



THE STUDY OF NOVEL ELECTROSTATIC ELECTRON LENSES

Thesis submitted for the degree of PhD
by Carol Trager
Physics Department
Royal Holloway and Bedford New College

ProQuest Number: 10090144

All rights reserved

INFORMATION TO ALL USERS

The quality of this reproduction is dependent upon the quality of the copy submitted.

In the unlikely event that the author did not send a complete manuscript and there are missing pages, these will be noted. Also, if material had to be removed, a note will indicate the deletion.



ProQuest 10090144

Published by ProQuest LLC(2016). Copyright of the Dissertation is held by the Author.

All rights reserved.

This work is protected against unauthorized copying under Title 17, United States Code.
Microform Edition © ProQuest LLC.

ProQuest LLC
789 East Eisenhower Parkway
P.O. Box 1346
Ann Arbor, MI 48106-1346

ABSTRACT

This thesis is concerned with the investigation, both numerically and experimentally of novel electrostatic lenses.

The properties of a five-element lens are described. This lens allows the variation of the magnification of an image of fixed position with fixed overall energy, and can be therefore considered a 'zoom' lens. This lens can also be constrained so that it is afocal and the separation between any pair of conjugate points is constant, and therefore independent of V_5/V_1 , with the magnification related very simply to V_5/V_1 .

A numerical technique involving matrix multiplication is used to compute the properties of the five-element lens from the tabulated properties of two-element lenses. Manipulation of the calculated data revealed that it is possible to define two 'universal' curves to summarise its properties. The calculated lens properties are compared with those previously obtained by experiment, (Heddle and Papadovassilakis 1984 †).

The aberration behaviour of a five-element lens was investigated. In particular, the dependence of the spherical aberration coefficient C_s on V_3/V_1 where $V_5/V_1 = 1$, and $V_2/V_1 = V_4/V_5$. C_s was also investigated for a number of afocal lenses. Finally, C_s was investigated for the lens where $V_5/V_1 = V_3/V_1 = 1$, V_2/V_1 is the variable and $\neq V_4/V_3$. This lens was found to have a minimum value for the product $MAG \times C_s$, therefore, **optimum** values of V_2/V_1 and the magnification exist for this lens. The values for C_s obtained by experiment are compared with those calculated by my supervisor Professor Heddle using the Bessel Function Expansion Method ‡, and the Fox-Goodwin Method §.

Finally, the properties of a three-element lens constructed from 31 discs electrically insulated from each other, and sandwiched between two ordinary cylindrical elements was investigated. Voltages were applied to this lens so that it simulated a three-element lens with a 'movable' centre element of variable length. The obtained experimental properties are also compared with those calculated by Professor Heddle.

† Heddle D W O and Papadovassilakis 1984 The magnification behaviour of a five-element electrostatic lens *J. Phys. E : Sci. Instrum.* **17** 559-605

‡ Cook R D and Heddle D W O 1976 The simple accurate calculation of cylinder lens potentials and focal properties *J. Phys. E : Sci Instrum.* **9** 279-282

§ Buckingham R A 1962 *Numerical Methods* (London : Pitman)

TABLE OF CONTENTS

CHAPTER ONE : INTRODUCTION

Section (1.1) General	19
Section (1.2) The Optical Analogy	20
Section (1.3) Fundamental Properties of Electron Lenses	
(a) Cardinal Points	23
(b) Other Lens Parameters and Lens Equations	26
Section (1.4) Lens Fields and Related Lens Properties	
(a) The Electrostatic Lens	31
(b) Magnetic Lens	42
(c) Comparison of Electrostatic and Magnetic Lenses	50
References : Bibliography	51
<i>(The References to this Introductory Chapter form the Bibliography. The Bibliography is also to be found at the end of the Thesis)</i>	

CHAPTER TWO : METHODS FOR CALCULATING THE PROPERTIES OF ELECTRON LENSES

Section (2.1) Introduction	56
Section (2.2) The Finite Difference Method or Relaxation Method	56
Section (2.3) The Charge Density Method	60
Section (2.4) The Separation of Variables Method	62
Section (2.5) The Finite Element Method	66
Section (2.6) Comparison of the various methods available for calculating the lens potential	71
Section (2.7) The Calculation of charged particle trajectories	73
References	81

CHAPTER THREE : METHODS FOR DETERMINING EXPERIMENTALLY THE PROPERTIES OF ELECTRON LENSES

Section (3.1) General Introduction	87
Section (3.2) Description of Experimental Methods other than those used in the present work	87
Section (3.3) Introduction to Experimental Methods used in the present work	93
Section (3.4) Description of the Lens Elements	93
Section (3.5) Description of the method used to determine the focal and magnification properties of a lens	
(a) Lens System	95
(b) Electronics	96
Section (3.6) Description of the method used to determine the spherical aberration coefficient	103
References	110

CHAPTER FOUR : CALCULATION OF MULTIPLE ELEMENT LENS
 PROPERTIES USING MATRIX TECHNIQUES

111-124

CHAPTER FIVE : FIVE-ELEMENT LENSES

Section (5.1) Why Five Elements?	133
Section (5.2) The Afocal Five-element lens with constant separation between conjugate planes	134
Section (5.3) Calculation of the Properties of the Afocal lens	136
Section (5.4) Five-element lens of Variable Magnification	143
Section (5.5) The Derivation of a 'Universal Curve' for the Voltage Ratios Required to Focus the Lens	148
Section (5.6) The 'Universal Curve' for the Magnification	161
Section (5.7) The 'Universal Curve' for the Angular Magnification	163
Section (5.8) The Investigation of the Aberration Behaviour of a Five-element Lens	163
References	182
Appendix	183

CHAPTER SIX : MULTI-DISC LENS

Section (6.1) Introduction	204
Section (6.2) Construction and Operation of the Multi-Disc Lens	206
Section (6.3) Acquiring data for the Multi-disc Lens	
(a) Experimental Data	214
(b) Calculated Data	218
Section (6.4) Presentation and Discussion of the Data for the Multi-Disc Lens	218
Section (6.5) Concluding Remarks	222
References	244
References : All	245
Bibliography	250

LIST OF TABLES

CHAPTER FOUR

Table 4.1 Table listing Matrix Elements for an Accelerating Lens	119
Table 4.2 Table listing Matrix Elements for a Decelerating Lens	120
Table 4.3 Table comparing the values obtained for V_2/V_1 using the Matrix and Bessel Function Expansion Methods for the symmetric three-element einzel lens, where $L_2 = L_3 = 2.0D$ and $0.5 \leq L_1 \leq 2.0D$	123

CHAPTER FIVE

Table 5.1 Table listing calculated lens properties illustrating the consistency of the calculations	142
Table 5A.1 Table defining the points A through to H	188

CHAPTER TWO

Figure 2.1 A five-point grid of equal mesh width	57
Figure 2.2 A nine-point grid of equal mesh width	60
Figure 2.3 Simple coaxial cylinder lens represented by a large number of circular strips in order to obtain the potential distribution by the charge density method	61
Figure 2.4 Schematic diagram of a two-cylinder lens showing the dimensions, the coordinate system and the regions in which different expressions for the potential apply in the Bessel function expansion method	65
Figure 2.5 Cross-section of a typical magnetic lens	67
Figure 2.6 Two finite element mesh for analyzing the pole piece region	68

LIST OF FIGURES

CHAPTER ONE

Figure 1.1 Snell's Law for Light	21
Figure 1.2 Snell's law for Electrons	22
Figure 1.3 Cardinal Points	25
(a) Principal Rays	
(b) Location of Focal Points	
(c) Location of Principal Planes and Principal Points	
(d) Location of Nodal Planes and Nodal Points	
Figure 1.4 Diagram Demonstrating that $AH_1 = BH_2$	24
Figure 1.5 Diagram Summarising Properties of Electron Lenses	27
Figure 1.6 Diagram for the Derivation of the Abbé Sine Rule	28
Figure 1.7 Examples of Electrostatic Electron Lenses	32
Figure 1.8 Diagram for Computing the electron trajectories in an axially symmetrical electric field	34
Figure 1.9 Diagram for proving that any axially symmetric electrostatic lens has the properties of an ideal lens	37
Figure 1.10 A Diverging Lens	39
Figure 1.11 Diagram for the proof that electrostatic lenses are always convergent when bounded by regions of constant potential	39
Figure 1.12 Crossed Nodal Points	41
Figure 1.13 Crossed Principal Points	41
Figure 1.14 Magnetic Lens	43
Figure 1.15 Components of the vector \mathbf{B} near the axis	42
Figure 1.16 Diagram showing force and field vectors for computing electron trajectories in an axially symmetrical magnetic field	48
 CHAPTER TWO	
Figure 2.1 A five-point grid of equal mesh width	57
Figure 2.2 A nine-point grid of equal mesh width	60
Figure 2.3 Simple coaxial cylinder lens represented by a large number of circular strips in order to obtain the potential distribution by the charge density method	61
Figure 2.4 Schematic diagram of a two-cylinder lens showing the dimensions, the coordinate system and the regions to which different expressions for the potential apply in the Bessel function expansion method	63
Figure 2.5 Cross section of a typical magnetic lens	67
Figure 2.6 The finite element mesh for analysing the pole piece region	68

Figure 2.7(a) A general finite element for the scalar potential calculation	69
Figure 2.7(b) Diagram for the generation of the finite element equations	69
CHAPTER THREE	
Figure 3.1 Diagram illustrating the Parallel Beam Method	87
Figure 3.2 Schematic Diagram of lens from which the Focal Distances F_1 and F_2 and the Focal Lengths f_1 and f_2 can be deduced	89
Figure 3.3 Diagram illustrating how the Cardinal Points of a lens can be deduced by extrapolating the paths of pencil rays from where they hit a target after they have passed through the lens	90
Figure 3.4 Diagram illustrating the Shadow Method for location of the cardinal points	92
Figure 3.5 A typical lens element	94
Figure 3.6 5-element lens system	97
Figure 3.7 Schematic diagram of 5-element lens system	98
Figure 3.8 Schematic Diagram of Aperture discs used to obtain the magnification of an electron lens	99
Figure 3.9 A lens element with deflection plates	100
Figure 3.10 Photograph of image displayed on display scope from which the lens magnification is deduced	101
Figure 3.11 Block Diagram of Electronics used to Operate and Display the image of the Lens	102
Figure 3.12 Diagram illustrating the effect of spherical aberration	104
Figure 3.13 Schematic diagram of 5-element lens system used to obtain Δr in order to obtain the spherical aberration coefficient C_s	106
Figure 3.14 Schematic Diagram of Aperture disc with five apertures whose use enables Δr and hence C_s to be determined	107
Figure 3.15 Photograph of image displayed on display scope from which Δr_h and Δr_v and hence C_s is deduced	108
Figure 3.16 Diagram comparing the distances at which a beam will cross a plane perpendicular to the lens axis when unaffected by lens action and when under the influence of a lens	109
CHAPTER FOUR	
Figure 4.1 Diagram illustrating the object and image sizes, angle of inclination at the object and angle of inclination at the image for a typical lens system	115
Figure 4.2 Schematic diagram of a two-tube electrostatic lens showing the focal points F_1 and F_2 , focal lengths f_1 and f_2 , principal planes H_1 and H_2 , and coordinates p, P, q, Q in object and image space respectively	117

Figure 4.3 The dependence of the matrix elements on voltage ratio (a) for accelerating lenses (b) for decelerating lenses	121
CHAPTER FIVE	
Figure 5.1 Five-element Electrostatic lens	135
Figure 5.2 Ray Diagram for 5-element Afocal Lens with constant separation between Conjugate Points	137
Figure 5.3 V_5/V_1 Versus V_2/V_1 as obtained from calculation using the matrix technique, for the lens with $L_1 = L_2 = L_4 = L_5 = 1.5D$ and $L_3 = 3.0D$	140
Figure 5.4 V_5/V_1 Versus V_2/V_1 as obtained from experiment, (<i>Heddle and Papadovassilakis (1984)</i>) for the lens with $L_1 = L_2 = L_4 = L_5 = 1.5D$ and $L_3 = 3.0D$	144
Figure 5.5 V_5/V_1 Versus the Magnification M as obtained from experiment, (<i>Heddle and Papadovassilakis (1984)</i>) for the lens with $L_1 = L_2 = L_4 = L_5 = 1.5D$ and $L_3 = 3.0D$	145
Figure 5.6 α Versus The Separation of the Conjugate Points	146
Figure 5.7 $(V_5/V_1)^\alpha$ Versus $(V_2/V_1)^\alpha$ as obtained from calculation using the matrix technique, for the lens with $S=1.5$	147
Figure 5.8 Lines of constant magnification M , angular magnification M_α , and overall voltage ratio V_5/V_1 , drawn on axes of V_2/V_1 and V_4/V_1 , as obtained by experiment by <i>Heddle and Papadovassilakis (1984)</i>	149
Figure 5.9 Lines of constant magnification M , angular magnification M_α , and overall voltage ratio V_5/V_1 , drawn on axes of V_2/V_1 and V_4/V_1 as obtained from calculation using the matrix technique, for the lens with $L_1 = L_2 = L_4 = L_5 = 1.5D$ and $L_3 = 3.0D$	150
Figure 5.10 $(V_2/V_1)/((V_5/V_1)^Q)$ Versus $(V_4/V_5)/((V_1/V_5)^Q)$ as obtained from calculation using the matrix technique, for the lens with $L_1 = L_2 = L_4 = L_5 = 1.5D$ and $L_3 = 3.0D$ for various values of V_5/V_1	152
Figure 5.11 Q Versus V_5/V_1 as obtained from calculation using the matrix technique, for the lens with $L_1 = L_2 = L_4 = L_5 = 1.5D$ and $L_3 = 3.0D$	153
Figure 5.12 $((V_2/V_1)/((V_5/V_1)^Q))^{ZETA}$ Versus $(V_4/V_5)/((V_1/V_5)^Q)^{ZETA}$ as obtained from calculation using the matrix technique, for the lens with $L_1 = L_2 = L_4 = L_5 = 1.5D$, and $L_3 = 3.0D$	154
Figure 5.13 $(V_5/V_1)^Q$ Versus V_5/V_1 as obtained from calculation using the matrix technique, for the lens with $L_1 = L_2 = L_4 = L_5 = 1.5D$ and $L_3 = 3.0D$	155
Figure 5.14 $ZETA$ Versus V_5/V_1 as obtained from calculation using the matrix technique, for the lens with $L_1 = L_2 = L_4 = L_5 = 1.5D$ and $L_3 = 3.0D$	156

Figure 5.15 $\left(\frac{(V_2/V_1)/((V_5/V_1)^Q)}{(V_4/V_5)/((V_1/V_5)^Q)}\right)^{ZETA}$ Versus $\left(\frac{(V_4/V_5)/((V_1/V_5)^Q)}{(V_2/V_1)/((V_5/V_1)^Q)}\right)^{ZETA}$	
as obtained from calculation using the matrix technique, for the lens with $L_1 = L_2 = L_4 = L_5 = 1.5D$, and $L_3 = 3.0D$ for $V_5/V_1 = 10$	157
Figure 5.16 $\left(\frac{(V_2/V_1)/((V_5/V_1)^Q)}{(V_4/V_5)/((V_1/V_5)^Q)}\right)^{ZETA}$ Versus $\left(\frac{(V_4/V_5)/((V_1/V_5)^Q)}{(V_2/V_1)/((V_5/V_1)^Q)}\right)^{ZETA}$	
as obtained from calculation using the matrix technique, for the lens with $L_1 = L_2 = L_4 = L_5 = 1.5D$, and $L_3 = 3.0D$ for $V_5/V_1 = 36$	158
Figure 5.17 $\left(\frac{(V_2/V_1)/((V_5/V_1)^Q)}{(V_4/V_5)/((V_1/V_5)^Q)}\right)^{ZETA}$ Versus $\left(\frac{(V_4/V_5)/((V_1/V_5)^Q)}{(V_2/V_1)/((V_5/V_1)^Q)}\right)^{ZETA}$	
as obtained from experiment, (<i>Heddle and Papadovassilakis (1984)</i>) for the lens with $L_1 = L_2 = L_4 = L_5 = 1.5D$, and $L_3 = 3.0D$ for various values of V_5/V_1	159
Figure 5.18 $(B \times (MAG)^A$ Versus $(C \times (V_2/V_4))^D$ as obtained from calculation using the matrix technique, for the lens with $L_1 = L_2 = L_4 = L_5 = 1.5D$ and $L_3 = 3.0D$	164
Figure 5.19 $(B \times (MAG)^A$ Versus $(C \times (V_2/V_4))^D$ as obtained from calculation using the matrix technique, for the lens with $L_1 = L_2 = L_4 = L_5 = 1.5D$ and $L_3 = 3.0D$ for $V_5/V_1 = 10$	165
Figure 5.20 $(B \times (MAG)^A$ Versus $(C \times (V_2/V_4))^D$ as obtained from calculation using the matrix technique, for the lens with $L_1 = L_2 = L_4 = L_5 = 1.5D$ and $L_3 = 3.0D$ for $V_5/V_1 = 36$	166
Figure 5.21 A Versus V_5/V_1 as obtained from calculation using the matrix technique, for the lens with $L_1 = L_2 = L_4 = L_5 = 1.5D$ and $L_3 = 3.0D$	167
Figure 5.22 B Versus V_5/V_1 as obtained from calculation using the matrix technique, for the lens with $L_1 = L_2 = L_4 = L_5 = 1.5D$ and $L_3 = 3.0D$	168
Figure 5.23 C Versus V_5/V_1 as obtained from calculation using the matrix technique, for the lens with $L_1 = L_2 = L_4 = L_5 = 1.5D$ and $L_3 = 3.0D$	169
Figure 5.24 D Versus V_5/V_1 as obtained from calculation using the matrix technique, for the lens with $L_1 = L_2 = L_4 = L_5 = 1.5D$ and $L_3 = 3.0D$	170
Figure 5.25 $(B \times (MAG)^A$ Versus $(C \times (V_2/V_4))^D$ as obtained from experiment, for the lens with $L_1 = L_2 = L_4 = L_5 = 1.5D$ and $L_3 = 3.0D$ (<i>Heddle and Papadovassilakis (1984)</i>) for various values of V_5/V_1	171
Figure 5.26 $\left(\frac{(V_2/V_1)/((V_5/V_1)^Q)}{(V_4/V_5)/((V_1/V_5)^Q)}\right)^{ZETA}$ Versus $\left(\frac{(V_4/V_5)/((V_1/V_5)^Q)}{(V_2/V_1)/((V_5/V_1)^Q)}\right)^{ZETA}$ (plotted on linear axes)	
as obtained from calculation using the matrix technique, for the lens with $L_1 = L_2 = L_4 = L_5 = 1.5D$, and $L_3 = 3.0D$	172

Figure 5.27 Photograph of display scope showing six dots for aberration measurements	176
Figure 5.28 C_s Versus V_3/V_1 , where $V_5/V_1 = 1$, $V_2/V_1 = V_4/V_5 > V_3/V_1$, for the lens where $L_1 = L_5 = 1.5D, L_2 = L_4 = 1.0D$ and $L_3 = 3.0D$	177
Figure 5.29 C_s Versus V_5/V_1 , for the afocal lens where $L_1 = L_5 = 1.5D, L_2 = L_4 = 1.0D$ and $L_3 = 3.0D$	178
Figure 5.30 C_s Versus V_2/V_1 , where $V_5/V_1 = V_3/V_1 = 1$, $V_2/V_1 \neq V_4/V_5$, for the lens where $L_1 = L_5 = 1.5D, L_2 = L_4 = 1.0D$ and $L_3 = 3.0D$	179
Figure 5.31 $MAG \times C_s$ Versus V_2/V_1 , where $V_5/V_1 = V_3/V_1 = 1$, $V_2/V_1 \neq V_4/V_5$, for the lens where $L_1 = L_5 = 1.5D, L_2 = L_4 = 1.0D$ and $L_3 = 3.0D$	180
Figure 5.32 $MAG \times C_s$ Versus MAG , where $V_5/V_1 = V_3/V_1 = 1$, $V_2/V_1 \neq V_4/V_5$, for the lens where $L_1 = L_5 = 1.5D, L_2 = L_4 = 1.0D$ and $L_3 = 3.0D$	181
Figure 5A.1 Diagram showing Afocal Locus, Defining the Points A through to H	187
CHAPTER SIX	
Figure 6.1 Read's Movable Electrostatic Lens	205
Figure 6.2 Photograph of Discs sandwiched between two Cylindrical Lens Elements	207
Figure 6.3 Diagram showing how the Voltages are stepped between L_1 and L_2 and L_2 and L_3 respectively	208
Figure 6.4 Photograph of a disc	209
Figure 6.5 Schematic Diagram of a disc	210
Figure 6.6 Diagram showing how discs were stacked to form the Disc Lens	212
Figure 6.7 End View of Disc Lens Sandwich	213
Figure 6.8 Schematic Diagram of Switching Unit	215
Figure 6.9 Photograph of Front Panel of Switching Unit	216
Figure 6.10 Diagram showing that if the change in voltage in the regions of 'stepping' voltage are approximated by a linear voltage variation, then the effective length of L_2 is (no. of discs connected together to form L_2-1) $\times 0.1D$	217
Figure 6.11 Typical Example of the 'image' displayed on the Display Scope from the Disc Lens	219
Figure 6.12 Example of a 'bad' image from the Disc lens	220

Figure 6.13 Lines of constant V_3/V_1 and lines of Constant magnification M plotted on axes of n_c Versus V_2/V_1 for various values of V_3/V_1 for the Disc Lens with a Centre Element length of 0.6D as obtained from the calculated data of Heddle	224
Figure 6.14 Lines of constant V_3/V_1 and lines of Constant magnification M plotted on axes of n_c Versus V_2/V_1 for various values of V_3/V_1 for the Disc Lens with a Centre Element length of 1.0D as obtained from the calculated data of Heddle	225
Figure 6.15 Lines of constant V_3/V_1 and lines of Constant magnification M plotted on axes of n_c Versus V_2/V_1 for various values of V_3/V_1 for the Disc Lens with a Centre Element length of 2.0D as obtained from the calculated data of Heddle	226
Figure 6.16 V_2/V_1 Versus n_c for various values of V_3/V_1 for the Disc Lens with a Centre Element length of 0.6D as obtained from experiment	228
Figure 6.17 V_2/V_1 Versus n_c for various values of V_3/V_1 for the Disc Lens with a Centre Element length of 1.0D as obtained from experiment	229
Figure 6.18 V_2/V_1 Versus n_c for various values of V_3/V_1 for the Disc Lens with a Centre Element length of 2.0D as obtained from experiment	230
Figure 6.19 Experimentally obtained and calculated values of V_2/V_1 Versus n_c for $V_3/V_1 = 0.6, 1.0$ and 3.0 for the Disc Lens with a Centre Element length of 0.6D	232
Figure 6.20 Experimentally obtained and calculated values of V_2/V_1 Versus n_c for $V_3/V_1 = 0.6, 1.0$ and 3.0 for the Disc Lens with a Centre Element length of 01.0D	233
Figure 6.21 Experimentally obtained and calculated values of V_2/V_1 Versus n_c for $V_3/V_1 = 0.6, 1.0$ and 3.0 for the Disc Lens with a Centre Element length of 2.0D	234
Figure 6.22 Experimentally obtained and calculated values of Magnification M Versus n_c for $V_3/V_1 = 0.6$ for the Disc Lens with a Centre Element Length of 0.6D	236
Figure 6.23 Experimentally obtained and calculated values of Magnification M Versus n_c for $V_3/V_1 = 1.0$ for the Disc Lens with a Centre Element Length of 0.6D	237
Figure 6.24 Experimentally obtained and calculated values of Magnification M Versus n_c for $V_3/V_1 = 3.0$ for the Disc Lens with a Centre Element Length of 0.6D	238
Figure 6.25 Experimentally obtained and calculated values of Magnification M Versus n_c for $V_3/V_1 = 0.6$ for the Disc Lens with a Centre Element Length of 1.0D	239
Figure 6.26 Experimentally obtained and calculated values of Magnification M Versus n_c for $V_3/V_1 = 1.0$ for the Disc Lens with a Centre Element Length of 1.0D	240

Figure 6.27 Experimentally obtained and calculated values of Magnification M Versus n_c for $V_3/V_1 = 3.0$ for the Disc Lens with a Centre Element Length of 1.0D	241
Figure 6.28 Experimentally obtained and calculated values of Magnification M Versus n_c for $V_3/V_1 = 0.6$ and 1.0 for the Disc Lens with a Centre Element Length of 2.0D	242
Figure 6.29 Experimentally obtained and calculated values of Magnification M Versus n_c for $V_3/V_1 = 0.6$ and 3.0 for the Disc Lens with a Centre Element Length of 2.0D	243

I would like to dedicate this thesis to my family and friends whose help, support and encouragement have made the presentation of this thesis possible.

ACKNOWLEDGEMENTS

I would like to thank Professor Heddle for proposing and supervising the work that is presented in this thesis, and also for his patience and support during the time I have been his supervisee. I would like to thank Dr Susan Kay for her help and advice and support with both the experimental work and with the preparation of the thesis, and for being a very sympathetic listener. I would like to thank Dr Ron Miller and Prof Milan Kurepa for their help and advice during their time as visiting Fellows in the Physics Department. I would like to thank Dr Janet Webster for her help and advice on Numerical Methods. I would like to dedicate this thesis to my family and friends whose help, support and encouragement have made the presentation of this thesis possible.

I would like to thank Dr Andrew Wroot, Sylvia Marshall, and Dr Leslie Morgan of the Computer Centre for their advice and help.

I would like to thank all the staff in the electronics and mechanical workshops, without whose help the work in this thesis would have never even been started. In particular, I would like to thank Leon Ellison, Ray Jordan and Rick Sams for designing and building the electronics I needed in order to investigate the losses, and for their patience when things 'blew up', I will be eternally grateful for their uncomplaining help and advice when I had a 'wee problem'. I would also like to thank Reg Elton, Steve Forman, Brian Porter, John Taylor and John Nodes for producing electron lens elements, etc yesterday. I would also like to thank John Nodes for keeping me supplied with liquid nitrogen.

I would like to thank Mike Thyer for his work, help and advice with the vacuum systems, and for his help with 'tidying' the lab.

I would like to thank Mary Walls and Pearl O'Neil for typing these things it was impossible to produce on the computer.

I would like to thank Sue May for producing the diagrams in this thesis, in particular, I would like to thank her for the work she did in her own time.

I would like to thank the SERC for supplying the money for the two year research assistantship which enabled me to do this work, and I would also like to thank the College for the award of the Amy Lady Tass postgraduate studentship, which helped support me in my third year.

ACKNOWLEDGEMENTS

I would like to thank Professor Heddle for proposing and supervising the work that is presented in this thesis, and also for his patience and support during the time I have been his supervisee. I would like to thank Dr Susan Kay for her help and advice and support with both the experimental work and with the preparation of the thesis, and for being a very sympathetic listener. I would like to thank Dr Ron Miller and Prof Milan Kurepa for their help and advice during their time as visiting Fellows in the Physics Department. I would like to thank Dr Janet Webster for her help and advice on Numerical Methods. I would like to thank Dr Eric Munro for the helpful discussion I had with him on his work and on general techniques used to calculate lens properties.

I would like to thank Dr Andrew Wroot, Sylvia Marshall, and Dr Leslie Morgan of the Computer Centre for their advice and help.

I would like to thank all the staff in the electronics and mechanical workshops, without whose help the work in this thesis would have never even been started. In particular, I would like to thank Leon Ellison, Ray Jordan and Rick Sams for designing and building the electronics I needed in order to investigate the lenses, and for their patience when things 'blew up', I will be eternally grateful for their uncomplaining help and advice when I had a 'wee problem'. I would also like to thank Reg Elton, Steve Foreman, Brian Porter, John Taylor and John Nodes for producing electron lens elements, etc yesterday. I would also like to thank John Nodes for keeping me supplied with liquid nitrogen.

I would like to thank Mike Thyer for his work, help and advice with the vacuum systems, and for his help with 'tidying' the lab.

I would like to thank Mary Walls and Pearl Olliff for typing those items it was impossible to produce on the computer.

I would like to thank Sue May for producing the diagrams in this thesis, in particular, I would like to thank her for the work she did in her own time.

I would like to thank the SERC for supplying the money for the two year research assistantship which enabled me to do this work, and I would also like to thank the College for the award of the Amy Lady Tate postgraduate studentship, which helped support me in my third year.

Finally, I would like to thank Amanda Nelson whose friendship has kept me sane.

CHAPTER ONE

INTRODUCTION

. This Thesis was produced using T_EX, created by D E Knuth

CONTENTS : CHAPTER ONE

	Page No
Section (1.1) General	12
Section (1.2) The Optical Analogy	20
Section (1.3) Fundamental Properties of Electron Lenses	
(a) Cardinal Points	25
(b) Other Lens Parameters and Lens Equations	28
Section (1.4) Lens Types	
(a) The Electrostatic Lens	31
(b) Magnetic Lenses	42
(c) Compound Lenses	50
(d) Spherical Lenses	50
References - Bibliography	54
<i>(The References in this Introductory Chapter form the Bibliography. The Bibliography is also to be found at the end of the Thesis)</i>	

CHAPTER ONE INTRODUCTION

CONTENTS : CHAPTER ONE

	Page No
Section (1.1) General	19
Section (1.2) The Optical Analogy	20
Section (1.3) Fundamental Properties of Electron Lenses	25
(a) Cardinal Points	23
(b) Other Lens Parameters and Lens Equations	26
(c) Location of Principal Planes and Principal Points	27
Section (1.4) Lens Fields and Related Lens Properties	31
(a) The Electrostatic Lens	31
(b) Magnetic Lens	42
(c) Comparison of Electrostatic and Magnetic Lenses	50
References : Bibliography	51
<i>(The References to this Introductory Chapter form the Bibliography. The Bibliography is also to be found at the end of the Thesis)</i>	
Figure 1.1 Examples of Electrostatic Electron Lenses	32
Figure 1.2 Diagram for computing the electron trajectories in an axially symmetrical electric field	34
Figure 1.3 Diagram for proving that any axially symmetrical electrostatic lens has the properties of an ideal lens	37
Figure 1.4 A Diverging Lens	39
Figure 1.5 Diagram for the proof that electrostatic lenses are always convergent when bounded by regions of constant potential	40
Figure 1.6 Crossed Nodal Points	41
Figure 1.7 Crossed Principal Points	41
Figure 1.8 Magnetic Lens	43
Figure 1.9 Components of the vector \mathbf{B} near the axis	45
Figure 1.10 Diagram showing force and field vectors for computing electron trajectories in an axially symmetrical magnetic field	46

LIST OF FIGURES : CHAPTER ONE

	Page No
Figure 1.1 Snell's Law for Light	21
Figure 1.2 Snell's law for Electrons	22
Figure 1.3 Cardinal Points	25
(a) Principal Rays	
(b) Location of Focal Points	
(c) Location of Principal Planes and Principal Points	
(d) Location of Nodal Planes and Nodal Points	
Figure 1.4 Diagram Demonstrating that $A H_1 = B H_2$	24
Figure 1.5 Diagram Summarising Properties of Electron Lenses	27
Figure 1.6 Diagram for the Derivation of the Abbé Sine Rule	28
Figure 1.7 Examples of Electrostatic Electron Lenses	32
Figure 1.8 Diagram for Computing the electron trajectories in an axially symmetrical electric field	34
Figure 1.9 Diagram for proving that any axially symmetric electrostatic lens has the properties of an ideal lens	37
Figure 1.10 A Diverging Lens	39
Figure 1.11 Diagram for the proof that electrostatic lenses are always convergent when bounded by regions of constant potential	39
Figure 1.12 Crossed Nodal Points	41
Figure 1.13 Crossed Principal Points	41
Figure 1.14 Magnetic Lens	43
Figure 1.15 Components of the vector B near the axis	42
Figure 1.16 Diagram showing force and field vectors for computing electron trajectories in an axially symmetrical magnetic field	48

INTRODUCTION

1.1 GENERAL†

Electron optics is the name given to the subject which describes the production, propagation and focusing of beams of electrons and ions. An electron lens is a device which manipulates beams of charged particles using electric and/or magnetic fields, –where the word electron is generally understood to apply to any charged particle–. Electron lenses are important in many fields, such as electron physics, electron microscopy, surface physics, high energy physics, plasma physics; and are found in such devices as the cathode ray tube, electron and ion microscopes and microscopes, mass and beta spectrometers, image intensifiers. . . . The diversity of the uses of electron optics is aptly illustrated by considering the range of energies of the electric and magnetic fields used. Energies of only a few eV are used by the atomic and molecular physicists, while the electron microscopist will use $100KeV$ or so, while the high energy physicist may encounter many GeV .

Today research in electron optics is concerned with improving the performance of existing devices, for example the understanding and elimination/minimisation of aberration effects. High powered computers have greatly facilitated the study of electron optics, as it has become possible, using various techniques, to calculate numerically the properties of lenses and lens systems and hence predict the optimum.

New fields in which electron optics is becoming important are the semiconductor industry where they are used in the analysis and production of semiconductor materials, for example in metal ion guns, secondary ion mass spectrometry (SIMS), and electron and ion lithography; and positron physics, where lenses are now being used to control and manipulate positron beams.

The problems encountered by the different users of electron lenses will differ, for example the aberration problems encountered by the atomic physicist, –because he must work with low energy electron beams–, will probably not be met by the semiconductor physicist using much higher energy ion beams. However, the semiconductor physicist may have problems with space charge, –due to the size of the ions and the intensity of the beam used–, a problem with which the atomic physicist will rarely need be concerned. However, *THE BASIC LAWS OF OPTICS AND THE LAWS GOVERNING ELECTRIC AND*

† References : See Bibliography

MAGNETIC FIELDS ARE THE SAME IN ANY FIELD, AS LONG AS THE DEVICE USED TO MANIPULATE THE CHARGED PARTICLES CAN BE CONSIDERED TO BE A LENS.

With the previous statement in mind, the remainder of this chapter will be concerned with outlining the basic principles of electron optics.

As implied by the word optics there is a close analogy between light rays and electron beams; electrons can in fact be reflected, refracted and focused very much as can light rays. It should therefore be possible to describe an electron optical system using the ideas of light optics, in fact the laws and principles as observed for light optics can be applied to electron lenses.

1.2 THE OPTICAL ANALOGY†

The fundamental theory of electron optics is based on the concept of Hamilton, that there exists a strong analogy between a light ray traversing a medium of continuously varying index of refraction and a mass point travelling through a potential field. This concept originated from a comparison of Fermat's principle of least time as applied to the path of a light ray, with Maupertuis' principle of least action as applied to any mechanical movement.

The principle of least time states that a light ray will assume a path such that the time taken between any two points of its path will be a minimum compared to that for all other possible paths between the same two points. Thus

$$T = \int \frac{1}{v} ds = \frac{1}{c} \int n ds = \min \quad (1.1)$$

where s is the distance, T is the time, v is the velocity of light in a medium of refractive index n , and c is the velocity of light in a vacuum.

The principle of least action states that a particle will assume a path such that the action, —that is the integral of momentum mv with distance—, is a minimum, i.e.,

$$\text{Action} = m \int v ds = \min \quad (1.2)$$

Comparison between the above two integrals clearly illustrates the correspondence between the two principles. It is also possible to deduce from the above that, excluding the constants

† References : See Bibliography

the refractive index of a medium in the optical case can be considered the equivalent of the corresponding velocity in the dynamical case. This implies that the path taken by a massive particle is the same as that taken by a light ray, in a medium whose refractive index at every point of motion is proportional to the velocity of the particle.

Another fundamental optical law which illustrates the analogy between light and electron optics, is Snell's law. Snell's law in light optics is illustrated in figure 1.1 below.

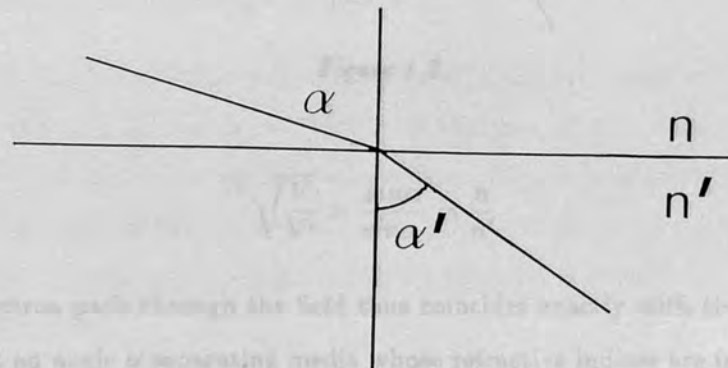


Figure 1.1

A beam travelling through a medium of refractive index n passes into another medium of refractive index n' , as shown in figure 1.1. The angle of incidence α and the angle of incidence α' are related by;

$$n \sin \alpha = n' \sin \alpha' \dots \dots \dots \text{Snell's Law} \quad (1.3)$$

Similarly, an electron travelling with uniform speed u through a space of constant potential V , which then passes a potential step into a space of constant potential V' , will have its path abruptly changed, as shown in figure 1.2 below.

Assuming that as in figure 1.2, V' is greater than V , the normal velocity component u_y is increased and the electron will be accelerated. The tangential component u_x will remain unchanged, so that $u'_x = u_x$. The velocity of the electron is proportional to the square root of the potential as

$$\frac{1}{2} m u^2 = - e V \quad (1.4)$$

and from figure 1.2

$$\sin \alpha = \frac{u_x}{u}$$

$$\sin \alpha' = \frac{u'_x}{u'}$$

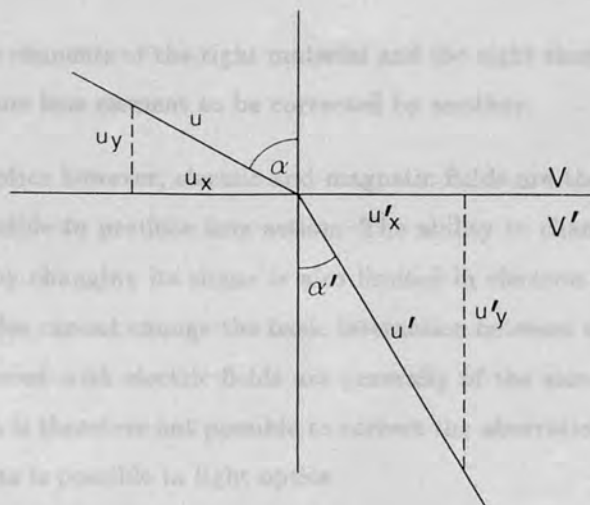


Figure 1.2

therefore

$$\sqrt{\frac{V}{V'}} = \frac{\sin \alpha'}{\sin \alpha} = \frac{n}{n'} \quad (1.5)$$

The electron path through the field thus coincides exactly with the path of a light ray incident at an angle α separating media whose refractive indices are in the ratio $\sqrt{\frac{V}{V'}}$. The electronic refractive index thus depends only on the position in the potential field. A continuously varying field will cause the divergence of an incident ray to decrease with the increase in refractive index, and may ultimately cause the ray to converge to a point, i.e., an appropriate continuously varying field can be used to 'focus' an electron beam and can therefore be regarded as an electron lens. This suggests that the action of an electron lens is similar to that of a thick optical lens, the electric field corresponding to an optical system of an infinite number of lenses of different refractive index in contact.

This discussion has so far been concerned with the similarities between light and electron optics. However, it must be pointed out that the analogy does have its limitations, and that there are principal differences between the two optics. For example, light rays are generally refracted by a finite number of refractive surfaces where the refractive index changes abruptly, whereas in electron optical systems there are no sharp changes in refractive index, but a continuous variation. Other differences exist between the two optics, such as the difference in the number of materials available to construct lenses.

In light optics there is a wide choice of materials available with which a lens can be built, for example various types of glass, plastics, quartz... in fact any transparent material can be used to construct a lens. It is therefore relatively easy to construct a light lens which will satisfy required specifications. The ability to change the properties of a given lens by

simply choosing lens elements of the right material and the right shape, allows for example, aberrations due to one lens element to be corrected by another.

In electron optics however, electric and magnetic fields are the only media available with which it is possible to produce lens action. The ability to change the properties of a given lens element by changing its shape is also limited in electron optics, as varying the shape of the electrodes cannot change the basic interaction between electron and field. The aberrations encountered with electric fields are generally of the same sign as those due to magnetic fields, so it is therefore not possible to correct the aberrations due to one medium by using the other, as is possible in light optics.

Although we are limited to only two media with which to construct an electron lens, the fact that refractive indices can be varied by the control of voltage or current makes an electron lens a lot more flexible than a light lens. The magnitudes of refractive indices which are frequently dealt with in electron lens systems would never occur in light optics. Ratios of refractive indices of the order of 10^3 are possible, compared to an upper limit of about 10 in light optics.

Even though there are differences between the two optics, –as discussed above–; the analogy between electron and light optics provides the foundation to introduce the concepts of electron optics and also to define the fundamental geometrical properties of electron lenses. The next section describes some of the fundamental parameters used to characterise electron lenses, and some of the laws they obey.

1.3 FUNDAMENTAL PROPERTIES OF ELECTRON LENSES

A. Cardinal Points†

When considering the imaging of objects by an electron lens, it is inconvenient to have to trace the ray paths from a particular point on the object to find the resulting point on the image. As in light optics it is possible to define six points known as the cardinal points, from which all the required imaging information can be deduced. The procedure is only exact however, for paraxial rays, that is those rays that move close to the axis and make a small angle with it, so that the angle can be equated to its sine. This approximation

† References : See Bibliography, in particular Hall 1953

is known as the Gaussian or first order approximation. The cardinal points are defined by figure 1.3 and the following discussion.

In order to define the cardinal points it is first necessary to define what are known as the principal rays of the lens. The principal rays are the two rays which enter and leave the lens parallel to the axis respectively, (see figure 1.3(a)). The ray which approaches the lens parallel to the axis from the right side of the lens is known as the first principal ray, the ray which approaches the lens parallel to the axis from the left side of the lens is known as the second principal ray. Any general ray can be expressed as a combination of these two rays.

FOCAL POINTS : The focal points F_1 and F_2 (see figure 1.3(b)), are defined as the points where the principal rays intersect the axis.

PRINCIPAL POINTS : The principal points H_1 and H_2 (see figure 1.3(c)), are defined as the points where the principal planes h_1 and h_2 cross the axis, where the principal planes are the planes of unit lateral magnification and can be located, (as shown in figure 1.3(c)) by asymptotically extending the straight line sections of the principal rays until they intersect, the points of intersection lying on the principal planes.

NOTE : All rays which converge to a point A on the first principal plane must, after passing through the lens, diverge from a point B on the second principal plane such that $AH_1 = BH_2$. This is illustrated by the two examples of figures 1.4(a) and 1.4(b) below, where figure 1.4(b) shows the principal points crossed as is the case for electron lenses, a point which will be discussed later.

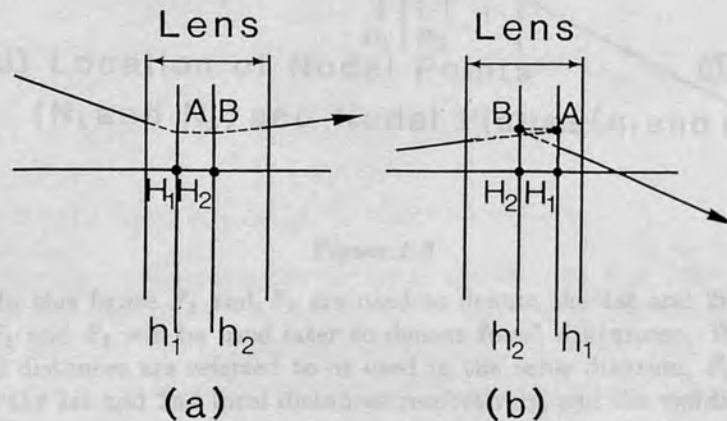
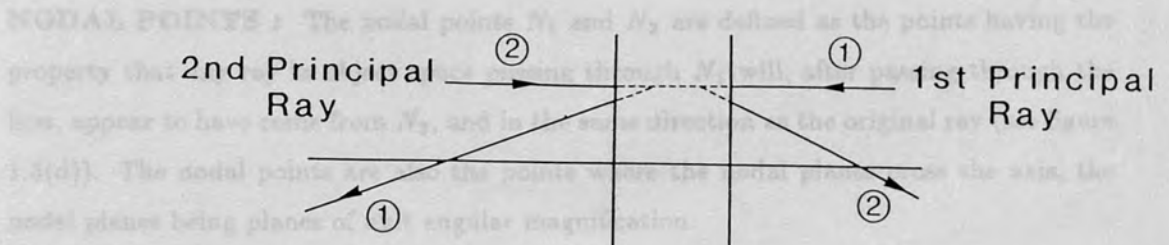
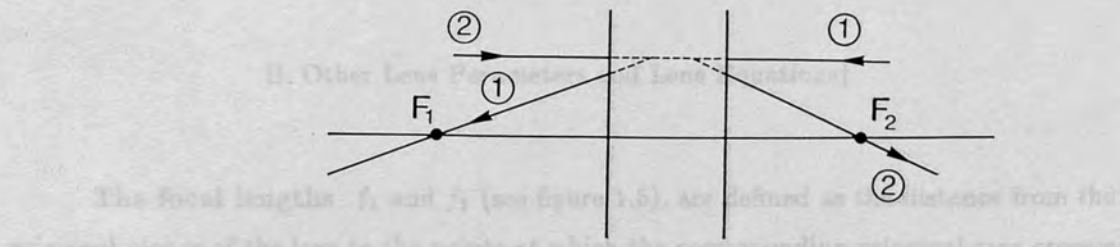


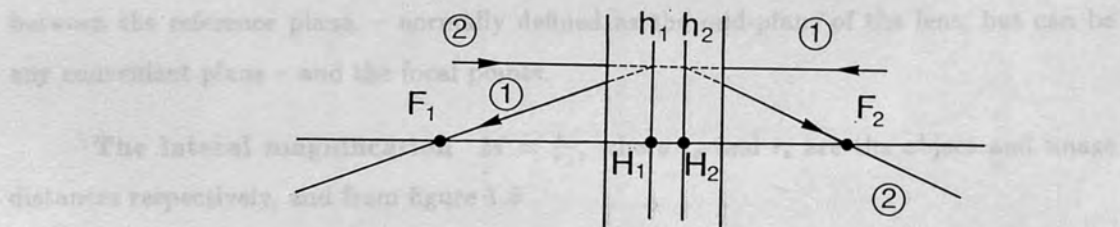
Figure 1.4



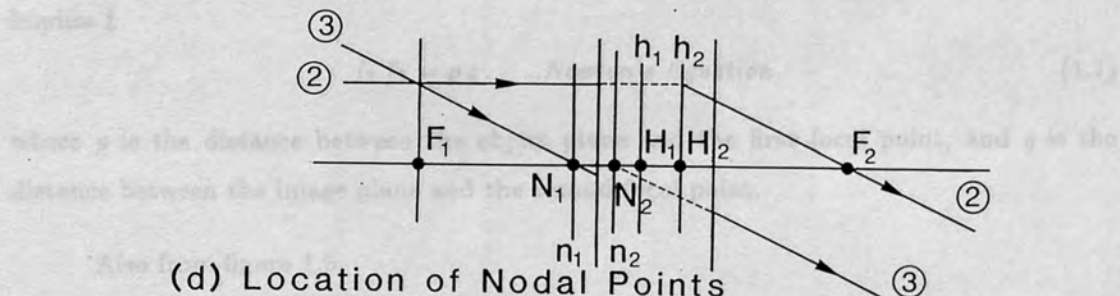
(a) Principal Rays



(b) Location of the Focal Points



(c) Location of Principal Points (H_1 and H_2) and Principal Planes (h_1 and h_2)



(d) Location of Nodal Points (N_1 and N_2) and Nodal Planes (n_1 and n_2)

Figure 1.3

Note : In this figure F_1 and F_2 are used to denote the 1st and 2nd focal points respectively. F_1 and F_2 will be used later to denote focal distances. Where both focal point and focal distances are referred to or used in the same diagram, F_1 and F_2 will be used to denote the 1st and 2nd focal distances respectively, and the words 1st Focal Point and 2nd Focal Point will be used to denote the 1st and second focal points respectively, so as to prevent any ambiguity.

NODAL POINTS : The nodal points N_1 and N_2 are defined as the points having the property that any ray in object space passing through N_1 will, after passing through the lens, appear to have come from N_2 , and in the same direction as the original ray (see figure 1.3(d)). The nodal points are also the points where the nodal planes cross the axis, the nodal planes being planes of unit angular magnification.

NOTE : From geometry it can be seen that the distances $N_1 N_2 = H_1 H_2$ are equal.

B. Other Lens Parameters and Lens Equations†

The focal lengths f_1 and f_2 (see figure 1.5), are defined as the distance from the principal planes of the lens to the points at which the corresponding principal rays crosses the axis, i.e., the focal points. The focal distances F_1 and F_2 are defined as the distances between the reference plane, – normally defined as the mid-plane of the lens, but can be any convenient plane – and the focal points.

The lateral magnification $M = \frac{r_i}{r_o}$, where r_o and r_i are the object and image distances respectively, and from figure 1.5

$$M = \frac{r_i}{r_o} = -\frac{f_1}{p} = -\frac{q}{f_2} \quad (1.6)$$

implies ‡

$$f_1 f_2 = p q \dots \text{Newton's Equation} \quad (1.7)$$

where p is the distance between the object plane and the first focal point, and q is the distance between the image plane and the second focal point.

Also from figure 1.5,

$$P = F_1 + p \text{ and } Q = F_2 + q \quad (1.8)$$

where P and Q are the object and image distances respectively.

† References : See Bibliography, in particular Grivet 1972, Hall 1953.

‡ Note: the sign convention used above and in the rest of this text is as follows. All quantities above the optic axis are positive, all quantities below the optic axis are negative. All quantities to the left of the reference plane of the lens are negative, all quantities to the right of the reference plane are positive, and the focal lengths are negative if the focal point is to the left of its corresponding principal plane.

The angular magnification $M_a = \frac{\tan \alpha_i}{\tan \alpha_o}$, where α_o and α_i are the angles made with the axis at the object and image respectively. From figure 1.5 it can be seen that

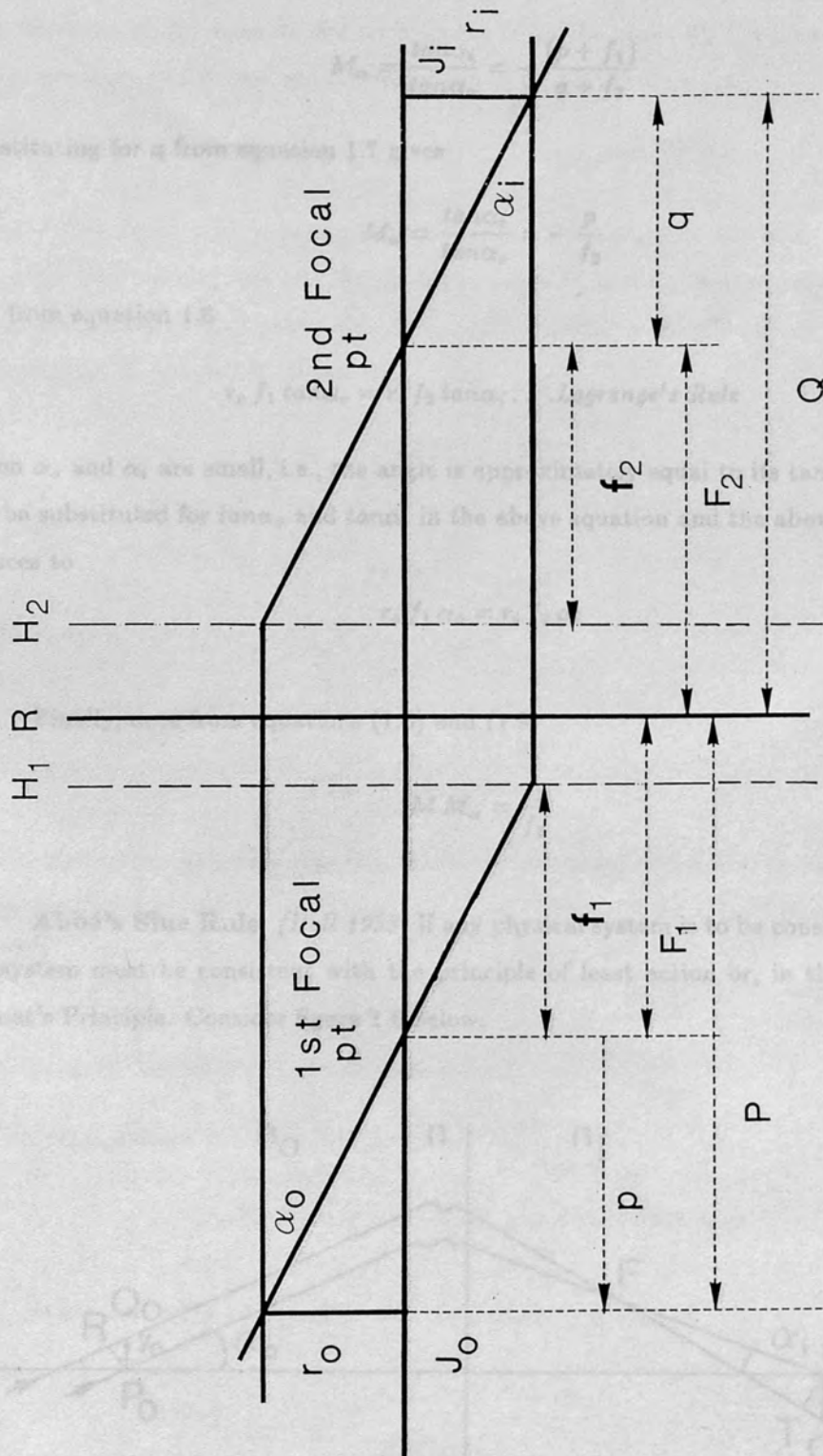


Figure 1.5

Lens
Figure 1.5 (from Hall 1958, figure 1.11)

The angular magnification $M_\alpha = \frac{\tan\alpha_i}{\tan\alpha_o}$, where α_o and α_i are the angles made with the axis at the object and image respectively. From figure 1.5 it can be seen that

$$M_\alpha = \frac{\tan\alpha_i}{\tan\alpha_o} = -\frac{(p+f_1)}{q+f_2}$$

Substituting for q from equation 1.7 gives

$$M_\alpha = \frac{\tan\alpha_i}{\tan\alpha_o} = -\frac{p}{f_2} \quad (1.9)$$

and from equation 1.6

$$r_o f_1 \tan\alpha_o = r_i f_2 \tan\alpha_i \dots \text{Lagrange's Rule} \quad (1.10)$$

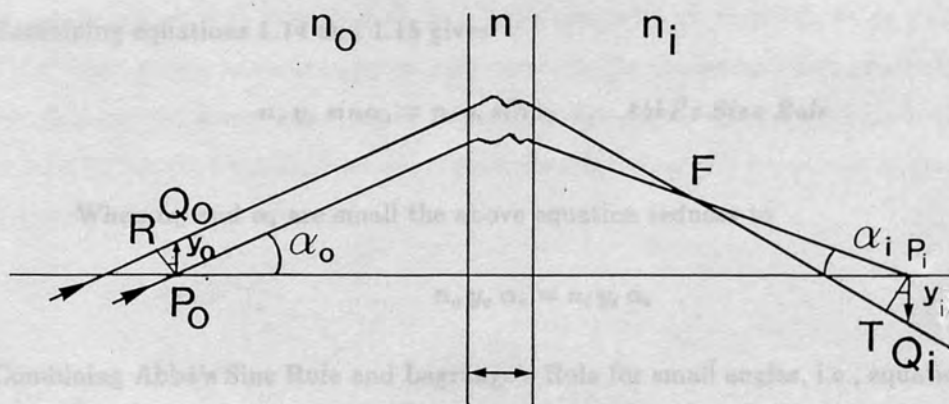
When α_o and α_i are small, i.e., the angle is approximately equal to its tangent, α_o and α_i can be substituted for $\tan\alpha_o$ and $\tan\alpha_i$ in the above equation and the above equation then reduces to

$$r_o f_1 \alpha_o = r_i f_2 \alpha_i \quad (1.11)$$

Finally, note from equations (1.6) and (1.9)

$$M M_\alpha = \frac{f_1}{f_2} \quad (1.12)$$

Abbé's Sine Rule (Hall 1953) If any physical system is to be considered as a lens, the system must be consistent with the principle of least action or, in the case of light, Fermat's Principle. Consider figure 1.6 below.



Lens

Figure 1.6 (from Hall 1953, figure 3.11)

Applying Fermat's principle to a small finite area imposes the condition that the path length from a point Q_o a small distance y_o from the axis, to a point Q_i a small distance y_i from the axis, is the same as the path length from the point P_o the normal projection of Q_o on the axis, and P_i the normal projection of Q_i on the axis. i.e.,

$$(Q_o F) + (F T) + (T Q_i) = (P_o F) + (F P_i) \quad (1.13)$$

where F (see figure 1.6), is located on the second focal plane of the lens, and is the point where the two parallel rays passing through points P_o and Q_o respectively will cross. The brackets indicate optical paths, i.e., index of refraction \times length. Since $P_i Q_i$ the angle subtended at F is small it follows that

$$(F P_i) \approx (F T)$$

and also

$$(T Q_i) = n_i y_i \sin \alpha_i$$

where n_i is the refractive index in image space.

Substituting the above two equations into equation 1.13 gives

$$(Q_o F) + n_i y_i \sin \alpha_i = (P_o F) \quad (1.14)$$

As F is located on the focal plane it is the image of a point at infinity. Since the paths from this point at infinity to R and P_o must be equal, $(R Q_o F)$ and $(P_o F)$ must also be equal, therefore

$$n_o y_o \sin \alpha_o + (Q_o F) = (P_o F) \quad (1.15)$$

where n_o is the refractive index of object space.

Combining equations 1.14 and 1.15 gives

$$n_o y_o \sin \alpha_o = n_i y_i \sin \alpha_i \dots \dots \text{Abbé's Sine Rule} \quad (1.16)$$

When α_o and α_i are small the above equation reduces to

$$n_o y_o \alpha_o = n_i y_i \alpha_i \quad (1.17)$$

Combining Abbé's Sine Rule and Lagrange's Rule for small angles, i.e., equations 1.11 and 1.17 gives

$$\frac{f_1}{f_2} = \frac{n_o}{n_i} \quad (1.18)$$

and from equation (1.5),

$$\frac{f_1}{f_2} = \sqrt{\frac{V_1}{V_2}} \quad (1.19)$$

Resolving Power : The Abbé Formula If a lens system is perfect in that it does not suffer from aberration effects, the resolving power is fixed by the wavelength of the radiation used and by the aperture of the system, i.e., the system is diffraction limited. The resolving power of such a system is given by the general formula due to Abbé, which states that

$$\rho = \frac{0.61 \lambda}{n \sin \alpha}$$

where λ is the wavelength of the radiation, n is the refractive index and α is the semi-angle subtended at the object by the objective lens of the system. In practice, the resolving power of any system incorporating electron lenses will be aberration limited. The theoretical limit of the resolving power of an electron microscope for example, is determined mainly by spherical aberration effects. An electron microscope with an accelerating voltage of 100 KeV will have a resolving power ρ of about 2Å.

This introductory chapter has thus far been mainly concerned with the optical analogy and the fundamental optical properties of electron lenses, very little has been said about the form of the electric and/or magnetic fields that make electron lenses possible. The next section will outline the fundamental rules and equations which determine the electric and magnetic fields which produce lens action.

1.4 LENS FIELDS AND RELATED LENS PROPERTIES

It has already been stated that both electric and magnetic fields can be used to obtain lens action in electron optics. However, as the the lenses being studied in this work are electrostatic lenses, most of the subsequent discussion will be concerned with this type of lens, although, for completeness, a short description of the properties of magnetic lenses has been included in this section.

A. The Electrostatic Lens†

Electron lenses are made from two or more elements separated by a small gap to which different voltages are applied. The equipotential lines at and near the gaps between the elements will be curved, as shown in figure 1.7, like the curved surface of a glass lens. These curved equipotentials cause the path of an electron to 'bend' just as the path of a light ray bends when it enters a glass lens, in fact, the curved equipotentials have all the properties of a lens with respect to electrons, a parallel beam of electrons will be focussed at a point F, and a beam of electrons diverging from a point O on the axis will be focussed at a point I on the axis.

The elements are typically metal cylinders or discs with a hole in the centre through which the electron beam passes. Two examples of simple electrostatic lenses are shown in figure 1.7.

Axially Symmetric Electric Fields and the Laplace Equation In general, rotationally symmetric fields are used to form electron lenses. The potential ϕ of a rotationally symmetric electrostatic field expressed in cylindrical coordinates (z, r, θ) , is a function of z and r only, i.e., it is independent of θ so $\phi = \phi(z, r)$. The dependence of ϕ on z and r is given by the Laplace equation which is

$$\frac{\partial^2 \phi}{\partial z^2} + \frac{\partial^2 \phi}{\partial r^2} + \frac{1}{r} \frac{\partial \phi}{\partial r} = 0 \quad (1.20)$$

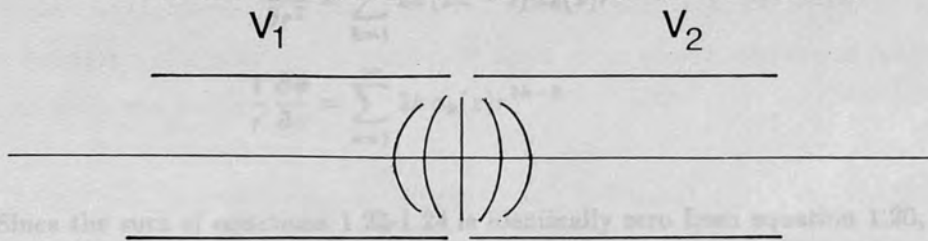
To determine the electric field in a given electron lens it is therefore necessary to solve the Laplace equation with boundary conditions determined by the geometry of the electron lens. It is generally not possible to do this analytically, only in geometrically simple cases and in the absence of space charge is an analytical solution possible, where the problem is essentially the same as the determination of the capacity of a given arrangement of conductors considered as a capacitor; parallel infinite planes, concentric spheres, an infinite cylinder, for example. For practical electrode configurations, numerical calculations or experimental measurements must be used to determine the distribution of the electric field.

The potential can be expanded around the z -axis into an even power series in r (Ximen Jiye 1986)

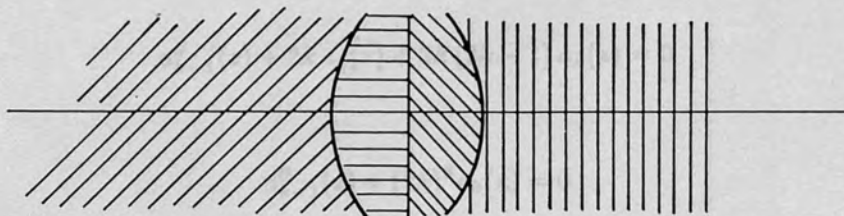
$$\phi(z, r) = \sum_{k=0}^{\infty} a_k(z) r^{2k} \quad k = 0, 1, 2, \dots \quad (1.21)$$

† References : See Bibliography, in particular Cosslett 1950, Grivet 1972, Hall 1953, Ximen Jiye 1986.

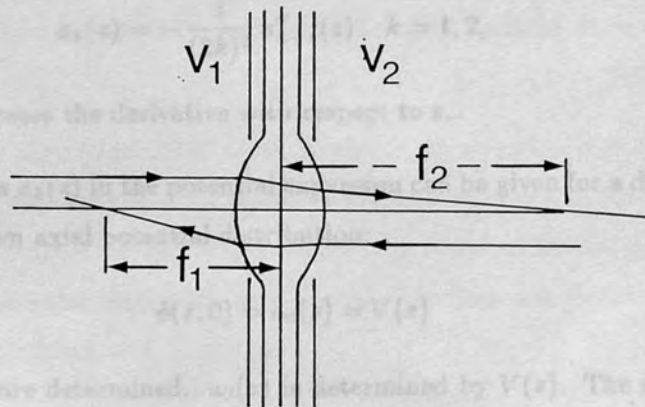
EXAMPLES OF ELECTRON LENSEES



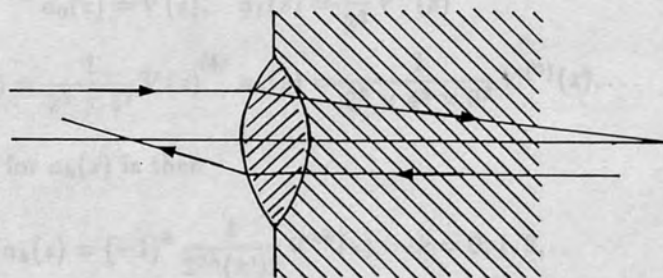
EQUAL DIAMETER TWO CYLINDER LENS



PHYSICAL EQUIVALENT



DOUBLE APERTURE LENS



PHYSICAL EQUIVALENT

Figure 1.7

$$\frac{\partial^2 \phi}{\partial z^2} = \sum_{k=0}^{\infty} a_k''(z) r^{2k} \quad (1.22)$$

$$\frac{\partial^2 \phi}{\partial r^2} = \sum_{k=1}^{\infty} 2k(2k-1) a_k(z) r^{2k-2} \quad (1.23)$$

$$\frac{1}{r} \frac{\partial \phi}{\partial r} = \sum_{k=1}^{\infty} 2k a_k(z) r^{2k-2} \quad (1.24)$$

Since the sum of equations 1.22-1.24 is identically zero from equation 1.20, the coefficients for all powers of r in the sum must be zero. Setting the coefficient of the general term r^{2k-2} to zero gives:

$$a_{k-1}''(z) + 2k a_k(z) + 2k(2k-1) a_k(z) = 0$$

implies

$$a_{k-1}''(z) + (2k)^2 a_k(z) = 0 \quad (1.25)$$

From the above equation the recursion formula can be obtained:

$$a_k(z) = -\frac{1}{(2k)^2} a_{k-1}''(z) \quad k = 1, 2, \dots \quad (1.26)$$

where the prime indicates the derivative with respect to z .

The coefficients $a_k(z)$ in the potential expansion can be given for a definite boundary condition. For a known axial potential distribution:

$$\phi(z, 0) = a_0(z) = V(z) \quad (1.27)$$

all coefficients $a_k(z)$ are determined. $a_0(z)$ is determined by $V(z)$. The remaining coefficients a_k are then given by the recursion formula equation 1.26:

$$a_0(z) = V(z), \quad a_1(z) = -\frac{1}{2^2} V''(z)$$

$$a_2(z) = \frac{1}{2^2 \times 4^2} V^{(4)}(z), \quad a_3(z) = -\frac{1}{2^2 \times 4^2 \times 6^2} V^{(6)}(z), \dots$$

The general equation for $a_k(z)$ is then

$$a_k(z) = (-1)^k \frac{1}{2^{2k} (k!)^2} V^{(2k)}(z), \quad k = 0, 1, 2, \dots \quad (1.28)$$

Substituting this into equation 1.21 gives

$$\phi(z, r) = \sum_{k=0}^{\infty} (-1)^k \frac{1}{(k!)^2} \left(\frac{r}{2}\right)^{2k} V^{(2k)}(z), \quad k = 0, 1, 2, \dots \quad (1.29)$$

Knowing the axial potential distribution allows rotationally symmetric electric fields to be expressed in a power series.

When the Gaussian dioptrics of an electron optical system are to be investigated, the first two terms of equation 1.29 suffice. If third order aberrations are of interest, the third term must also be included:

$$\phi(z, r) = V(z) - \frac{1}{4} V''(z) r^2 + \frac{1}{64} V^{(4)}(z) r^4 - \dots \quad (1.30)$$

The components of the electric field can be deduced from equation 1.30:

$$E_r(z, r) = -\frac{\partial \phi}{\partial r} = \frac{1}{2} V''(z) r - \frac{1}{16} V^{(4)}(z) r^3 + \dots,$$

$$E_z(z, r) = -\frac{\partial \phi}{\partial z} = -V'(z) + \frac{1}{4} V^{(3)}(z) r^2 - \dots \quad (1.31)$$

$$E_\theta = -\frac{1}{r} \frac{\partial \phi}{\partial \theta} = 0$$

Thus in the rotationally symmetric electric field, E_r is odd in r and E_z is even in r .

Paraxial-Ray Equation (Hall 1953) To obtain the equation of motion of an axially symmetrical field, it is assumed that the potential is constant except in the region $0 < z < l$. The problem then reduces to finding the differential equation for the rays in the region $0 < z < l$, as outside this region the rays are straight lines, see figure 1.8. There is no restriction in this assumption as l is arbitrary.

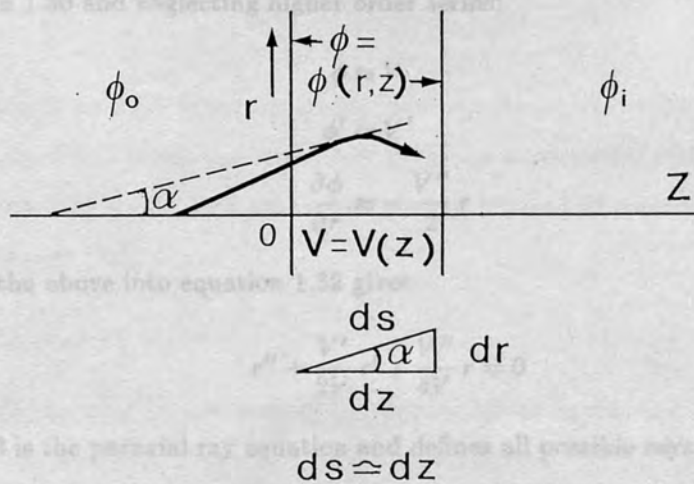


Figure 1.8 (adapted from Hall 1953, figure 4.3)

Certain assumptions are made which are similar to those used in first order lens theory in light optics:

- (1) The discussion is confined to meridional rays, i.e., rays in planes containing the axis.
- (2) r is assumed to be small (i.e., the rays are paraxial) and it is assumed that high powers of r can be neglected.
- (3) The angle $\alpha = \tan^{-1} r'$ which rays make with the axis is so small that $\tan \alpha \approx \alpha$, where r' is the differential of r with respect to z . [This approximation is equivalent to neglecting terms containing powers of α equal to 3 and greater with respect to α , since $\tan \alpha = \alpha + (\frac{\alpha^3}{3}) + (\frac{2\alpha^5}{15}) + \dots$] It follows that if ds is an element of the trajectory, $ds \approx dz$.

Applying Newton's second law, the rate of change of momentum is equal to the force acting, i.e.,

$$\frac{d}{dt} (m \dot{r}) = e \frac{\partial \phi}{\partial r}$$

where \dot{r} indicates differentiation with respect to time. Substituting $\dot{r} = \frac{dr}{dz} \dot{z} = r' \sqrt{\frac{2e\phi}{m}}$, (from $\dot{z} \approx v = \sqrt{\frac{2e\phi}{m}}$) and $\frac{d}{dt} = \dot{z} \frac{d}{dz}$, implies

$$\sqrt{\frac{2e\phi}{m}} \frac{d}{dz} \left(r' \sqrt{\frac{2e\phi}{m}} \right) = \frac{e}{m} \frac{\partial \phi}{\partial r} \quad (1.31)$$

and finally

$$r'' + \frac{\phi' r'}{2\phi} - \frac{1}{2\phi} \frac{\partial \phi}{\partial r} = 0 \quad (1.32)$$

From equation 1.30 and neglecting higher order terms:

$$\phi \approx V$$

$$\phi' \approx V'$$

$$\frac{\partial \phi}{\partial r} \approx -\frac{V''}{2} r$$

Substituting the above into equation 1.32 gives

$$r'' + \frac{V'}{2V} r' + \frac{V''}{4V} r = 0 \quad (1.33)$$

Equation 1.33 is the paraxial ray equation and defines all possible rays near the axis of any axially symmetrical electrostatic field. The solutions of this equation, r as a function of z , are the equations of possible trajectories in the region $0 < z < l$.

The Reduced or Picht Equation It is often convenient to express the paraxial-ray equation in a simpler form by introducing a new variable R through the substitution

$$R = r \phi^{\frac{1}{2}} \quad (1.34)$$

The curve $R(z)$ is referred to as a reduced ray. With the substitution, the reduced paraxial-ray equation is obtained, i.e.,

$$R'' + \frac{3}{16} \left(\frac{V'}{V} \right)^2 R = 0 \quad (1.35)$$

Note that this equation has no R' term. This equation also displays an interesting feature in that it possesses a single expression characteristic of the lens. All the paraxial properties of the lens are determined by the characteristic function

$$T(z) = \frac{V'}{V} \quad (1.36)$$

General Solution of the Paraxial-Ray Equation (Hall 1953) The paraxial-ray equation is a linear differential equation of the second order and therefore must have two linearly independent solutions $r_1 = f_1(z)$ and $r_2 = f_2(z)$. The general solution is therefore

$$r = c_1 f_1(z) + c_2 f_2(z) \quad (1.37)$$

where c_1 and c_2 are arbitrary constants to be determined by two boundary conditions, i.e., for $z = 0$, (1) $r = r_0$ and (2) $r' = r'_0$. Applying the first condition gives

$$r_0 = c_1 f_1(0) + c_2 f_2(0)$$

If c_1 and c_2 are to be kept arbitrary (independent), either $f_1(0)$ must equal zero or $f_2(0)$ must equal zero. If this is not the case, there would be a numerical relation between c_1 and c_2 , and equation 1.37 would be a particular solution instead of a general solution. If $f_2(0)$ is chosen to be zero then:

$$c_1 = \frac{r_0}{f_1(0)}$$

Similarly, c_2 may be determined by differentiating equation 1.37 with respect to z and applying the condition that $r' = r'_0$ when $z = 0$. Thus

$$r'_0 = c_1 f'_1(0) + c_2 f'_2(0)$$

Here again either $f_1'(0) = 0$ or $f_2'(0) = 0$. Otherwise there is a numerical relation between c_1 and c_2 . But $f_2'(0)$ cannot be zero because if it were, c_2 would be indeterminate. Therefore, f_1 must be zero and

$$c_2 = \frac{r'_0}{f_2(0)}$$

Therefore, the general solution is

$$r = r_0 \frac{f_1(z)}{f_1(0)} + r'_0 \frac{f_2(z)}{f_2(0)} \quad (1.38)$$

or

$$r = r_0 P(z) + r'_0 Q(z) \quad (1.39)$$

where $P(z)$ and $Q(z)$ are functions of z only.

Lens Action (Hall 1953) It may be shown that to the order of approximation used to derive the paraxial-ray equation, any axially symmetrical electrostatic field has the properties of an ideal lens. Referring to figure 1.9 below, take through any point A on an object a ray 1 parallel to the axis and another arbitrary ray 2 with a slope r'_0 . For z greater than zero the general solution of the paraxial ray equation becomes:

$$\text{For ray 1 : } r = yP(z)$$

$$\text{For ray 2 : } r = (y + r'_0 z_0)P(z) + r'_0 Q(z)$$

The point A_i where the two rays cross on the image is located from the condition that r is the same, (i.e., $r = y_i$) for both rays at this point.

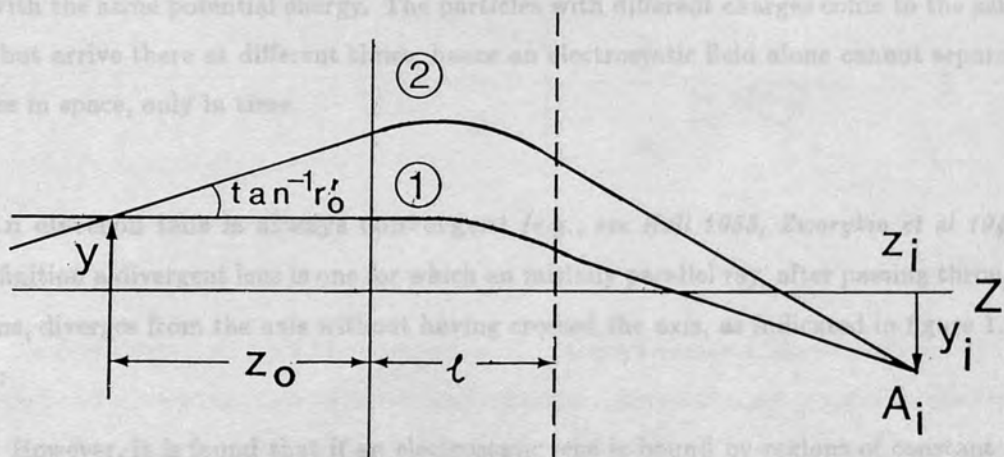


Figure 1.9 (from Hall 1953, figure 4.4)

Therefore, equating the right-hand sides of the above two equations

$$yP(z_i) = (y + r'_0 z_0)P(z_i) + r'_0 Q(z_i)$$

which becomes

$$z_0 P(z_i) + Q(z_i) = 0$$

Note that r'_0 has divided out, therefore, the above equation states that z_i is independent of the arbitrary ray 2. This means that all rays through a point A regardless of their slope, reunite at the same point on the image. Note also that z_i is independent of y . The following conclusions can be drawn:

- (1) All rays leaving A will converge at A_i
- (2) z_i is independent of y for all points A . Therefore, the image of a plane perpendicular to the axis at z_0 is a plane perpendicular to the axis at z_i .
- (3) The lateral magnification $y_i/y = P(z_i)$ depends only on z_i and is therefore a constant throughout any pair of conjugate planes perpendicular to the axis.

These three conditions are sufficient to specify an ideal lens, therefore, it has been shown that any axially symmetrical field has the properties of an ideal lens to the order of approximation used for the derivation of the paraxial-ray equation.

Consequences of the Paraxial-Ray Equation on the Properties of the Electrostatic Lens

(1) **The paraxial equation is independent of $\frac{e}{m}$** The ratio $\frac{e}{m}$ does not appear in the paraxial equation, so the path is the same for any charged particle, provided it enters the field with the same potential energy. The particles with different charges come to the same focus but arrive there at different times, hence an electrostatic field alone cannot separate charges in space, only in time.

(2) **An electron lens is always convergent** (*e.g.*, see Hall 1953, Zworykin et al 1945) By definition a divergent lens is one for which an initially parallel ray, after passing through the lens, diverges from the axis without having crossed the axis, as indicated in figure 1.10 below:

However, it is found that if an electrostatic lens is bound by regions of constant V , i.e., $V'_0 = V'_i = 0$, the lens is always convergent. This can be illustrated if the reduced

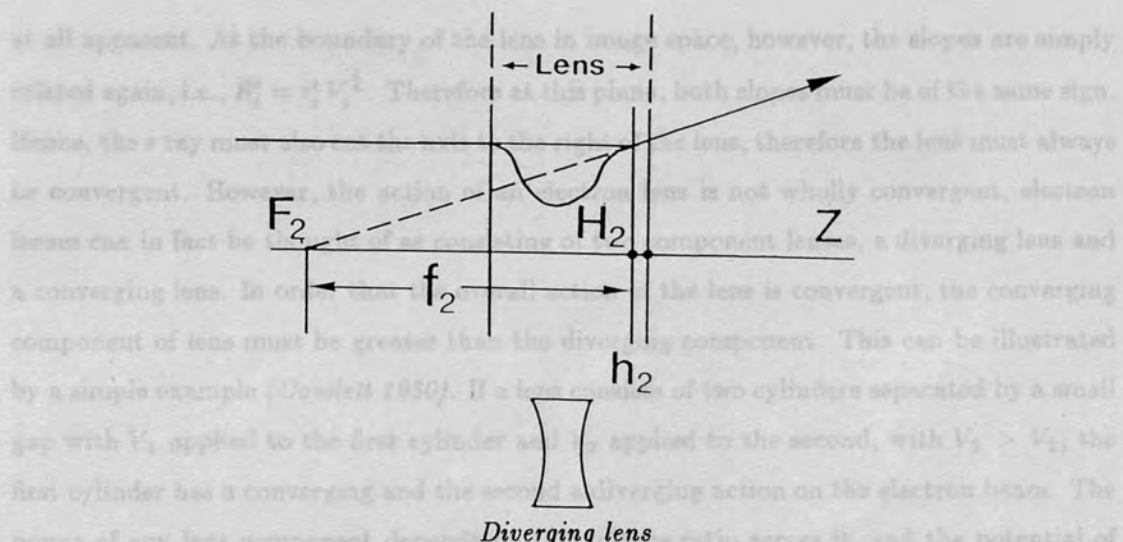


Figure 1.10 (from Hall 1953, figure 4.8)

equation is rewritten as

$$R'' = -\frac{3}{16} \left(\frac{V'}{V}\right)^2 R$$

It can be seen that R'' is always negative when R is positive because of the square term. In regions where $R = \text{constant}$, $R' = r' V_{\text{constant}}^{\frac{1}{4}}$, and therefore when $r' = 0$ in such regions, R' is also zero.

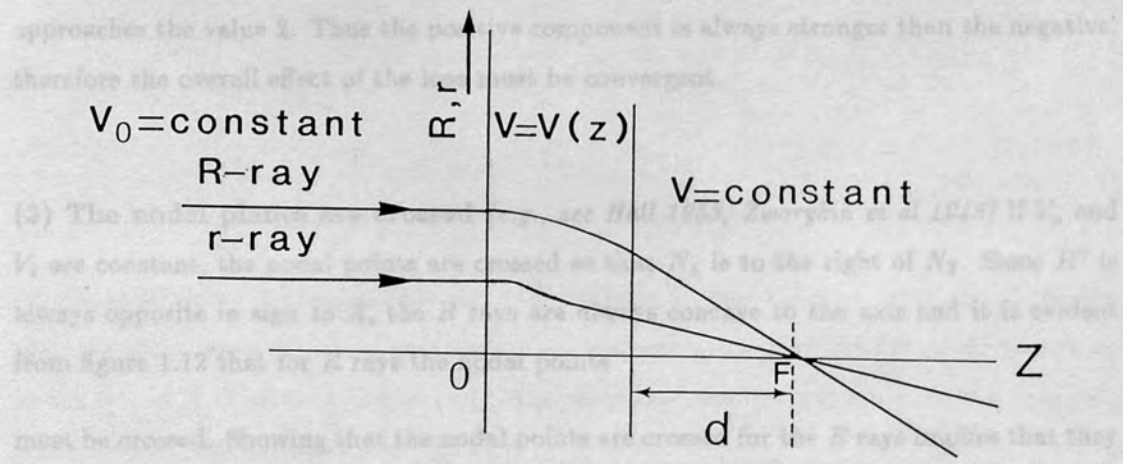


Figure 1.11 (adapted from Hall 1953, figure 4.9)

As illustrated in figure 1.11 above, since R'' is always negative, the initially parallel R ray must be concave to the axis as drawn and must cut the axis at some point F to the right of the lens. For R rays the lens is obviously always convergent. But the corresponding r ray must always be parallel to the axis in object space, though its slope within the lens is not

at all apparent. At the boundary of the lens in image space, however, the slopes are simply related again, i.e., $R'_i = r'_i V_i^{\frac{1}{4}}$. Therefore at this plane, both slopes must be of the same sign. Hence, the r ray must also cut the axis to the right of the lens, therefore the lens must always be convergent. However, the action of an electron lens is not wholly convergent, electron lenses can in fact be thought of as consisting of two component lenses, a diverging lens and a converging lens. In order that the overall action of the lens is convergent, the converging component of lens must be greater than the diverging component. This can be illustrated by a simple example (Cosslett 1950). If a lens consists of two cylinders separated by a small gap with V_1 applied to the first cylinder and V_2 applied to the second, with $V_2 > V_1$, the first cylinder has a converging and the second a diverging action on the electron beam. The power of any lens component depends on the voltage ratio across it, and the potential of the mid-plane is $V_M = \frac{1}{2}(V_1 + V_2)$. Hence the power of the positive semi-lens depends on the ratio

$$\frac{V_M}{V_1} = \frac{(V_1 + V_2)}{2V_1}$$

and that of the succeeding negative semi-lens on the ratio

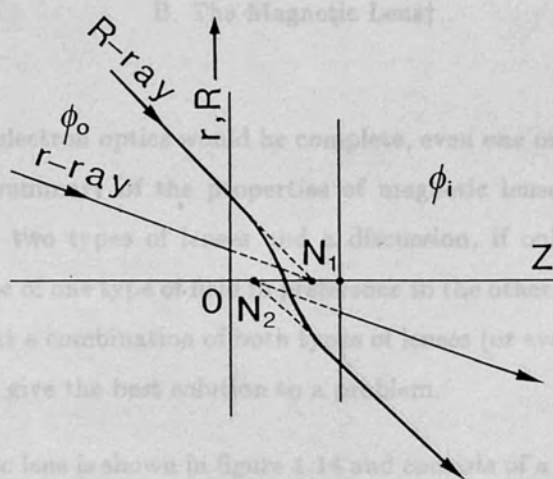
$$\frac{V_2}{V_M} = \frac{2V_2}{(V_1 + V_2)}$$

It can be seen that as the voltage ratio is increased, $\frac{V_M}{V_1}$ increases without limit, whereas $\frac{V_2}{V_M}$ approaches the value 2. Thus the positive component is always stronger than the negative, therefore the overall effect of the lens must be convergent.

(3) The nodal planes are crossed (e.g., see Hall 1953, Zworykin et al 1945) If V_o and V_i are constant, the nodal points are crossed so that N_1 is to the right of N_2 . Since R'' is always opposite in sign to R , the R rays are always concave to the axis and it is evident from figure 1.12 that for R rays the nodal points

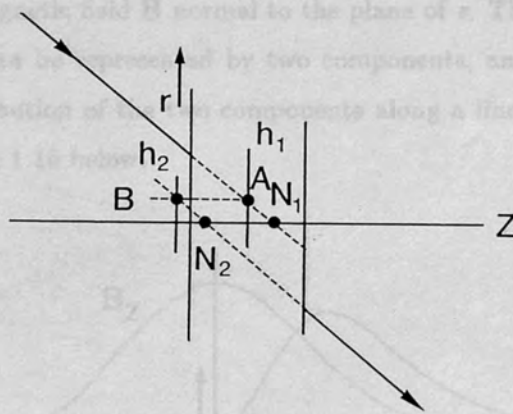
must be crossed. Showing that the nodal points are crossed for the R rays implies that they are also crossed for the r rays, as the nodal points must be the same for both the R and the r rays, as both types of ray converge to or diverge from the same points on the axis.

(4) The principal planes are crossed (e.g., see Hall 1953, Zworykin et al 1945) Consider a ray aimed at N_1 and emergent parallel to itself and therefore diverging from N_2 as shown in figure 1.13.



Crossed Nodal Points

Figure 1.12 (from Hall 1953, figure 4.10)



Crossed Principal Planes

Figure 1.13 (from Hall 1953, figure 4.11)

At whatever point A the incident ray or its extension cuts the first principal plane, the corresponding point of unit magnification on the second part of the ray must always be to the left of A. Therefore the second principal plane must be 'behind' the first principal plane, so the principal planes are crossed.

B. The Magnetic Lens†

No discussion on electron optics would be complete, even one on electrostatic lenses, without at the least a summary of the properties of magnetic lenses, thus allowing for some comparison of the two types of lenses and a discussion, if only superficial, of the appropriateness of the use of one type of field in preference to the other, in a given situation. It may even be found that a combination of both types of lenses (or even both types of field in the same lens), would give the best solution to a problem.

A typical magnetic lens is shown in figure 1.14 and consists of a short coil fitted with an iron shield with a narrow gap; the gap has the effect of concentrating the field into a small region.

The field of the lens of figure 1.14 is symmetrical about the z -axis and therefore there is no component of the magnetic field \mathbf{B} normal to the plane of z . This means that at any point the magnetic field can be represented by two components, an axial one B_z , and a radial one, B_r . The distribution of the two components along a line parallel and near to the axis is plotted in figure 1.15 below.

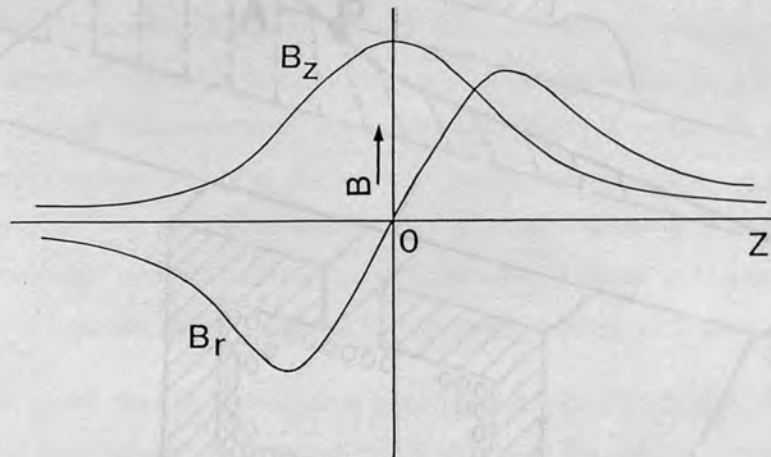
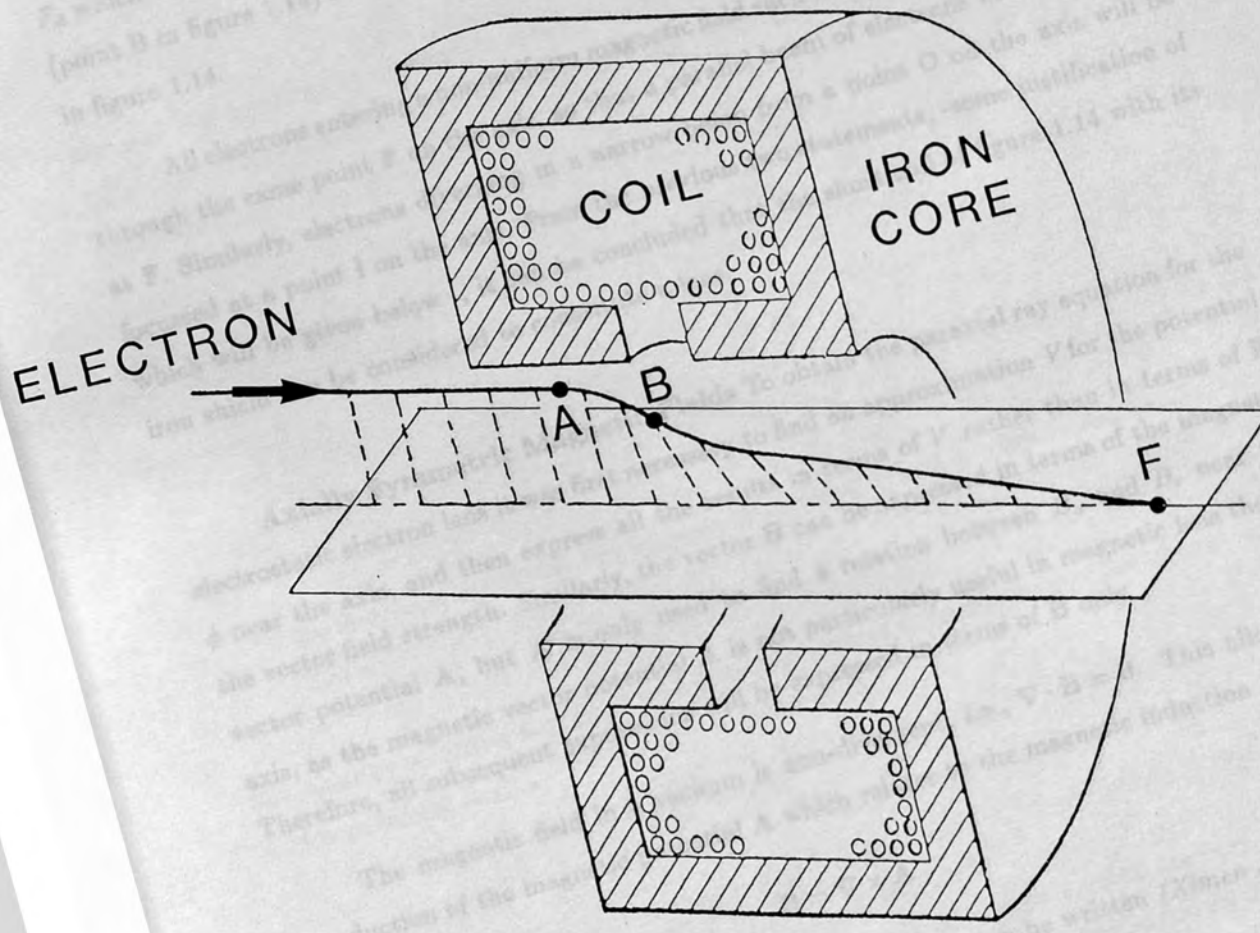


Figure 1.15 (from Hall 1953, figure 5.2)

As an electron enters the field of the lens of figure 1.14, (point A) parallel to the axis, it encounters no force due to B_z as the electron is moving parallel to it, but it will encounter a relatively strong radial component B_r . An application of the left-hand rule

† References : Grivet 1972, Hall 1953, Ximen Jiye 1986, Pierce 1954.

forces that B_z will produce a force in a direction mutually perpendicular to the direction of the electron and B , i.e., a force directed out of the figure and towards us will act on the electron. This force F_y (see figure 1.14) accelerates the electron giving it a sideways velocity v_y , which increases as the electron approaches the mid-plane of the field (point O of figure 1.15). As shown in figure 1.15 beyond the mid-plane B_z reverses, and this gradually reduces the sideways velocity of the electron until it again becomes zero when the electron emerges from the lens. Because the sideways velocity v_y is perpendicular to the axial component of the field B_z , a second application of the left-hand rule shows that B_z will produce a force F_x which will act on the electron, urging it towards the axis with an increasing velocity v_x (point B in figure 1.14) so that the electron eventually crosses the axis at point F as shown in figure 1.14.



A Magnetic Lens

Figure 1.14 (adapted from Pierce 1954, figure 6.9)

shows that B_z will produce a force in a direction mutually perpendicular to the direction of the electron and B_r i.e., a force directed out of the figure and towards us will act on the electron. This force F_s , (see figure 1.14) accelerates the electron giving it a sideways velocity v_s , which increases as the electron approaches the mid-plane of the field (point O of figure 1.15). As shown in figure 1.15 beyond the mid-plane B_r reverses, and this gradually reduces the sideways velocity of the electron until it again becomes zero when the electron emerges from the lens. Because the sideways velocity v_s is perpendicular to the axial component of the field B_z , a second application of the left-hand rule shows that B_z will produce a force F_d which will act on the electron, urging it towards the axis with an increasing velocity v_d , (point B in figure 1.14) so that the electron eventually crosses the axis at point F as shown in figure 1.14.

All electrons entering a non-uniform magnetic field such as that of figure 1.14 will pass through the same point F on the axis, so that a parallel beam of electrons will be focussed at F. Similarly, electrons diverging in a narrow beam from a point O on the axis will be focussed at a point I on the axis. From the previous two statements, -some justification of which will be given below -, it can be concluded that the short coil of figure 1.14 with its iron shield can be considered to constitute a lens.

Axially Symmetric Magnetic Fields To obtain the paraxial ray equation for the electrostatic electron lens it was first necessary to find an approximation V for the potential ϕ near the axis, and then express all the results in terms of V rather than in terms of \mathbf{E} the vector field strength. Similarly, the vector \mathbf{B} can be expressed in terms of the magnetic vector potential \mathbf{A} , but \mathbf{A} is only used to find a relation between B_z and B_r near the axis, as the magnetic vector potential \mathbf{A} is not particularly useful in magnetic lens theory. Therefore, all subsequent expressions will be expressed in terms of \mathbf{B} only.

The magnetic field in a vacuum is non-divergent, i.e., $\nabla \cdot \mathbf{B} = 0$. This allows the introduction of the magnetic potential \mathbf{A} which relates to the magnetic induction \mathbf{B} :

$$\mathbf{B} = \nabla \times \mathbf{A}$$

In cylindrical coordinates (z, r, θ) , the above equation can be written (Ximen Jiye 1986) :

$$\begin{aligned} B_z &= \frac{1}{r} \left(\frac{\partial(r A_\theta)}{\partial r} - \frac{\partial A_r}{\partial \theta} \right) \\ B_r &= \frac{1}{r} \left(\frac{\partial(A_z)}{\partial \theta} - \frac{\partial(r A_\theta)}{\partial z} \right) \end{aligned} \quad (1.40)$$

$$B_\theta = \frac{\partial A_r}{\partial z} - \frac{\partial A_z}{\partial r}$$

The rotationally symmetric magnetic vector potential \mathbf{A} is a function of z and r only and is independent of θ , i.e.,

$$\frac{\partial A_r}{\partial \theta} = \frac{\partial A_z}{\partial \theta} = \frac{\partial A_\theta}{\partial \theta} = 0$$

Equation 1.40 then gives

$$B_z = \frac{1}{r} \frac{\partial(r A_\theta)}{\partial r} \quad (1.40)$$

$$B_r = -\frac{1}{r} \frac{\partial(r A_\theta)}{\partial z}$$

$$B_\theta = \frac{\partial A_r}{\partial z} - \frac{\partial A_z}{\partial r}$$

Because the rotationally symmetric magnetic field is generated by currents flowing in circular conductors about the axis of symmetry, the vector potential has only an azimuthal component A_θ , i.e.,

$$A_\theta = A(z, r) \equiv A, \quad A_r = A_z = 0$$

So finally:

$$B_z = \frac{1}{r} \frac{\partial(r A)}{\partial r} \quad (1.41)$$

$$B_r = -\frac{1}{r} \frac{\partial(r A)}{\partial z}$$

$$B_\theta = 0 \quad (1.41)$$

Furthermore, in current free regions, the magnetic field is irrotational, i.e.,

$$\nabla \times \mathbf{B} = \mathbf{0} \quad (1.42)$$

Substituting equation 1.41 into 1.42 gives the partial differential equation obeyed by the vector potential \mathbf{A} i.e.,

$$\frac{\partial^2(r A)}{\partial z^2} + r \frac{\partial}{\partial r} \left(\frac{1}{r} \frac{\partial(r A)}{\partial r} \right) = 0$$

or

$$\frac{\partial^2 A}{\partial z^2} + \frac{\partial^2 A}{\partial r^2} + \frac{1}{r} \frac{\partial A}{\partial r} - \frac{A}{r^2} = 0 \quad (1.43)$$

Using the above equation, and following the same procedure used in the case of the rotationally symmetric electric field, the spatial magnetic vector potential can be expanded into the following series:

$$A(z, r) = \sum_{k=0}^{\infty} (-1)^k \frac{1}{(k!)(k+1)!} \left(\frac{r}{2}\right)^{2k+1} B^{(2k)}(z) \quad k = 0, 1, 2, \dots \quad (1.44)$$

From equation 1.41, the components of magnetic induction are

$$\begin{aligned}
 B_z(z, r) &= \sum_{k=0}^{\infty} (-1)^k \frac{1}{(k!)^2} \left(\frac{r}{2}\right)^{2k} B^{(2k)}(z) \\
 B_r(z, r) &= \sum_{k=0}^{\infty} (-1)^{k+1} \frac{1}{(k!)(k+1)!} \left(\frac{r}{2}\right)^{2k+1} B^{(2k+1)}(z) \\
 B_\theta &= 0
 \end{aligned}
 \tag{1.45}$$

where $B(z) = B_z(z, 0)$ is the axial distribution of the magnetic induction. Hence, it is possible to obtain, by using the axial magnetic induction distribution, the spatial distribution of the vector potential \mathbf{A} or magnetic induction \mathbf{B} of the rotationally symmetric field expressed in a power series. Thus equations 1.44 and 1.45 are the basic formula of the rotationally symmetric magnetic field.

Again, for the study of Gaussian dioptrics and aberrations, only the first two terms of the above two equations are required, i.e.,

$$\begin{aligned}
 A(z, r) &= \frac{1}{2} B(z) r - \frac{1}{16} B''(z) r^3 + \dots \\
 B_z(z, r) &= B(z) - \frac{1}{4} B''(z) r^2 + \dots \\
 B_r(z, r) &= -\frac{1}{2} B'(z) r + \frac{1}{16} B^{(3)}(z) r^3 - \dots
 \end{aligned}
 \tag{1.46}$$

Thus for rotationally symmetric magnetic fields, B_z is even in r and B_r is odd in r .

Paraxial-Ray Equation (Hall 1953) The force \mathbf{F} on an electron moving with a velocity \mathbf{v} in a magnetic field of strength \mathbf{B} is given by the equation

$$\mathbf{F} = -e\mathbf{v} \times \mathbf{B}
 \tag{1.47}$$

The magnitude of \mathbf{F} is

$$F = Bev \sin\chi$$

where χ is the angle between \mathbf{B} and \mathbf{v} . Since the force is always at right angles to the velocity and to \mathbf{B} , the velocity changes in direction but not in magnitude.

In cylindrical coordinates r, θ, z for a field of axial symmetry, equation (1.47) may be written as the determinant of a matrix,

$$\begin{vmatrix}
 \dot{r} & \dot{\theta} & \dot{z} \\
 -e\dot{r} & -e\dot{\theta} & -e\dot{z} \\
 B_r & 0 & B_z
 \end{vmatrix}
 \tag{1.48}$$

where i_r, i_θ, i_z are unit vectors as shown in figure 1.16 below

Then, from equation 1.48

$$F_r = -er\dot{\theta}B_z$$

$$F_\theta = -e\dot{z}B_r + e\dot{r}B_z$$

Substituting F_r into Newton's second law in the r direction i.e, $F_r = \frac{d}{dt}mv_r$ gives

$$m\frac{d}{dt}\dot{r} = -er\dot{\theta}B_z + m\dot{\theta}^2r \quad (1.49)$$

In the θ direction, equating the rate of change of angular momentum to the moments of the forces acting (i.e., $F_\theta r$), gives

$$\frac{d}{dt}(mr^2\dot{\theta}) = -e\dot{z}B_r r + e\dot{r}B_z r$$

Substituting $-\frac{r}{2}\frac{\partial B_z}{\partial z} \approx B_r$ deduced from equation 1.46 for B_r in the above equation, gives

$$mr^2\dot{\theta} = \frac{er^2B_z}{2} + a \text{ constant} \quad (1.50)$$

It is useful to eliminate the time from the equations of motion and obtain equations locating rays in space. Using the approximation that

$$\dot{z} \approx v = \sqrt{\frac{2eV}{m}}$$

giving

$$\dot{\theta} = \theta'\dot{z} = \theta'\sqrt{\frac{2eV}{m}}$$

allows the time dependence in equation 1.50 to be eliminated, and equation 1.50 becomes

$$\theta' = \sqrt{\frac{e}{8mV}}B_z + \frac{C}{r^2} \quad (1.51)$$

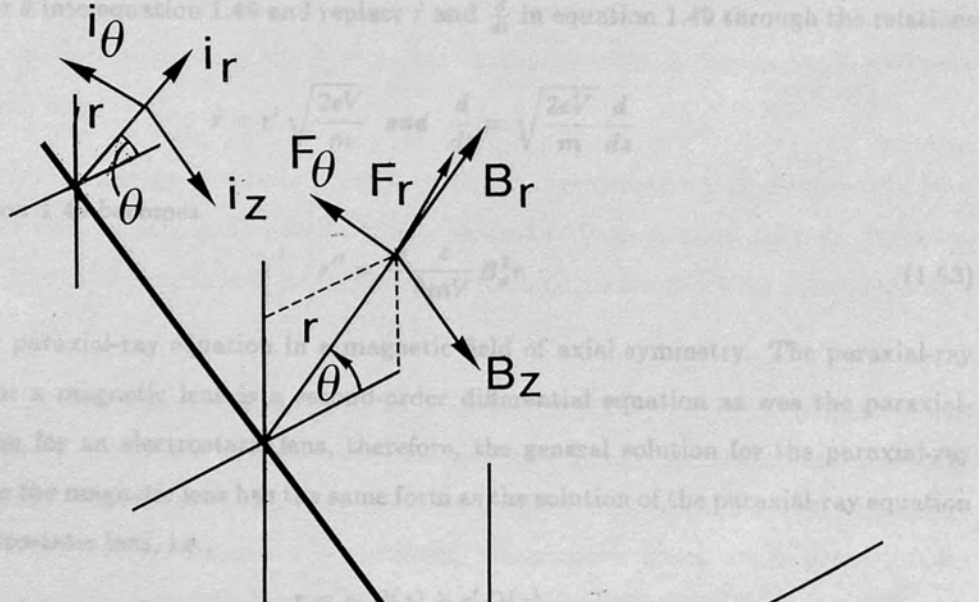
The integration constant C in the above equation is not zero for all rays, and it is not possible in general, to do any further integration, without a relation between r and z . C is zero however, for all rays such that $\theta' = 0$ when $B_z = 0$. These are rays contained in meridional planes in any region where $B_z = 0$, for example, before they enter the lens field. Therefore, confining the discussion to meridional rays, C can be assumed to be zero.

When C is zero, integrating equation 1.51 yields

$$\theta = \sqrt{\frac{e}{8mV}} \int_{z_1}^{z_2} B_z dz \quad (1.52)$$

Rays passing through the lens are turned through an angle which does not depend on the distance of the rays from the axis. All electrons in a given meridional plane before entering the field are contained in a rotating meridional plane as they pass through the lens, and they leave the lens convergent.

Equating the constant in equation 1.50 to zero, and substituting the resultant expression for $\dot{\theta}$ in equation 1.49 and replacing \dot{r} and $\frac{d}{dt}$ in equation 1.49 through the relations



This is the paraxial-ray equation for a magnetic lens. It is identical to the paraxial-ray equation for an electrostatic lens, therefore, the general solution for the paraxial-ray equation for the magnetic lens has the same form as the solution of the paraxial-ray equation for an electrostatic lens, i.e.,

The form of equation 1.53 is identical to the form of the ray equation (in B) for the electrostatic lens, therefore conclusions drawn on the optics of the electrostatic lens with respect to the ray equation for the magnetic lens, can be adopted for the magnetic lens without proof and are listed below.

- (1) Any axially symmetric field has the properties of an ideal lens to the approximations made in deriving the paraxial-ray equation.
- (2) Magnetic lenses are always convergent. Since r'' is always negative for positive r , this conclusion holds whether the object is in the magnetic field or not.
- (3) In the absence of electrostatic fields, the refractive index is the same in object and image space, and therefore $f_1 = f_2$. The nodal points coincide with the principal points.
- (4) The nodal points are crossed.
- (5) r'' is dependent on the magnitude of B_z . Therefore the focusing properties depend on B_z .

Figure 1.16 (from Hall 1953, figure 5.5)

Rays passing through the lens are turned through an angle which does not depend on the distance of the rays from the axis. All electrons in a given meridional plane before entering the field are contained in a rotating meridional plane as they pass through the lens, and they leave the lens coplanar.

Equating the constant in equation 1.50 to zero, and substituting the resultant expression for $\dot{\theta}$ into equation 1.49 and replace \dot{r} and $\frac{d}{dt}$ in equation 1.49 through the relations

$$\dot{r} = r' \sqrt{\frac{2eV}{m}} \quad \text{and} \quad \frac{d}{dt} = \sqrt{\frac{2eV}{m}} \frac{d}{dz}$$

and equation 1.49 becomes

$$r'' = -\frac{e}{8mV} B_z^2 r \quad (1.53)$$

This is the paraxial-ray equation in a magnetic field of axial symmetry. The paraxial-ray equation for a magnetic lens is a second-order differential equation as was the paraxial-ray equation for an electrostatic lens, therefore, the general solution for the paraxial-ray equation for the magnetic lens has the same form as the solution of the paraxial-ray equation for an electrostatic lens, i.e.,

$$r = r_0 P(z) + r'_0 Q(z)$$

The form of equation 1.53 is identical to the form of the reduced paraxial-ray equation (in R) for the electrostatic lens, therefore conclusions reached on the optics of the electrostatic lens with respect to the reduced equation for the electrostatic lens, can be adopted for the magnetic lens without proof and are listed below.

- (1) Any axially symmetrical field has the properties of an ideal lens to the approximations made in deriving the paraxial-ray equation.
- (2) Magnetic lenses are always convergent. Since r'' is always negative for positive r , this conclusion holds whether the object is in the magnetic field or not.
- (3) In the absence of electrostatic fields, the refractive index is the same in object and image space, and therefore $f_1 = f_2$. The nodal points coincide with the principal points.
- (4) The nodal points are crossed.
- (5) r'' is dependent on the magnitude of $\frac{e}{m}$. Therefore the focussing properties depend on $\frac{e}{m}$. The cardinal points will in general be different for different $\frac{e}{m}$.

Comparison of Electrostatic and Magnetic Lenses

BIBLIOGRAPHY

The ratio $\frac{e}{m}$ does not appear in the paraxial ray equation for the electrostatic lens, however, it does appear in the paraxial equation for the magnetic lens. This means that any charged particles of the same sign, which enter an electrostatic lens with the same kinetic energy, will follow the same path. Particles with different charges come to the same focus but arrive there at different times, therefore, they are separated in time, but not in space. Because of this independence of the $\frac{e}{m}$ ratio, the electrostatic lens is favoured to focus heavy particles, i.e., ions.

The kinetic energy of a particle can be changed considerably by an electrostatic lens, particles can even be reflected; a fact which is utilised to form electron mirrors. However, the kinetic energy of a particle in a magnetic lens remains unchanged after passing through a magnetic lens.

The above two paragraphs can be summarised by simply stating that electrostatic lenses are energy dispersive devices, whereas magnetic lenses are momentum dispersive devices and the choice of lens in a given situation will reflect which type of device, i.e., energy dispersive or momentum dispersive is preferred. Electrostatic lenses are in general easier to manufacture than magnetic lenses. However, it is very difficult to build a satisfactory electrostatic lens to act as an objective lens for an electron microscope, as a very high voltage lens with a very short focal length is required, therefore electrostatic lenses are rarely found in the imaging lens system of a high voltage electron microscope, but are confined to the electron gun part of the instrument.

Jacob L 1950 *An Introduction to Electron Optics* (Butterworths - London)

Wimperley D 1983 *Electron Optics 2nd Edition* (Cambridge University Press - England)

Wimperley D and Barbeta M B 1971 *Electron Optics 3rd Edition* (Cambridge University Press - England)

Lawson J D 1977 *The Physics of Charged Particle Beams* (Oxford University Press - England)

Hagena L M 1970 *Electron Optics* (Gordon and Breach - London)

Melroy T and Willington M J 1978 *Electron Lenses Rep. Prog. Phys.* 20 341-427

Preussner B 1966 *Electron Optics* (SIF - London)

REFERENCES : CHAPTER ONE
BIBLIOGRAPHY

- Cosslett V E 1950 *Introduction to Electron Optics, the Production, Propagation, and Focusing of Electron Beams* (Oxford University Press : England)
- Drummond I W 1984 The Ion Optics of Low Energy Ion Beams *Vacuum* **34** (*Vacuum Special Issue, Proceedings of the 3rd International Conference on Low Energy Ion Beams*) 1-61
- El-Kareh A B and El-Kareh J C 1970 *Electron Beams, Lenses, and Optics* Vols. I and II (Academic Press : New York)
- Gabor D 1945 *The Electron Microscope* (Hutton : London)
- Grivet P 1972 *Electron Optics* 2nd Edition (1st Ed. 1965) (Pergamon : Oxford)
- Hall C E 1966 *Introduction to Electron Microscopy* 2nd Edition (1st Ed. 1953) (McGraw-Hill : New York)
- Harting E and Read F H 1976 *Electrostatic Lenses* (Amsterdam : Elsevier)
- Hawkes P W 1972 *Electron Optics and Electron Microscopy* (Taylor and Francis Ltd : London)
- Hawkes P W (editor) 1973 *Image Processing and Computer Aided Design in Electron Optics* (Academic Press : London)
- Jacob L 1950 *An Introduction to Electron Optics* (Methuen : London)
- Klemperer O 1953 *Electron Optics* 2nd Edition (Cambridge University Press : England)
- Klemperer O and Barnett M E 1971 *Electron Optics* 3rd Edition (Cambridge University Press : England)
- Lawson J D 1977 *The Physics of Charged Particle Beams* (Oxford University Press : England)
- Meyers L M 1939 *Electron Optics* (Chapman and Hall : London)
- Mulvey T and Wallington M J 1973 Electron Lenses *Rep. Prog. Phys.* **36** 347-421
- Paszkowski B 1968 *Electron Optics* (Iliffe : London)

- Pierce J R 1954 *Theory and Design of Electron Beams* (D. Van Nostrand Company, Inc. : U.S.A)
- Septier A (editor) 1967 *Focusing of charged particles* (Academic Press : London)
- Spangenberg K 1948 *Vacuum Tubes* (McGraw-Hill : New York)
- Sturrock P A 1955 *Electron Optics* (Cambridge University Press : England)
- Ximen Jiye 1986 *Aberration Theory in Electron and Ion Optics*; Suppl. *Advances in Electronic and Electron Physics* **17**
- Zworykin V K, Morton G A, Ramberg E G, Hillier J and Vance A W 1945 *Electron Optics and the Electron Microscope* (Wiley : New York)
- Zworykin V K and Morton 1956 *Television. The Electronics of Image Transmission in Colour and Monochrome* 2nd Edition (1st Ed. 1940 *Television*) (Wiley : New York)

CONTENTS ; CHAPTER TWO

	Page No
Section (2.1) Introduction	58
Section (2.2) The Finite Difference Method or Relaxation Method	58
Section (2.3) The Charge Density Method	60
Section (2.4) The Separation of Variables Method	62
CHAPTER TWO	66
METHODS FOR CALCULATING	71
THE PROPERTIES OF	71
ELECTRON LENSES	71
Section (2.1) The Calculation of charged particle trajectories	73
References	81

CONTENTS : CHAPTER TWO

	Page No
Section (2.1) Introduction of equal mesh width	56
Section (2.2) The Finite Difference Method or Relaxation Method	56
Section (2.3) The Charge Density Method	60
Section (2.4) The Separation of Variables Method	62
Section (2.5) The Finite Element Method	66
Section (2.6) Comparison of the various methods available for calculating the lens potential	71
Section (2.7) The Calculation of charged particle trajectories	73
References	81
Figure 2.7(a) A general finite element for the scalar potential calculation	
Figure 2.7(b) Diagram for the generation of the finite element equations	88

METHODS OF ANALYSIS OF ELECTRON LENSES

LIST OF FIGURES : CHAPTER TWO

	Page No
Figure 2.1 A five-point grid of equal mesh width	57
Figure 2.2 A nine-point grid of equal mesh width	60
Figure 2.3 Simple coaxial cylinder lens represented by a large number of circular strips in order to obtain the potential distribution by the charge density method	61
Figure 2.4 Schematic diagram of a two-cylinder lens showing the dimensions, the coordinate system and the regions to which different expressions for the potential apply in the Bessel function expansion method	63
Figure 2.5 Cross section of a typical magnetic lens	67
Figure 2.6 The finite element mesh for analysing the pole piece region	68
Figure 2.7(a) A general finite element for the scalar potential calculation	
Figure 2.7(b) Diagram for the generation of the finite element equations	69

2.2 THE FINITE DIFFERENCE METHOD OR RELAXATION METHOD †

To find the solution of the two Laplace equation $\nabla^2 = 0$, it can be replaced by set of difference equations. In its simplest form, the potential V_0 in a cylindrical lens at a point P_0 , is expressed in terms of the potentials V_1, V_2, V_3 and V_4 at the four points P_1, P_2, P_3 and P_4 , where P_1, P_2, P_3 and P_4 are the four nearest points to P_0 on a square mesh surrounding the point P_0 , see figure 2.1 below.

The potentials at points P_1, P_2, P_3 and P_4 are expanded as a Taylor series in the neigh-

† References : Edwards 1983, Grivet 1973, Ximen Jye 1986, Klempner 1953, Mulvey and Wellington 1973, Nosal et al 1973, Reber 1957

METHODS FOR CALCULATING THE PROPERTIES OF ELECTRON LENSES

2.1 INTRODUCTION

The computation of the properties of electron lenses can normally be separated into two parts, – the determination of the potential distribution of the lens followed by the calculation of the electron trajectories through the lens.

This chapter will summarise the techniques most commonly used to determine the potential distribution, i.e., solution of the Laplace or Poisson equation, for a given electron lens. From the potential distribution the electric or magnetic field distribution can be derived and the electron lens trajectories through the lens calculated. Once the lens trajectories have been obtained, the imaging properties of the lens can be deduced.

There exist four main techniques for determining the potential distribution of an electron lens, these are,

- (1) The finite difference method *or* relaxation method,
- (2) The charged density method,
- (3) The Separation of variables method, and
- (4) The finite element method.

2.2 THE FINITE DIFFERENCE METHOD OR RELAXATION METHOD †

To find the solution of the the Laplace equation $\nabla^2 = 0$, it can be replaced by set of difference equations. In its simplest form, the potential V_0 in a cylindrical lens at a point P_0 , is expressed in terms of the potentials V_1, V_2, V_3 and V_4 at the four points P_1, P_2, P_3 and P_4 , where P_1, P_2, P_3 and P_4 are the four nearest points to P_0 on a square mesh surrounding the point P_0 , see figure 2.1 below.

The potentials at points P_1, P_2, P_3 and P_4 are expanded as a Taylor series in the neigh-

† References : Edwards 1983, Grivet 1972, Ximen Jiye 1986, Klemperer 1953, Mulvey and Wallington 1973, Natali et al 1972, Weber 1967

When the point P_0 lies on the axis $r_0 = 0$ and the above formula no longer applies. However symmetry dictates that $(\frac{\partial V}{\partial r})_0 = 0$ as the potential is constant in the r direction.

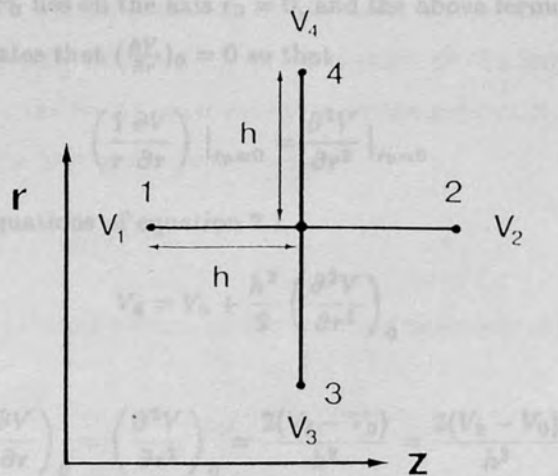


Figure 2.1

Neighbourhood of the point P_0 with cylindrical coordinates (z_0, r_0) as follows,

$$\begin{aligned}
 V_1 &= V_0 - h \left(\frac{\partial V}{\partial z} \right)_0 + \frac{h^2}{2} \left(\frac{\partial^2 V}{\partial z^2} \right)_0 - \dots, \\
 V_2 &= V_0 + h \left(\frac{\partial V}{\partial z} \right)_0 + \frac{h^2}{2} \left(\frac{\partial^2 V}{\partial z^2} \right)_0 + \dots, \\
 V_3 &= V_0 - h \left(\frac{\partial V}{\partial r} \right)_0 + \frac{h^2}{2} \left(\frac{\partial^2 V}{\partial r^2} \right)_0 - \dots, \\
 V_4 &= V_0 + h \left(\frac{\partial V}{\partial r} \right)_0 + \frac{h^2}{2} \left(\frac{\partial^2 V}{\partial r^2} \right)_0 + \dots
 \end{aligned} \tag{2.1}$$

where h is the mesh width. From the above it can be deduced that

$$V_1 + V_2 + V_3 + V_4 - 4V_0 = h^2 \left(\frac{\partial^2 V}{\partial r^2} + \frac{\partial^2 V}{\partial z^2} \right) \tag{2.2}$$

The right hand side of equation 2.2 can be replaced by

$$-\frac{h^2}{r_0} \frac{\partial V}{\partial r}$$

using the Laplace equation expressed in cylindrical coordinates, i.e.,

$$\frac{\partial^2 V}{\partial z^2} + \frac{\partial^2 V}{\partial r^2} + \frac{1}{r} \frac{\partial V}{\partial r} = 0$$

which, from taking the difference of the last two equations of 2.1 is found to equal

$$-\frac{h}{2r_0} (V_4 - V_3)$$

so finally,

$$V_1 + V_2 + V_3 \left(1 - \frac{h}{2r_0} \right) + V_4 \left(1 + \frac{h}{2r_0} \right) = 0 \tag{2.3}$$

When the point P_0 lies on the axis $r_0 = 0$, and the above formula no longer applies. However symmetry dictates that $(\frac{\partial V}{\partial r})_0 = 0$ so that

$$\left(\frac{1}{r} \frac{\partial V}{\partial r}\right) \Big|_{r_0=0} = \frac{\partial^2 V}{\partial r^2} \Big|_{r_0=0}$$

and from the last two equations of equation 2.1

$$V_4 = V_0 + \frac{h^2}{2} \left(\frac{\partial^2 V}{\partial r^2}\right)_0$$

Hence

$$\left(\frac{1}{r} \frac{\partial V}{\partial r}\right)_0 = \left(\frac{\partial^2 V}{\partial r^2}\right)_0 = \frac{2(V_4 - V_0)}{h^2} = \frac{2(V_3 - V_0)}{h^2} \quad (2.1)$$

which implies that $V_3 = V_4$ and equation 2.2 becomes

$$V_1 + V_2 + 2V_4 - 4V_0 = 2V_0 - 2V_4$$

implies

$$V_1 + V_2 + 4V_4 - 6V_0 = 0 \quad (2.4)$$

Difference equations 2.3 and 2.4 are linear algebraic equations relating the potential at arbitrary mesh points to the potentials of neighbouring mesh points. Suppose the total number of mesh points is N , therefore, there exist N linear equations in N unknowns, where the potentials at the mesh points are the unknowns. The assembly of equations for the whole lattice is normally solved by 'the method of relaxation', however, the finite difference equations can be assembled into a 'band' matrix, the inversion of which yields a direct solution for the potential at each lattice point (Hawkes and Armstrong 1970). Unfortunately very large computer memories are required to contain the elements of a band matrix, therefore, relaxation is the most commonly used way of solving the finite difference equations, which is why this method of finding the potential distribution is often referred to as the relaxation method.

The relaxation method consists of making repeated estimates of the values of V at all the mesh points using the set of difference equations, until the difference between $V_i^{(k+1)}$ and $V_i^{(k)}$ is less than a preselected amount, in the manner outlined below.

The difference equations 2.3 and 2.4 can be written in a more general form, i.e.,

$$c_1 V_1 + c_2 V_2 + c_3 V_3 + c_4 V_4 - c_0 V_0 = 0$$

the above can then be rewritten as

$$V_0 = (c_1 V_1 + c_2 V_2 + c_3 V_3 + c_4 V_4) / c_0 \quad (2.5)$$

Initially, arbitrary values for the potentials at the mesh points are assumed, which satisfy the boundary conditions imposed by the geometry of the lens. These potentials $V_0^{(0)}, V_2^{(0)}, V_3^{(0)}, V_4^{(0)}, \dots$, the zeroth approximation for the potentials, are then substituted into equation 2.5 to give a first approximation, i.e.,

$$V_0^{(1)} = (c_1V_1^{(0)} + c_2V_2^{(0)} + c_3V_3^{(0)} + c_4V_4^{(0)})/c_0 \quad (2.6)$$

This process is repeated k times for every mesh point until the required precision is obtained, i.e.,

$$V_0^{(k+1)} = (c_1V_1^{(k)} + c_2V_2^{(k)} + c_3V_3^{(k)} + c_4V_4^{(k)})/c_0 \quad (2.7)$$

This process is called simultaneous displacement, i.e., for each cycle all the potentials are calculated from the potentials of the previous cycle and after each cycle **all** the potentials of the previous cycle are displaced simultaneously by the potentials of the cycle just calculated. Alternatively it is possible to displace successively the previous potentials by the new ones as soon as they have been calculated. This method is known as successive displacement. $V_0^{(k+1)}$ is then given by

$$V_0^{(k+1)} = (c_1V_1^{(k+1)} + c_2V_2^{(k)} + c_3V_3^{(k+1)} + c_4V_4^{(k)})/c_0 \quad (2.8)$$

if the iterative procedure is running from left to right in the z direction, and from bottom to top in the r direction.

After k cycles the error at each mesh point is given by

$$E_0^{(k+1)} = V_0^{(k+1)} - V_0^k \quad (2.9)$$

For the method of successive displacement, it is possible to speed up the rate of convergence by multiplying the error of equation 2.9 by a factor ω and adding it to the potential $V_0^{(k)}$, to obtain the potential at point 0 to the $k + 1 - th$ approximation :

$$V_0^{(k+1)} = (1 - \omega)V_0^{(k)} + \omega(c_1V_1^{(k+1)} + c_2V_2^{(k)} + c_3V_3^{(k+1)} + c_4V_4^{(k)})/c_0 \quad (2.10)$$

This is the five-point difference formula in successive overrelaxation, and ω is the overrelaxation factor, and its optimum value is lens dependent.

The above has been a basic outline of the relaxation method for calculating the potential distribution of a lens. In practice, the mesh used may not be square but rectangular, and the density of the mesh can be variable, *e.g.*, where the potential is changing rapidly a denser mesh may be used. The technique is also not restricted to five points, more accurate

difference equations can be derived to include terms with potentials at points $P_5, P_6, P_7,$ and P_8 , i.e., a nine-point difference formula can be derived, see figure 2.2 below.

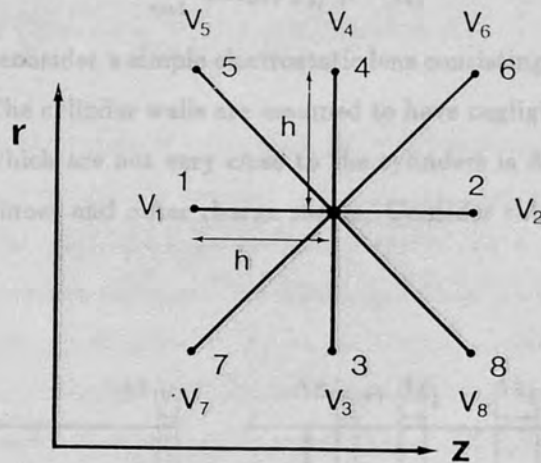


Figure 2.2

2.3 THE CHARGE DENSITY METHOD †

In the charge density method of calculating the lens potential, the surfaces of the electrodes which make up a given lens are divided up into rings, each of which carries a uniform surface charge density. Each electrode is considered as the superposition of N rings, each with a different charge, so that the sum of the potentials created by the rings is, for each electrode, equal to the potential applied to that electrode.

A ring i has an area s_i and carries a uniform surface charge density σ_i and therefore has a total charge $q_i = \sigma_i s_i$. The potential at a point $R_j = (\rho_j, z_j)$ on a ring j due to the charges on the N rings is

$$V(R_j) = V_j = \sum_{i=1}^N A_{ji} q_i$$

where

$$A_{ji} = \frac{1}{4\pi\epsilon_0 s_i} \int_{s_i} \frac{dr_i}{|R_j - r_i|}$$

In order to obtain the lens potential the matrix \mathbf{A} must be evaluated. Once \mathbf{A} has been calculated the column vector \mathbf{q} is obtained by inverting \mathbf{A} and using

$$\mathbf{q} = \mathbf{A}^{-1} \mathbf{V}$$

† References : Mulvey and Wallington 1973, Read et al 1971, Renau et al 1982

The potential at any point \mathbf{r} that is not on a boundary ring is then given by

$$V(\mathbf{r}) = \sum_{i=1}^N \frac{q_i}{4\pi\epsilon_0 s_i} \int_{s_i} \frac{d\mathbf{r}_i}{|\mathbf{r} - \mathbf{r}_i|}$$

To illustrate the method, consider a simple electrostatic lens consisting of two coaxial cylinders, (Read et al 1971). The cylinder walls are assumed to have negligible thickness so that the potential in regions which are not very close to the cylinders is determined simply by the algebraic sum of the inner and outer charge sheets. Consider the cylinder lens shown in figure 2.3 below.

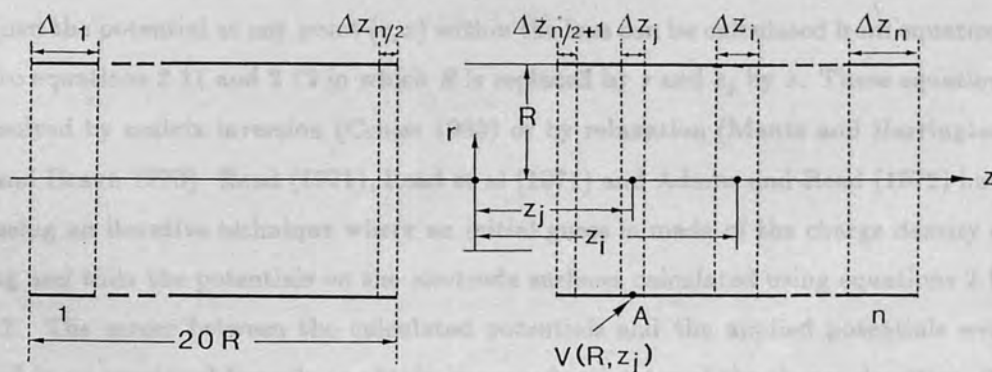


Figure 2.3 (from Mulvey and Wallington 1973 figure 8)

The cylinders of radius R have length $20R$ so that the cylinder ends have a negligible effect on the potential distribution in the neighbourhood of the gap. The first step in the solution is to divide the cylinders into a total of n rings of variable width, which are made narrowest near the gap where the charge density changes most rapidly. The potential V_i at a point A on the j th element with coordinates (R, z_j) due to a charge q_i uniformly distributed around a circle of Radius R lying in the plane $z = z_i$ is given by the expression (Weber 1950)

$$V_i(R, z_j) = \frac{q_i k_i}{4\pi\epsilon_0 R} K(k_i)$$

where

$$k_i^2 = \frac{4R^2}{4R^2 + (z_j - z_i)^2}$$

and $K(k_i)$ is the complete elliptic integral of the first kind. The charge density σ_i on the upper and lower surface of the element of width Δz_i is given by

$$\sigma_i = \frac{q_i}{4\pi R \Delta z_i} \quad (2.11)$$

The potential at point A due to the summed contributions from all the elements of the two cylinders is therefore

$$V(R, z_j) = \frac{1}{\pi \epsilon_0} \sum_{\substack{i=1 \\ i \neq j}}^n \sigma_i k_i K(k_i) \Delta z_i + I_{i=j} \quad (2.12)$$

where $I_{i=j}$ is the term for the region of integration ($z_i = z_j$) at which the elliptic integral has a singularity. The lens is completely specified by n such equations each of which specifies the potential on a particular ring. Now since the strip potential is the applied potential and therefore known, the assembly of equations is a soluble system of n linear equations where the n unknowns are the charge densities of the rings. Once the charge density has been determined the potential at any point (r, z) within the lens can be calculated from equations similar to equations 2.11 and 2.12 in which R is replaced by r and z_j by z . These equations can be solved by matrix inversion (Cruise 1963) or by relaxation (Mautz and Harrington, Singer and Braun 1970). Read (1971), Read et al (1971) and Adams and Read (1972) have solved using an iterative technique where an initial guess is made of the charge density of each ring and then the potentials on the electrode surfaces calculated using equations 2.11 and 2.12. The errors between the calculated potentials and the applied potentials were then used in an empirical formula to obtain improved estimates of the charge densities. By repeating this process, convergence to the true values was achieved.

2.4 THE SEPARATION OF VARIABLES METHOD †

In the separation of variables method the solution of the Laplace equation is written as a product of functions, each of which contains only one of the variables of the coordinate system employed. In the case of cylindrical symmetry, the solution can be expressed as the product of two functions, one depending on the radial component r and the other on the axial component z . This solution can be expressed as an infinite Fourier series, (Bonjour 1979, Cook and Heddle 1976, Read 1969a,b,1970, Renau and Heddle 1986)

$$V(r, z) = \sum_n A_n \exp(k_n z) J_0(k_n r)$$

where J_0 is the Bessel function of order zero and the constants A_n must be determined so as to satisfy the boundary conditions. A method defined by Cook and Heddle (1975), using the variational principle and the expansion of Bessel functions, and is therefore referred

† References : Bertram 1940,1942, Bonjour 1979, Cook and Heddle 1976, Grivet 1972, Fink and Kisker 1980, Read 1969a,b,1970, Renau and Heddle 1986

to either as the variational method or the Bessel function expansion method, was used to obtain the lens potential, and is outlined below.

A solution ψ of Laplace's equation $\nabla^2\psi = 0$ in a volume Ω can be found which satisfies the condition that $\psi = \psi_B$ on some closed boundary of Ω . Initially an approximate solution ϕ is assumed and a functional $W(\phi)$ defined, i.e.,

$$W(\phi) = \frac{1}{2} \int_{\Omega} (\nabla\phi)^2 d\Omega$$

The variational principle indicates that

$$W(\psi) \leq W(\phi)$$

The approximate solution is constructed so that

$$\phi = \sum_{i=1}^n \alpha_i \phi_i$$

and the coefficients α_i determined by minimising $W(\phi)$. In other words, the appropriate potential distribution is the one of minimum potential energy.

Consider the geometry shown in figure 2.4. The potential in the three

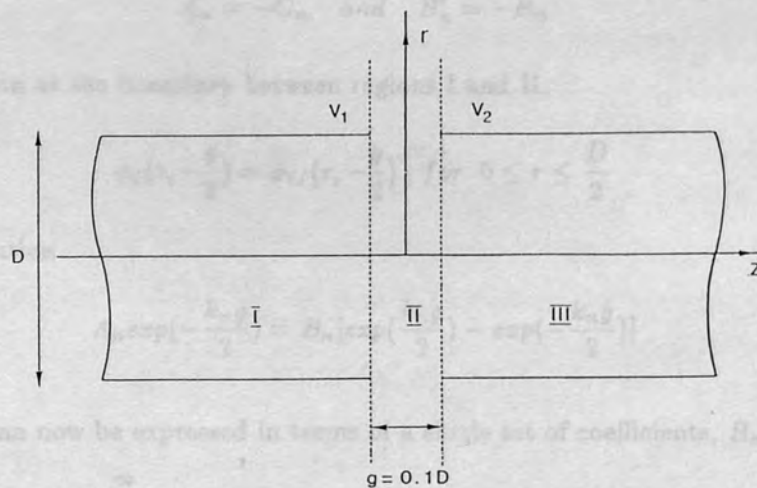


Figure 2.4 (from Cook and Heddle 1976 figure 1)

labelled regions is as follows

$$\phi_I(r, z) = V_1 + \sum_{n=1}^{\infty} A_n \exp(k_n z) J_0(k_n r) \quad (2.13a)$$

$$\phi_{II}(r, z) = \frac{V_1 + V_2}{2} + \left(\frac{V_2 - V_1}{g} \right) z + \sum_{n=1}^{\infty} [B_n \exp(-k_n z) + B'_n \exp(k_n z)] J_0(k_n r) \quad (2.13b)$$

$$\phi_{III}(r, z) = V_2 + \sum_{n=1}^{\infty} C_n \exp(-k_n z) J_0(k_n r) \quad (2.13c)$$

Each term of equation (2.13) is a formal solution of Laplace's equation with unspecified boundary conditions. A_n , B_n , B'_n and C_n are coefficients to be determined, $J_0(t)$ is the Bessel function of order zero and cylindrical polar coordinates are used with the origin at the centre of the lens. The cylinder potentials are V_1 and V_2 and the signs of the arguments of the exponentials were chosen by Cook and Heddle (1976) to satisfy the boundary condition at $z = \pm\infty$. The boundary condition at the cylindrical surfaces is satisfied if the values of k_n are restricted to those for which $J_0(k_n D/2) = 0$. This restriction implies, from equation 2.13b, that the potential in the gap between the cylinders at $r = D/2$ changes linearly with z . This is known to be an approximation, however, Bonjour (1979) has shown how a more realistic dependence may be incorporated into the variational method but the effect is small for a lens having a small gap and thick walls.

The relationship between the coefficients can be found from

(1) Symmetry about the origin

Symmetry about the origin implies that

$$A_n = -C_n \quad \text{and} \quad B'_n = -B_n$$

(2) The condition at the boundary between regions I and II,

$$\phi_I(r, -\frac{g}{2}) = \phi_{II}(r, -\frac{g}{2}) \quad \text{for} \quad 0 \leq r \leq \frac{D}{2}$$

leads to the relation

$$A_n \exp(-\frac{k_n g}{2}) = B_n [\exp(\frac{k_n g}{2}) - \exp(-\frac{k_n g}{2})] \quad (2.14a)$$

The potential can now be expressed in terms of a single set of coefficients, B_n , as

$$\phi_I(r, z) = V_1 + \sum_{i=1}^{\infty} B_i [\exp(k_i g) - 1] \exp(k_i z) J_0(k_i r) \quad (2.14a)$$

$$\phi_{II}(r, z) = \frac{V_1 + V_2}{2} + \left(\frac{V_2 - V_1}{g} \right) z + \sum_{i=1}^{\infty} B_i [\exp(-k_i z) - \exp(k_i z)] J_0(k_i r) \quad (2.14b)$$

$$\phi_{III}(r, z) = V_2 - \sum_{i=1}^{\infty} B_i [\exp(k_i g) - 1] \exp(-k_i z) J_0(k_i r) \quad (2.14c)$$

The functional to be minimised is therefore

$$\pi \left\{ \int_0^{D/2} \int_{-g/2}^{g/2} \left[\left(\frac{\partial \phi_I}{\partial z} \right)^2 + \left(\frac{\partial \phi_I}{\partial r} \right)^2 \right] r dr dz \right. \\ \left. + \int_0^{D/2} \int_{-g/2}^{g/2} \left[\left(\frac{\partial \phi_{II}}{\partial z} \right)^2 + \left(\frac{\partial \phi_{II}}{\partial r} \right)^2 \right] r dr dz \right. \\ \left. + \int_0^{D/2} \int_{g/2}^{\infty} \left[\left(\frac{\partial \phi_{III}}{\partial z} \right)^2 + \left(\frac{\partial \phi_{III}}{\partial r} \right)^2 \right] r dr dz \right\}$$

When the condition $\partial W / \partial B_n = 0$ it is found that

$$B_n = (V_2 - V_1) \exp\left(-\frac{k_n g}{2}\right) / \left(\frac{g}{2}\right) k_n D J_1\left(\frac{k_n D}{2}\right)$$

where J_1 is the Bessel function of order one. The dimensions are all expressed in terms of the cylinder diameter, D , as

$$G = \frac{g}{D}, \quad Z = \frac{z}{D}, \quad R = \frac{2r}{D}$$

with

$$K_n = \frac{k_n D}{2}$$

Values of K_n and the corresponding values of $J_1(K_n)$ to ten decimal places are given in the British Association Mathematical Tables (1958) for $1 \leq n \leq 150$. It is convenient for calculation to write

$$Q_n = \frac{1}{2K_n J_1(K_n)} \quad (\text{Note : } D = \frac{2r}{R} = 1 \text{ when } \frac{r}{R} = 1)$$

and

$$B_n = \frac{(V_2 - V_1) Q_n \exp(-K_n G)}{G}$$

The potentials can then be expressed as

$$\phi_I(R, Z) = V_1 + \frac{V_2 - V_1}{G} \sum_{n=1}^{\infty} Q_n \{ \exp[K_n(2Z + G)] - \exp[K_n(2Z - G)] \} J_0(K_n R) \quad (2.15a)$$

$$\phi_{II}(R, Z) = \frac{V_1 + V_2}{2} + \frac{V_2 - V_1}{G} Z + \frac{V_2 - V_1}{G} \sum_{n=1}^{\infty} Q_n \{ \exp[-K_n(2Z + G)] - \exp[K_n(2Z - G)] \} J_0(K_n R) \quad (2.15b)$$

$$\phi_{III}(R, Z) = V_2 - \frac{V_2 - V_1}{G} \sum_{n=1}^{\infty} Q_n \{ \exp[-K_n(2Z - G)] - \exp[-K_n(2Z + G)] \} J_0(K_n R) \quad (2.15c)$$

For the limiting case of a lens having zero gap an exact analytic expansion exists (Grivet 1972). The expressions for ϕ_I and ϕ_{III} reduce to this exact expression as $G \rightarrow 0$.

Cook and Heddle (1976) found that the evaluation of the potential from the expressions of equations 2.15 required a little care. For values of Z close to $\pm G/2$ the convergence was found to be extremely slow. Successive terms alternate in sign, however, and it was found that a greatly improved approximation was obtained by taking the means of the sums to N and $N + 1$ terms.

Another method used to obtain the solution of the Laplace equation, using the method of separation of variables, involves expressing the solution of the Laplace equation as a Fourier integral, (rather than an infinite Fourier series, Bertram 1940,1942, Fink and Kisker 1980) as,

$$V(r, z) = \frac{1}{2\pi} \int_{-\infty}^{\infty} a(k) I_0(kr) e^{ikz} dk$$

where $I_0(kr) = J_0(ikr)$ is the Bessel function of order zero with imaginary argument and where $a(k)$ is a function of the arbitrary parameter k , where $a(k)$ must be chosen so that $V(r, z)$ satisfies the boundary conditions. The above integral can be approximated to give an analytical expression for the lens potential, (Bertram 1940,1942, Fink and Kisker 1980). Approximating the integral gives a very rapid method of calculating the potential, however, the Bessel function expansion method gives a more accurate solution.

Finally, Read 1969a,b,1970 used the separation of variables method to obtain the potential of two and three aperture immersion lenses, using Bessel series for the potentials, chosen to satisfy the boundary condition at $z = \pm\infty$, and restricting the values of k_n to those values for which $J_0(k_n D/2) = 0$, (i.e., the same boundary conditions as applied in the Bessel function expansion method of solution described above). The boundary conditions which remain to be satisfied are that the radial and longitudinal components of the field are continuous across the lens apertures. The application of this boundary condition alone was found to be insufficient to obtain convergence, and a 'least squares' criterion had to be applied to finally obtain a satisfactory solution. This method gives good results, however, the Bessel function expansion method is a more rapid method of obtaining a solution.

2.5 THE FINITE ELEMENT METHOD †

To obtain the potential of a lens using the finite element method, as with the relax-

† References : Ximen Jiye 1986, Mulvey and Wallington 1973, Munro 1973

ation method, the lens is divided into a network of grids. However, in the finite element case, the elements are quadrilaterals with no special symmetry, where each quadrilateral is subsequently divided into two triangles. A potential value is assigned to each lattice node, (i.e., each corner of the triangle) and the potential is assumed to vary linearly across each triangular finite element.

The finite element method like the variational or Bessel function expansion method, uses the variational principle, i.e., a functional is defined whose minimisation is equivalent to solving the original differential equation. As the potential is assumed to vary linearly across each triangular finite element, the potential over each element is uniquely determined by the potential at its vertices, so that the contribution from the functional can be expressed in terms of the potentials at the corners of the triangles. The condition that the functional be minimised is used to derive a set of simultaneous algebraic equations, which when solved give the potential at each mesh point.

To illustrate the method, consider the unsaturated magnetic lens of figure 2.5, (Munro 1973).

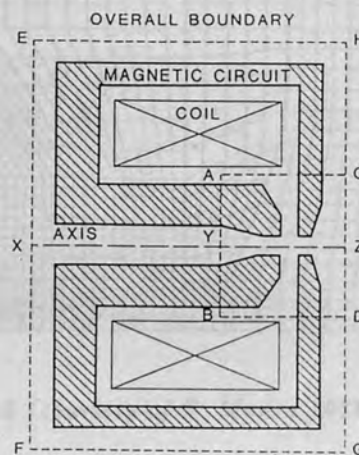


Figure 2.5 courtesy of E. Munro 1973 figure 1)

Suppose the field distribution in the pole-piece region ABCD is to be computed. The region ABCD encloses no currents and the magnetic field \mathbf{B} may be represented by a scalar potential V , defined such that

$$\mathbf{B} = \nabla V$$

where V satisfies the differential equation

$$\nabla \cdot (\mu \nabla V) = 0 \tag{2.16}$$

where μ is the permeability at any point. The solution of equation 2.16 subject to prescribed boundary conditions, (listed below) can be obtained by minimising the functional

$$F = \int \int \int_{\text{TOTAL VOLUME}} \frac{1}{2} \mu \nabla V \cdot \nabla V dV \quad (2.17)$$

subject to the same boundary conditions. For a rotationally-symmetric lens, the equation 2.17 becomes

$$F = \int \int_{\text{TOTAL AREA}} \frac{1}{2} \mu \left[\left(\frac{\partial V}{\partial z} \right)^2 + \left(\frac{\partial V}{\partial r} \right)^2 \right] 2\pi r dz dr \quad (2.18)$$

The entire region in the rz is divided into small quadrilaterals, which are subdivided into small triangular finite elements, (figure 2.6).

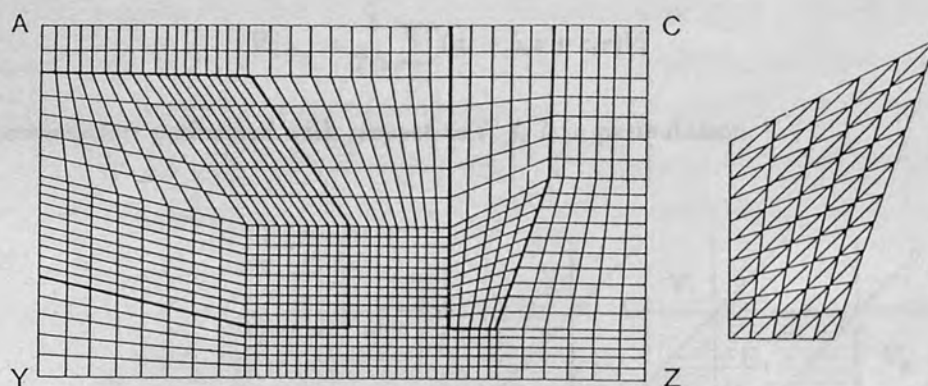


Figure 2.6 (courtesy of E. Munro 1973 figure 2)

The contribution from such an element to the functional F in equation 2.18 is

$$F_{\Delta_e} = \int_{\Delta_e} \int \frac{1}{2} \mu \left[\left(\frac{\partial V}{\partial z} \right)^2 + \left(\frac{\partial V}{\partial r} \right)^2 \right] 2\pi r dz dr \quad (2.19)$$

which is evaluated over the element Δ_e . For the finite element approximation, V is assumed to vary linearly across the element, and is thus given by

$$V(z, r)|_{\Delta_e} = \alpha_i + \alpha_j z + \alpha_k r \quad (2.20)$$

where $\alpha_i, \alpha_j, \alpha_k$ can be expressed in terms of three vertex potentials V_i, V_j, V_k as follows (figure 2.7)

$$\begin{aligned}\alpha_i &= \frac{1}{2\Delta}(a_i V_i + a_j V_j + a_k V_k) \\ \alpha_j &= \frac{1}{2\Delta}(b_i V_i + b_j V_j + b_k V_k) \\ \alpha_k &= \frac{1}{2\Delta}(c_i V_i + c_j V_j + c_k V_k)\end{aligned}\quad (2.21)$$

In the above formula Δ is the area of the triangular element

$$\Delta = \frac{1}{2} \begin{vmatrix} 1 & z_i & r_i \\ 1 & z_j & r_j \\ 1 & z_k & r_k \end{vmatrix} \quad (2.22)$$

while the coefficients become

$$a_i = z_j r_k - z_k r_j, \quad b_i = r_j - r_k, \quad c_i = -z_j + z_k$$

and so forth. Substituting equation 2.21 into equation 2.20 gives

$$V|_{\Delta_c} = \frac{1}{2\Delta} \sum (a_i + b_i z + c_i r) V_i \quad (2.23)$$

where summation is performed with respect to i, j, k in permutation.

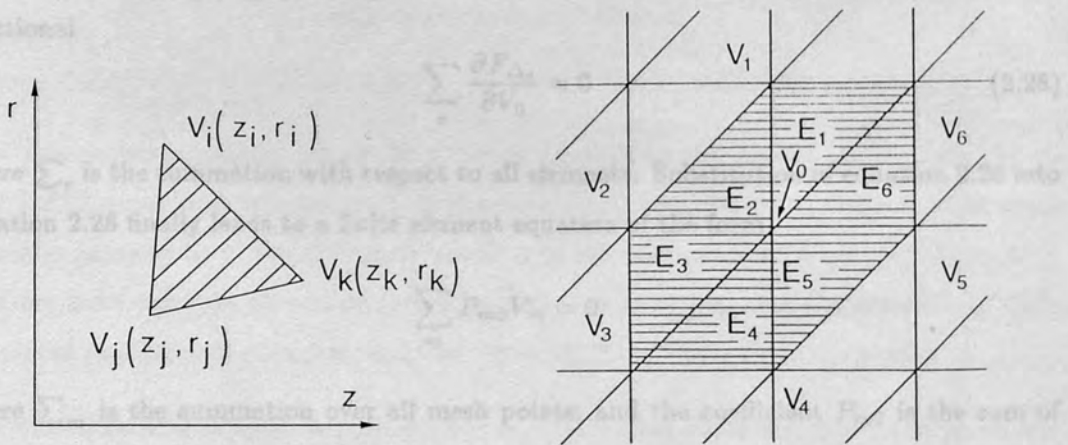


Figure 2.7 (courtesy of E. Munro 1973 figures 3 & 4)

The gradient of the scalar potential in each finite element is given by

$$\frac{\partial V}{\partial z} = \frac{1}{2\Delta} \sum (b_i V_i), \quad \frac{\partial V}{\partial r} = \frac{1}{2\Delta} \sum (c_i V_i) \quad (2.24)$$

Substituting into equation 2.19 gives the contribution from such an element Δ_e to the functional F

$$F_{\Delta_e} = \frac{1}{8\Delta^2} \int \int \mu [(b_i V_i + b_j V_j + b_k V_k)^2 (c_i V_i + c_j V_j + c_k V_k)^2] 2\pi r dr dz$$

The above can be rewritten as follows

$$F_{\Delta_e} = \frac{\pi\mu}{4\Delta} \bar{r} \sum [(b_i V_i)^2 + (c_i V_i)^2] \quad (2.25)$$

where \bar{r} is the value of r at the centroid.

Differentiating equation 2.25 with respect to V_i gives the following matrix formula

$$\left[\frac{\partial F_{\Delta_e}}{\partial V_i} \right] = [F_{ij}] [V_{ij}] \quad (i, j, k) \quad (2.26)$$

where

$$F_{ij} = \mu \frac{\pi \bar{r}}{2\Delta} (b_i b_j + c_i c_j) \quad (2.27)$$

For each element of the mesh the 3×3 matrix $[F_{ij}]$ is computed using equation 2.27. For example, in figure 2.7b, let the node 0 be a general mesh point, and let the adjacent elements be $\Delta_1, \Delta_2, \Delta_3, \Delta_4, \Delta_5, \Delta_6$, with the corresponding vertex potentials $V_0, V_1, V_2, V_3, V_4, V_5, V_6$. Using equations 2.25 and 2.26 to sum up the contributions from each element, and inserting the total contributions into equation 2.18 gives the condition for minimizing the functional

$$\sum_e \frac{\partial F_{\Delta_e}}{\partial V_0} = 0 \quad (2.28)$$

where \sum_e is the summation with respect to all elements. Substitution of equation 2.26 into equation 2.28 finally leads to a finite element equation of the form

$$\sum_m P_{m0} V_m = 0$$

where \sum_m is the summation over all mesh points, and the coefficient P_{m0} is the sum of the appropriate terms of F_{ij} with respect to the node 0. A finite element equation is generated in this way for each mesh point, a seven-point equation being obtained for each non-axial mesh point, and a five-point equation for each axial mesh point. The resulting linear algebraic equations for scalar potentials of mesh points leads finally to the matrix equation

$$[P][V] = 0$$

and this set of linear algebraic equations can be solved by Gaussian elimination or iteration.

2.6 COMPARISON OF THE VARIOUS METHODS AVAILABLE FOR CALCULATING THE LENS POTENTIAL

There are pros and cons to all the methods described above. In choosing which method to use to calculate the potential distribution of a given lens, it is necessary to consider,

- (1) the geometry of the lens, as some methods are restricted to certain geometries,
- (2) is the potential to be evaluated at every point of the lens, or is it sufficient to only know the potential at discrete points, (i.e., the nodes of a mesh) or is it only necessary to know the axial potential,
- (3) what accuracy is required,
- (4) how much computer memory is available,
- (5) how much time is available to do the calculations.

With these points in mind, the following lists the good and bad points of the methods described above.

Finite Difference Method

Good Points

This is an accurate method, where the accuracy depends on the density of the mesh. Natali et al (1972) quote that "the accuracy of the relaxation technique using five point formulas, is usually taken to be of the order $1/N$ where N is the number of mesh points." Since they used the more accurate nine-point formulas, Natali et al believe that the accuracy of their calculated potentials is considerably better than 10^{-4} of the maximum potential.

The finite difference method can be used to calculate the potential of lenses of any geometry.

Bad Points

The potential is obtained only at discrete points, i.e., the node of a mesh, and interpolation is necessary if the potential is required at points lying between the mesh points. Interpolation must be done with extreme care if the accuracy of the method is to be maintained.

The finite difference method requires a lot of computing time and computer memory because of the need for iteration or the inversion of a large matrix.

Charge Density Method

Good Points

This is an accurate method, where the accuracy depends on the number of segments into which the lens is divided which are assumed to carry a uniform charge density. Harting and Read (1976) obtained accuracies of ($\approx 0.1\%$).

The potential is obtained at all points in the lens.

This method can be used to calculate the potential of lenses of any geometry, provided that it is possible to divide the lens into segments, where each segment has a uniform charge density.

Bad Points

The axial potential can be found quite simply, but the calculation of the potential at off axis points requires the numerical evaluation of elliptical integrals.

The charge density method requires a lot of computing time and computer memory because of the need for iteration or the inversion of a large matrix.

Separation of Variables Method (Bessel function Expansion Method)

Good Points

This is a fast and accurate method for computing the potential of cylindrical lenses of constant diameter where the cylinders are separated by a small gap ($\leq 0.1D$), or when the potential in the gap is known. It requires a very simple computer program; no iteration or matrix inversion is necessary. The precision of the Bessel function technique depends on the number of terms considered in the infinite sum of Bessel functions. To test the accuracy of this method the results obtained are compared with those obtained using other methods. The lens potentials obtained using the Bessel function expansion method, were compared with the potentials calculated by Natali et al (1972) using the finite difference method, (Cook and Heddle (1976), Edwards 1983) and with those calculated by Read et al (1971) using the charge density method, (Edwards 1983). The agreement was found to be within 0.01%.

The potential is obtained at all points of the lens.

Bad Points

This method is limited to cylindrical lenses where the cylinders are of the same diameter D , and the cylinders are separated by a small gap, or the potential in the gap is known and can be approximated by some function.

Finite Element Method

Good Points

This method can be used to calculate the potential of a lens of any geometry, and is particularly useful where the lens geometry is complicated, and the lens boundaries have peculiar shapes.

Bad Points

This method is not as accurate as the previous three methods, Munro (1973) obtained accuracies of ($\approx 1\%$).

The finite element method requires a lot of computing time and computer memory because of the need for the inversion of a very large matrix.

2.7 THE CALCULATION OF CHARGED PARTICLE TRAJECTORIES †

Once the potential distribution within a lens has been calculated, by whatever method, in order to finally find the focal properties of the lens, the trajectories of charged particles through the lens have to be determined. To obtain the charge particle trajectories it is necessary to solve the trajectory equation. This equation is an ordinary differential equation, the solution of which can be found by numerical integration.

Consider a first order differential equation inside a region G in the $x y$ plane :

$$\frac{dy}{dx} = f(x, y)$$

The initial condition is

$$y(x_0) = y_0$$

† References : Buckingham 1966, Hamming 1973, Kisker 1982, Ximen Jiye 1986, Ralston 1965, Renau and Heddle 1986

The independent variable is x , and the dependent variable is y . If inside the region G , the function $f(x, y)$ is sufficiently differentiable or possesses continuous derivatives of all orders with respect to x and y , then a unique and well behaved solution satisfying the above two equations does exist inside the region G . Numerical integration can then be performed in the following way to find a solution. If an initial value $y(x_0)$ at the initial point $x = x_0$ is known, using the slope y'_0 at this point it is possible to move forward by a step of length h to the next value $y(x_1)$ at the next point $x = x_1$. Repeating this process allows the approximate values $y(x_2), y(x_3), \dots, y(x_n)$ at the consecutive points $x = x_2, x_3, \dots, x_n$, thus a numerical approximation to the solution of the differential equation can be generated.

The methods available to obtain the solution of ordinary differential equations by numerical integration may be grouped into two broad classes

- (1) Single-step methods. In these methods the value of $y(x_{n+1})$ is obtained from a knowledge of the previous $y(x_n)$ and the calculation of $f(x, y)$ within the interval (x_n, x_{n+1}) . The Runge-Kutta method is of this type, as is the method described by Renau and Heddle (1986), both methods will be described below.
- (2) Multi-step methods. In these methods the value $y(x_{n+1})$ is obtained from a knowledge of a number of previous points, i.e., y_n, y_{n-1}, \dots and y'_n, y'_{n-1}, \dots . The predictor-corrector formulae is of this type and will be described below. Finally, if only the Gaussian approximation of trajectory equation is considered, i.e., the paraxial equation, a simpler method than either of the above, known as the Fox-Goodwin method (or Numerov-Manning-Millmann method) can be used, and this method is also described below.

RUNGE-KUTTA SINGLE STEP METHOD†

The Runge-Kutta method estimates the value of y_{n+1} from y_n and a weighted average of values of $f(x, y)$ where x and y lie between x_n and x_{n+1} , and y_n and y_{n+1} respectively. Where the values of $f(x, y)$ are chosen so that the truncation error is comparable to that of a p th order Taylor series, i.e., (to fourth order)

$$y(x_{n+1}) = y(x_n) + h[aK_1 + bK_2 + cK_3 + dK_4] + O(h^5) \quad (2.29)$$

Expanding both sides of equation 2.29 into Taylor series at the point $x = x_n$ and comparing

† References : Ximen Jiye 1986

corresponding terms gives

$$y_{n+1} = y_n + \frac{h}{6}(K_1 + 2K_2 + 2K_3 + K_4) + O(h^5) \quad (2.30)$$

where h is the step length and,

$$\begin{aligned} K_1 &= f(x_n, y_n) \\ K_2 &= f\left(x_n + \frac{h}{2}, y_n + \frac{hK_1}{2}\right) \\ K_3 &= f\left(x_n + \frac{h}{2}, y_n + \frac{hK_2}{2}\right) \\ K_4 &= f(x_n + h, y_n + hK_3) \end{aligned} \quad (2.31)$$

The advantages of the Runge-Kutta method are its high accuracy, self-starting and stability, and also its ease in changing step length in numerical integration. Its main disadvantage is the number of function evaluations required per step, which means that considerable computer time may be needed to finally compute trajectories.

RENAU-HEDDLE SINGLE STEP METHOD †

Renau and Heddle (1986) described a single step method for calculating the trajectories through an electrostatic lens. The electron trajectories were calculated by numerically integrating the Newtonian equations of motion, using the power series expansion of the electron co-ordinates in terms of time

$$z(t) = z_0 + \left(\frac{dz}{dt}\right)_0 t + \frac{1}{2} \left(\frac{d^2z}{dt^2}\right)_0 t^2 + \frac{1}{6} \left(\frac{d^3z}{dt^3}\right)_0 t^3 + \dots \quad (2.32)$$

$$r(t) = r_0 + \left(\frac{dr}{dt}\right)_0 t + \frac{1}{2} \left(\frac{d^2r}{dt^2}\right)_0 t^2 + \frac{1}{6} \left(\frac{d^3r}{dt^3}\right)_0 t^3 + \dots \quad (2.33)$$

where $z(t)$ and $r(t)$ are the co-ordinates of an electron, with initial coordinates denoted by suffix 0 after a short time interval, t . The accuracy of the trajectories depends on the number of terms used and on the value t used for integration. Renau and Heddle (1986) found that very accurate results could be obtained by considering (for each step) variation in potential up to the second order and therefore the first four terms of equations 2.32 and 2.33.

The electron velocities at the end of a step are given by

$$\frac{dz(t)}{dt} = \left(\frac{dz}{dt}\right)_0 + \left(\frac{d^2z}{dt^2}\right)_0 t + \frac{1}{2} \left(\frac{d^3z}{dt^3}\right)_0 t^2$$

† References : Renau and Heddle 1986

$$\frac{dr(t)}{dt} = \left(\frac{dr}{dt}\right)_0 + \left(\frac{d^2r}{dt^2}\right)_0 t + \frac{1}{2} \left(\frac{d^3r}{dt^3}\right)_0 t^2$$

The second differentials of z and r with respect to t are given by Newton's equations, i.e.,

$$\left(\frac{d^2z}{dt^2}\right)_0 = -\frac{e}{m} \left(\frac{\partial V}{\partial z}\right)_0$$

$$\left(\frac{d^2r}{dt^2}\right)_0 = -\frac{e}{m} \left(\frac{\partial V}{\partial r}\right)_0$$

and the third differentials of z and r with respect to t are found by differentiating the above two equations with respect to t where $\frac{d}{dt} = \frac{\partial}{\partial z} \frac{dz}{dt} + \frac{\partial}{\partial r} \frac{dr}{dt}$, i.e.,

$$\left(\frac{d^3z}{dt^3}\right)_0 = -\frac{e}{m} \left(\frac{\partial^2 V}{\partial z^2}\right)_0 \left(\frac{dz}{dt}\right)_0 - \frac{e}{m} \left(\frac{\partial^2 V}{\partial z \partial r}\right)_0 \left(\frac{dr}{dt}\right)_0$$

$$\left(\frac{d^3r}{dt^3}\right)_0 = -\frac{e}{m} \left(\frac{\partial^2 V}{\partial r^2}\right)_0 \left(\frac{dr}{dt}\right)_0 - \frac{e}{m} \left(\frac{\partial^2 V}{\partial z \partial r}\right)_0 \left(\frac{dz}{dt}\right)_0$$

where e/m is the charge to mass ratio for an electron. The final expressions can be simplified if the parameter T is used to replace t , where T is given by,

$$T = -\left(\frac{2e}{m}\right)^{\frac{1}{2}} t$$

Finally, the recurrence relations for the position and velocity of the electron become

$$z(t) = z_0 + \left(\frac{dz}{dT}\right)_0 T + \frac{1}{4} \left(\frac{\partial V}{\partial z}\right)_0 T^2 + \frac{1}{12} \left[\left(\frac{\partial^2 V}{\partial z^2}\right)_0 \left(\frac{dz}{dT}\right)_0 + \left(\frac{\partial^2 V}{\partial z \partial r}\right)_0 \left(\frac{dr}{dT}\right)_0 \right] T^3$$

$$r(t) = r_0 + \left(\frac{dr}{dT}\right)_0 T + \frac{1}{4} \left(\frac{\partial V}{\partial r}\right)_0 T^2 + \frac{1}{12} \left[\left(\frac{\partial^2 V}{\partial r^2}\right)_0 \left(\frac{dr}{dT}\right)_0 + \left(\frac{\partial^2 V}{\partial z \partial r}\right)_0 \left(\frac{dz}{dT}\right)_0 \right] T^3$$

$$\left(\frac{dz(t)}{dT}\right) = \left(\frac{dz}{dT}\right)_0 + \frac{1}{2} \left(\frac{\partial V}{\partial z}\right)_0 T + \frac{1}{4} \left[\left(\frac{\partial^2 V}{\partial z^2}\right)_0 \left(\frac{dz}{dT}\right)_0 + \left(\frac{\partial^2 V}{\partial z \partial r}\right)_0 \left(\frac{dr}{dT}\right)_0 \right] T^2$$

$$\left(\frac{dr(t)}{dT}\right) = \left(\frac{dr}{dT}\right)_0 + \frac{1}{2} \left(\frac{\partial V}{\partial r}\right)_0 T + \frac{1}{4} \left[\left(\frac{\partial^2 V}{\partial r^2}\right)_0 \left(\frac{dr}{dT}\right)_0 + \left(\frac{\partial^2 V}{\partial z \partial r}\right)_0 \left(\frac{dz}{dT}\right)_0 \right] T^2$$

The values of $(dz/dT)_0$ and $(dr/dT)_0$ at the beginning of a trajectory are derived from the angle θ that the trajectory makes with the optic axis, where

$$\left(\frac{dz}{dT}\right)_0 = V_0^{\frac{1}{2}} \cos(\theta_0)$$

$$\left(\frac{dr}{dT}\right)_0 = V_0^{\frac{1}{2}} \sin(\theta_0)$$

Better results will be obtained from either of the above methods if a variable step length is used. If the step length is taken to be equal to a small value h and moving forward by this step gives $r^{(h)}$ and $z^{(h)}$. Going back to the starting point and moving forward two steps of length $h/2$, gives $r^{(h/2+h/2)}$ and $z^{(h/2+h/2)}$. Therefore a relative error can be defined as follows

$$\delta = \max \left[\left| \frac{r^{(h)} - r^{(\frac{h}{2} + \frac{h}{2})}}{r^{(\frac{h}{2} + \frac{h}{2})}} \right|, \left| \frac{z^{(h)} - z^{(\frac{h}{2} + \frac{h}{2})}}{z^{(\frac{h}{2} + \frac{h}{2})}} \right| \right]$$

If δ is greater than a prescribed amount h is halved, if it is less than a prescribed amount h is doubled. An alternative way of choosing the step length by is considering the energy of the electron. The change in electron kinetic energy during a step is given by

$$\Delta K.E = -\frac{m(v_1^2 - v_0^2)}{2}$$

which should be equal but of opposite sign to the change in potential energy

$$\Delta P.E = -e(V_1 - V_0)$$

if the calculation was exact. An error ε can therefore be defined as the apparent change in the total energy of the electron, i.e.,

$$\varepsilon = |\Delta P.E| - |\Delta K.E|$$

Again, if ε is greater than a prescribed amount h is halved, if it less than a prescribed amount h is doubled.

PREDICTOR-CORRECTOR MULTI-STEP METHOD †

In order to improve the accuracy and stability of numerical integration, the predictor-corrector method can be used. However, the predictor-corrector method is not self starting, and a single-step method must be used to compute the first few trajectory values.

To find a solution y_{n+1} of a differential equation of the form

$$\frac{dy}{dx} = f(x, y)$$

using the predictor-corrector method, involves making an initial prediction of y_{n+1} from a knowledge of $y_n, y_{n-1} \dots$, where the value of n is the order of the approximation. An

† References : Hamming 1973, Ralston 1965

iterative formula is then used to correct the prediction, until the difference between two corrected values is sufficiently small; hence the name predictor-corrector. An example of a fourth order predictor-corrector system using corresponding open and closed Newton-Cotes integration formulae is given by

$$\begin{aligned}
 \text{Predictor : } \quad y_{n+1}^{(0)} &= y_{n-3} + \frac{4h}{3}(2y' - y_{n-1} + 2y'_{n-2}) \\
 (y_{n+1}^{(0)})' &= f(x_{n+1}, y_{n+1}^{(0)}) \\
 \text{Corrector : } \quad y_{n+1}^{(j+1)} &= y_{n-1} + \frac{h}{3}[(y_{n+1}^{(j)})' + 4y'_n + y'_{n-1}] \quad (2.34)
 \end{aligned}$$

The precision of the predictor-corrector system can be improved by modifying the predictor by adding a term $T_n^{(0)}$ to it, where $T_n^{(0)}$ is an estimate of the truncation error in the predictor, i.e., the error incurred because the Predictor formulae is not of infinite order but is truncated after a finite number of terms. $T_n^{(0)}$ can be written in terms of the difference between the predicted and corrected values as

$$T_n^{(0)} = c(y_n - y_n^{(0)})$$

where c is a constant and for the system given above, it can be shown that, (Ralston 1965) $c = 28/29$. Equation 2.34 then becomes

$$\begin{aligned}
 \text{Predictor : } \quad y_{n+1}^{(0)} &= y_{n-3} + \frac{4h}{3}(2y' - y_{n-1} + 2y'_{n-2}) \\
 \text{Modifier : } \quad \bar{y}_{n+1}^{(0)} &= y_{n+1}^{(0)} + \frac{28}{29}(y_n - y_n^{(0)}) \\
 (\bar{y}_{n+1}^{(0)})' &= f(x_{n+1}, \bar{y}_{n+1}^{(0)}) \\
 \text{Corrector : } \quad y_{n+1}^{(j+1)} &= y_{n-1} + \frac{h}{3}[(\bar{y}_{n+1}^{(0)})' + 4y'_n + y'_{n-1}] \quad (2.35)
 \end{aligned}$$

The above is just one example of a predictor-corrector system. When deriving predictor and corrector formulae, it is necessary to consider (1) the truncation error, and (2) stability, and to a lesser extent (3) roundoff errors and (4) the ease with which they may be computed. Natali et al (1972), used the following formulae (defined by Hamming)

$$\begin{aligned}
 \text{Predictor : } \quad y_{n+1}^{(0)} &= y_{n-3} + \frac{4h}{3}(2y' - y_{n-1} + 2y'_{n-2}) \\
 \text{Modifier : } \quad \bar{y}_{n+1}^{(0)} &= y_{n+1}^{(0)} + \frac{112}{121}(y_n - y_n^{(0)}) \\
 (\bar{y}_{n+1}^{(0)})' &= f(x_{n+1}, \bar{y}_{n+1}^{(0)}) \\
 \text{Corrector : } \quad y_{n+1}^{(j+1)} &= \frac{1}{8}(9y_n - y_{n-2}) + \frac{3h}{8}[(\bar{y}_{n+1}^{(0)})' + 2y'_n + y'_{n-1}] \quad (2.36)
 \end{aligned}$$

to calculate z , r , $u = dz/d\tau$ and $v = dr/d\tau$, where $\tau^2 = \frac{2e}{m}t^2$, and $dz/d\tau = u(r, z)$, $dr/d\tau = v(r, z)$, $du/d\tau = -\frac{1}{2}E_z(r, z)$ and $dv/d\tau = -\frac{1}{2}E_r(r, z)$. Natali et al (1972) iterated the corrector formulae until the required precision was reached; they then calculated ultimate values using formulae of the form

$$y_{i+1} = y_{n+1}^{(j+1)} + T_n$$

where T_n is the truncation error, and in this case is given by

$$T_n = \frac{9}{121}(y_{n+1} - y_{n+1}^0)$$

A variable step length h was used, where the value of h was chosen so that the Hamming stability condition $hk < 0.4$ was satisfied, where

$$k = \left| \frac{\partial u}{\partial z} \right| + \left| \frac{\partial v}{\partial r} \right| + \left| \frac{\partial E_z}{\partial u} \right| + \left| \frac{\partial E_r}{\partial v} \right|$$

Before calculating the ultimate values z_{i+1} , r_{i+1} , u_{i+1} and v_{i+1} , the step length h was checked against the above stability criterion. If satisfied, the next trajectory point was calculated with the same h . If not, h was divided by two until the stability criterion was satisfied. Vice versa, if the stability criterion could be satisfied with a value for the step length twice as large, h was doubled.

FOX-GOODWIN or NUMEROV-MANNING-MILLMANN METHOD †

This method is only applicable to the Gaussian trajectory equation, i.e., the paraxial equation of motion, i.e.,

$$r'' + \frac{V'}{2V}r' + \frac{V''}{4V}r = 0$$

(i.e., equation 1.33, the paraxial ray equation for the electrostatic lens)

or

$$r'' + \frac{e}{8mV}B_z^2r = 0$$

(i.e., equation 1.53, the paraxial ray equation for the magnetic lens)

Since the paraxial equation is a linear and homogeneous second order differential equation, a simpler method than those described above, known as the Fox-Goodwin or Numerov-Manning-Millmann method, can be used. Its application to the paraxial equation

† References : Buckingham 1966, Kisker 1982

for an electrostatic lens will be described below. This method uses the reduced paraxial equation or Picht equation, i.e.,

$$R'' + TR = 0 \quad (\text{i.e., equation 1.38})$$

where

$$R = rV^{\frac{1}{2}}$$

and

$$T = \frac{3}{16} \left(\frac{V'}{V} \right)^2$$

R_{n+1} is given by a Taylor series expansion from R_n i.e.,

$$R_{n+1} = R_n + h \frac{dr}{dz} + \frac{h^2}{2} \frac{d^2 R}{dz^2} + \frac{h^3}{6} \frac{d^3 R}{dz^3} + \frac{h^4}{24} \frac{d^4 R}{dz^4} + \dots \quad (2.37)$$

similarly, R_{n-1} is given by

$$R_{n-1} = R_n - h \frac{dr}{dz} + \frac{h^2}{2} \frac{d^2 R}{dz^2} - \frac{h^3}{6} \frac{d^3 R}{dz^3} + \frac{h^4}{24} \frac{d^4 R}{dz^4} + \dots \quad (2.38)$$

Adding R_{n-1} to R_{n+1} and then subtracting $2R_n$ gives

$$R_{n+1} - R_{n-1} - 2R_n = h^2 \frac{d^2 R}{dz^2} + \frac{h^4}{24} \frac{d^4 R}{dz^4} + O(h^6) \quad (2.39)$$

From equation 1.38

$$\frac{d^2}{dz^2} = -TR \quad (2.40)$$

and

$$\frac{d^4}{dz^4} = \frac{d^2(-TR)}{dz^2}$$

and from equation 2.39, neglecting the fourth order term

$$\frac{d^4}{dz^4} = - \frac{[T_{n+1}R_{n+1} + T_{n-1}R_{n-1} - 2T_nR_n]}{h^2} \quad (2.41)$$

Substituting equations 2.40 and 2.41 into equation 2.39 finally gives

$$R_{n+1} = \frac{2R_n - R_{n-1} - \frac{h^2}{12}[T_{n-1}R_{n-1} + 10T_nR_n]}{\left[\frac{1+h^2}{12} \right]} \quad (2.42)$$

Note : Because this method uses the paraxial equation of motion for the electrons, it implicitly only takes into account the first order terms of the lens potential, so the ray tracing does not take place through the true lens potential, but through a first order approximation to it, i.e., the axial potential. It is also worth noting at this point, that the accuracy of the trajectories obtained in a given ray trace, not only depend on the precision of the numerical integration technique used to solve the trajectory equation, but also on how close the calculated potential used in the solution, approximates the real potential of the lens.

REFERENCES : CHAPTER TWO

- Bertram S 1940 Determination of the Axial Potential Distribution in Axially Symmetric Electrostatic Fields *Proc. IRE* **28** 418-20
- Bertram S 1942 Calculation of Axially Symmetric Fields *J. Appl. Phys.* **13** 496-502
- Bonjour P 1979 A simple accurate expression of the potential in electrostatic lenses. Part I : Two cylinder lenses *Revue Phys. Appl.* **14** 533-40
- British Association Mathematical Tables **6** 1958 (Cambridge Royal Society)
- Buckingham R A 1966 *Numerical Methods* (Pitman : London)
- Cook R D and Heddle D W O 1976 The simple accurate calculation of cylinder lens potentials and focal properties *J. Phys. E : Sci. Instrum.* **9** 279-282
- Cruise D R 1963 A Numerical Method for the Determination of an Electric Field about a Complicated Boundary *J. Appl. Phys.* **34** 3477-3479
- Edwards D 1983 Accurate calculations of electrostatic potentials for cylindrically symmetric lenses *Rev. Sci. Instrum.* **54** 1729-1735
- Fink J and Kisker E 1980 A method for rapid calculations of electron trajectories in multi-element electrostatic cylinder lenses *Rev. Sci. Instrum.* **51** 918-920
- Grivet P 1972 *Electron Optics* (Pergamon : Oxford)
- Hamming R W 1973 *Numerical Methods for Scientists and Engineers* (MacGraw Hill : London)
- Harting E and Read F H 1976 *Electrostatic Lenses* (Amsterdam : Elsevier)
- Hawkes P W and Armstrong R J 1970 Note on the Calculation of Potential and Field Functions in Electron Optics *Optik* **30** 546-548
- Kisker E 1982 Simple method for accurate ray tracing in electrostatic lenses *Rev. Sci. Instrum.* **53** 114-116
- Klemperer O 1953 *Electron Optics* (Cambridge University Press : England)
- Mautz J R and Harrington R F 1970 Computation of Rotationally Symmetric Laplacian Potentials *Proc. IEE* **117** 850-852

- Mulvey T and Wallington M J 1973 Electron Lenses *Rep. Prog. Phys.* **36** 347-421
- Munro E 1973 Computer-Aided Design of Electron Lenses by the Finite Element Method in *Image Processing and Computer Aided Design in Electron Optics*, ed. Hawkes P W (Academic Press : London) 284-323
- Natali S, DiChio D and Kuyatt C E 1972 Accurate Calculations of Properties of the Two-Tube Electrostatic Lens. 1. Improved Digital Methods for the Precise Calculation of Electric Fields and Trajectories *J. Research NBS* **76A** 27-35
- Ralston A 1965 *A first Course in Numerical Analysis* (McGraw-Hill:New York)
- Read F H 1969a Accurate Calculations of double-aperture electrostatic immersion lenses *J. Phys. E: Sci. Instrum.* **2** 165-169
- Read F H 1969b Calculated properties of electrostatic einzel lenses of three apertures *J. Phys. E: Sci. Instrum.* **2** 679-684
- Read F H 1970 Asymmetric electrostatic lenses of three apertures *J. Phys. E: Sci. Instrum.* **3** 127-31
- Read F H, Adams A and J R Soto-Montiel 1971 Electrostatic cylinder lenses 1: Two element lenses *J. Phys. E: Sci. Instrum.* **4** 625-632
- Renau A, Read F H and Brunt J N H 1982 The charge-density method of solving electrostatic problems with and without the inclusion of space-charge *J. Phys. E: Sci. Instrum.* **15** 347-354
- Renau A and Heddle D W O 1986 Geometric aberrations in electrostatic lenses I. A simple and accurate computer model *J. Phys. E : Sci. Instrum.* **19** 284-288
- Singer B and Braun M 1970 Integral Equation Method for Computer Evaluation of Electron Optics *IEEE Trans. Electron. Devices* **17** 926-934
- Weber C 1950 *Electromagnetic Fields* Vol. 1 (Wiley : New York)
- Weber C 1967 Numerical Solution of Laplace's and Poissons's equations and the Calculation of Electron Trajectories and Electron Beams in *Focusing of Charged Particles* Vol 1, ed Septier A (Academic Press : London) 45-99
- Ximen Jiye 1986 *Aberration Theory in Electron and Ion Optics*; Suppl. *Advances in Electronic and Electron Physics* **17**

CONTENTS : CHAPTER THREE

	Page No
Introduction	27
Experimental Methods other than the present work	27
Experimental Methods used in the present work	93
CHAPTER THREE	93
METHODS FOR DETERMINING EXPERIMENTALLY THE PROPERTIES OF ELECTRON LENSES	95
1.1. Introduction	95
1.2. Experimental Methods used in the present work	103
1.3. Summary	110

CONTENTS : CHAPTER THREE

	Page No
Section (3.1) General Introduction	87
Section (3.2) Description of Experimental Methods other than those used in the present work	87
Section (3.3) Introduction to Experimental Methods used in the present work	93
Section (3.4) Description of the Lens Elements	93
Section (3.5) Description of the method used to determine the focal and magnification properties of a lens	
(a) Lens System	95
(b) Electronics	96
Section (3.6) Description of the method used to determine the spherical aberration coefficient	103
References	110

LIST OF FIGURES : CHAPTER THREE

	Page No
Figure 3.1 Diagram illustrating the Parallel Beam Method	87
Figure 3.2 Schematic Diagram of lens from which the Focal Distances F_1 and F_2 and the Focal Lengths f_1 and f_2 can be deduced	89
Figure 3.3 Diagram illustrating how the Cardinal Points of a lens can be deduced by extrapolating the paths of pencil rays from where they hit a target after they have passed through the lens	90
Figure 3.4 Diagram illustrating the Shadow Method for location of the cardinal points	92
Figure 3.5 A typical lens element	94
Figure 3.6 5-element lens system	97
Figure 3.7 Schematic diagram of 5-element lens system	98
Figure 3.8 Schematic Diagram of Aperture Discs used to obtain the magnification of an electron lens	99
Figure 3.9 A lens element with deflection plates	100
Figure 3.10 Photograph of image displayed on display scope from which the lens magnification is deduced	101
Figure 3.11 Block Diagram of Electronics used to Operate and Display the image of the Lens	102

ME LIST OF FIGURES (cont) : CHAPTER THREE BY
 THE PROPERTIES OF ELECTRON LENSES

	Page No
Figure 3.12 Diagram illustrating the effect of spherical aberration	104
Figure 3.13 Schematic diagram of 5-element lens system used to obtain Δr in order to obtain the spherical aberration coefficient C_s	106
Figure 3.14 Schematic Diagram of Aperture disc with five apertures whose use enables Δr and hence C_s to be determined	107
Figure 3.15 Photograph of image displayed on display scope from which Δr_h and Δr_v and hence C_s is deduced <i>(courtesy of N Papadovassilakis)</i>	108
Figure 3.16 Diagram comparing the distances at which a beam will cross a plane perpendicular to the lens axis when unaffected by lens action and when under the influence of a lens	109



Figure 3.1 (from Orlin 1972, Paper 22)

it is now possible to deduce the semi-aperture β of the lens, and the image focal length f_i is

$$\tan \beta = \frac{R_1 - R_2}{f}$$

METHODS FOR DETERMINING EXPERIMENTALLY THE PROPERTIES OF ELECTRON LENSES

3.1 GENERAL INTRODUCTION

This chapter will describe some of the experimental methods used to determine the properties of electron lenses. It will outline those methods which have been used by other workers, and will then go on to describe in more detail the methods used in the present work.

3.2 DESCRIPTION OF EXPERIMENTAL METHODS OTHER THAN THOSE USED IN THE PRESENT WORK

The simplest method, known as the **parallel beam method** (Grivet 1972), involves a parallel beam of electrons being incident on the lens, where r_0 , the radius of the beam, is small in comparison with the radius of the lens. Once the beam has passed through the lens it produces a spot of radius R_1 on a fluorescent screen at E_1 (see figure 3.1 below). The screen is then moved to a new position E_2 a distance D away from E_1 , where the radius of the spot is R_2 .

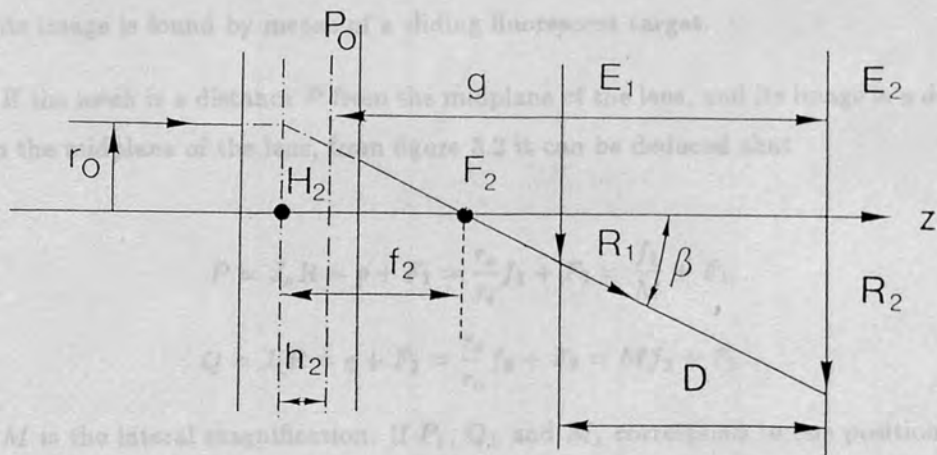


figure 3.1 (from Grivet 1972, figure 32)

It is now possible to deduce the semi-aperture β of the beam, and the 'image' focal length f_2 , i.e.,

$$\tan \beta \approx \beta = \frac{R_2 - R_1}{D} \quad (3.1)$$

$$f_2 = \frac{r_o}{\beta} = \frac{r_o D}{R_2 - R_1}$$

The position of the 'image' principal plane H_2 is a distance h_2 from the reference plane P_0 , whose position is arbitrary, but will be positioned, for convenience, in the symmetry plane of a symmetrical lens. h_2 is then given by

$$h_2 = H_2 P_0 = H_2 F_2 - P_0 F_2$$

and as $f_2 = H_2 F_2$,

$$h_2 = f_2 - (P_0 E_2 - F_2 E_2)$$

denoting the distance $P_0 E_2$ as g , and noting that $F_2 E_2 = R_2 / \tan \beta$ gives finally

$$h_2 = f_2 - \left(g - \frac{R_2}{\tan \beta} \right)$$

The lens is then turned round, leaving the plane P_0 fixed, so that values for f_1 and h_1 can be deduced. Once values for f_1 , f_2 , F_1 and F_2 have been found, it is possible, (see Chapter One) to deduce the position of all the cardinal points of the lens, and hence its paraxial properties.

A second method (Epstein 1936, Klemperer 1953, Klemperer and Barnett 1971) involves the illumination with electrons of a wire mesh target which acts as an object, where its image is found by means of a sliding fluorescent target.

If the mesh is a distance P from the midplane of the lens, and its image is a distance Q from the midplane of the lens, from figure 3.2 it can be deduced that

$$P = J_o R = p + F_1 = \frac{r_o}{r_i} f_1 + F_1 = \frac{f_1}{M} + F_1$$

$$Q = J_i R = q + F_2 = \frac{r_i}{r_o} f_2 + F_2 = M f_2 + F_2$$

where M is the lateral magnification. If P_1 , Q_1 and M_1 correspond to one position of the wire mesh, the resultant position of its image on the fluorescent target, and the subsequent magnification, and P_2 , Q_2 and M_2 correspond to a second position of the wire mesh, etc, it follows that

$$f_1 = \frac{P_1 - P_2}{\frac{1}{M_1} - \frac{1}{M_2}} \quad (3.1a)$$

$$f_2 = \frac{Q_1 - Q_2}{M_1 - M_2} \quad (3.1b)$$

$$F_1 = \frac{B_2 M_1 - B_1 M_2}{M_2 - M_1} \quad (3.11)$$

$$F_2 = \frac{B_1 M_1 - B_2 M_2}{M_2 - M_1} \quad (3.12)$$

A third method devised by Klemperer, Wright, Klemperer and Wright (1949, Klemperer 1953, Klemperer and Barrett 1957) is a 'pepper-pot diagram' to select a series of narrow pencil rays from an initial pencil beam, which then pass through the electron lens under investigation. The emerging pencil rays which are once again travelling in straight lines, (i.e., having escaped the lens), are then detected with a detector. The detector target has target spots on the back of the target and their mutual separations are measured by means of a calibrated microscope. The cardinal points of the lens are deduced from the separation of these spots by extrapolation of straight lines back through the lens, i.e., see Figure 3.2.

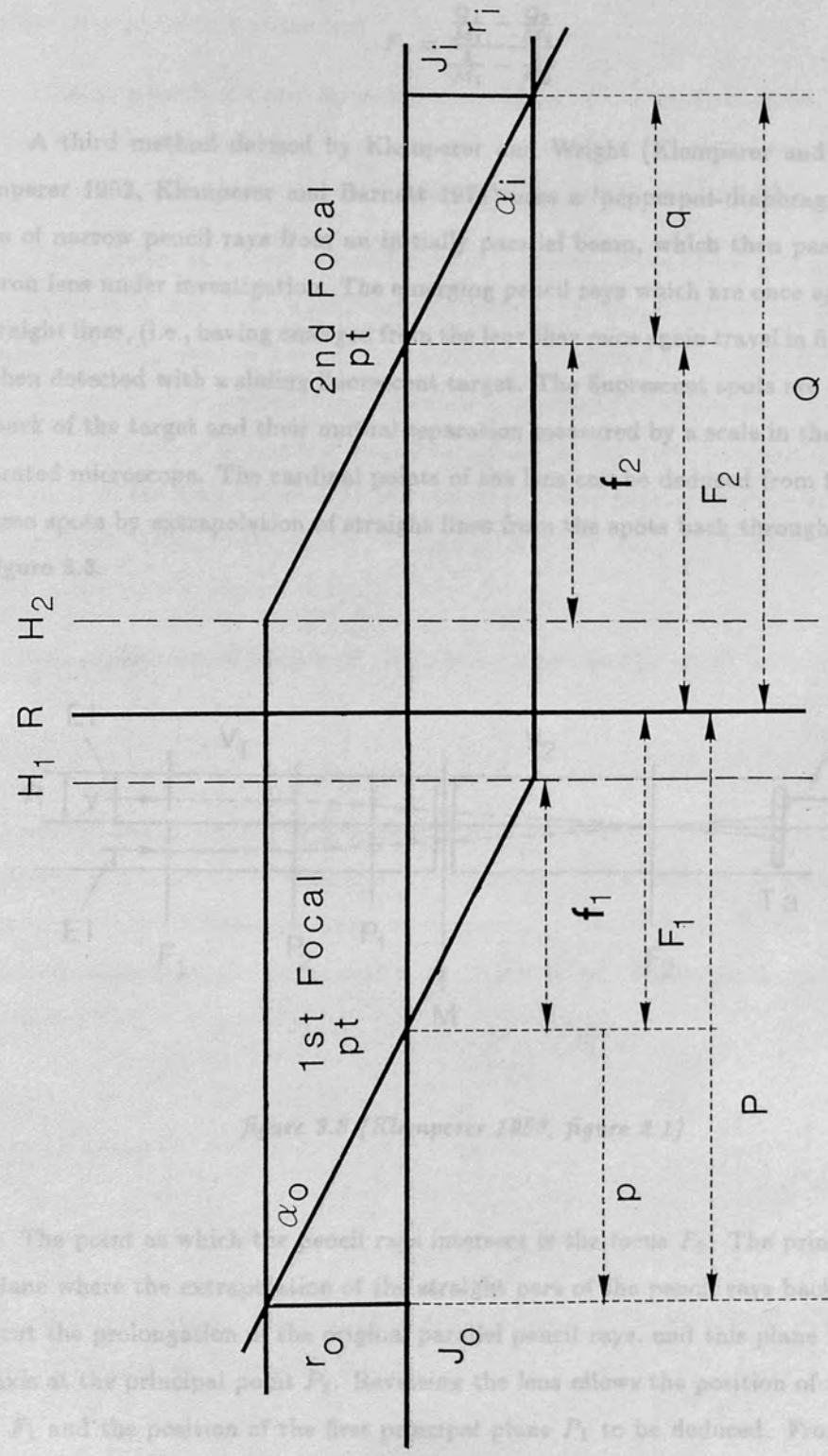


Figure 3.2

The point at which the pencil ray intersects the vertical axis is the point F_1 . The principal plane is the plane where the extrapolation of the straight parts of the pencil rays back through the lens, cut the prolongation of the optical axis of the lens, and this plane intersects the lens axis at the principal point F_1 . Reversing the lens allows the position of the first focal point F_1 and the position of the first principal plane H_1 to be deduced. From F_1 , H_1 , F_2 and H_2 , the position of the nodal points N_1 and N_2 can be deduced, hence the location of all the cardinal points of a lens can be found, and the paraxial properties of the lens can be deduced. Using the 'pepper-pot diagram', parallel pencils of marginal rays can be

$$F_1 = \frac{P_1 M_1 - P_2 M_2}{M_1 - M_2} \quad (3.1c)$$

$$F_2 = \frac{\frac{Q_1}{M_1} - \frac{Q_2}{M_2}}{\frac{1}{M_1} - \frac{1}{M_2}} \quad (3.1d)$$

A third method devised by Klemperer and Wright (Klemperer and Wright 1939, Klemperer 1953, Klemperer and Barnett 1971) uses a 'pepperpot-diaphragm' to select a series of narrow pencil rays from an initially parallel beam, which then pass through the electron lens under investigation. The emerging pencil rays which are once again travelling in straight lines, (i.e., having emerged from the lens they once again travel in field free space) are then detected with a sliding fluorescent target. The fluorescent spots are observed from the back of the target and their mutual separation measured by a scale in the eyepiece of a calibrated microscope. The cardinal points of the lens can be deduced from the separation of these spots by extrapolation of straight lines from the spots back through the lens, i.e., see figure 3.3.

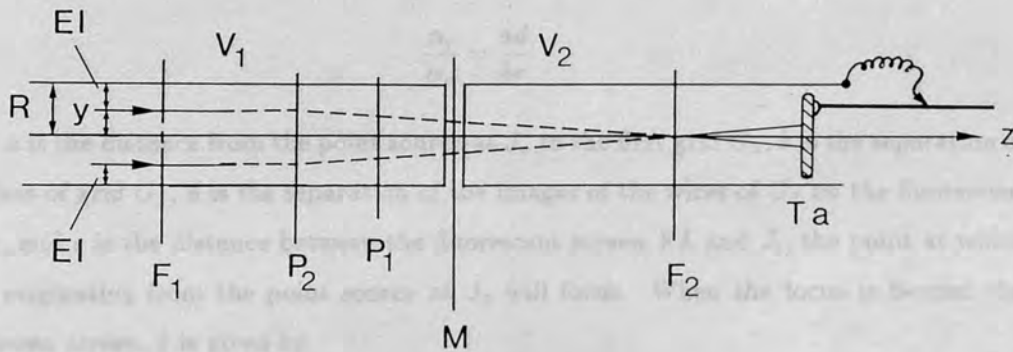


figure 3.3 (Klemperer 1953, figure 2.1)

The point at which the pencil rays intersect is the focus F_2 . The principal plane is the plane where the extrapolation of the straight part of the pencil rays back through the lens, cut the prolongation of the original parallel pencil rays, and this plane intersects the lens axis at the principal point P_2 . Reversing the lens allows the position of the first focal point F_1 and the position of the first principal plane P_1 to be deduced. From F_1 , P_1 , F_2 and P_2 , the position of the nodal points N_1 and N_2 can be deduced, hence the location of all the cardinal points of a lens can be found, and the paraxial properties of the lens can be deduced. Using the 'pepper-pot diaphragm', parallel pencils of marginal rays can be

produced, allowing the 'third order, fifth order, . . .' properties of the lens to be investigated, where the 'third order, fifth order, . . .' properties of the lens are commonly referred to as the aberration properties of the lens.

Finally, a method based upon the observation of the shadows of two grids G_1 and G_2 , which are illuminated by a point source and placed in front of and behind respectively the lens being investigated, was used by Spangenberg and Field (1942,1948), see figure 3.4.

The grids are composed of parallel wires, where the wires of one grid are perpendicular to the wires of the other, so that their shadows on the target (fluorescent screen), can be distinguished from one another. The method uses equation 3.1, i.e., in order to determine f_1 , f_2 , F_1 and F_2 it is necessary to find two sets of associated values of the object distance P , the image distance Q and the magnification M for the same lens voltage ratio V_f/V_i . In this method the magnification M is deduced from the angular magnification M_α , using Lagrange's rule $MM_\alpha = (V_i/V_f)^{1/2}$, where M_α is found using the images of the grids G_1 and G_2 in the manner described below.

The angular magnification M_α is given by α_i/α_o and for small angles (see figure 3.4)

$$\frac{\alpha_i}{\alpha_o} = \frac{ad}{bc}$$

where a is the distance from the point source at J_o to the first grid G_1 , b is the separation of the wires of grid G_1 , d is the separation of the images of the wires of G_1 on the fluorescent screen, and c is the distance between the fluorescent screen FL and J_i , the point at which a ray originating from the point source at J_o will focus. When the focus is beyond the fluorescent screen, c is given by

$$c = \frac{e}{1 - \frac{s}{g}}$$

For focus between G_2 and the fluorescent screen

$$-c = \frac{e}{1 + \frac{s}{g}}$$

where s is the separation of the wires of grid G_2 and g is the separation of the images of the wires of G_2 on the fluorescent screen.

3.3 INTRODUCTION TO EXPERIMENTAL METHODS USED IN THE PRESENT WORK

The following is concerned with the description of the 'apparatus' used in the present work to investigate the properties of electron lenses. The basic components, i.e., the lens elements, used to build a given lens are described, and this is followed by a description of the techniques used which allow the lens properties to be determined.

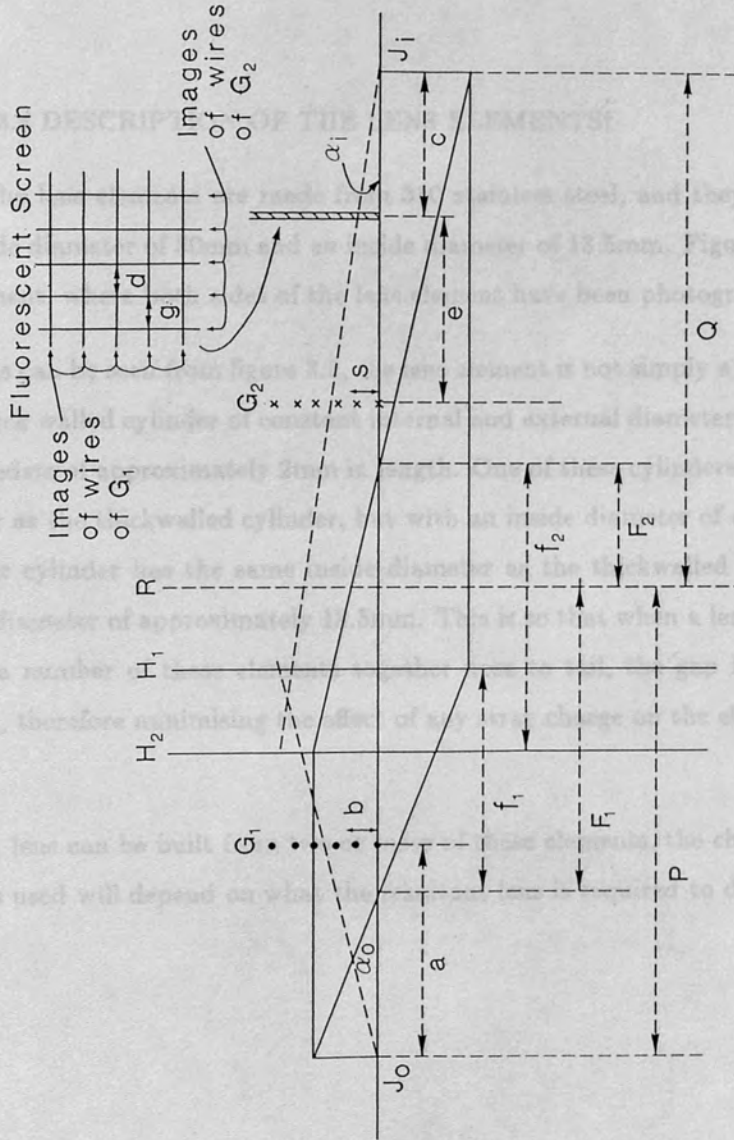


Figure 3.4 (Spangenberg and Field 1942, figure 2)

References: Hechle and Kurek 1970

3.3 INTRODUCTION TO EXPERIMENTAL METHODS USED IN THE PRESENT WORK

The following is concerned with the description of the 'apparatus' used in the present work to investigate the properties of electron lenses. The basic components, i.e., the lens elements, used to build a given lens are described, and this is followed by a description of the techniques used which allow the lens properties to be determined.

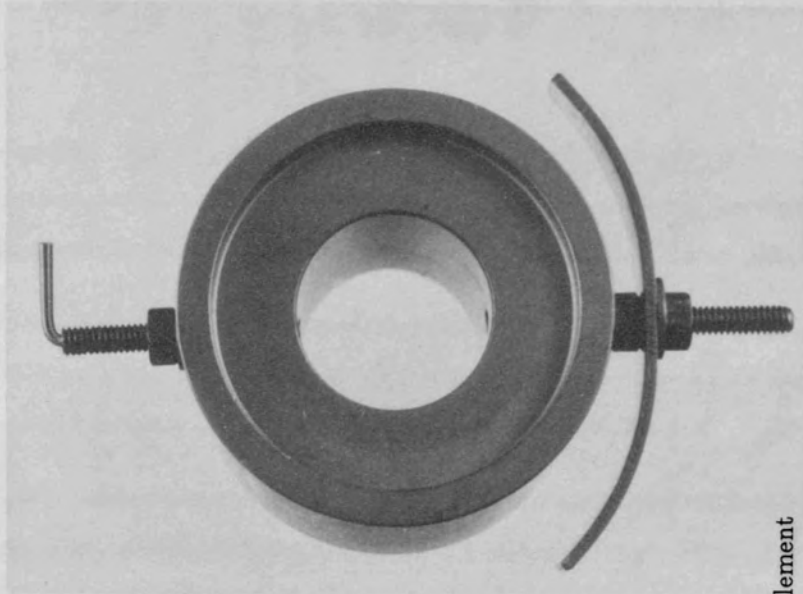
3.4 DESCRIPTION OF THE LENS ELEMENTS†

The lens elements are made from 310 stainless steel, and they are cylindrical with an outside diameter of 30mm and an inside diameter of 13.5mm. Figure 3.5 shows a typical lens element, where both sides of the lens element have been photographed.

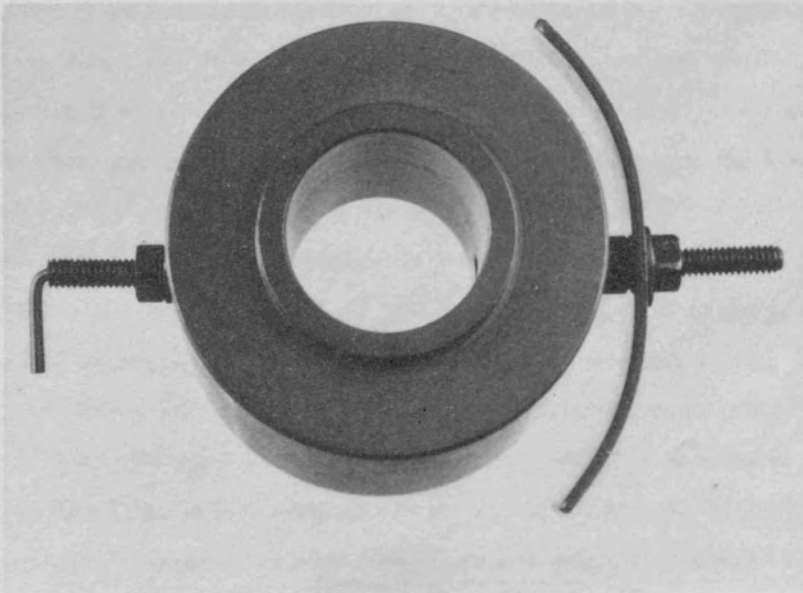
As can be seen from figure 3.5, the lens element is not simply a thick walled cylinder, but a thick walled cylinder of constant internal and external diameter, sandwiched between two cylinders of approximately 2mm in length. One of these cylinders has the same outside diameter as the thickwalled cylinder, but with an inside diameter of approximately 26mm, the other cylinder has the same inside diameter as the thickwalled cylinder but with an outside diameter of approximately 18.5mm. This is so that when a lens is constructed from placing a number of these elements together nose to tail, the gap between them can be screened, therefore minimising the effect of any stray charge on the electric field within the gap.

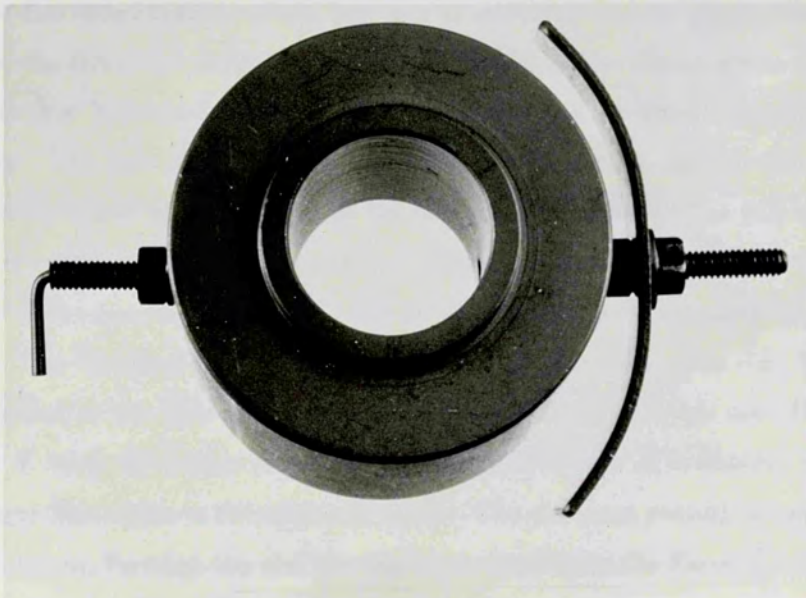
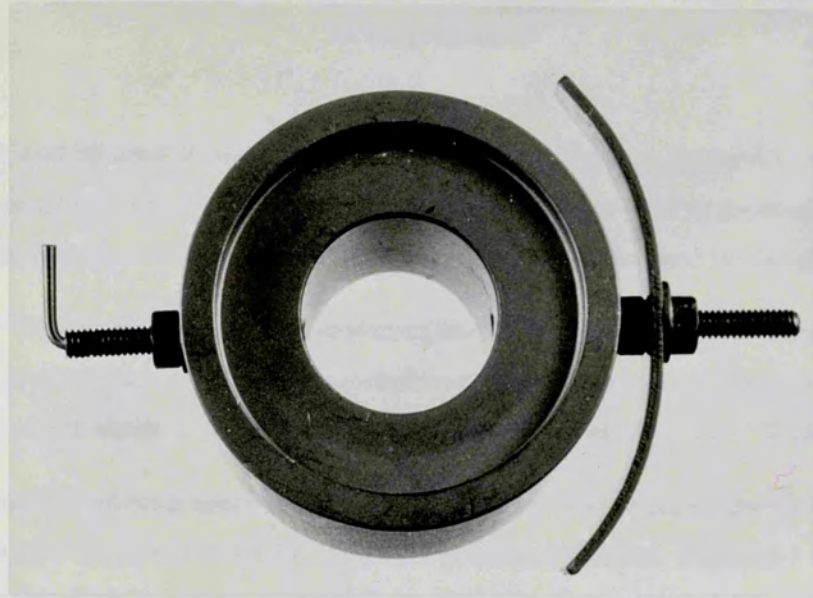
A lens can be built from two or more of these elements, the choice of the number of elements used will depend on what the resultant lens is required to do.

† References : Heddle and Kurepa 1970



A Typical Lens Element
Figure 9.5





3.5 DESCRIPTION OF THE METHOD USED TO DETERMINE THE FOCAL AND MAGNIFICATION PROPERTIES OF A LENS

A. Lens System‡

The system used to measure the focal and magnification properties of a given lens, basically consists of the lens itself, an oxide coated flat cathode used to produce the electrons, and a Faraday cup to collect the electrons once they have traversed the length of the lens.

The lens system is aligned by mounting the lens elements on a pair of parallel ceramic rods supported on a stainless or aluminium frame. The lens system is then contained within a mumetal shield inside a vacuum system at pressures below 2.0×10^{-6} Torr.

Figure 3.6 shows a typical lens system, where the lens being studied is a five-element lens, the properties of which will be described in a future chapter. Figure 3.7 is a schematic diagram of the same lens system, showing the location of the aperture discs and deflection plates whose presence enable the properties of the lens to be measured.

Figure 3.7 shows the location of the aperture discs (see figure 3.8) and deflection plates, (figure 3.9 shows deflection plates mounted inside a lens element) whose use enable a picture to be displayed on the screen of an display scope when the lens is focussed. From this picture the magnification of the lens can be deduced. A pair of apertures in the disc **X** (refer to the schematic diagram, figure 3.7) located at the object plane of the lens, are imaged onto disc **Y** located on the image plane of the lens, in which there is a second pair of apertures. The pair of apertures of disc **X** are arranged so that the line joining their centres is vertical and at right angles to the optic axis of the lens. The pair of apertures of disc **Y** are arranged so that the line joining their centres is at right angles to the line joining the centres of the apertures of disc **X**, i.e., horizontal and at right angles to the optic axis of the lens. The image of the two apertures of disc **X** is scanned over disc **Y** by scanning voltages applied to the deflection plates. Electrons will pass through one of the apertures in the disc **Y** when the image of one of the apertures of disc **X** is scanned across it, and this will occur four times in the course of a scan. The electrons passing through disc **Y** are collected in a deep Faraday cup and the resultant signal from the Faraday cup is then used to modulate the intensity of the picture displayed on an display scope when the scanning voltages are applied to its X and Y plates. The picture consists of four dots sited on the

‡ References : Heddle and Kurepa 1970, Heddle et al 1982

corners of a rectangle; the magnification can be deduced from the ratio of the separation of the dots in the X direction to that of the separation of the dots in the Y direction, (see figure 3.10).

B. Electronics

A block diagram of the power supplies, scanning unit, amplifiers, etc used to operate the lens, and display and analyse the 'image' from the lens is given in figure 3.11.

1. Power Supplies

The voltages to the individual lens elements and to the Faraday cup are derived from floating stabilised power supplies, (stabilised to 0.1% of the output voltage) designed and built in the department's electronics workshop. The power supplies produced voltages of between 0 and 700 volts which could float at a common voltage of between -1000 and 1000 volts. The power supplies were built so that they could float so that it would be possible to have the Faraday cup at 'earth' potential, and the cathode therefore at a negative potential and the power supplies which supply the voltages to the lens elements floating at the cathode potential.

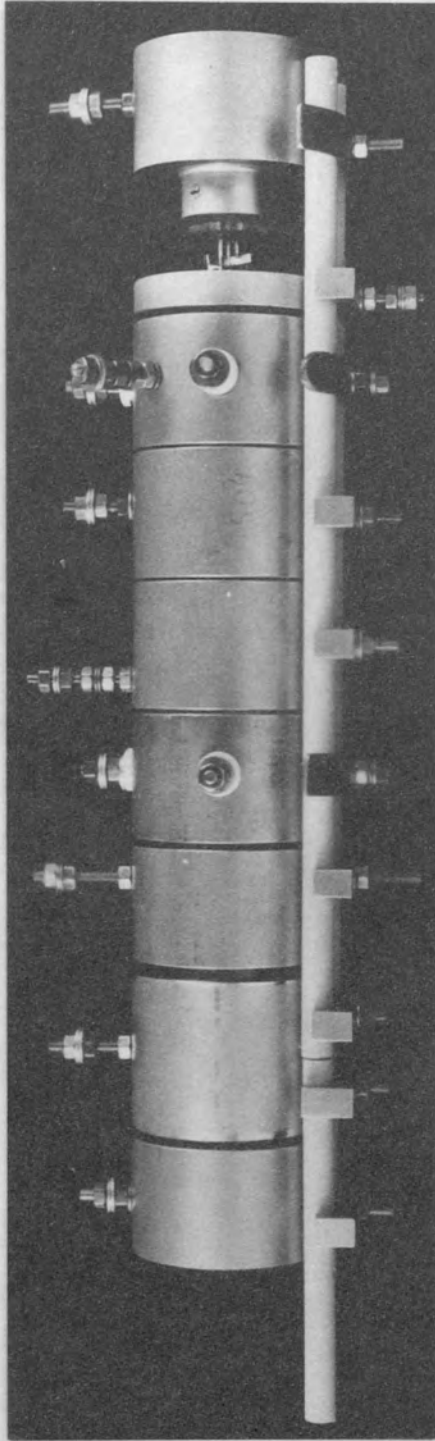
2. Scanning Unit

The scanning unit supplies a 'fast' ramp at 1KHz to the x -deflection plates of one of the lens elements, (the first element in the case of the disc lens described in chapter six, the third element in the case of the five-element lens described in chapter five) and a 'slow' ramp at 10Hz to the y -deflection plates of the same lens element. Great care was taken to ensure that the **magnitudes** of the x and y ramps were **the same**, so that the deflection of the electrons would be the same in both the x and y directions. The magnitude of the ramps could be set at between 7 and 30 volts. The x and y ramps both float at the DC voltage applied to the lens element in which the deflection plates are sited. Both ramps were also applied to the x and y plates respectively of the display scope.

It was also possible to apply small DC offset voltages of between -12 and 12 volts to the deflection plates to 'steer' the electron beam if required. In the five-element lens described in chapter five, in addition to the deflection plates incorporated into the third element of the lens, to which the scanning voltages were applied, a further set of deflection plates were contained within the first element; small DC deflection voltages could be applied

FIVE - ELEMENT ELECTROSTATIC LENS.

Faraday Cup →
Elements
Containing
Deflection Plates →
Electrode at
Cathode → Potential



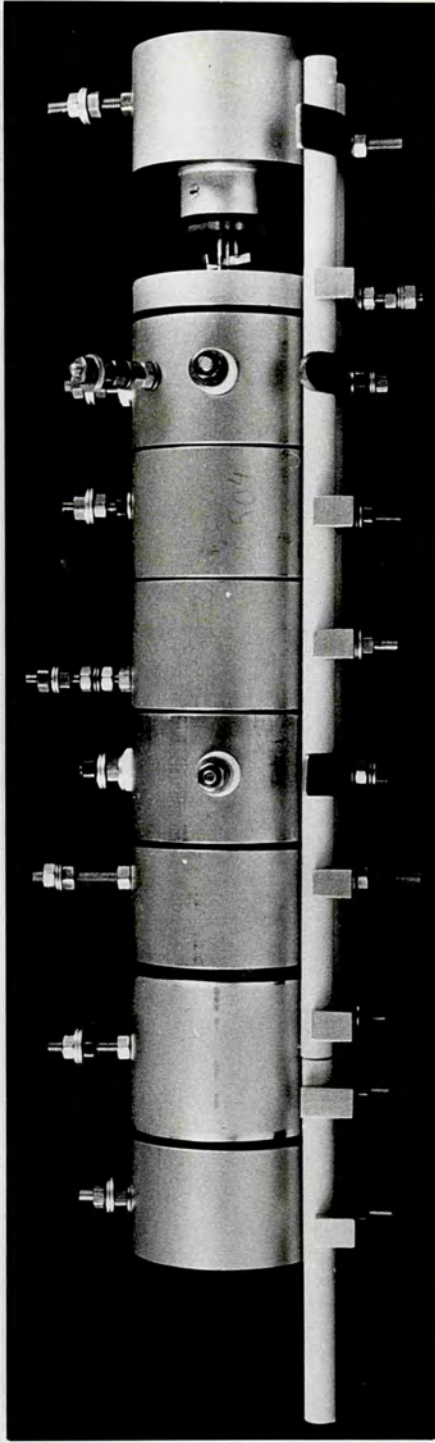
5th 4th 3rd 2nd 1st
Cathode

Elements of Lens

Figure 3.6

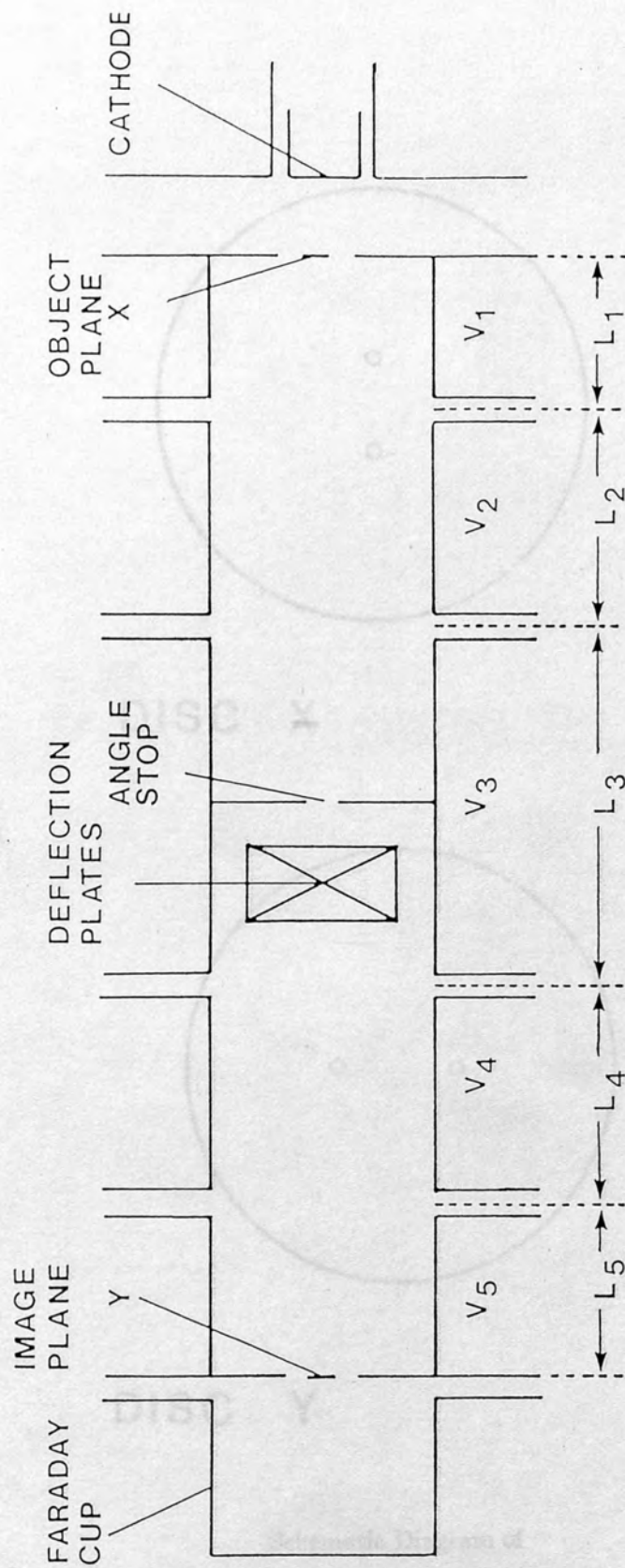
FIVE - ELEMENT ELECTROSTATIC LENS.

Faraday Cup →
Elements Containing Deflection Plates →
Electrode at Cathode Potential →



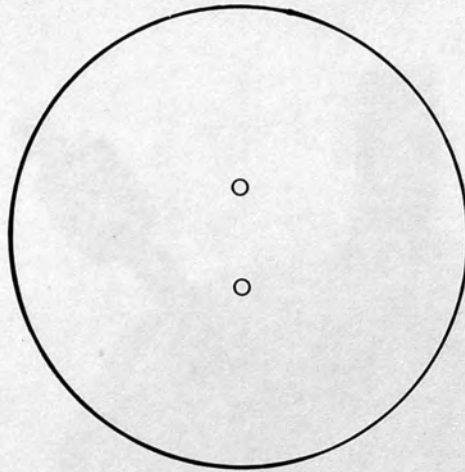
5th 4th 3rd 2nd 1st Cathode

Elements of Lens

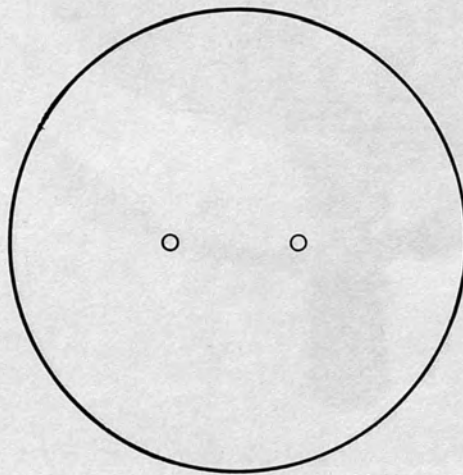


Schematic Diagram of Five-element Lens System

Figure 3.7



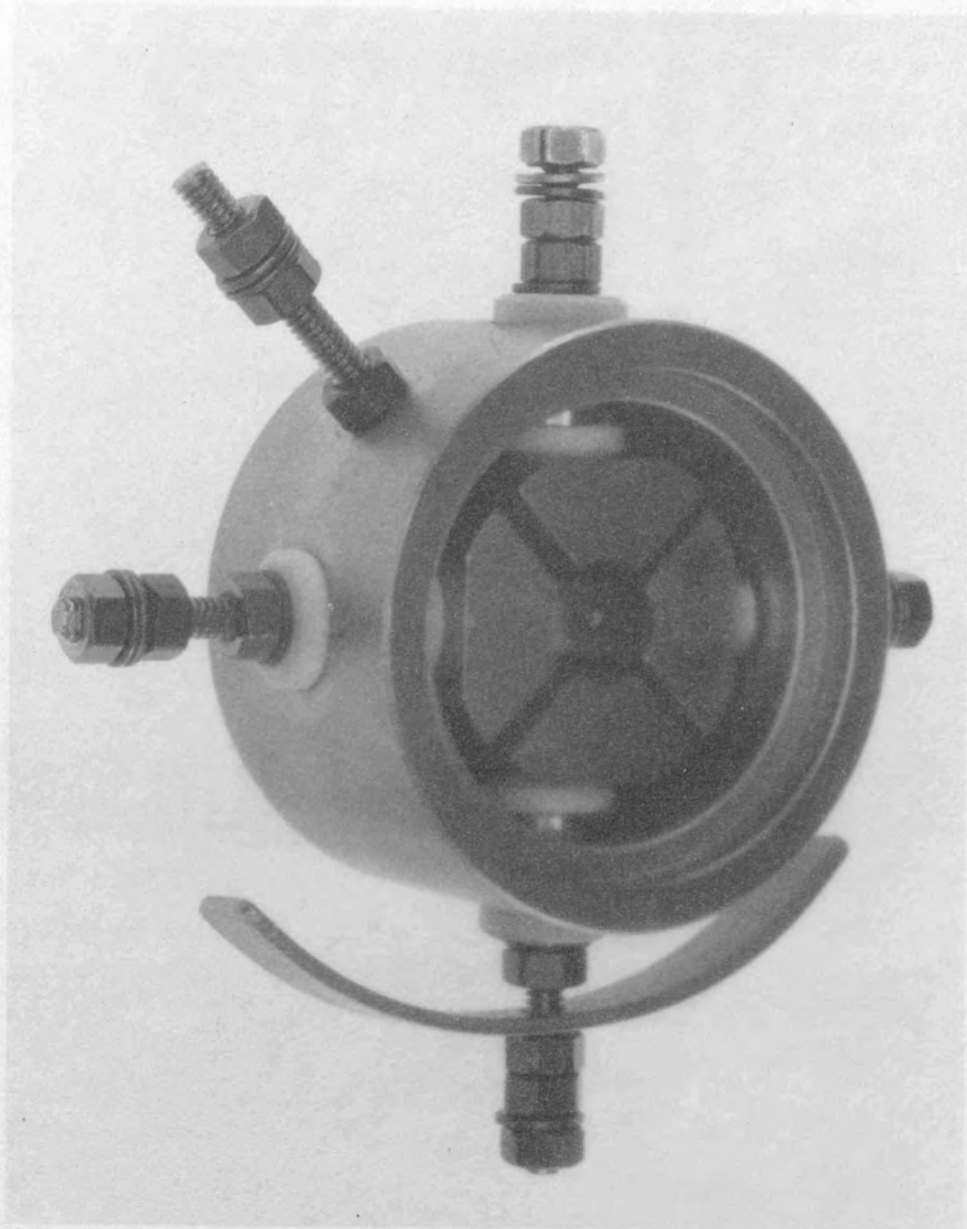
DISC X



DISC Y

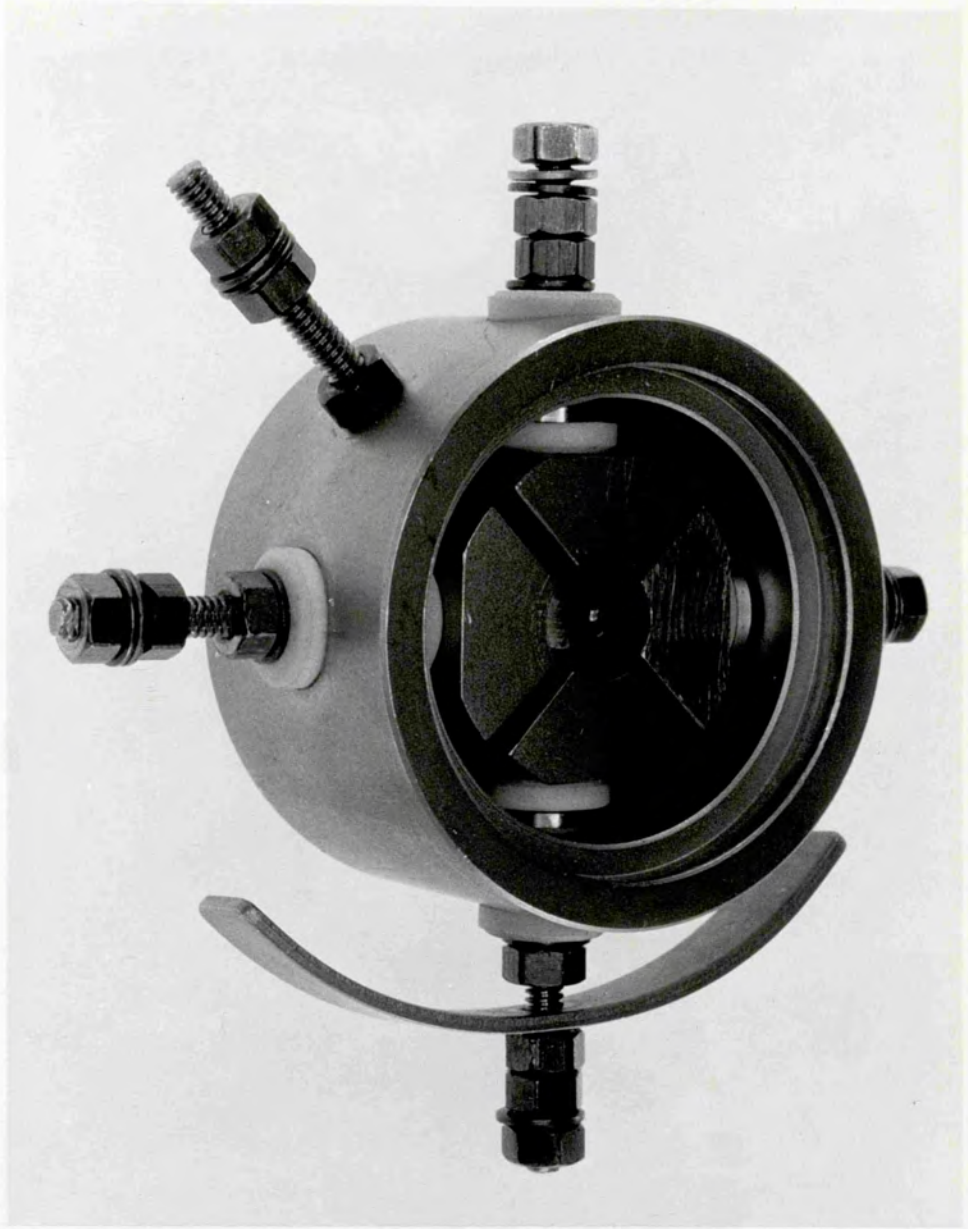
Schematic Diagram of
Aperture Discs

figure 3.8



A Lens Element with
Deflection Plates

figure 3.9



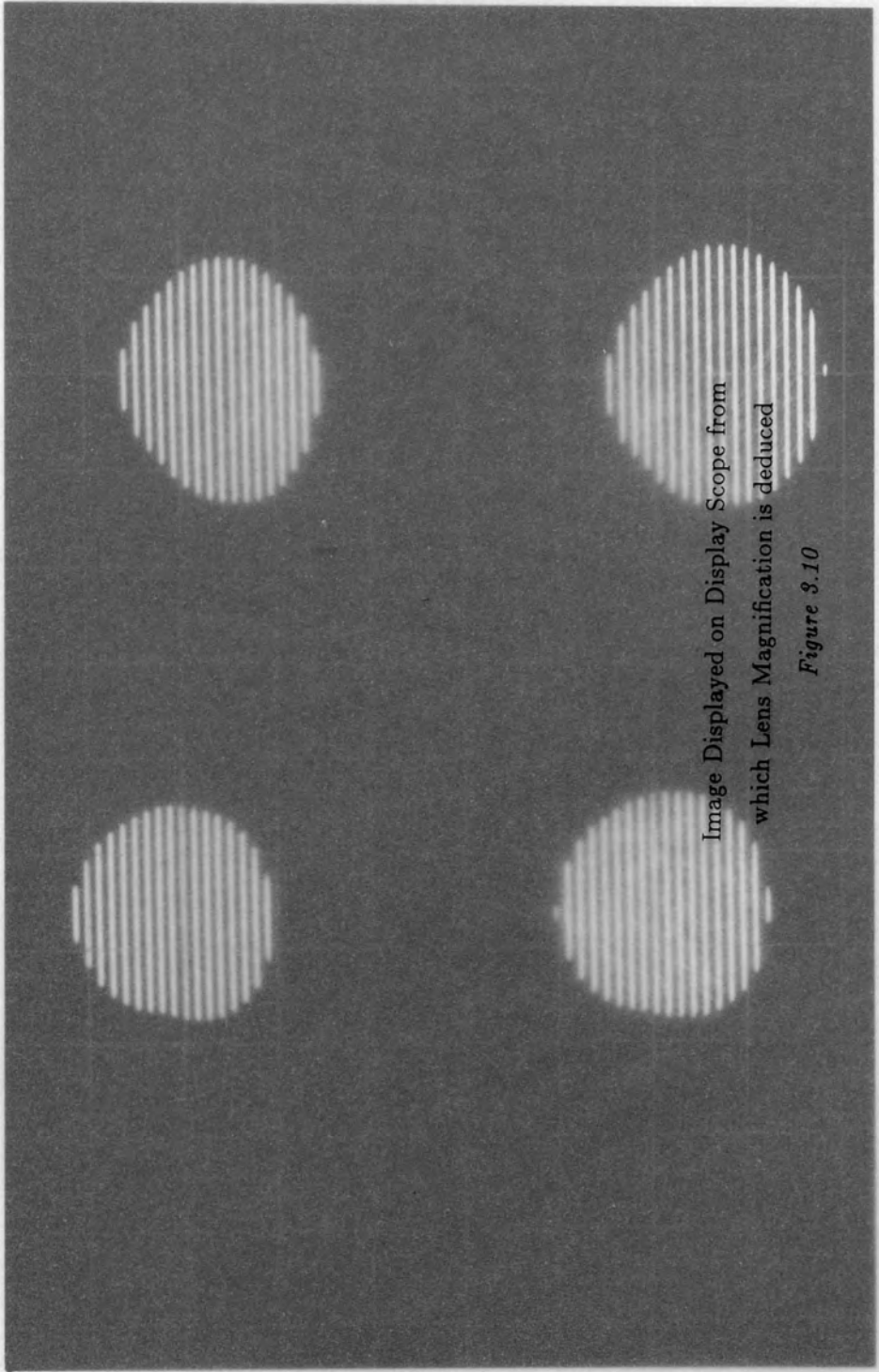
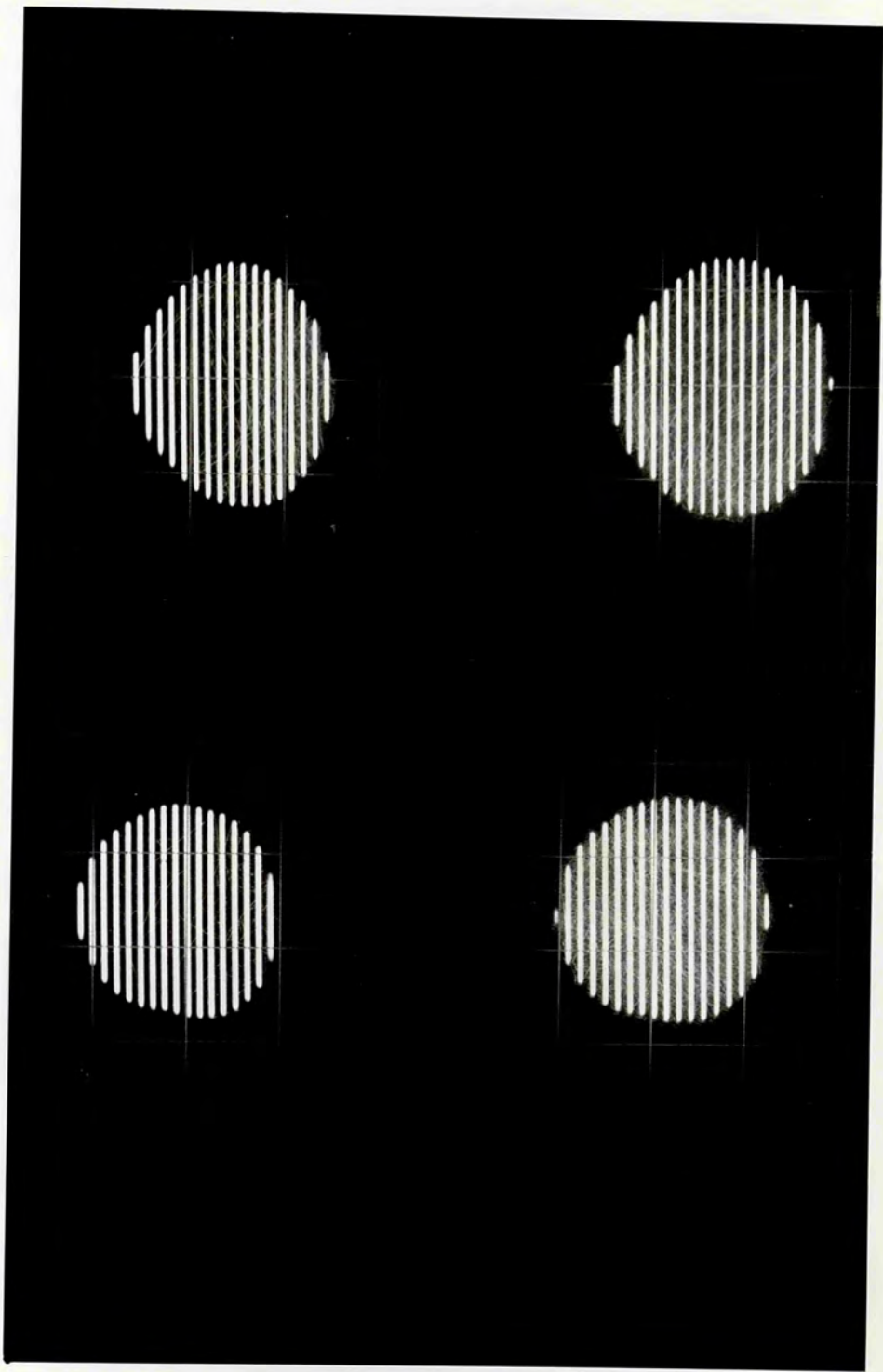
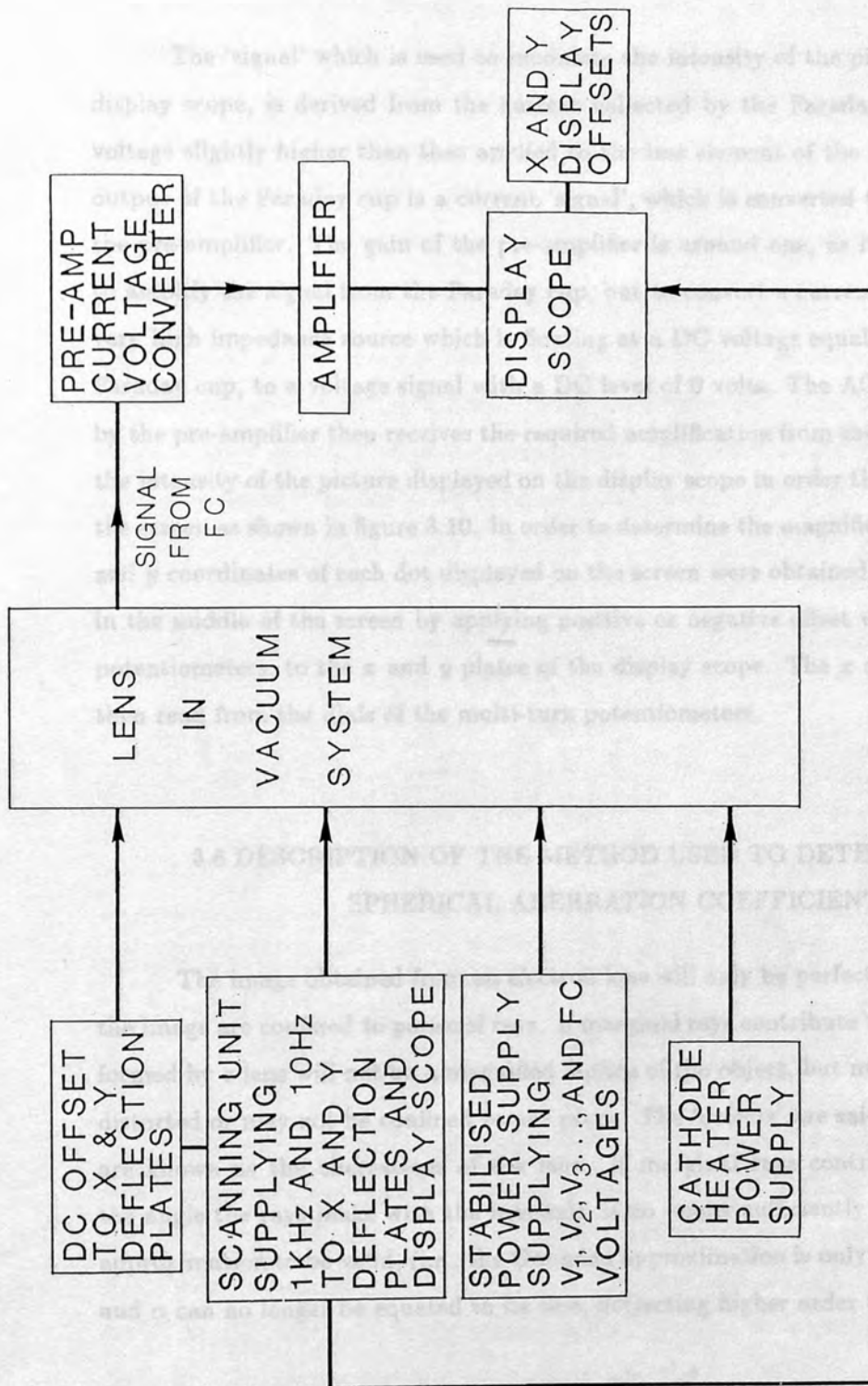


Image Displayed on Display Scope from
which Lens Magnification is deduced

Figure 9.10





Block Diagram of Electronics
Figure 8.11

to these plates for added control of the electron beam.

3. Pre-amplifier, Amplifier and Display Scope

The 'signal' which is used to modulate the intensity of the picture displayed on the display scope, is derived from the current collected by the Faraday cup, which sits at a voltage slightly higher than that applied to the last element of the lens (≥ 20 volts). The output of the Faraday cup is a current 'signal', which is converted to a voltage 'signal' by the pre-amplifier. The gain of the pre-amplifier is around one, as its main purpose is not to amplify the signal from the Faraday cup, but to convert a current signal coming from a very high impedance source which is floating at a DC voltage equal to that applied to the Faraday cup, to a voltage signal with a DC level of 0 volts. The AC voltage signal output by the pre-amplifier then receives the required amplification from the amplifier to modulate the intensity of the picture displayed on the display scope in order that four dots appear on the screen as shown in figure 3.10. In order to determine the magnification of the lens, the x and y coordinates of each dot displayed on the screen were obtained. Each dot was centred in the middle of the screen by applying positive or negative offset voltages, via multi-turn potentiometers, to the x and y plates of the display scope. The x and y coordinates were then read from the dials of the multi-turn potentiometers.

3.6 DESCRIPTION OF THE METHOD USED TO DETERMINE THE SPHERICAL ABERRATION COEFFICIENT

The image obtained from an electron lens will only be perfect if the rays which form the image are confined to paraxial rays. If marginal rays contribute to the image, the image formed by a lens will not be a magnified replica of the object, but may for example, appear distorted or may not be confined to one plane. The 'defects' are said to be caused by what are known as the aberrations of the lens. If marginal rays contribute to the image, α , the angle the rays make with the lens axis, is no longer sufficiently small for the Gaussian approximation to be valid, (i.e., the Gaussian approximation is only valid for paraxial rays) and α can no longer be equated to its sine, neglecting higher order terms in the expansion,

$$\sin\alpha = \alpha - \frac{\alpha^3}{3!} + \frac{\alpha^5}{5!} - \dots$$

the higher order terms must be included if an accurate description of the resultant image is to be obtained.

Aberrations are referred to as third-order aberrations, fifth-order aberrations, etc, depending on which term in the above expansion they are a consequence of. Only third-order aberrations will be considered here, as their effect is sufficiently large in comparison to the fifth-order aberrations for the fifth-order aberrations to be neglected. The total 'error' of a point on the image due to third-order aberrations, can be expressed as a number of terms in a series, the separate terms are named individually, after the similar aberrations which occur with glass lenses. For electrostatic lenses there are five third-order aberrations just as there are for glass lenses, and these are spherical aberration, distortion, curvature of field, astigmatism and coma.

Spherical aberration is the most important of the third-order errors mainly because it is the only geometric defect which occurs even for axial objects, and it is the aberration whose effect is investigated in the present work. The effect of this aberration on the image of an axial point P is illustrated in figure 3.12 below.

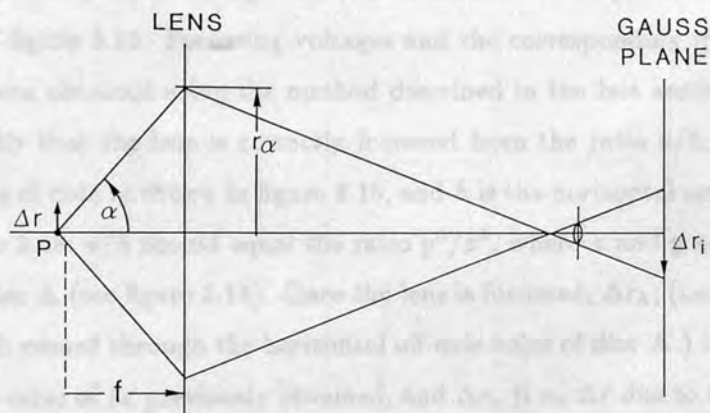


figure 3.12

The power of the lens is greater for rays the larger the distance r_α at which they pass through the lens. Rays contained within the launch angle α i.e., the angle at which rays leave the lens axis at the object plane, are spread over a disc of radius Δr_i at the image plane, where $\Delta r_i \propto r_\alpha$. The point P therefore appears to have an apparent diameter $\Delta r = \Delta r_i/M$, where M is the magnification. Now, $r_\alpha \propto \alpha$ and therefore to third order $\Delta r \propto \alpha^3$. Writing the constant of proportionality as C_s ,

$$\Delta r = C_s \alpha^3$$

In order to obtain the spherical aberration coefficient C_s it is necessary to determine Δr and α , and they are obtained in the manner described below.

Figure 3.13 is a schematic diagram of the lens system used to obtain Δr by experiment for a five-element lens.

In the lens denoted by the schematic diagram of figure 3.13 the single hole in the disc **X** located at the object plane of the lens will be imaged onto the disc **Y** located at the image plane of the lens. If there is a pair of apertures in disc **Y** and the image of this single hole is scanned across disc **Y** in the manner described in the last section, a picture of two dots will be obtained on the display scope screen. If however, the rays which traverse the lens from the object to form the image at **Y** encounter a further disc **A** in which there are five apertures arranged as shown in figure 3.14, the image of the single hole of disc **X** will appear as five dots in the image plane, as the rays constrained to pass through the off-axis holes of disc **A** will form an image in the image plane which is displaced from the true image by a distance dictated by the degree of aberration suffered by the rays forming the image. If this image of five dots is scanned across the pair of apertures located in the image plane, a picture like that depicted in figure 3.15 will be obtained. It is not possible to determine at precisely what voltages the lens is focussed from pictures on the display scope like that of figure 3.15. Focussing voltages and the corresponding magnification M must first have been obtained using the method described in the last section. However, it is possible to verify that the lens is correctly focussed from the ratio v/h , where v is the vertical separation of dots as shown in figure 3.15, and h is the horizontal separation of dots as shown in figure 3.15. v/h should equal the ratio y^3/x^3 , where x and y are separation of the holes in the disc **A** (see figure 3.14). Once the lens is focussed, Δr_h , (i.e., Δr due to the off-axis rays which passed through the horizontal off-axis holes of disc **A**) is then found by dividing h by the value of M previously obtained, and Δr_v (i.e., Δr due to the off-axis rays which passed through the vertical off-axis holes of disc **A**) is found by dividing v by M .

The launch angle α is equal to the ratio r_a/L , where r_a is the distance a ray launched at an angle of α unaffected by any lens action, (see figure 3.16) will cross a plane P_a perpendicular to the lens axis. L is the distance of the plane P_a from the object plane.

Now,

$$\alpha = \frac{r_a}{L} = \frac{r_c}{L} \times \left(\frac{r_a}{r_c}\right)$$

r_c is the distance at which a ray launched at α under the influence of the lens, will cross the plane P_a . In the present case r_c equals the distance of the off axis holes (either x or y) from the lens axis. The ratio r_a/r_c is deduced from ray tracing using the Fox-Goodwin method described in the last chapter.

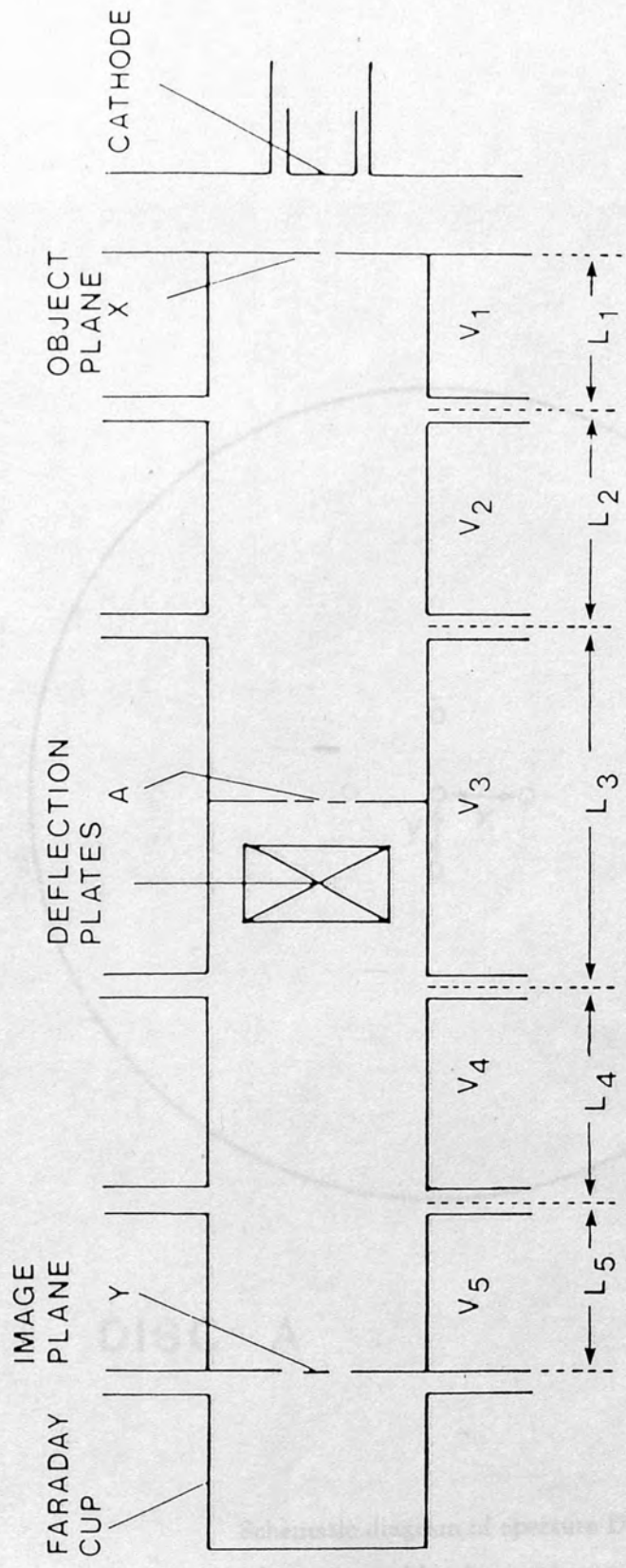
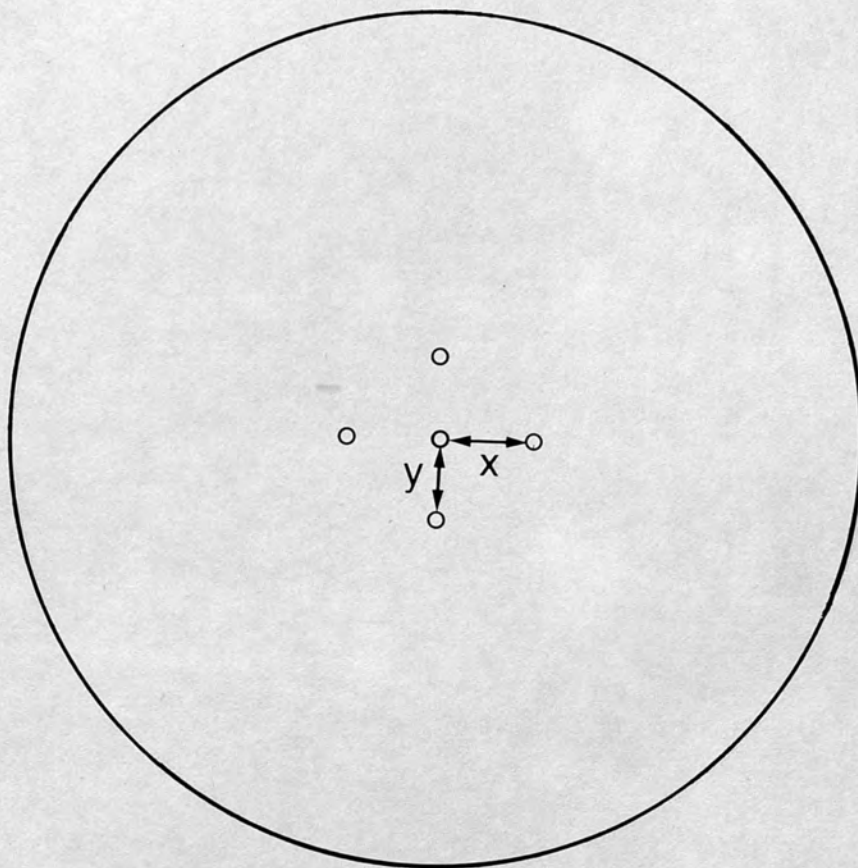


Figure 3.13



DISC A

Schematic diagram of aperture Disc
whose use enables Δr and hence C_s

to be determined

figure 3.14

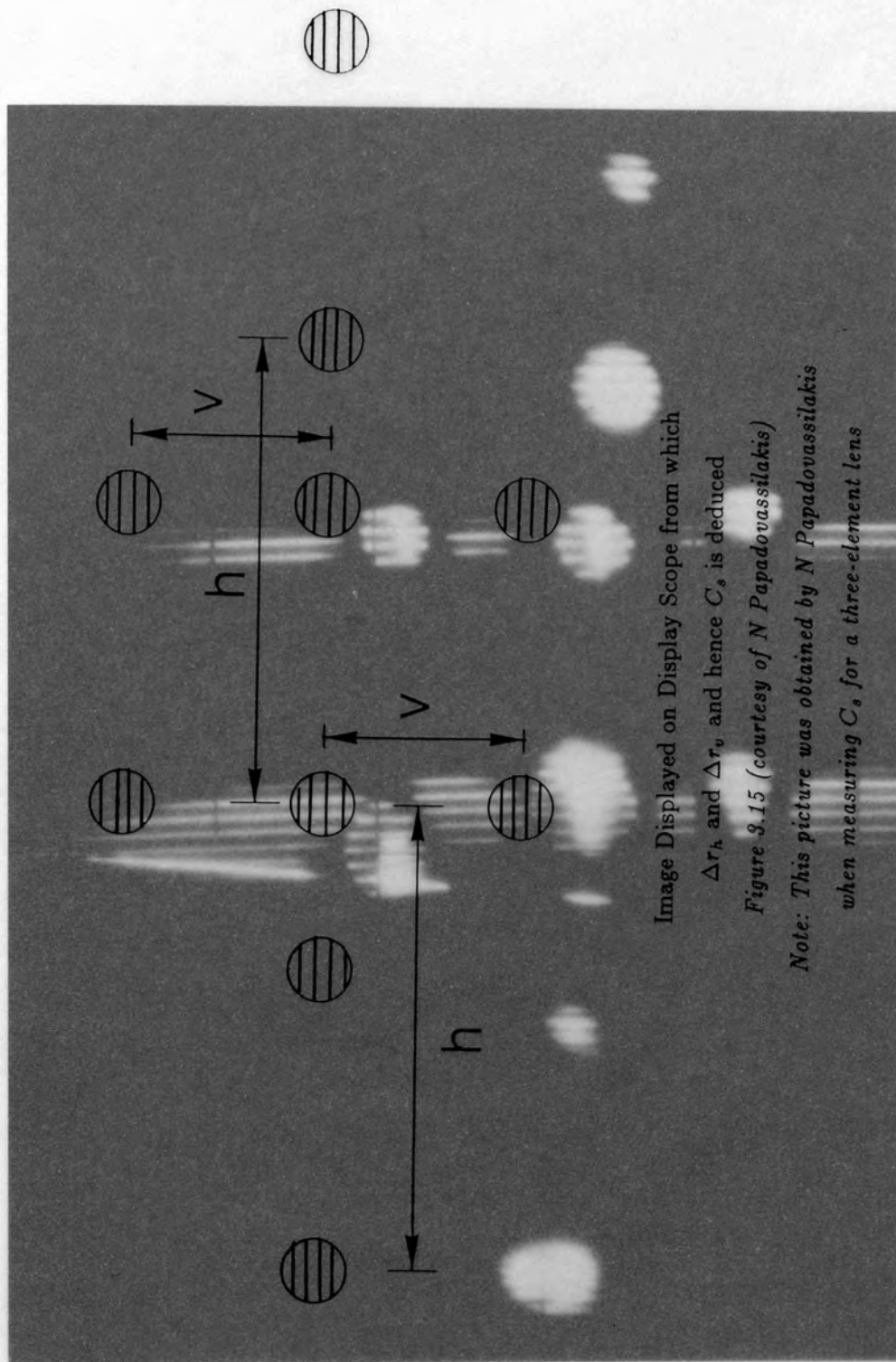
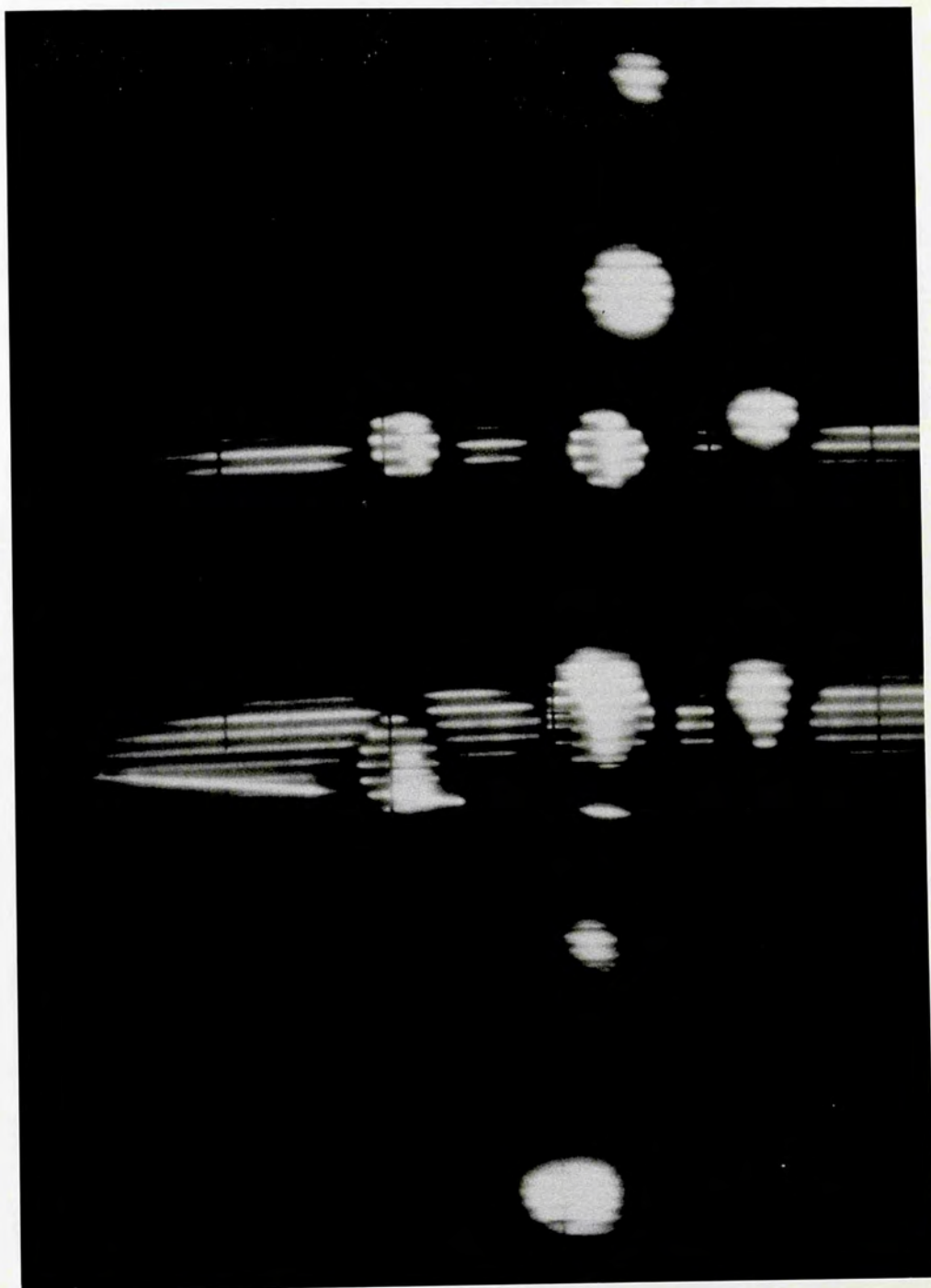


Image Displayed on Display Scope from which

Δr_h and Δr_v and hence C_s is deduced

Figure 9.15 (courtesy of N Papadovassilakis)

Note: This picture was obtained by N Papadovassilakis
when measuring C_s for a three-element lens



REFERENCES, CHAPTER THREE

Epstein D W 1936 Electron Optical System of Two Cylinders as applied to Cathode-Ray Tubes *Proc. Inst. Radio Eng.* 23 1275-1279

Griest P 1973 *Electron Beams and Tubes* (2nd Ed. 1973) (Pergamon: Oxford)

Heddie D W D and Heddie M V 1959 The focal properties of three-element electrostatic electron lenses. *Proc. R. Soc. London* 252A

Heddie D W D, Pappasovitch M and Heddie M V 1962 Measurement of the magnification behaviour of some magnetic and electrostatic lenses. *Phys. J: Sci Instrum.* 35 1210-1213

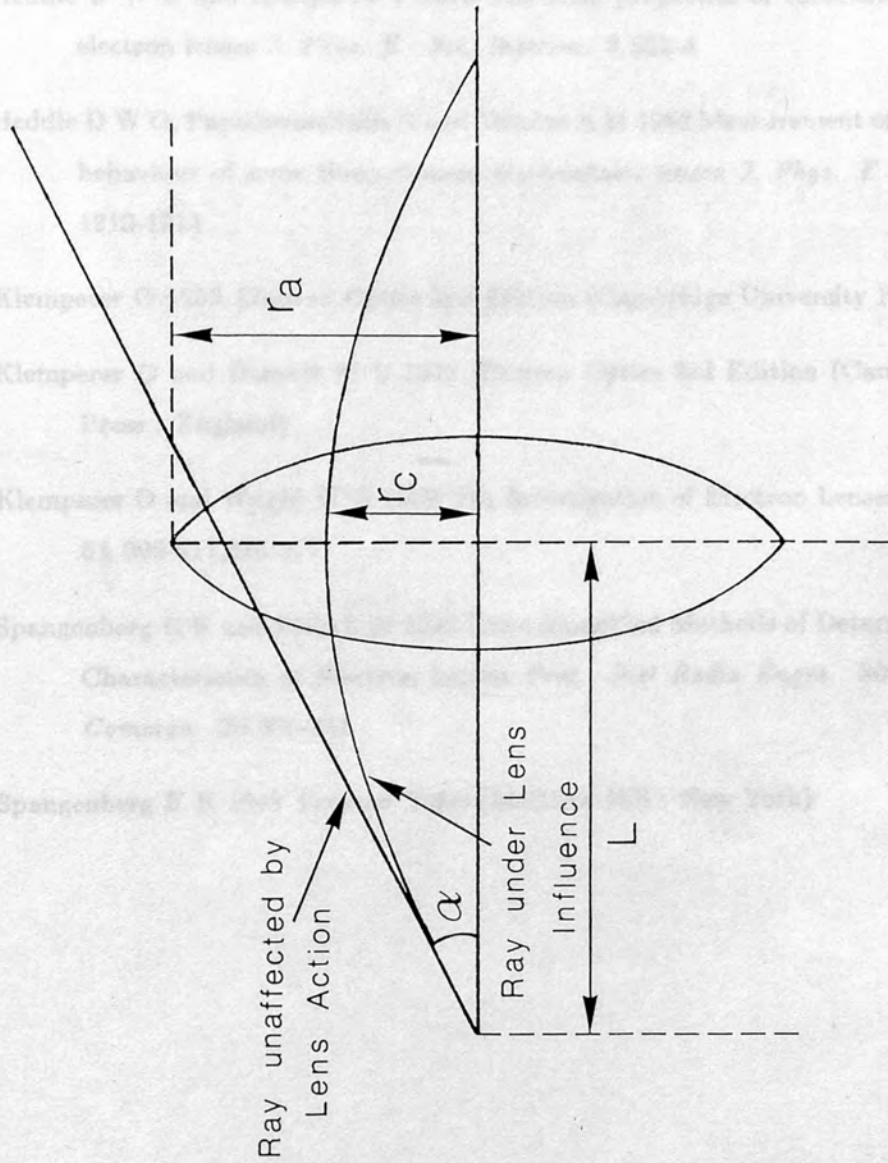
Klemperer O 1958 *Electron Optics* (Cambridge University Press: England)

Klemperer O 1962 *Electron Optics* 2nd Edition (Cambridge University Press: England)

Klemperer O 1963 *Electron Optics* (Cambridge University Press: England)

Spangenberg K R 1948 *Electron Optics* (McGraw-Hill: New York)

Spangenberg K R 1954 *Electron Optics* (McGraw-Hill: New York)



PLANE Pa
Figure 3.16

REFERENCES : CHAPTER THREE

- Epstein D W 1936 Electron Optical System of Two Cylinders as applied to Cathode-Ray Tubes *Proc. Inst. Radio Engrs* **24** 1095-1139
- Grivet P 1972 *Electron Optics* 2nd Edition (1st Ed. 1965) (Pergamon : Oxford)
- Heddle D W O and Kurepa M V 1970 The focal properties of three-element electrostatic electron lenses *J. Phys. E : Sci. Instrum.* **3** 552-4
- Heddle D W O, Papadovassilakis N and Yateem A M 1982 Measurement of the magnification behaviour of some three-element electrostatic lenses *J. Phys. E : Sci Instrum.* **15** 1210-1213
- Klemperer O 1953 *Electron Optics* 2nd Edition (Cambridge University Press : England)
- Klemperer O and Barnett M E 1971 *Electron Optics* 3rd Edition (Cambridge University Press : England)
- Klemperer O and Wright W D 1939 The Investigation of Electron Lenses *Proc. Phys. Soc.* **51** 296-317,376-377
- Spangenberg K R and Field L M 1942 Some Simplified Methods of Determining the Optical Characteristics of Electron Lenses *Proc. Inst Radio Engrs.* **30** 138-144 & *Elect. Commun.* **20** 305-313
- Spangenberg K R 1948 *Vacuum Tubes* (McGraw-Hill : New York)

LIST OF FIGURES : CHAPTER FOUR

	Page No.
Figure 4.1 Diagram illustrating the effect and image size, angle of inclination of the object and angle of inclination at the image for a typical lens system	115
Figure 4.2 Schematic diagram of a two-focal electrostatic lens showing the focal points F_1 and F_2 , focal lengths f_1 and f_2 , principal planes H_1 and H_2 , and construction	117

CHAPTER FOUR

CALCULATION OF MULTIPLE ELEMENT LENS PROPERTIES USING MATRIX TECHNIQUES

LIST OF FIGURES : CHAPTER FOUR

	Page No
Figure 4.1 Diagram illustrating the object and image sizes, angle of inclination at the object and angle of inclination at the image for a typical lens system	115
Figure 4.2 Schematic diagram of a two-tube electrostatic lens showing the focal points F_1 and F_2 , focal lengths f_1 and f_2 , principal planes H_1 and H_2 , and coordinates p, P, q, Q in object and image space respectively	117
Figure 4.3 The dependence of the matrix elements on voltage ratio (a) for accelerating lenses (b) for decelerating lenses	121

CALCULATING LIST OF TABLES: CHAPTER FOUR PROPERTIES
USING MATRIX TECHNIQUES

	Page No
Table 4.1 Table listing Matrix Elements for an Accelerating Lens	119
Table 4.2 Table listing Matrix Elements for a Decelerating Lens	120
Table 4.3 Table comparing the values obtained for V_2/V_1 using the Matrix and Bessel Function Expansion Methods for the symmetric three-element einzel lens, where $L_2 = L_3 = 2.0D$ and $0.5 \leq L_1 \leq 2.0D$	123

Typically, in either light or electron optics

$$\begin{pmatrix} r_i \\ \alpha_i \end{pmatrix} = \begin{pmatrix} A_{11} & A_{12} \\ A_{21} & A_{22} \end{pmatrix} \begin{pmatrix} r_o \\ \alpha_o \end{pmatrix} \quad (4.1)$$

where r_o and r_i are the object and image sizes respectively, α_o is the inclination of the ray leaving the object, and α_i is the inclination of the ray arriving at the image, (see figure 4.1)

The matrix $\begin{pmatrix} A_{11} & A_{12} \\ A_{21} & A_{22} \end{pmatrix}$ is known as the object-image matrix, and as illustrated by equation (4.1) transforms a ray with position and angle coordinates (r_o, α_o) to a ray with coordinates (r_i, α_i) .

A_{11} is equal to the lateral magnification M ,

A_{12} equals zero,

A_{21} is equal to $-n_o/f = -n_i/f'$, where n_o and n_i are the refractive indices of the media of object and image space respectively, and $-f$ and f' are the corresponding focal lengths,

A_{22} is equal to the angular magnification M' .

Note that in light optics, the media of object space and image space respectively, are, in most cases, the same, usually air, so that the refractive indices are the same, i.e.

$$n_o = n_i = 1$$

so that,

$$A_{21} = -1/f = -1/f'$$

therefore,

$$-f = f'$$

CALCULATION OF MULTIPLE ELEMENT LENS PROPERTIES USING MATRIX TECHNIQUES

Matrices may be used to calculate the imaging and focal properties of electron and/or ion lenses, and can therefore be a powerful tool in the design of electron/ion lens systems. In the present work, the parameters of lenses of three or more elements have been calculated by a process of matrix multiplication, using matrix elements calculated by DiChio et al (1974a) for two-element lenses. The physical principles involved are similar to those used in light optics, and are outlined below.

Typically, in either light or electron optics

$$\begin{pmatrix} r_i \\ \alpha_i \end{pmatrix} = \begin{pmatrix} A_{11} & A_{12} \\ A_{21} & A_{22} \end{pmatrix} \begin{pmatrix} r_o \\ \alpha_o \end{pmatrix} \quad (4.1)$$

where r_o and r_i are the object and image sizes respectively, α_o is the inclination of the ray leaving the object, and α_i is the inclination of the ray arriving at the image, (see figure 4.1).

The matrix $\begin{pmatrix} A_{11} & A_{12} \\ A_{21} & A_{22} \end{pmatrix}$ is known as the object-image matrix, and as illustrated by equation (4.1) transforms a ray with position and angle coordinates (r_o, α_o) to a ray with coordinates (r_i, α_i) .

A_{11} is equal to the lateral magnification M ,

A_{12} equals zero,

A_{21} is equal to $-n_o/f = n_i/f'$, where n_o and n_i are the refractive indices of the media of object and image space respectively, and $-f$ and f' are the corresponding focal lengths,

A_{22} is equal to the angular magnification M_α .

Note that in light optics, the media of object space and image space respectively, are, in most cases, the same, usually air, so that the refractive indices are the same, i.e.,

$$n_o = n_i = 1$$

so that,

$$A_{21} = -\frac{1}{f} = \frac{1}{f'}$$

therefore,

$$-f = f'$$

As shown in Chapter 3, the angle subtended by the object is $\alpha_i = (h/f)$ and in this case, as $|h| = |f'|$, Lagrange's relation $h h' = -f f'$ gives the angular magnification as therefore equal to the reciprocal of the lateral magnification, i.e., $M_{\alpha} = M_L = 1/M$.

In electron optics, as in geometrical optics, the electron beam for an optical lens, it is rare to find an electron lens which is a single element. An electron lens typically consists of a number of curved thin plates or rods, which are held in position by a supporting structure. The electric field within the lens is produced by the potential difference which the electron travels. The electric field varies along the length of the lens, the nature of this variation being dependent on the geometry of the lens. For an electron lens the overall ratio for the values of n_o and n_i is given by $n_o/n_i = V_o/V_i$ is the voltage applied to the first element of the lens and V_i/V_o is the voltage applied to the last element. Therefore the overall magnification M is also equal to this ratio.

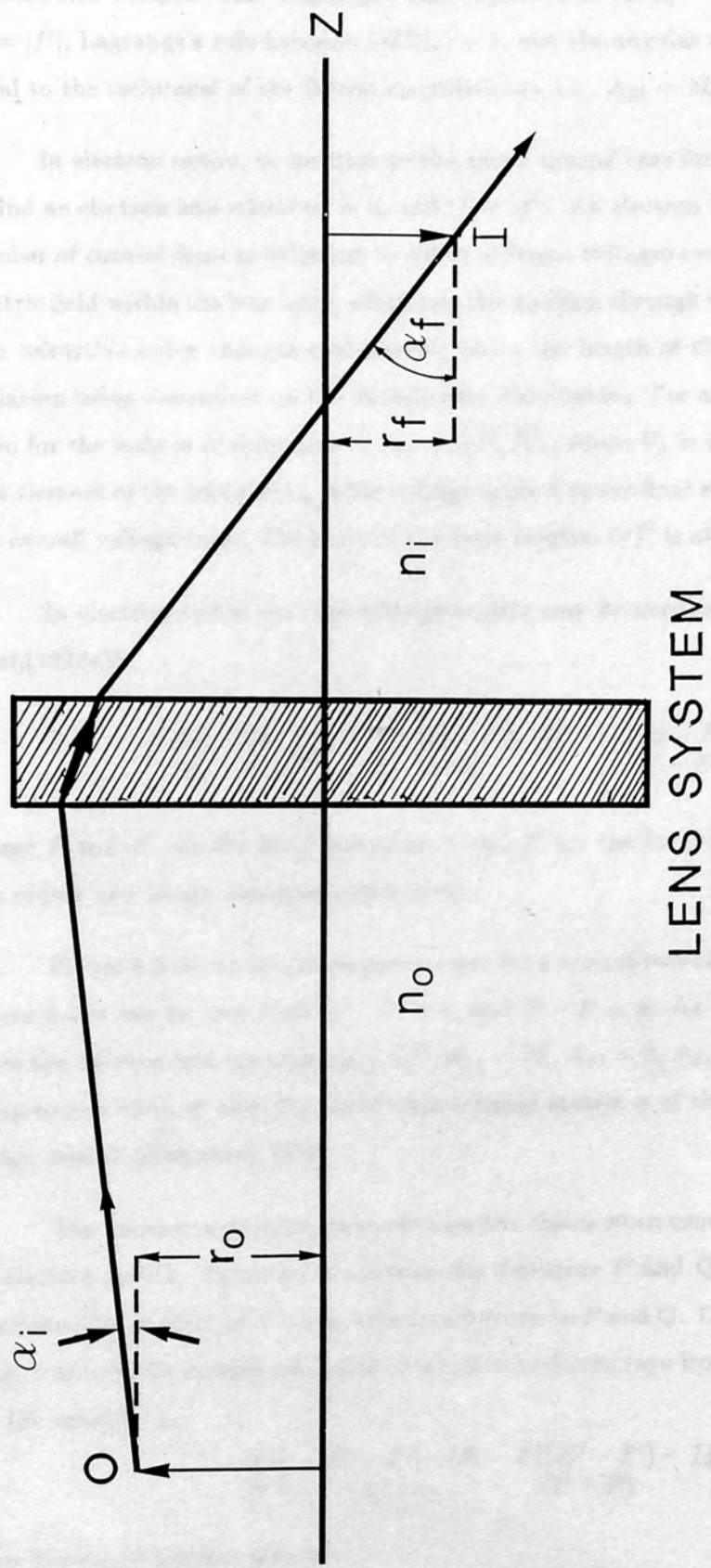


Figure 4.1

As shown in Chapter One, Lagrange's rule implies that $MM_\alpha = f/f'$ and in this case, as $|f| = |f'|$, Lagrange's rule becomes $|MM_\alpha| = 1$, and the angular magnification is therefore equal to the reciprocal of the lateral magnification, i.e., $A_{22} = M_\alpha = 1/M$.

In electron optics, in contrast to the above typical case for an optical lens, it is rare to find an electron lens where $n_o = n_i$ and $|f| = |f'|$. An electron lens typically consists of a number of coaxial discs or cylinders to which different voltages can be applied, the resulting electric field within the lens being effectively the medium through which the electrons travel. The refractive index changes continuously along the length of the lens, the nature of this variation being dependent on the electric field distribution. For an electron lens the overall ratio for the indices of refraction $n_i/n_o = \sqrt{V_n/V_1}$, where V_1 is the voltage applied to the first element of the lens and V_n is the voltage applied to the final element, V_n/V_1 is therefore the overall voltage ratio. The ratio of the focal lengths f/f' is also equal to this ratio.

In electron optics the object-image matrix may be expressed as follows (see DiChio et al,(1974a));

$$\begin{pmatrix} A_{11} & A_{12} \\ A_{21} & A_{22} \end{pmatrix} = \frac{1}{f'} \begin{pmatrix} -(Q - F') & (P - F)(Q - F') - ff' \\ -1 & (P - F) \end{pmatrix} \quad (4.2)$$

where F and F' are the focal distances, f and f' are the focal lengths, and P and Q are the object and image distances respectively.

Figure 4.2 shows the above parameters for a typical two-element electron lens. From figure 4.2 it can be seen that $Q - F' = q$, and $P - F = p$. As $M = -q/f' = -f/p$, and from the Newton lens equation $pq = ff'$, $A_{11} = M$, $A_{12} = 0$, $A_{21} = -1/f'$, and $A_{22} = M_\alpha$, (Lagrange's rule), so that the above object-image matrix is of the same form as the object image matrix of equation (4.1).

The above matrix is the most obvious first choice when considering the use of matrices in electron optics. However, it contains the distances P and Q , and it is more useful to represent the properties of a lens with no reference to P and Q . DiChio et al (1974a) discuss this, and initially considered a matrix which transforms rays from the first principal plane to the second, i.e;

$$\frac{1}{f'} \begin{pmatrix} -(H - F') & (H - F)(H' - F') - ff' \\ -1 & (P - F) \end{pmatrix} \quad (4.3)$$

The free space transfer matrix

$$\begin{pmatrix} 1 & \Delta Z \\ 0 & 1 \end{pmatrix} \quad (4.4)$$

would then translate rays to and from the principal planes. For entering rays $\Delta Z = P - F$, and for exiting rays $\Delta Z = Q - F'$.

However, DiChio et al (1974a) rejected this approach for two reasons, (i) the focal properties are not all included in the matrix, and (ii) for lenses for voltage ratios near unity or with very large voltage ratios F and F' become very large.

DiChio et al (1974a) instead concluded that the following matrix contained all the essential properties of the lens, it transforms entering asymptotic rays at the reference plane to exiting asymptotic rays at the reference plane.

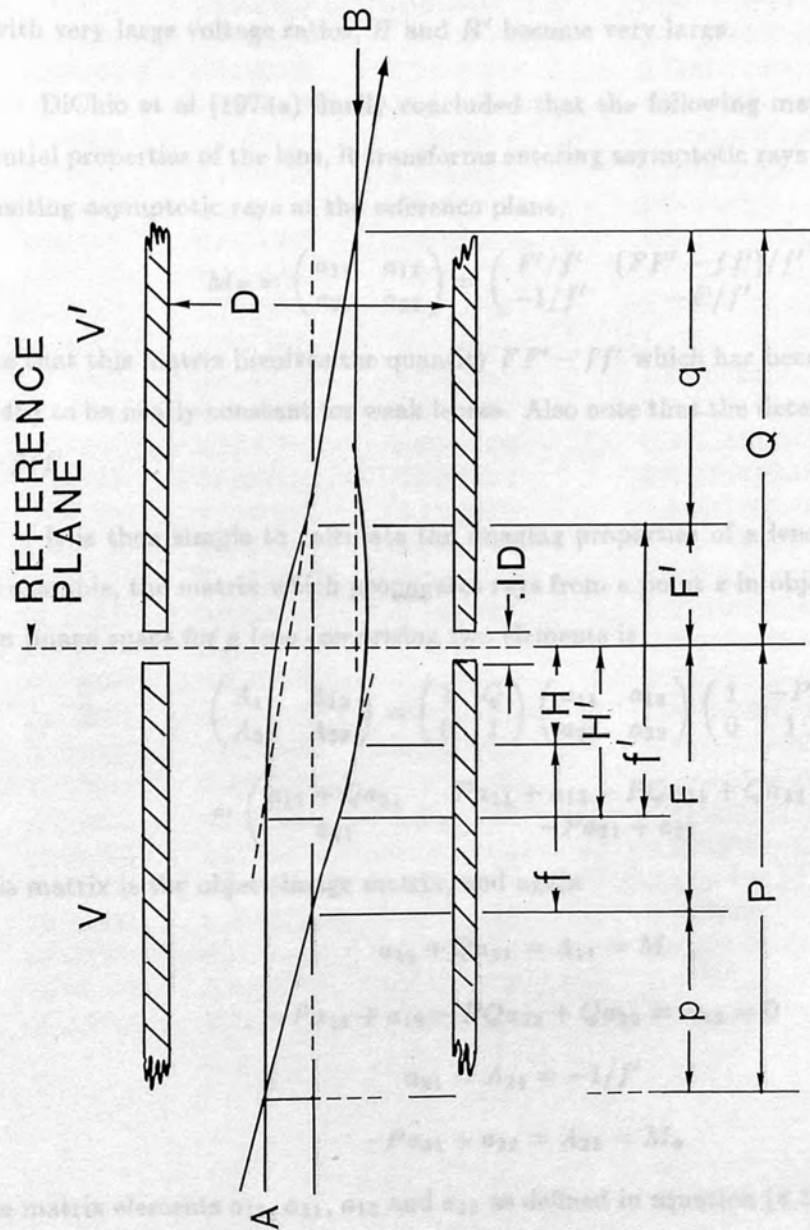


Figure 4.2 (adapted from DiChio et al 1974, figure 1)

would then translate rays to and from the principal planes. For entering rays $\Delta Z = P - F$, and for exiting rays $\Delta Z = Q - F'$.

However, DiChio et al (1974a) rejected this approach for two reasons, (i) the focal properties are not all included in the matrix, and (ii) for lenses for voltage ratios near unity or with very large voltage ratios, H and H' become very large.

DiChio et al (1974a) finally concluded that the following matrix contained all the essential properties of the lens, it transforms entering asymptotic rays at the reference plane to exiting asymptotic rays at the reference plane,

$$M_R = \begin{pmatrix} a_{11} & a_{12} \\ a_{21} & a_{22} \end{pmatrix} = \begin{pmatrix} F'/f' & (FF' - ff')/f' \\ -1/f' & -F/f' \end{pmatrix} \quad (4.5)$$

Note that this matrix involves the quantity $FF' - ff'$ which has been shown (DiChio et al 1974b) to be nearly constant for weak lenses. Also note that the determinant of the matrix is $-f/f'$.

It is then simple to calculate the imaging properties of a lens from equation (4.5). For example, the matrix which propagates rays from a point z in object space to any point z' in image space for a lens comprising two elements is

$$\begin{aligned} \begin{pmatrix} A_{11} & A_{12} \\ A_{21} & A_{22} \end{pmatrix} &= \begin{pmatrix} 1 & Q \\ 0 & 1 \end{pmatrix} \begin{pmatrix} a_{11} & a_{12} \\ a_{21} & a_{22} \end{pmatrix} \begin{pmatrix} 1 & -P \\ 0 & 1 \end{pmatrix} \\ &= \begin{pmatrix} a_{11} + Qa_{21} & -Pa_{11} + a_{12} - PQa_{21} + Qa_{22} \\ a_{21} & -Pa_{21} + a_{22} \end{pmatrix} \end{aligned} \quad (4.6)$$

This matrix is the object-image matrix, and again

$$\begin{aligned} a_{11} + Qa_{21} &= A_{11} = M \\ -Pa_{11} + a_{12} - PQa_{21} + Qa_{22} &= A_{12} = 0 \\ a_{21} &= A_{21} = -1/f' \\ -Pa_{21} + a_{22} &= A_{22} = M_\alpha \end{aligned} \quad (4.7)$$

The matrix elements a_{11} , a_{21} , a_{12} and a_{22} as defined in equation (4.5) were calculated from the focal properties of two-element lenses calculated by Harting and Read (1976) for voltage ratios of between 1.5 and 50, and from the calculated focal properties of two element lenses of DiChio et al (1974a) for voltage ratios of between 1.1 and 1.5. Tables 4.1 and 4.2 list the voltage ratios and the matrix elements calculated for accelerating and decelerating lenses respectively. Figures 4.3a and 4.3b show graphically the relationship between the matrix elements and the voltage ratio for voltage ratios up to 1000 as calculated by DiChio et al (1974a).

TABLE 4.1

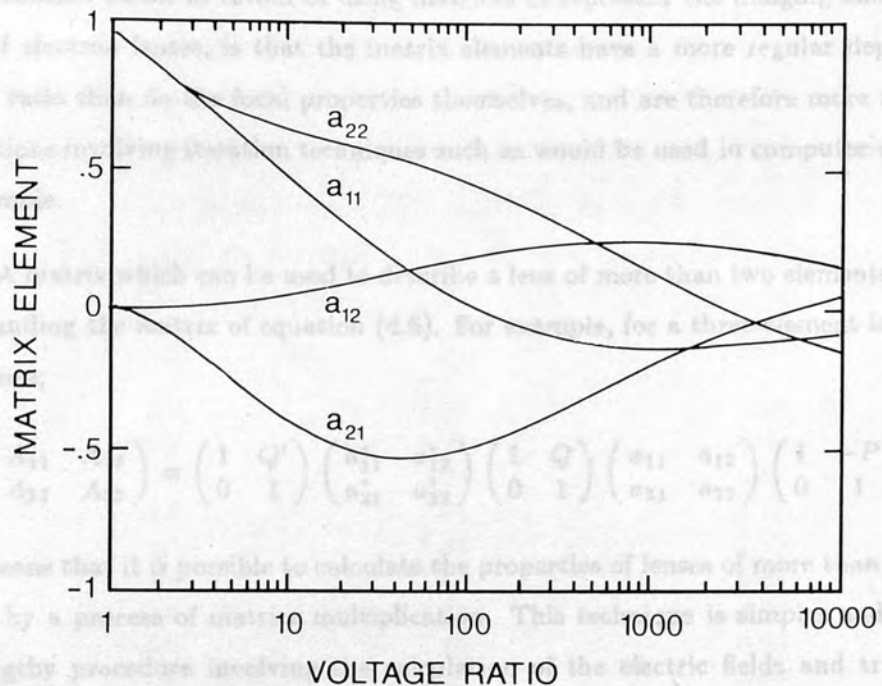
MATRIX ELEMENTS FOR AN ACCELERATING LENS

$\frac{V'}{V}$	a_{11}	a_{21}	a_{12}	a_{22}
1.000000	1.000000	0.000000E+00	0.000000E+00	1.000000
1.100000	0.9764606	-1.4383999E-03	6.8237998E-05	0.9764692
1.200000	0.9553902	-5.1453034E-03	2.4287000E-04	0.9554931
1.300000	0.9363202	-1.0429051E-02	4.9591000E-04	0.9367269
1.400000	0.9188472	-1.6808983E-02	8.0790999E-04	0.9197875
1.500000	0.9026574	-2.3940627E-02	1.1655000E-03	0.9045008
1.700000	0.8738229	-3.9566353E-02	1.9827001E-03	0.8775817
2.000000	0.8365273	-6.4308681E-02	3.3821000E-03	0.8449517
2.500000	0.7858491	-0.1048218	5.5377088E-03	0.8039832
3.000000	0.7443214	-0.1419648	9.7038122E-03	0.7738501
3.500000	0.7091801	-0.1751927	1.1454784E-02	0.7508759
4.000000	0.6786079	-0.2047083	1.3940434E-02	0.7324463
5.000000	0.6272264	-0.2544529	2.0582864E-02	0.7048346
6.000000	0.5847557	-0.2942908	2.6273474E-02	0.6848146
7.000000	0.5491990	-0.3269042	3.0691151E-02	0.6698267
8.000000	0.5180467	-0.3538570	3.5951179E-02	0.6578202
9.000000	0.4905874	-0.3765060	4.1189775E-02	0.6475904
10.00000	0.4663766	-0.3955696	4.5335460E-02	0.6392405
12.00000	0.4245524	-0.4262575	5.3756990E-02	0.6257460
14.00000	0.3890386	-0.4492363	6.2795229E-02	0.6145552
16.00000	0.3591779	-0.4670714	6.9505416E-02	0.6053246
18.00000	0.3333333	-0.4810005	7.5999990E-02	0.5974026
20.00000	0.3098869	-0.4918839	8.3135754E-02	0.5902607
22.00000	0.2892893	-0.5005005	8.8399388E-02	0.5840841
26.00000	0.2539764	-0.5130836	9.8562323E-02	0.5726014
30.00000	0.2251173	-0.5211048	0.1070985	0.5622720
34.00000	0.1998948	-0.5260389	0.1157107	0.5533929
38.00000	0.1782126	-0.5288207	0.1232628	0.5452142
42.00000	0.1595125	-0.5299417	0.1292544	0.5373609
46.00000	0.1426299	-0.5302227	0.1355127	0.5296925
50.00000	0.1275807	-0.5293806	0.1409502	0.5230280

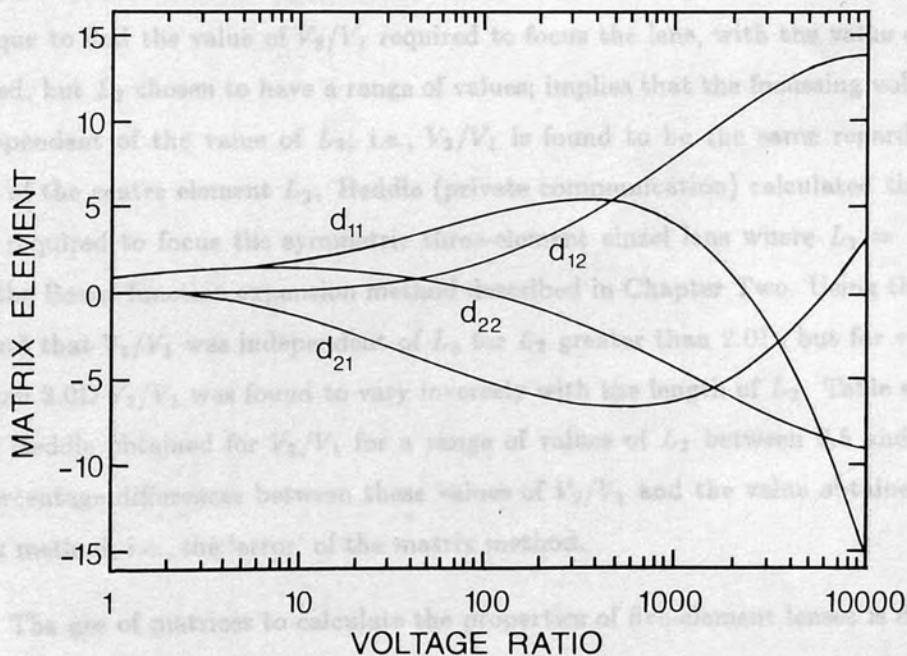
TABLE 4.2

MATRIX ELEMENTS FOR A DECELERATING LENS

$\frac{v'}{v}$	a_{11}	a_{21}	a_{12}	a_{22}
2.0000000E-02	3.700375	-3.745318	0.9972098	0.9026217
2.1739131E-02	3.593525	-3.597122	0.9193419	0.9676259
2.3809524E-02	3.484536	-3.436426	0.8381547	1.034364
2.6315790E-02	3.358306	-3.257329	0.7592508	1.097720
2.9411765E-02	3.226994	-3.067485	0.6747423	1.165644
3.3333335E-02	3.082857	-2.857143	0.5872056	1.234286
3.8461540E-02	2.921466	-2.617801	0.5028743	1.295812
4.5454547E-02	2.739437	-2.347418	0.4146056	1.356808
5.0000001E-02	2.637363	-2.197802	0.3714615	1.384615
5.5555556E-02	2.534694	-2.040816	0.3224571	1.414286
6.2500000E-02	2.422430	-1.869159	0.2781516	1.437383
7.1428575E-02	2.299160	-1.680672	0.2349280	1.455462
8.3333336E-02	2.168390	-1.477105	0.1862835	1.471197
0.1000000	2.022528	-1.251564	0.1434394	1.475595
0.1111111	1.943503	-1.129943	0.1236159	1.472316
0.1250000	1.860861	-1.001001	0.1016997	1.465465
0.1428571	1.772491	-0.8650519	8.1214733E-02	1.453287
0.1666667	1.677722	-0.7209805	6.4367175E-02	1.432588
0.2000000	1.575654	-0.5688282	4.6012886E-02	1.402161
0.2500000	1.465193	-0.4095004	2.7886579E-02	1.357494
0.2857143	1.404785	-0.3277614	2.1430321E-02	1.326778
0.3333333	1.340300	-0.2458815	1.6806899E-02	1.289157
0.4000000	1.271341	-0.1657550	8.7567950E-03	1.242665
0.5000000	1.194998	-9.0950429E-02	4.7831000E-03	1.183083
0.5882353	1.144243	-5.1588938E-02	2.5851999E-03	1.139342
0.6666667	1.107785	-2.9321214E-02	1.4275000E-03	1.105527
0.7142857	1.088320	-1.9894954E-02	9.5592003E-04	1.087180
0.7692308	1.068015	-1.1890748E-02	5.6542002E-04	1.067551
0.8333333	1.046692	-5.6364066E-03	2.6604999E-04	1.046579
0.9090909	1.024107	-1.5085732E-03	7.1567003E-05	1.024098
1.0000000	1.000000	0.0000000E+00	0.0000000E+00	1.000000



The matrix elements a_{ij} for accelerating lenses



The matrix elements d_{ij} for decelerating lenses

Figure 4.3 (DiChio et al 1974, figures 2 & 3)

Another factor in favour of using matrices to represent the imaging and focal properties of electron lenses, is that the matrix elements have a more regular dependence on voltage ratio than do the focal properties themselves, and are therefore more amenable to calculations involving iteration techniques such as would be used in computer calculations, for example.

A matrix which can be used to describe a lens of more than two elements is obtained by expanding the matrix of equation (4.6). For example, for a three-element lens equation 6 becomes;

$$\begin{pmatrix} A_{11} & A_{12} \\ A_{21} & A_{22} \end{pmatrix} = \begin{pmatrix} 1 & Q' \\ 0 & 1 \end{pmatrix} \begin{pmatrix} a_{11}^* & a_{12}^* \\ a_{21}^* & a_{22}^* \end{pmatrix} \begin{pmatrix} 1 & Q \\ 0 & 1 \end{pmatrix} \begin{pmatrix} a_{11} & a_{12} \\ a_{21} & a_{22} \end{pmatrix} \begin{pmatrix} 1 & -P \\ 0 & 1 \end{pmatrix} \quad (4.8)$$

This means that it is possible to calculate the properties of lenses of more than one element simply by a process of matrix multiplication. This technique is simpler and faster than the lengthy procedure involving the calculation of the electric fields and trajectories in the lens to obtain its properties. The only limitation to this technique is that it must be confined to lenses where the focussing action of the gaps between the lens elements must not overlap. This means that the properties of lenses with elements shorter than one diameter in length cannot be accurately calculated using this technique. To illustrate this, consider a symmetric three-element einzel lens, i.e., $L_1 = L_3$ and $V_3/V_1 = 1$. Using the matrix technique to find the value of V_2/V_1 required to focus the lens, with the value of $L_1 = L_3$ specified, but L_2 chosen to have a range of values; implies that the focussing voltage V_2/V_1 is independent of the value of L_2 ; i.e., V_2/V_1 is found to be the same regardless of the length of the centre element L_2 . Heddle (private communication) calculated the values of V_2/V_1 required to focus the symmetric three-element einzel lens where $L_1 = L_3 = 2.0D$ using the Bessel function expansion method described in Chapter Two. Using this method, he found that V_2/V_1 was independent of L_2 for L_2 greater than $2.0D$, but for values of L_2 less than $2.0D$ V_2/V_1 was found to vary inversely with the length of L_2 . Table 4.3 lists the values Heddle obtained for V_2/V_1 for a range of values of L_2 between 0.5 and $2.0D$, and the percentage differences between these values of V_2/V_1 and the value obtained from the matrix method, i.e., the 'error' of the matrix method.

The use of matrices to calculate the properties of five-element lenses is described in the next chapter.

TABLE 4.3
 COMPARING THE VALUES OBTAINED FOR V_2/V_1
 USING THE MATRIX AND BESSEL FUNCTION EXPANSION METHODS
 FOR THE SYMMETRIC THREE-ELEMENT EINZEL LENS, WHERE

$$L_1 = L_3 = 2.0D \text{ and } 0.5 \leq L_2 \leq 2.0D$$

V_2/V_1 was calculated to be 7.23 using the matrix method

L_2	$\frac{V_2}{V_1}$	%DIFF
2.0	7.23	0.00
1.5	7.26	0.41
1.4	7.28	0.67
1.3	7.32	1.23
1.2	7.37	1.90
1.1	7.44	2.82
1.0	7.55	4.24
0.9	7.72	6.35
0.8	7.98	9.40
0.7	8.37	13.62
0.6	8.98	19.49
0.5	9.99	27.63

REFERENCES : CHAPTER FOUR

- DiChio D, Natali S V, Kuyatt C E and Galejs A 1974a Use of matrices to represent electron lenses. Matrices for the two tube electrostatic lens *Rev. Sci. Instrum.* **45** 566-569
- DiChio D, Natali S V and Kuyatt C E 1974b Focal properties of the two tube electrostatic lens for large and near-unity voltage ratios *Rev. Sci. Instrum* **45** 559-565
- Harting E and Read F H 1976 *Electrostatic Lenses* (Amsterdam : Elsevier)

CHAPTER FIVE

FIVE-ELEMENT LENSES

CONTENTS : CHAPTER FIVE

	Page No
Section 5.1: 'Mag. Five Elements'	133
Section 5.2: The afocal five-element lens with constant separation between conjugate planes	134
Section 5.3: Calculation of the Properties of the Afocal lens	136
Section 5.4: Properties of Variable Magnification	143
CHAPTER FIVE	
FIVE-ELEMENT LENSES	148
Section 5.5: The 'Universal Curve' for the Magnification	161
Section 5.6: The 'Universal Curve' for the Angular Magnification	169
Section 5.7: The Description of the Aberration Behaviour of a Five-Element Lens	183
Appendix	183
Appendix	183

CONTENTS : CHAPTER FIVE

	Page No
Section (5.1) Why Five Elements?	133
Section (5.2) The Afocal Five-element lens with constant separation between conjugate planes	134
Section (5.3) Calculation of the Properties of the Afocal lens	136
Section (5.4) Five-element lens of Variable Magnification	143
Section (5.5) The Derivation of a 'Universal Curve' for the Voltage Ratios Required to Focus the Lens	148
Section (5.6) The 'Universal Curve' for the Magnification	161
Section (5.7) The 'Universal Curve' for the Angular Magnification	163
Section (5.8) The Investigation of the Aberration Behaviour of a Five-element Lens	163
References	182
Appendix	183

LIST OF FIGURES : CHAPTER FIVE

	Page No
Figure 5.1 Five-element Electrostatic lens	135
Figure 5.2 Ray Diagram for 5-element Afocal Lens with constant separation between Conjugate Points	137
Figure 5.3 V_5/V_1 Versus V_2/V_1 as obtained from calculation using the matrix technique, for the lens with $L_1 = L_2 = L_4 = L_5 = 1.5\text{D}$ and $L_3 = 3.0\text{D}$	140
Figure 5.4 V_5/V_1 Versus V_2/V_1 as obtained from experiment, (<i>Heddle and Papadovassilakis (1984)</i>) for the lens with $L_1 = L_2 = L_4 = L_5 = 1.5\text{D}$ and $L_3 = 3.0\text{D}$	144
Figure 5.5 V_5/V_1 Versus the Magnification M as obtained from experiment, (<i>Heddle and Papadovassilakis (1984)</i>) for the lens with $L_1 = L_2 = L_4 = L_5 = 1.5\text{D}$ and $L_3 = 3.0\text{D}$	145
Figure 5.6 α Versus The Separation of the Conjugate Points	146
Figure 5.7 $(V_5/V_1)^\alpha$ Versus $(V_2/V_1)^\alpha$ as obtained from calculation using the matrix technique, for the lens with $S=1.5$	147
Figure 5.8 Lines of constant magnification M , angular magnification M_α , and overall voltage ratio V_5/V_1 , drawn on axes of V_2/V_1 and V_4/V_1 , as obtained by experiment by <i>Heddle and Papadovassilakis (1984)</i>	149
Figure 5.9 Lines of constant magnification M , angular magnification M_α , and overall voltage ratio V_5/V_1 , drawn on axes of V_2/V_1 and V_4/V_1 as obtained from calculation using the matrix technique, for the lens with $L_1 = L_2 = L_4 = L_5 = 1.5\text{D}$ and $L_3 = 3.0\text{D}$	150

LIST OF FIGURES (cont) : CHAPTER FIVE

	Page No
<p>Figure 5.10 $(V_2/V_1)/((V_5/V_1)^Q)$ Versus $(V_4/V_5)/((V_1/V_5)^Q)$ as obtained from calculation using the matrix technique, for the lens with $L_1 = L_2 = L_4 = L_5 = 1.5D$ and $L_3 = 3.0D$ for various values of $V_5/V_1 = 1.5D$, and $L_3 = 3.0D$</p>	152
<p>Figure 5.11 Q Versus V_5/V_1 as obtained from calculation using the matrix technique, for the lens with $L_1 = L_2 = L_4 = L_5 = 1.5D$ and $L_3 = 3.0D$</p>	153
<p>Figure 5.12 $((V_2/V_1)/((V_5/V_1)^Q))^{ZETA}$ Versus $(V_4/V_5)/((V_1/V_5)^Q)^{ZETA}$ as obtained from calculation using the matrix technique, for the lens with $L_1 = L_2 = L_4 = L_5 = 1.5D$, and $L_3 = 3.0D$</p>	154
<p>Figure 5.13 $(V_5/V_1)^Q$ Versus V_5/V_1 as obtained from calculation using the matrix technique, for the lens with $L_1 = L_2 = L_4 = L_5 = 1.5D$ and $L_3 = 3.0D$</p>	155
<p>Figure 5.14 $ZETA$ Versus V_5/V_1 as obtained from calculation using the matrix technique, for the lens with $L_1 = L_2 = L_4 = L_5 = 1.5D$ and $L_3 = 3.0D$</p>	156
<p>Figure 5.15 $(B \times (MAG))^A$ Versus $(C \times (V_1/V_4))^D$ as obtained from calculation using the matrix technique, for the lens with $L_1 = L_2 = L_4 = L_5 = 1.5D$ and $L_3 = 3.0D$ for $V_5/V_1 = 10$</p>	157
<p>Figure 5.16 $(B \times (MAG))^A$ Versus $(C \times (V_1/V_4))^D$ as obtained from calculation using the matrix technique, for the lens with $L_1 = L_2 = L_4 = L_5 = 1.5D$ and $L_3 = 3.0D$ for $V_5/V_1 = 20$</p>	158

LIST OF FIGURES (cont) : CHAPTER FIVE

	Page No
<p>Figure 5.15 $\left(\frac{V_2/V_1}{(V_5/V_1)^Q}\right)^{ZETA}$ Versus $\frac{V_4/V_5}{(V_1/V_5)^Q}$ as obtained from calculation using the matrix technique, for the lens with $L_1 = L_2 = L_4 = L_5 = 1.5D$, and $L_3 = 3.0D$ for $V_5/V_1 = 10$</p>	157
<p>Figure 5.16 $\left(\frac{V_2/V_1}{(V_5/V_1)^Q}\right)^{ZETA}$ Versus $\frac{V_4/V_5}{(V_1/V_5)^Q}$ as obtained from calculation using the matrix technique, for the lens with $L_1 = L_2 = L_4 = L_5 = 1.5D$, and $L_3 = 3.0D$ for $V_5/V_1 = 36$</p>	158
<p>Figure 5.17 $\left(\frac{V_2/V_1}{(V_5/V_1)^Q}\right)^{ZETA}$ Versus $\frac{V_4/V_5}{(V_1/V_5)^Q}$ as obtained from experiment, (<i>Hedde and Papadovassilakis (1984)</i>) for the lens with $L_1 = L_2 = L_4 = L_5 = 1.5D$, and $L_3 = 3.0D$ for various values of V_5/V_1</p>	159
<p>Figure 5.18 $(B \times (MAG)^A)$ Versus $(C \times (V_2/V_4))^D$ as obtained from calculation using the matrix technique, for the lens with $L_1 = L_2 = L_4 = L_5 = 1.5D$ and $L_3 = 3.0D$</p>	164
<p>Figure 5.19 $(B \times (MAG)^A)$ Versus $(C \times (V_2/V_4))^D$ as obtained from calculation using the matrix technique, for the lens with $L_1 = L_2 = L_4 = L_5 = 1.5D$ and $L_3 = 3.0D$ for $V_5/V_1 = 10$</p>	165
<p>Figure 5.20 $(B \times (MAG)^A)$ Versus $(C \times (V_2/V_4))^D$ as obtained from calculation using the matrix technique, for the lens with $L_1 = L_2 = L_4 = L_5 = 1.5D$ and $L_3 = 3.0D$ for $V_5/V_1 = 36$</p>	166

LIST OF FIGURES (cont) : CHAPTER FIVE

	Page No
Figure 5.21 <i>A</i> Versus V_5/V_1 as obtained from calculation using the matrix technique, for the lens with $L_1 = L_2 = L_4 = L_5 = 1.5D$ and $L_3 = 3.0D$	167
Figure 5.22 <i>B</i> Versus V_5/V_1 as obtained from calculation using the matrix technique, for the lens with $L_1 = L_2 = L_4 = L_5 = 1.5D$ and $L_3 = 3.0D$	168
Figure 5.23 <i>C</i> Versus V_5/V_1 as obtained from calculation using the matrix technique, for the lens with $L_1 = L_2 = L_4 = L_5 = 1.5D$ and $L_3 = 3.0D$	169
Figure 5.24 <i>D</i> Versus V_5/V_1 as obtained from calculation using the matrix technique, for the lens with $L_1 = L_2 = L_4 = L_5 = 1.5D$ and $L_3 = 3.0D$	170
Figure 5.25 $(B \times (MAG)^A$ Versus $(C \times (V_2/V_4))^D$ as obtained from experiment, for the lens with $L_1 = L_2 = L_4 = L_5 = 1.5D$ and $L_3 = 3.0D$ (Heddle and Papadovassilakis (1984)) for various values of V_5/V_1	171
Figure 5.26 $((V_2/V_1)/((V_5/V_1)^Q))^{ZETA}$ Versus $(V_4/V_5)/((V_1/V_5)^Q)^{ZETA}$ (plotted on linear axes) as obtained from calculation using the matrix technique, for the lens with $L_1 = L_2 = L_4 = L_5 = 1.5D$, and $L_3 = 3.0D$	172

LIST OF FIGURES (cont) : CHAPTER FIVE

	Page No
Figure 5.27 Photograph of display scope showing six dots for aberration measurements	176
Figure 5.28 C_s Versus V_3/V_1 , where $V_5/V_1 = 1$, $V_2/V_1 = V_4/V_5 > V_3/V_1$, for the lens where $L_1 = L_5 = 1.5D, L_2 = L_4 = 1.0D$ and $L_3 = 3.0D$	177
Figure 5.29 C_s Versus V_5/V_1 , for the afocal lens where $L_1 = L_5 = 1.5D, L_2 = L_4 = 1.0D$ and $L_3 = 3.0D$	178
Figure 5.30 C_s Versus V_2/V_1 , where $V_5/V_1 = V_3/V_1 = 1$, $V_2/V_1 \neq V_4/V_5$, for the lens where $L_1 = L_5 = 1.5D, L_2 = L_4 = 1.0D$ and $L_3 = 3.0D$	179
Figure 5.31 $MAG \times C_s$ Versus V_2/V_1 , where $V_5/V_1 = V_3/V_1 = 1$, $V_2/V_1 \neq V_4/V_5$, for the lens where $L_1 = L_5 = 1.5D, L_2 = L_4 = 1.0D$ and $L_3 = 3.0D$	180
Figure 5.32 $MAG \times C_s$ Versus MAG , where $V_5/V_1 = V_3/V_1 = 1$, $V_2/V_1 \neq V_4/V_5$, for the lens where $L_1 = L_5 = 1.5D, L_2 = L_4 = 1.0D$ and $L_3 = 3.0D$	181

LIST OF TABLES: CHAPTER FIVE

5.1 WHY FIVE ELEMENTS?

Table 5.1 Table listing calculated lens properties illustrating the consistency of the calculations

Page No

141-42

The argument which a lens will comprise, is most easily approached by considering a simple optical lens. A single optical lens has three interdependent parameters. These are the object distance, the image distance and the magnification. If for example the object distance is fixed, for the single lens the image distance and the magnification are also fixed (i.e., by $1/u + 1/v = 1/f$, and $M = v/u$, where u and v are the object and image distances respectively, and M is the magnification. To be able to change either the image distance or the magnification and leave the object distance fixed, requires the use of a second lens, to be able to change all three independently would require the use of three lenses.

We have a similar situation in electron optics. However, in electron optics there is one extra parameter, the ratio of the energy of the electrons leaving the lens to the energy of the electrons entering it, which is equal to the overall voltage ratio of the lens, V_2/V_1 , where V_1 is the voltage applied to the first element, and V_2 is the voltage applied to the last element of the lens. A two element lens allows the choice of one parameter which may for example be the energy ratio, a three element lens allows the choice of two parameters, which may be the energy and the image distance and so on. In general n elements are required to allow the choice of $n - 1$ properties of the lens.

In the application of electron optics, such as in atomic physics or in solid state physics, it is often necessary to form an image in a fixed position, for example, forming an image on a target or on a detector. If this constraint is imposed, then the simplest lens comprising two elements can only be used if the electrons being manipulated are confined to one energy. However, if an image has to be formed in a fixed position over a wide range of electron energies, then an electron lens built from more than two elements is required. Three element lenses have been widely used to form images in a fixed position over a wide range of electron energies, and their properties have been well documented (see for example Heddle (1989), Heddle (1970), Heddle and Kurita (1970), Hasting and Head (1975)), and Heddle et al (1982)).

However, it may be necessary to maintain two properties of an image constant, for example the position and the magnification, in this case three elements are not enough. Another constraint which could be imposed that would require a lens with more than three elements, would be that the lens not only produces one image in a position which does not

FIVE ELEMENT LENSES

5.1 WHY FIVE ELEMENTS?

The argument regarding the choice of the number of elements which a given lens will comprise, is most easily approached by considering a simple optical lens. A single optical lens has three interdependent parameters. These are the object distance, the image distance and the magnification. If for example the object distance is fixed, for the single lens the image distance and the magnification are also fixed i.e., by $1/u + 1/v = 1/f$, and $M = v/u$, where u and v are the object and image distances respectively, and M is the magnification. To be able to change either the image distance or the magnification and leave the object distance fixed, requires the use of a second lens, to be able to change all three independently would require the use of three lenses.

We have a similar situation in electron optics. However, in electron optics there is one extra parameter, the ratio of the energy of the electrons leaving the lens to the energy of the electrons entering it, which is equal to the overall voltage ratio of the lens, V_n/V_1 , where V_1 is the voltage applied to the first element, and V_n is the voltage applied to the last element of the lens. A two element lens allows the choice of one parameter which may for example be the energy ratio, a three element lens allows the choice of two parameters, which may be the energy and the image distance and so on. In general n elements are required to allow the choice of $n - 1$ properties of the lens.

In the application of electron optics, such as in atomic physics or in solid state physics, it is often necessary to form an image in a fixed position, for example, forming an image on a target or on a detector. If this constraint is imposed, then the simplest lens comprising two elements can only be used if the electrons being manipulated are confined to one energy. However, if an image has to be formed in a fixed position over a wide range of electron energies, then an electron lens built from more than two elements is required. Three element lenses have been widely used to form images in a fixed position over a wide range of electron energies, and their properties have been well documented, (see for example Heddle (1969), Heddle (1970), Heddle and Kurepa (1970), Harting and Read (1976)), and Heddle et al (1982)).

However, it may be necessary to maintain two properties of an image constant, for example the position and the magnification; in this case three elements are not enough. Another constraint which could be imposed that would require a lens with more than three elements, would be that the lens not only produces one image in a position which does not

depend on the voltage ratio, but also forms a second image in a fixed position, independent of the first, of another object in the lens system such as an angle stop or an exit pupil, and it is often desirable to have such a second image at infinity.

It is now possible to sum up the reasons for choosing a five-element lens. The choice of five elements allows the energy, the image position, and the magnification all to be changed independently so this lens is the 'true zoom' lens of electron optics. This would also be true for an electron lens of four elements but with a five-element lens it is also possible to construct a lens as described by Heddle (1971), with two very useful and interesting properties. Heddle (1971) described the properties of a lens constructed from a pair of identical three-element lenses, with the third element of the first lens joined to the first element of the second lens, forming one element, thus creating a five-element lens, (see figure 5.1). This lens, as shown by Heddle (1971), (and will be shown in the next section), is afocal or telescopic, with the separation of the conjugate planes independent of the position of the object, and the magnification dependent only on the overall voltage ratio.

5.2 THE AFOCAL FIVE-ELEMENT LENS WITH CONSTANT SEPARATION BETWEEN CONJUGATE PLANES

A lens system, (see figure 5.2) arranged so that the second focal point of the first lens and the first focal point of the second lens coincide, is necessarily afocal, as a ray incident parallel to the axis will pass through this common focal point and leave the lens system still parallel to the axis. From figure 5.2 and from Newton's equation the first lens will produce an image **I** of the object **O** at a distance q from the common focal point i.e.,

$$q = \frac{f_1 f_2}{p} \quad (5.1)$$

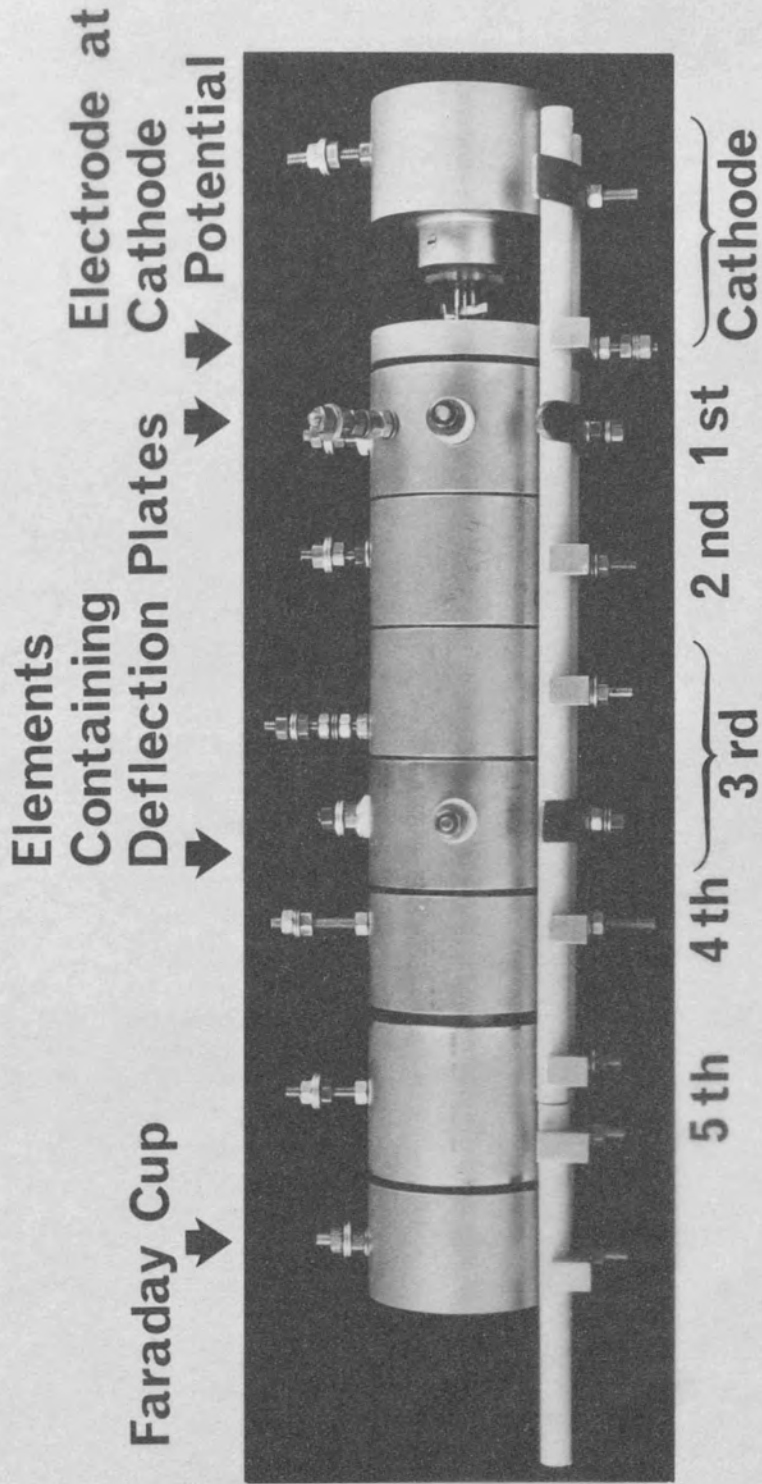
where p is the distance of the object from the first focal point of the first lens and f_1 and f_2 are the first and second focal lengths respectively of this first lens. This image **I** then becomes the object **O'** for the second lens so $p' = q$ where p' is the distance from **O'** to the first focal point of the second lens. Again from figure 5.2 and Newton's equation,

$$q' = \frac{f'_1 f'_2}{p'} = \frac{f'_1 f'_2}{q} \quad (5.2)$$

where f'_1 and f'_2 are the first and second focal lengths respectively of the second lens. From equations (5.1) and (5.2)

$$q' = \left(\frac{f'_1 f'_2}{f_1 f_2} \right) p \quad (5.3)$$

FIVE - ELEMENT ELECTROSTATIC LENS .

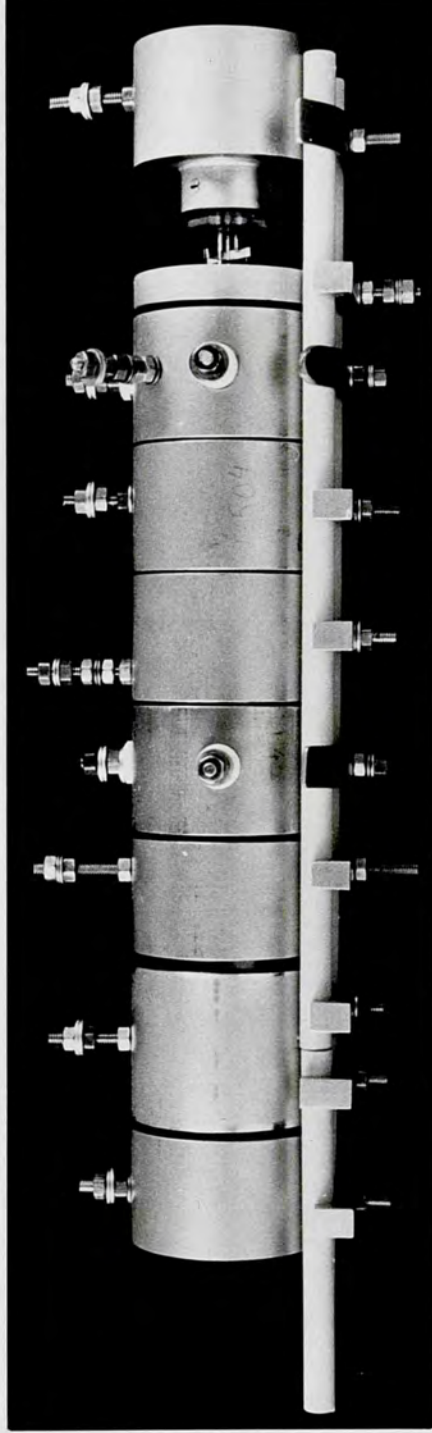


Elements of Lens

Figure 5.1

FIVE - ELEMENT ELECTROSTATIC LENS.

Faraday Cup →
Elements Containing Deflection Plates →
Electrode at Cathode Potential →



5 th 4 th 3 rd 2 nd 1 st Cathode

Elements of Lens

If the two lenses are further constrained to be identical, (i.e., $f_1 = f'_1$ and $f_2 = f'_2$) $q' = p$.

The distance between the object O and the final image I' is equal to

$$p + F_1 - q - F_2 + p' + F'_1 - q' - F'_2 = 2(F_2 - F_1)$$

as $p' = q$, $q' = p$, $F_1 = F'_1$, and $F_2 = F'_2$; the negative signs are due to sign convention.

N.B The separation between the reference planes of the two identical lenses is equal to $F_2 - F_1$, (see figure 5.2), which is a constant, therefore the separation of the conjugate planes is equal to a constant and therefore independent of object position.

The magnification of the lens system is given by f_1/f_2 . The angular magnification is given by

$$M_\alpha = \frac{\alpha'}{\alpha} = \left(\frac{h}{f'_2}\right) / \left(\frac{h}{f_1}\right) = \frac{f_1}{f'_2} = f_1/f_2 = M \quad (5.4)$$

(see figure 5.2 for definition of α , α' and h)

The law of Helmholtz and Lagrange relates the magnification, the angular magnification and the overall voltage ratio by;

$$MM_\alpha \left(\frac{V'}{V}\right)^{\frac{1}{2}} = 1 \quad (5.5)$$

therefore,

$$M = M_\alpha = \left(\frac{V'}{V}\right)^{-\frac{1}{4}} \quad (5.6)$$

therefore the magnification of the lens is dependent only on the overall voltage ratio.

5.3 CALCULATION OF THE LENS PROPERTIES

Because of the constraints imposed on this lens, for a given value for the overall voltage ratio V_5/V_1 , the only parameter which has to be calculated is V_2/V_1 , where $V_2/V_1 = V_4/V_3$. The magnification can be immediately deduced from V_5/V_1 , as $M = (V_5/V_1)^{-1/4}$, and once V_2/V_1 is known the remaining voltage ratios can be immediately found. To summarise,

$$V_5/V_3 = V_3/V_1 \text{ implies } V_3/V_1 = (V_5/V_1)^{1/2}$$

$$V_2/V_1 = V_4/V_3$$

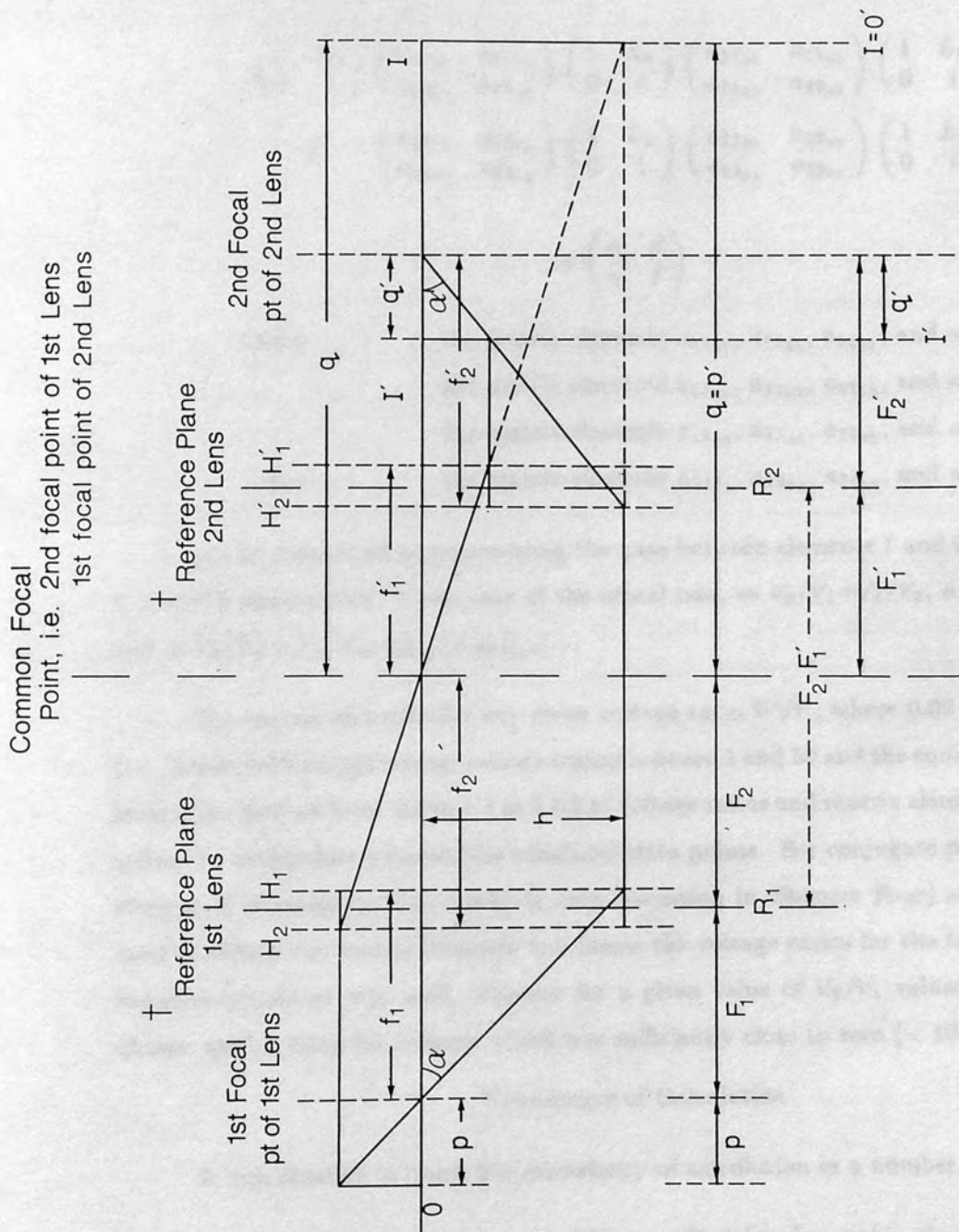


Figure 5.2

(2) As mentioned in the previous chapter, and as matrix element β is equal to the magnification, as $1/(MM_0) = f_2/f_1$, comparing the values obtained for f_2/f_1 to those given will give a check on the accuracy of the calculation.

$$V_3/V_2 = (V_3/V_1)/(V_2/V_1) \quad (5.7)$$

$$V_5/V_4 = (V_5/V_3)/(V_4/V_3) = V_3/V_2$$

$$M = (V_5/V_1)^{-1/4}$$

(b) A five-element lens can be represented by the following object-image matrix;

$$X = \begin{pmatrix} 1 & L_5 \\ 0 & 1 \end{pmatrix} \begin{pmatrix} a_{11_{54}} & a_{12_{54}} \\ a_{21_{54}} & a_{22_{54}} \end{pmatrix} \begin{pmatrix} 1 & L_4 \\ 0 & 1 \end{pmatrix} \begin{pmatrix} a_{11_{43}} & a_{12_{43}} \\ a_{21_{43}} & a_{22_{43}} \end{pmatrix} \begin{pmatrix} 1 & L_3 \\ 0 & 1 \end{pmatrix} \\ \begin{pmatrix} a_{11_{32}} & a_{12_{32}} \\ a_{21_{32}} & a_{22_{32}} \end{pmatrix} \begin{pmatrix} 1 & L_2 \\ 0 & 1 \end{pmatrix} \begin{pmatrix} a_{11_{21}} & a_{12_{21}} \\ a_{21_{21}} & a_{22_{21}} \end{pmatrix} \begin{pmatrix} 1 & L_1 \\ 0 & 1 \end{pmatrix} \quad (5.8)$$

$$= \begin{pmatrix} \alpha & \beta \\ \gamma & \delta \end{pmatrix}$$

where the matrix elements $a_{11_{21}}$, $a_{12_{21}}$, $a_{21_{21}}$, and $a_{22_{21}}$,
the matrix elements $a_{11_{32}}$, $a_{12_{32}}$, $a_{21_{32}}$, and $a_{22_{32}}$,
the matrix elements $a_{11_{43}}$, $a_{12_{43}}$, $a_{21_{43}}$, and $a_{22_{43}}$,
and the matrix elements $a_{11_{54}}$, $a_{12_{54}}$, $a_{21_{54}}$, and $a_{22_{54}}$,

can be considered as representing the gaps between elements 1 and 2, 2 and 3, 3 and 4, 4 and 5 respectively. In the case of the afocal lens, as $V_2/V_1 = V_4/V_3$, $a_{11_{21}} = a_{11_{43}}, \dots$, and as $V_3/V_2 = V_5/V_4$, $a_{11_{32}} = a_{11_{54}}, \dots$

The matrix elements for any given voltage ratio V'/V , where $0.02 \leq V'/V \leq 50.0$, (i.e., lenses with overall voltage ratios ranging between 1 and 50 and the equivalent reciprocal lenses) are derived from tables 4.1 and 4.2 of voltage ratios and matrix elements, using cubic splines to interpolate between the tabulated data points. For conjugate points the matrix element β of equation (5.8) equals 0, (see discussion in Chapter Four) and this fact was used to obtain the matrix elements and hence the voltage ratios for the focussed lens. An iterative procedure was used, whereby for a given value of V_5/V_1 values for V_2/V_1 were chosen until a value for β found which was sufficiently close to zero ($< 10^{-4}$).

Consistency of Calculation

It was possible to check the consistency of calculation in a number of ways.

- (1) As matrix element α is equal to the magnification (see again the discussion of the last chapter), which in this case is equal to $(V_5/V_1)^{-1/4}$, a check of the accuracy of the final choice of V_2/V_1 is possible, by comparing the values obtained for α and $(V_5/V_1)^{-1/4}$.

- (2) As mentioned above, α is equal to the magnification, and as matrix element δ is equal to the angular magnification, a value for f_2/f_1 can be deduced, as $1/(MM_\alpha) = f_2/f_1$, (Lagrange's rule). As $(V_5/V_1)^{1/2}$ should also equal f_2/f_1 , comparing the values obtained for f_2/f_1 in both cases will give a check on the accuracy of the calculation.
- (3) Finally, it is possible to extract the matrix elements for the three-element lens from which the five-element lens is constructed as

$$\begin{aligned} & \begin{pmatrix} a_{11_{32}} & a_{12_{32}} \\ a_{21_{32}} & a_{22_{32}} \end{pmatrix} \begin{pmatrix} 1 & L_2 \\ 0 & 1 \end{pmatrix} \begin{pmatrix} a_{11_{21}} & a_{12_{21}} \\ a_{21_{21}} & a_{22_{21}} \end{pmatrix} \\ &= \begin{pmatrix} 1 & \frac{L_2}{2} \\ 0 & 1 \end{pmatrix} \begin{pmatrix} a_{11_{31}} & a_{12_{31}} \\ a_{21_{31}} & a_{22_{31}} \end{pmatrix} \begin{pmatrix} 1 & \frac{L_2}{2} \\ 0 & 1 \end{pmatrix} \end{aligned} \quad (5.9)$$

where $a_{11_{31}}$, $a_{12_{31}}$, $a_{21_{31}}$, and $a_{22_{31}}$ are the matrix elements for the three-element lens, and as the focal distances F_{3_1} and F_{3_2} for the three-element lens can be deduced from these matrix elements, $F_{3_2} - F_{3_1}$ can be calculated and compared to $L_2 + L_3$, where L_2 and L_3 are the lengths of the second and third elements of the five-element lens.

Figure 5.3 shows V_5/V_1 versus V_2/V_1 for the five-element lens where $L_1 = L_2 = L_4 = L_5 = 1.5D$ and $L_3 = 3.0D$, and Table 5.1 lists some of the calculated results.

As the programs written to obtain the properties of the afocal lens are typical of those written to calculate lens properties using the matrix technique, a description and copies of these Fortran programs are included in an appendix to this chapter, entitled 'Examples of programs used to calculate lens properties'.

TABLE 5.1

TABLE LISTING CALCULATED LENS PROPERTIES
 ILLUSTRATING THE CONSISTENCY OF THE CALCULATIONS

$L_1 = L_2 = L_3 = L_4 = 1.5D$ and $L_5 = 3.0D$, $L_2 + L_3 = 4.5D$

$L_1 = L_2 = L_4 = L_5 = 1.5D$ $L_3 = 3.0D$
 AFOCAL 5-ELEMENT LENS

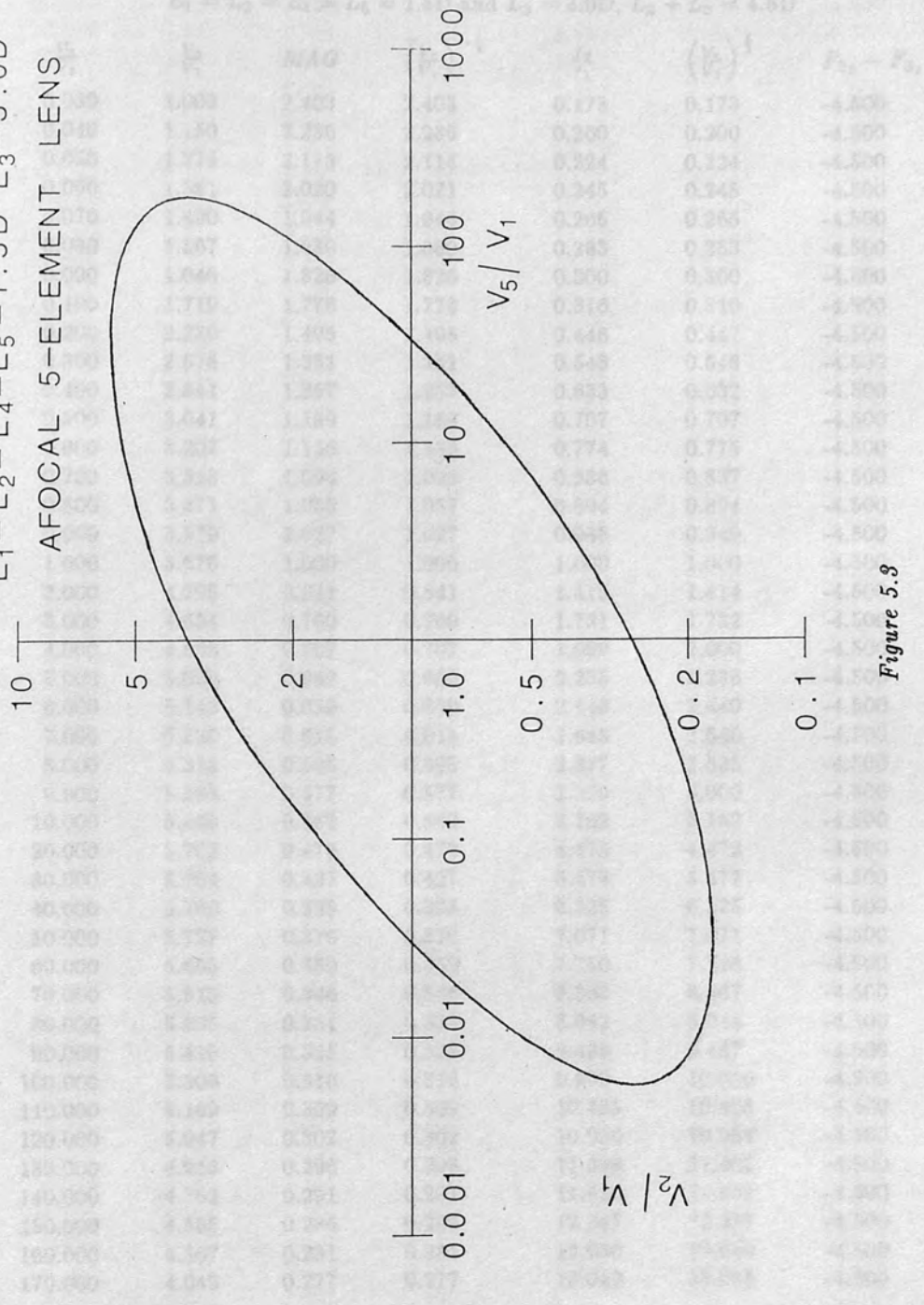


Figure 5.3

TABLE 5.1

TABLE LISTING CALCULATED LENS PROPERTIES
ILLUSTRATING THE CONSISTENCY OF THE CALCULATIONS

$L_1 = L_2 = L_4 = L_5 = 1.5D$ and $L_3 = 3.0D$, $L_2 + L_3 = 4.5D$

$\frac{V_5}{V_1}$	$\frac{V_2}{V_1}$	MAG	$\left(\frac{V_5}{V_1}\right)^{-\frac{1}{4}}$	$\frac{f_2}{f_1}$	$\left(\frac{V_5}{V_1}\right)^{\frac{1}{2}}$	$F_{3_2} - F_{3_1}$
0.030	1.003	2.403	2.403	0.173	0.173	-4.500
0.040	1.150	2.236	2.236	0.200	0.200	-4.500
0.050	1.275	2.115	2.115	0.224	0.224	-4.500
0.060	1.381	2.020	2.021	0.245	0.245	-4.500
0.070	1.490	1.944	1.944	0.265	0.265	-4.500
0.080	1.567	1.880	1.880	0.283	0.283	-4.500
0.090	1.646	1.826	1.826	0.300	0.300	-4.500
0.100	1.719	1.778	1.778	0.316	0.316	-4.500
0.200	2.239	1.495	1.495	0.448	0.447	-4.500
0.300	2.578	1.351	1.351	0.548	0.548	-4.500
0.400	2.841	1.257	1.257	0.633	0.632	-4.500
0.500	3.041	1.189	1.189	0.707	0.707	-4.500
0.600	3.207	1.136	1.136	0.774	0.775	-4.500
0.700	3.348	1.094	1.093	0.836	0.837	-4.500
0.800	3.471	1.058	1.057	0.894	0.894	-4.500
0.900	3.579	1.027	1.027	0.948	0.949	-4.500
1.000	3.676	1.000	1.000	1.000	1.000	-4.500
2.000	4.295	0.841	0.841	1.415	1.414	-4.500
3.000	4.634	0.760	0.760	1.731	1.732	-4.500
4.000	4.858	0.707	0.707	1.999	2.000	-4.500
5.000	5.020	0.669	0.669	2.235	2.236	-4.500
6.000	5.142	0.639	0.639	2.448	2.449	-4.500
7.000	5.239	0.615	0.615	2.645	2.646	-4.500
8.000	5.318	0.595	0.595	2.827	2.828	-4.500
9.000	5.383	0.577	0.577	2.999	3.000	-4.500
10.000	5.438	0.562	0.562	3.162	3.162	-4.500
20.000	5.702	0.473	0.473	4.473	4.472	-4.500
30.000	5.764	0.427	0.427	5.478	5.477	-4.500
40.000	5.769	0.398	0.398	6.325	6.325	-4.500
50.000	5.727	0.376	0.376	7.071	7.071	-4.500
60.000	5.665	0.359	0.359	7.750	7.746	-4.500
70.000	5.515	0.346	0.346	8.366	8.367	-4.500
80.000	5.505	0.334	0.334	8.942	8.944	-4.500
90.000	5.410	0.325	0.325	9.486	9.487	-4.500
100.000	5.306	0.316	0.316	9.999	10.000	-4.500
110.000	5.169	0.309	0.309	10.485	10.488	-4.500
120.000	5.047	0.302	0.302	10.950	10.954	-4.500
130.000	4.913	0.296	0.296	11.398	11.402	-4.500
140.000	4.762	0.291	0.291	11.830	11.832	-4.500
150.000	4.585	0.286	0.286	12.247	12.247	-4.500
160.000	4.367	0.281	0.281	12.650	12.649	-4.500
170.000	4.045	0.277	0.277	13.042	13.038	-4.500

$\frac{V_2}{V_1}$	$\frac{V_2}{V_1}$	MAG	$\left(\frac{V_2}{V_1}\right)^{-\frac{1}{4}}$	$\frac{f_2}{f_1}$	$\left(\frac{V_2}{V_1}\right)^{\frac{1}{2}}$	$F_{3_2} - F_{3_1}$
30.000	0.946	0.427	0.427	5.478	5.477	-4.500
40.000	1.101	0.398	0.398	6.325	6.325	-4.500
50.000	1.241	0.376	0.376	7.071	7.071	-4.500
60.000	1.382	0.359	0.359	7.750	7.746	-4.500
70.000	1.514	0.346	0.346	8.366	8.367	-4.500
80.000	1.645	0.334	0.334	8.942	8.944	-4.500
90.000	1.777	0.325	0.325	9.486	9.487	-4.500
100.000	1.911	0.316	0.316	9.998	10.000	-4.500
110.000	2.049	0.309	0.309	10.485	10.488	-4.500
120.000	2.188	0.302	0.302	10.950	10.954	-4.500
130.000	2.342	0.296	0.296	11.398	11.402	-4.500
140.000	2.511	0.291	0.291	11.830	11.832	-4.500
150.000	2.701	0.286	0.286	12.248	12.247	-4.500
160.000	2.933	0.281	0.281	12.651	12.649	-4.500
170.000	3.265	0.277	0.277	13.042	13.038	-4.500
30.000	0.946	0.427	0.427	5.478	5.477	-4.500
20.000	0.781	0.473	0.473	4.473	4.472	-4.500
10.000	0.580	0.562	0.562	3.162	3.162	-4.500
9.000	0.561	0.577	0.577	2.999	3.000	-4.500
8.000	0.537	0.595	0.595	2.827	2.828	-4.500
7.000	0.510	0.615	0.615	2.645	2.646	-4.500
6.000	0.482	0.639	0.639	2.448	2.449	-4.500
5.000	0.451	0.669	0.669	2.235	2.236	-4.500
4.000	0.418	0.707	0.707	1.999	2.000	-4.500
3.000	0.380	0.760	0.760	1.732	1.732	-4.500
2.000	0.335	0.841	0.841	1.415	1.414	-4.500
1.000	0.278	1.000	1.000	1.000	1.000	-4.500
0.900	0.270	1.027	1.027	0.948	0.949	-4.500
0.800	0.263	1.058	1.057	0.894	0.894	-4.500
0.700	0.255	1.094	1.093	0.836	0.837	-4.500
0.600	0.246	1.137	1.136	0.774	0.775	-4.500
0.500	0.237	1.189	1.189	0.707	0.707	-4.500
0.400	0.227	1.257	1.257	0.633	0.632	-4.500
0.300	0.215	1.351	1.351	0.548	0.548	-4.500
0.200	0.201	1.495	1.495	0.448	0.447	-4.500
0.100	0.185	1.778	1.778	0.316	0.316	-4.500
0.090	0.183	1.826	1.826	0.300	0.300	-4.500
0.080	0.181	1.880	1.880	0.283	0.283	-4.500
0.070	0.179	1.944	1.944	0.265	0.265	-4.500
0.060	0.177	2.020	2.021	0.245	0.245	-4.500
0.050	0.175	2.115	2.115	0.224	0.224	-4.500
0.040	0.174	2.236	2.236	0.200	0.200	-4.500
0.030	0.173	2.403	2.403	0.173	0.173	-4.500
0.020	0.176	2.659	2.659	0.141	0.141	-4.500
0.010	0.191	3.162	3.162	0.100	0.100	-4.500
0.009	0.195	3.246	3.247	0.095	0.095	-4.500
0.008	0.203	3.343	3.344	0.089	0.089	-4.500
0.007	0.215	3.457	3.457	0.084	0.084	-4.500
0.006	0.243	3.594	3.593	0.077	0.077	-4.500
0.030	1.003	2.403	2.403	0.173	0.173	-4.500
0.020	0.806	2.659	2.659	0.141	0.141	-4.500
0.010	0.530	3.162	3.162	0.100	0.100	-4.500
0.009	0.477	3.246	3.247	0.095	0.095	-4.500
0.008	0.444	3.343	3.344	0.089	0.089	-4.500
0.007	0.394	3.457	3.457	0.084	0.084	-4.500
0.006	0.322	3.593	3.593	0.077	0.077	-4.500

Comparison of the Calculated and Experimental Results
Obtained for the Afocal Lens

Heddle and Papadovassilakis (1984) investigated experimentally the properties of a five-element lens where $L_1 = L_2 = L_4 = L_5 = 1.5D$ and $L_3 = L_1 + L_5 = 3.0D$, this lens will subsequently be referred to as the **HP** lens. Figure 5.4 shows the values of V_5/V_1 and V_2/V_1 obtained experimentally for the **HP** lens; the solid line represents the calculated values. Figure 5.5 shows V_5/V_1 versus the magnification M , as obtained from experiment for the **HP** lens; the solid line corresponds to V_5/V_1 versus $(V_5/V_1)^{-1/4}$.

Representation of the Lens Properties of the Afocal Lens
with Constant Separation between Conjugate Points
with Graphs of $(V_5/V_1)^\alpha$ Versus $(V_2/V_1)^\alpha$

As this lens is the sum of two identical three-element lenses its properties can be represented by a single graph of $(V_5/V_1)^\alpha$ versus $(V_2/V_1)^\alpha$ where α is a function of the separation between the conjugate points, (see figure 5.6) using the property of three-element lenses found by Heddle (1970 and 1971). He discovered that all three-element lenses with the same centre element length S could be represented by a single graph of $(V_3/V_1)^\alpha$ versus $(V_2/V_1)^\alpha$ where α is a function of the sum of the focal distances of each lens. Therefore all five-element lenses whose second element (and therefore fourth element, i.e., the second element and the fourth element of the five-element lens are the centre elements of the three-element lens) are of the same length can similarly be represented by the one curve. Figure 5.7 shows $(V_5/V_1)^\alpha$ versus $(V_2/V_1)^\alpha$ for lenses where $S = 1.5D$ as calculated using the matrix technique.

5.4 FIVE-ELEMENT LENS OF VARIABLE MAGNIFICATION

In the above case V_2/V_1 was constrained to equal V_4/V_3 , (i.e., equation (1)) when this constraint is relaxed the lens can be operated as a lens of variable magnification. For this lens, of variable magnification, for every value of V_5/V_1 there exists a set of pairs of values of V_2/V_1 and V_4/V_3 which will focus the lens, and for each pair of values of V_2/V_1 and V_4/V_3 there will be a corresponding value for the magnification.

From the above it can be seen that by simply relaxing the one constraint to give a lens of variable magnification, the representation of the lens parameters becomes rather more complicated than it was in the afocal case. It is no longer possible to represent all the parameters of the lens by a simple graph of $(V_5/V_1)^\alpha$ versus $(V_2/V_1)^\alpha$, instead, for

$L_1=L_2=L_4=L_5=1.5D$ $L_3=3.0D$
 AFOCAL 5-ELEMENT LENS

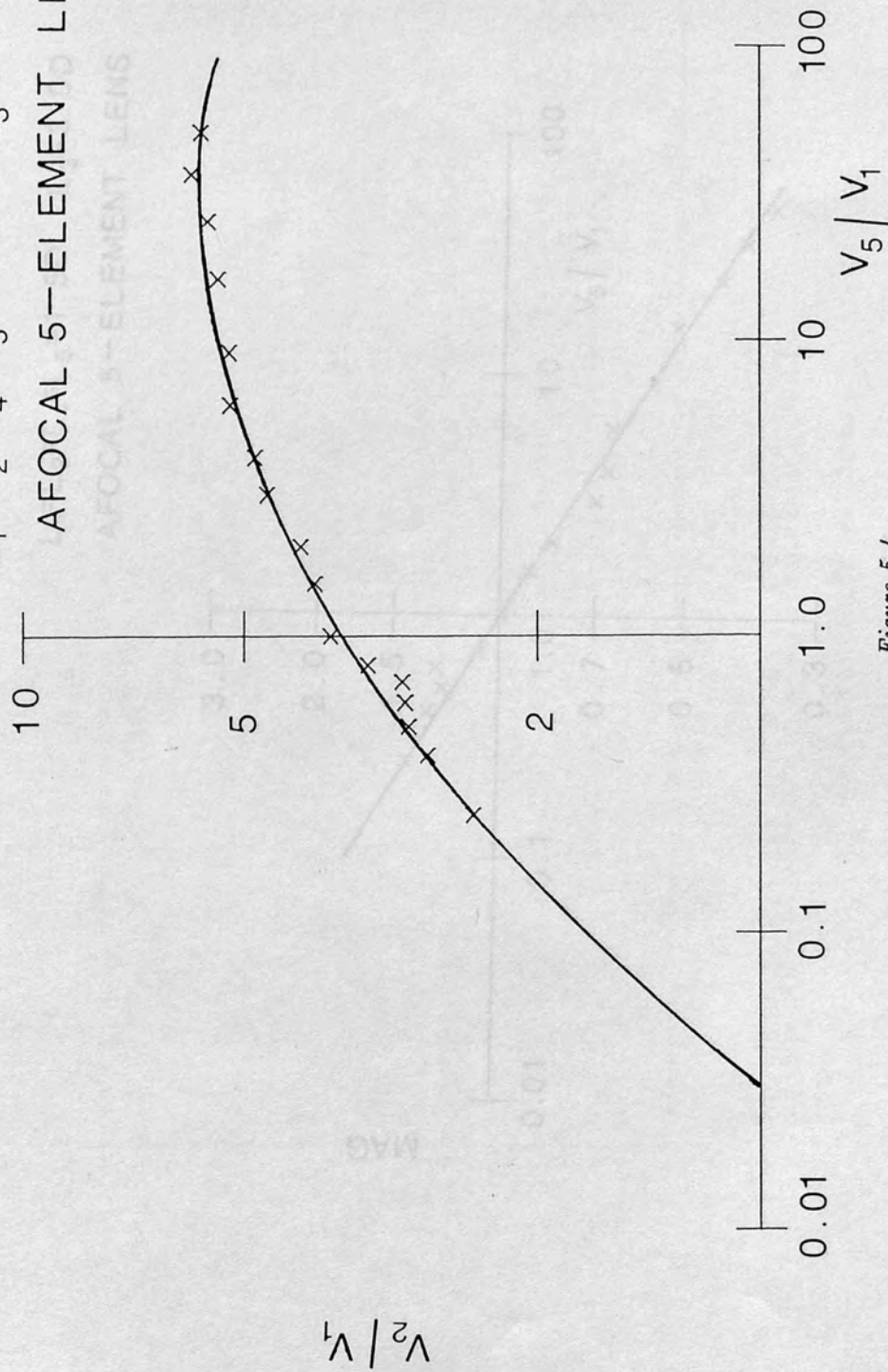
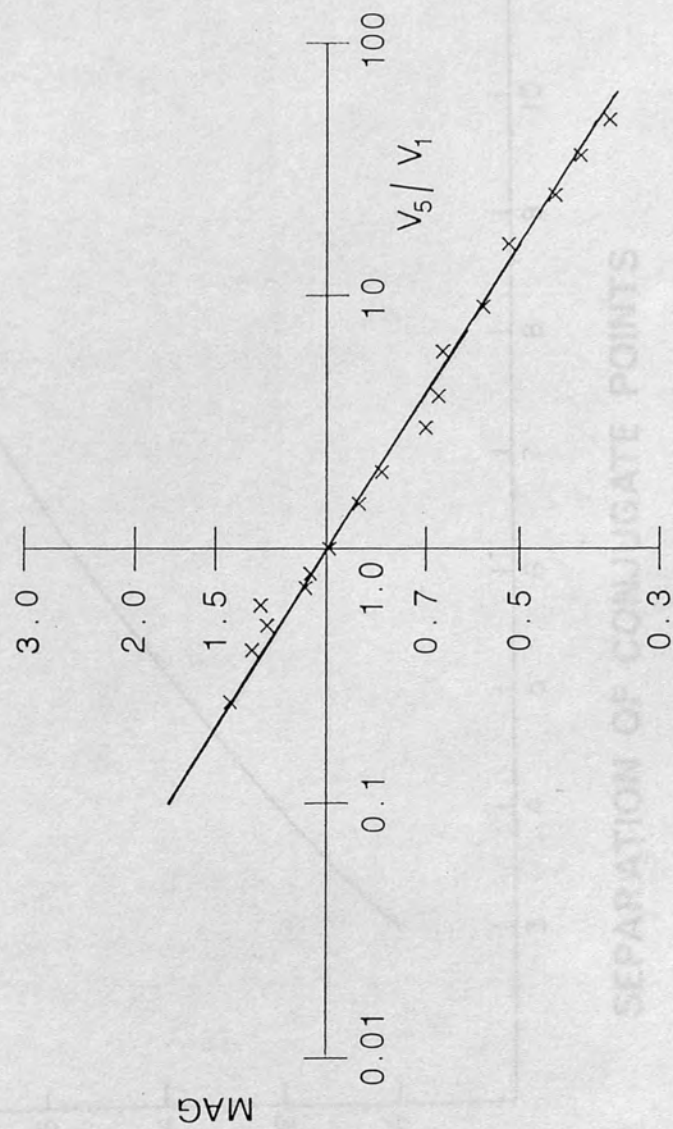


Figure 5.4

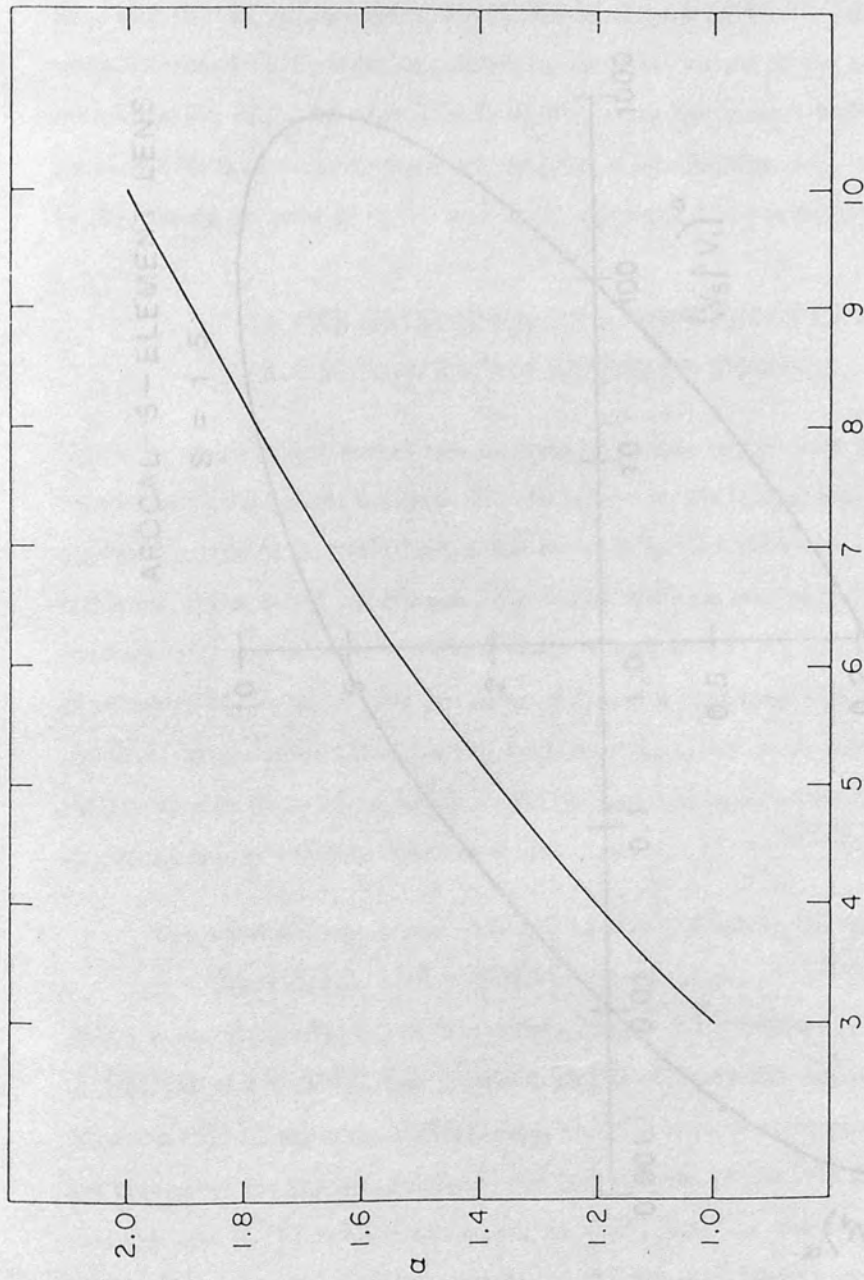
$L_1=L_2=L_4=L_5=1.5D$ $L_3=3.0D$
 AFOCAL 5-ELEMENT LENS



SEPARATION OF CONJUGATE POINTS

adapted from Hecht, 1971, figure 4

Figure 5.5



SEPARATION OF CONJUGATE POINTS

adapted from Heddle 1971, figure 4

Figure 5.6

every possible value of V_2/V_1 a three dimensional graph of V_3/V_1 versus V_4/V_1 versus the magnification for example, is required to represent the lens. Heddlie and Papadovassilakis (1984) represented the lens properties they had obtained experimentally, (i.e., the HP lens) with a graph (figure 5.8) showing lines of constant magnification M , angular magnification M_a , and overall voltage ratio, V_5/V_1 drawn on axes of V_2/V_1 and V_4/V_1 . In the present work, values of V_2/V_1 were calculated for constant values of the magnification M , angular magnification M_a , and overall ratio V_5/V_1 using the matrix technique. Figure 5.9 shows lines of constant magnification M , angular magnification M_a , and overall voltage ratio V_5/V_1 drawn on axes of V_2/V_1 and $(V_5/V_1)^\alpha$ using calculated data for the HP lens.

AFOCAL 5-ELEMENT LENS
 $S = 1.5$

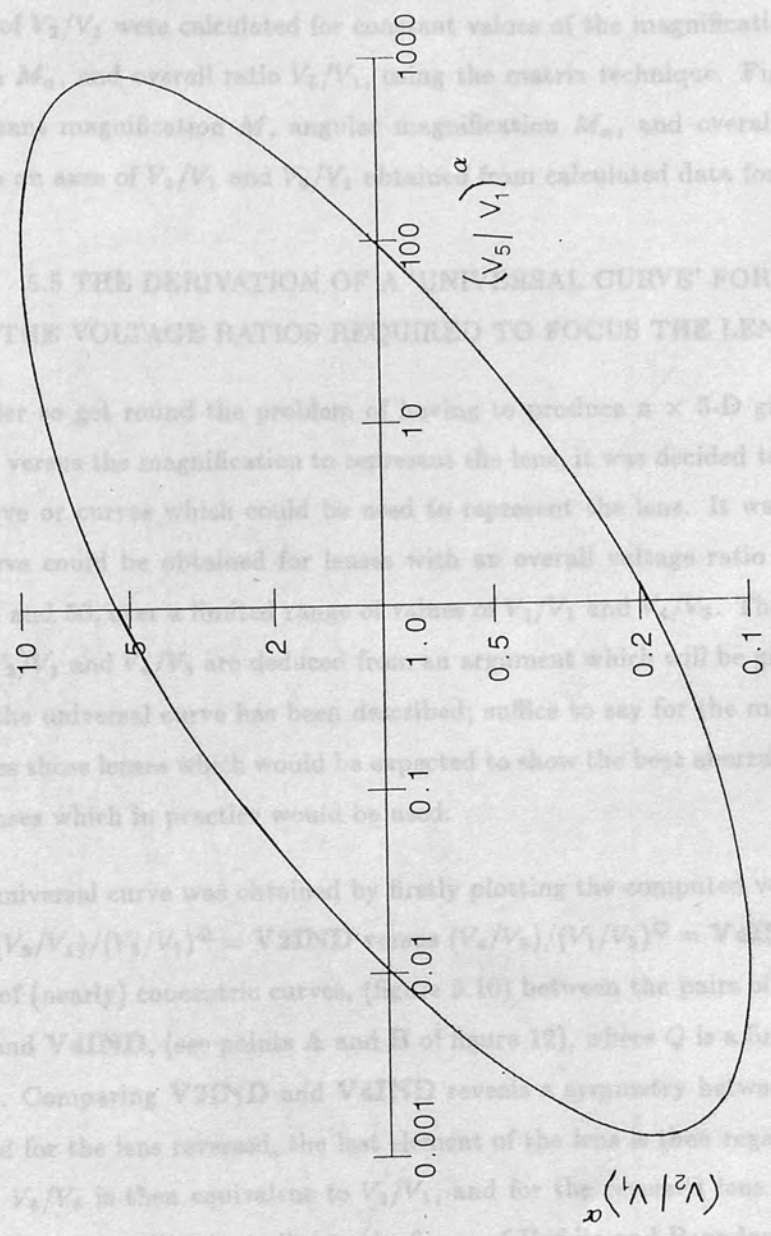


Figure 5.7

THE DERIVATION OF THE 'UNIVERSAL CURVE' FOR THE VOLTAGE RATIOS REQUIRED TO FOCUS THE LENS

The authors got round the problem of introducing a 3-D graph of V_3/V_1 versus V_4/V_1 versus the magnification to represent the lens, by deciding to look for some universal curve or curves which could be used to represent the lens. It was found that a universal curve could be obtained for lenses with an overall voltage ratio V_5/V_1 ranging between 0.02 and 10.0. A number of pairs of limiting values of V_2/V_1 and V_4/V_1 are deduced from an alignment which will be given later, after the form of the universal curve has been described; suffice to say for the moment that the range includes those lenses which would be expected to show the best aberration behaviour, i.e., those lenses which in practice would be used.

The universal curve was obtained by firstly plotting the computer values of $(V_3/V_1)/(V_2/V_1)^\alpha = V_3 \text{IND} / (V_2/V_1)^\alpha$ and $(V_4/V_1)/(V_2/V_1)^\alpha = V_4 \text{IND} / (V_2/V_1)^\alpha$ giving a set of (nearly) concentric curves, (see figure 5.10) between the pairs of limiting values of $V_3 \text{IND}$ and $V_4 \text{IND}$, (see points A and B of figure 10), where Q is a function of V_2/V_1 (figure 5.11). Comparing $V_3 \text{IND}$ and $V_4 \text{IND}$ reveals a symmetry between them if they are compared for the lens reversed, the best element of the lens then regarded as its first element and V_2/V_1 is then equivalent to V_1/V_2 , and for the lens as lens V_2/V_1 becomes V_1/V_2 . Note that figure 5.10 is similar to the figure of Heddlie and Papadovassilakis (figure 5.8) but in a more condensed form.

A 'UNIVERSAL CURVE' is then obtained relating these functions of V_2/V_1 and V_3/V_2 for all values of the overall voltage ratio V_5/V_1 , if these nearly concentric curves are expanded by using a scaling factor ZETA (ZETA being a function of V_1/V_2), which is chosen to make the curves overlap exactly on the axes. The curves do not scale exactly, but

every possible value of V_5/V_1 a three dimensional graph of V_2/V_1 versus V_4/V_3 versus the magnification for example, is required to represent the lens. Heddle and Papadovassilakis (1984) represented the lens properties they had obtained experimentally, (i.e., the **HP** lens) with a graph (figure 5.8) showing lines of constant magnification M , angular magnification M_α , and overall voltage ratio, V_5/V_1 drawn on axes of V_2/V_1 and V_4/V_1 . In the present work, values of V_2/V_1 were calculated for constant values of the magnification M , angular magnification M_α , and overall ratio V_5/V_1 , using the matrix technique. Figure 5.9 shows lines of constant magnification M , angular magnification M_α , and overall voltage ratio V_5/V_1 , drawn on axes of V_2/V_1 and V_4/V_1 obtained from calculated data for the **HP** lens.

5.5 THE DERIVATION OF A 'UNIVERSAL CURVE' FOR THE VOLTAGE RATIOS REQUIRED TO FOCUS THE LENS

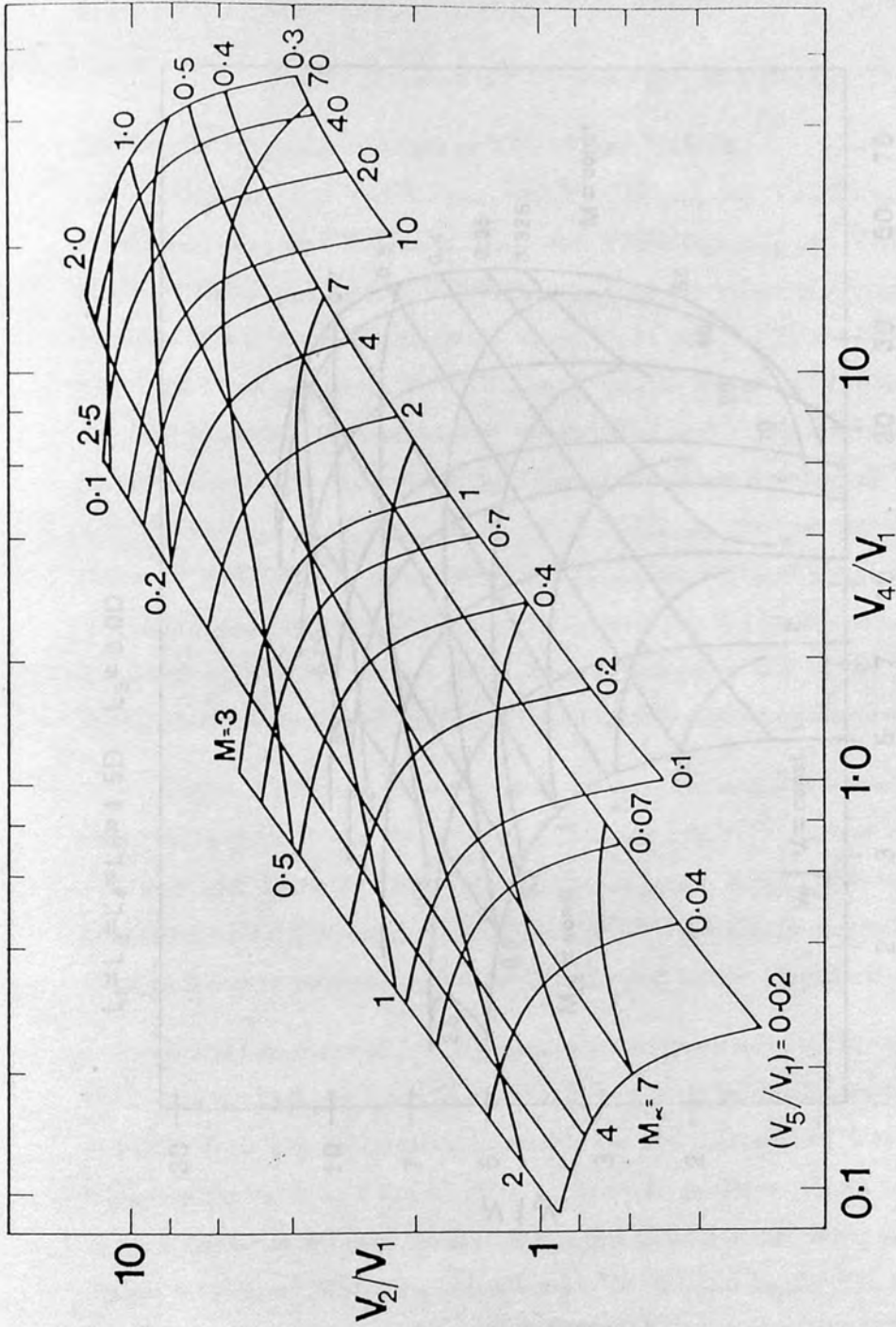
In order to get round the problem of having to produce $n \times 3$ -D graphs of V_2/V_1 versus V_4/V_3 versus the magnification to represent the lens, it was decided to look for some universal curve or curves which could be used to represent the lens. It was found that a universal curve could be obtained for lenses with an overall voltage ratio V_5/V_1 ranging between 0.02 and 50, over a limited range of values of V_2/V_1 and V_4/V_3 . The limiting pairs of values of V_2/V_1 and V_4/V_3 are deduced from an argument which will be given later, after the form of the universal curve has been described; suffice to say for the moment that the range includes those lenses which would be expected to show the best aberration behaviour, i.e., those lenses which in practice would be used.

The universal curve was obtained by firstly plotting the computed values of

$$(V_2/V_1)/(V_5/V_1)^Q = \mathbf{V2IND} \text{ versus } (V_4/V_5)/(V_1/V_5)^Q = \mathbf{V4IND}$$

giving a set of (nearly) concentric curves, (figure 5.10) between the pairs of limiting values of $\mathbf{V2IND}$ and $\mathbf{V4IND}$, (see points **A** and **B** of figure 12), where Q is a function of V_5/V_1 (figure 5.11). Comparing $\mathbf{V2IND}$ and $\mathbf{V4IND}$ reveals a symmetry between them if they are compared for the lens reversed, the last element of the lens is then regarded as its first element and V_4/V_5 is then equivalent to V_2/V_1 , and for the reversed lens V_5/V_1 becomes V_1/V_5 . Note that figure 5.10 is similar to the figure of Heddle and Papadovassilakis (figure 5.8) but in a more condensed form.

A 'UNIVERSAL CURVE' is then obtained relating these functions of V_2/V_1 and V_4/V_5 for all values of the overall voltage ratio V_5/V_1 , if these nearly concentric curves are expanded by using a scaling factor $ZETA$ ($ZETA$ being a function of V_5/V_1), which is chosen to make the curves overlap exactly on the axes. The curves do not scale exactly, but



from Heddle and Papadovassilakis 1984

Figure 5.8

are consistent in better than 2% in the worst case plotted.

To sum up, a universal curve is obtained if V_2/V_1 is plotted against V_4/V_1 for all values of V_5/V_1 where Q and $XPTA$ are functions of V_5/V_1 , between limiting pairs of values of V_2/V_1 and V_4/V_1 , see Figure 5.15, i.e., UNIVERSAL CURVE.

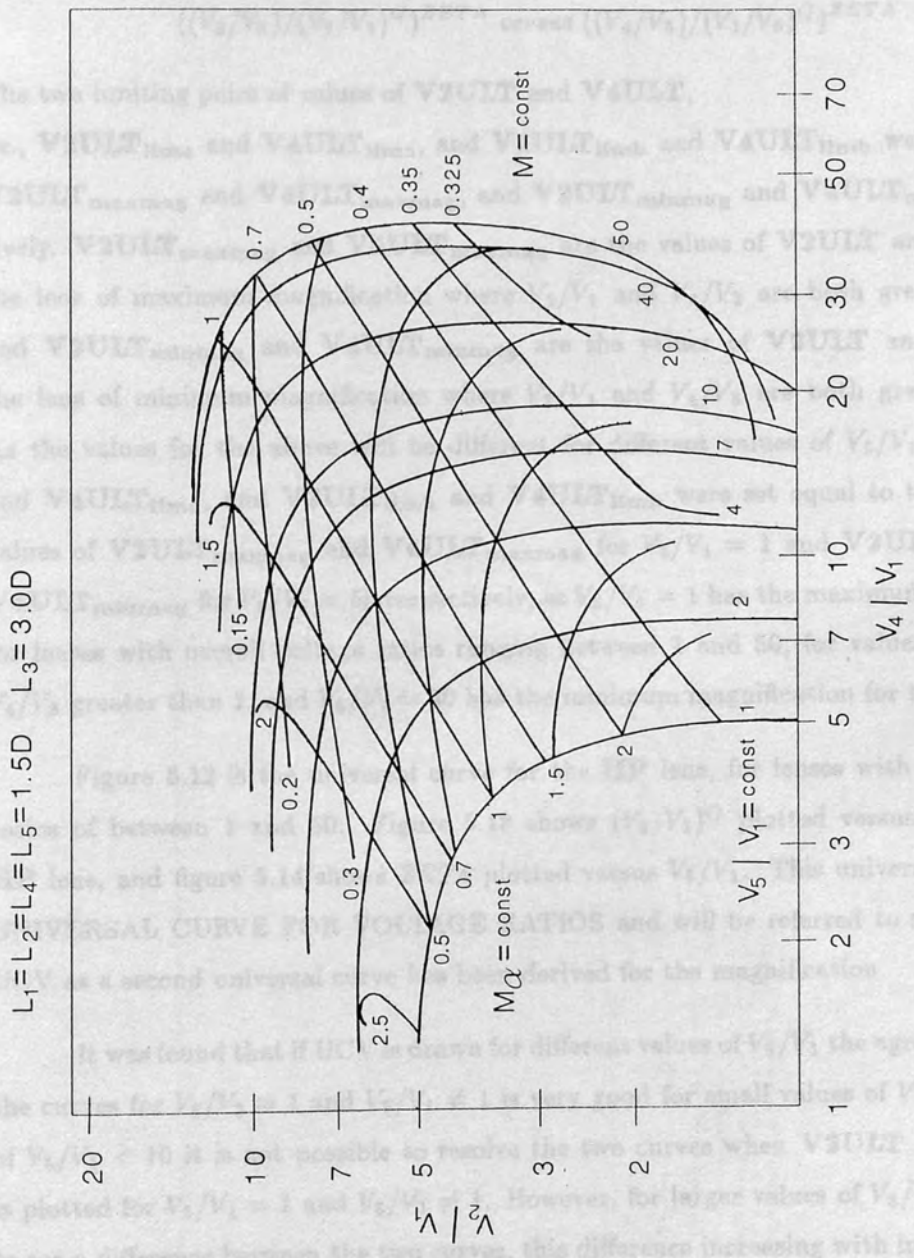


Figure 5.9

It was found that if the curves for different values of V_5/V_1 the agreement between the curves for $V_5/V_1 = 1$ and $V_5/V_1 = 2.5$ is very good for small values of V_4/V_1 , for values of $V_4/V_1 > 10$ it is possible to resolve the two curves when V_2/V_1 versus V_4/V_1 is plotted for $V_5/V_1 = 1$ and $V_5/V_1 = 2.5$. However, for larger values of V_4/V_1 it is possible to see a difference between the two curves, this difference increasing with increasing V_4/V_1 . Figure 5.15 shows V_2/V_1 plotted versus V_4/V_1 for $V_5/V_1 = 1$ and $V_5/V_1 = 10$, for the HP lens, and Figure 5.16 shows V_2/V_1 plotted versus V_4/V_1 for $V_5/V_1 = 1$ and $V_5/V_1 = 15$, for the HP lens.

V_2/V_1 and V_4/V_1 as derived from the values of $V_1/V_1, V_2/V_2$ etc. obtained

are consistent to better than 2% in the worst case plotted.

To sum up, a universal curve is obtained if $((V_2/V_1)/(V_5/V_1)^Q)^{ZETA} = \mathbf{V2ULT}$ is plotted against $((V_4/V_5)/(V_1/V_5)^Q)^{ZETA} = \mathbf{V4ULT}$, for all values of V_5/V_1 where Q and $ZETA$ are functions of V_5/V_1 , between limiting pairs of values of $\mathbf{V2ULT}$ and $\mathbf{V4ULT}$, see figure 5.12, i.e., *UNIVERSAL CURVE*;

$$((V_2/V_1)/(V_5/V_1)^Q)^{ZETA} \text{ versus } ((V_4/V_5)/(V_1/V_5)^Q)^{ZETA} \quad (5.10)$$

The two limiting pairs of values of $\mathbf{V2ULT}$ and $\mathbf{V4ULT}$, i.e., $\mathbf{V2ULT}_{llma}$ and $\mathbf{V4ULT}_{llma}$, and $\mathbf{V2ULT}_{llmb}$ and $\mathbf{V4ULT}_{llmb}$ were set equal to $\mathbf{V2ULT}_{maxmag}$ and $\mathbf{V4ULT}_{maxmag}$, and $\mathbf{V2ULT}_{minmag}$ and $\mathbf{V4ULT}_{minmag}$ respectively. $\mathbf{V2ULT}_{maxmag}$ and $\mathbf{V4ULT}_{maxmag}$ are the values of $\mathbf{V2ULT}$ and $\mathbf{V4ULT}$ for the lens of maximum magnification where V_2/V_1 and V_4/V_3 are both greater than one, and $\mathbf{V2ULT}_{minmag}$ and $\mathbf{V4ULT}_{minmag}$ are the values of $\mathbf{V2ULT}$ and $\mathbf{V4ULT}$ for the lens of minimum magnification where V_2/V_1 and V_4/V_3 are both greater than one. As the values for the above will be different for different values of V_5/V_1 , $\mathbf{V2ULT}_{llma}$ and $\mathbf{V4ULT}_{llma}$, and $\mathbf{V2ULT}_{llmb}$ and $\mathbf{V4ULT}_{llmb}$ were set equal to the appropriate values of $\mathbf{V2ULT}_{maxmag}$ and $\mathbf{V4ULT}_{maxmag}$ for $V_5/V_1 = 1$ and $\mathbf{V2ULT}_{minmag}$ and $\mathbf{V4ULT}_{minmag}$ for $V_5/V_1 = 50$ respectively, as $V_5/V_1 = 1$ has the maximum magnification for lenses with overall voltage ratios ranging between 1 and 50, for values of V_2/V_1 and V_4/V_3 greater than 1, and $V_5/V_1 = 50$ has the minimum magnification for the same range.

Figure 5.12 is the universal curve for the **HP** lens, for lenses with overall voltage ratios of between 1 and 50. Figure 5.13 shows $(V_5/V_1)^Q$ plotted versus V_5/V_1 for the **HP** lens, and figure 5.14 shows $ZETA$ plotted versus V_5/V_1 . This universal curve is the **UNIVERSAL CURVE FOR VOLTAGE RATIOS** and will be referred to subsequently as **UCV** as a second universal curve has been derived for the magnification.

It was found that if **UCV** is drawn for different values of V_5/V_1 the agreement between the curves for $V_5/V_1 = 1$ and $V_5/V_1 \neq 1$ is very good for small values of V_5/V_1 ; for values of $V_5/V_1 < 10$ it is not possible to resolve the two curves when $\mathbf{V2ULT}$ versus $\mathbf{V4ULT}$ is plotted for $V_5/V_1 = 1$ and $V_5/V_1 \neq 1$. However, for larger values of V_5/V_1 it is possible to see a difference between the two curves, this difference increasing with increasing V_5/V_1 . Figure 5.15 shows $\mathbf{V2ULT}$ plotted versus $\mathbf{V4ULT}$ for $V_5/V_1 = 1$ and $V_5/V_1 = 10$, for the **HP** lens, and figure 5.16 shows $\mathbf{V2ULT}$ plotted versus $\mathbf{V4ULT}$ for $V_5/V_1 = 1$ and $V_5/V_1 = 36$, for the **HP** lens.

$\mathbf{V2ULT}$ and $\mathbf{V4ULT}$ as derived from the values of V_2/V_1 , V_4/V_3 etc, obtained

$L_1=L_2=L_4=L_5=1.5D$ $L_3=3.0D$

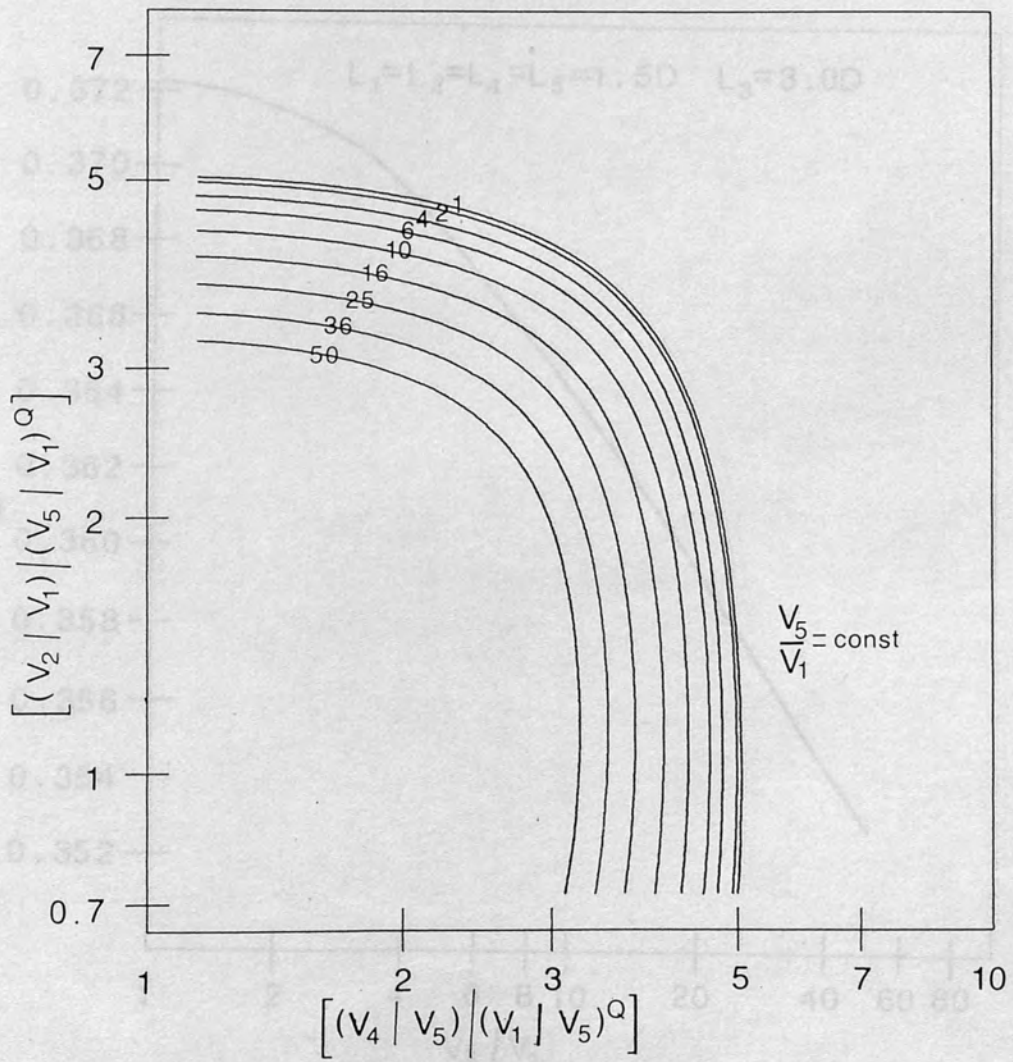


Figure 5.10

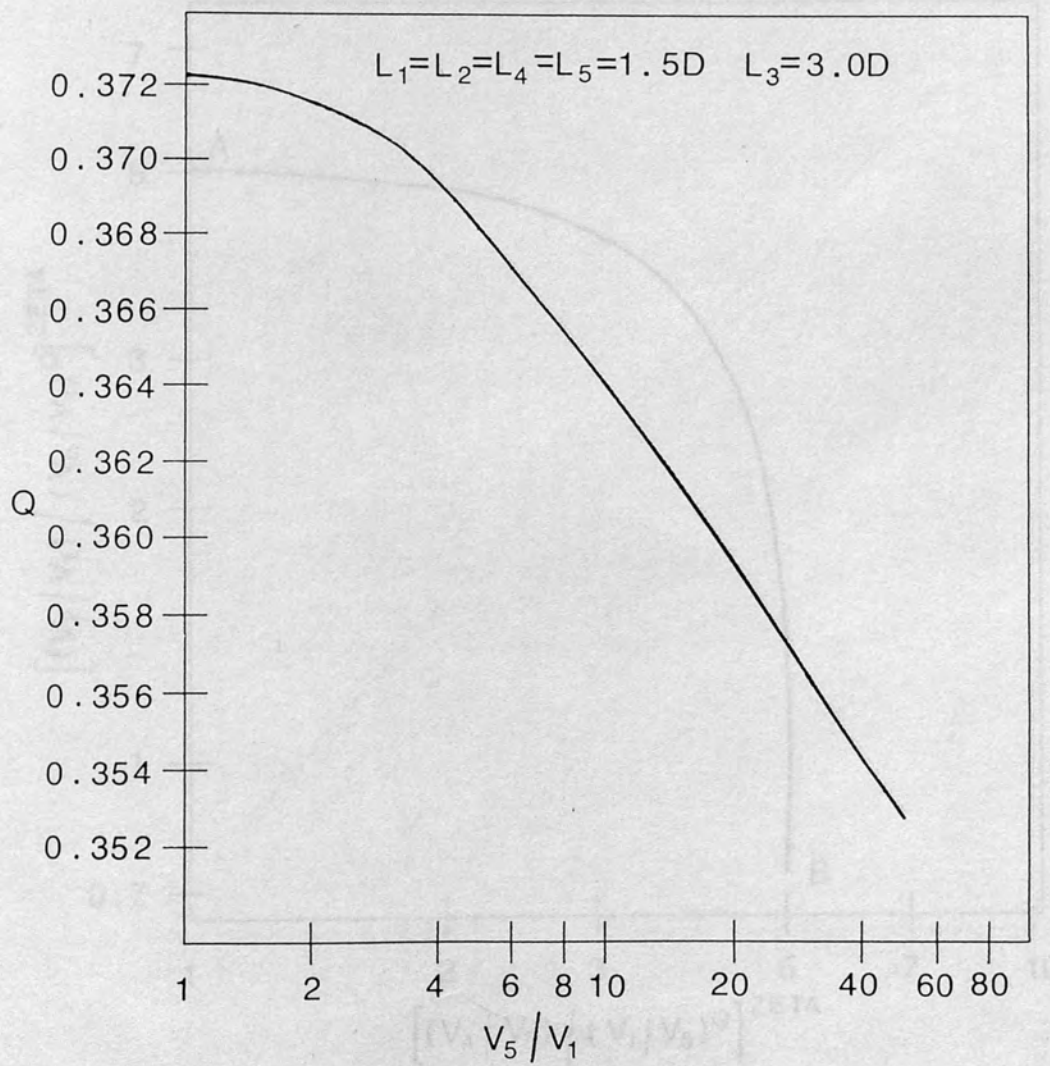


Figure 5.11

$$L_1=L_2=L_4=L_5=1.5D \quad L_3=3.0D$$

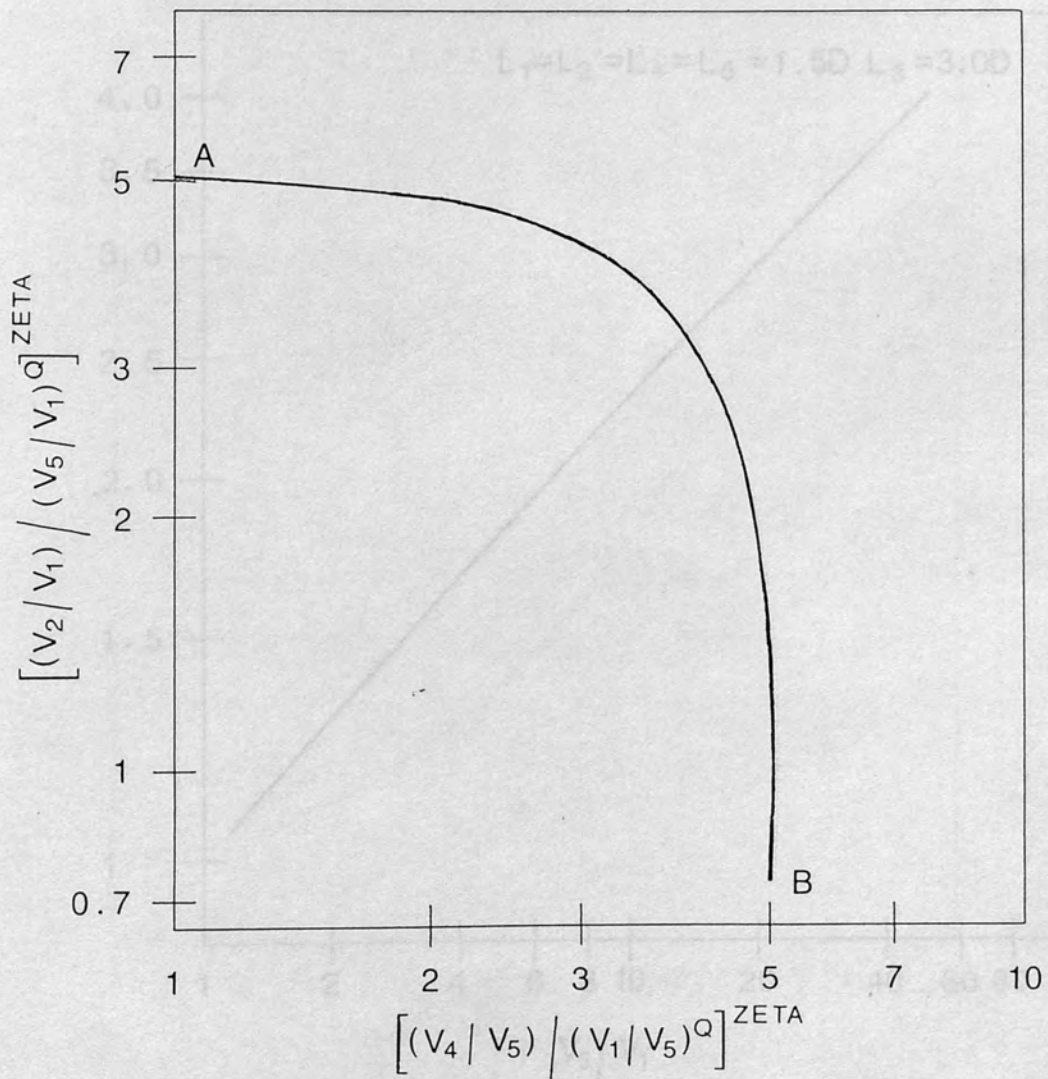


Figure 5.12

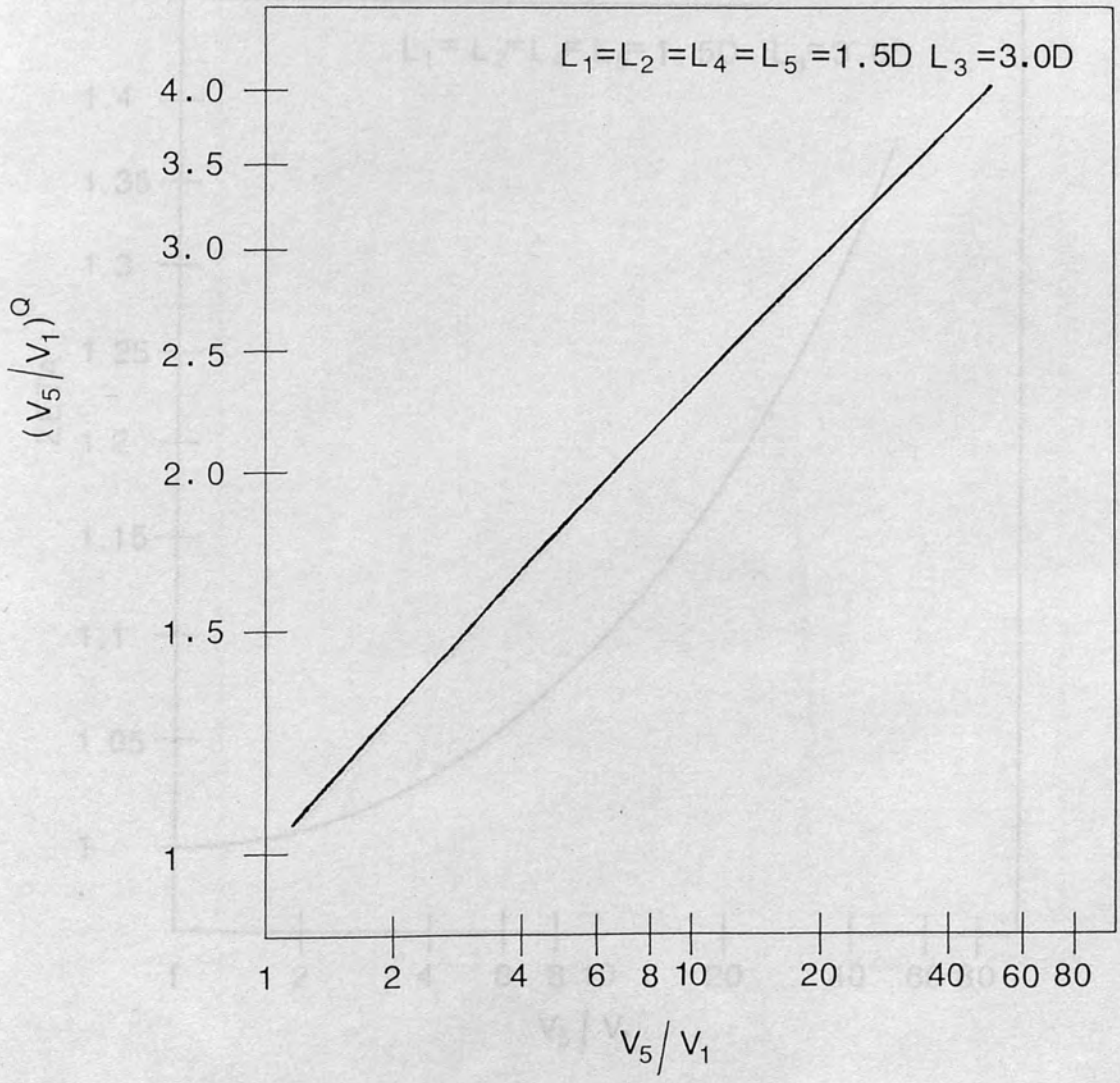


Figure 5.13

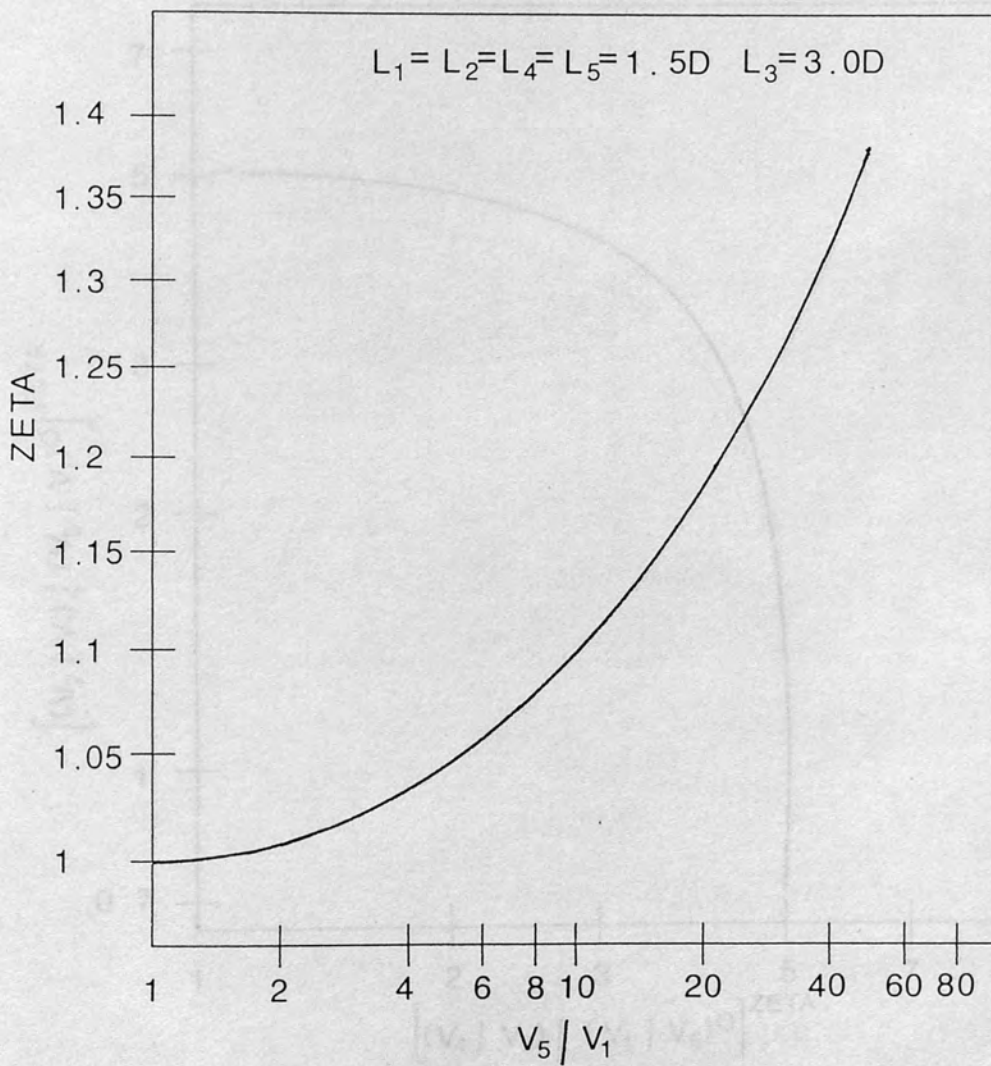


Figure 5.14

$$L_1 = L_2 = L_4 = L_5 = 1.5D \quad L_3 = 3.0D$$

$$V_5 / V_1 = 1 \quad \text{AND} \quad V_5 / V_1 = 10$$

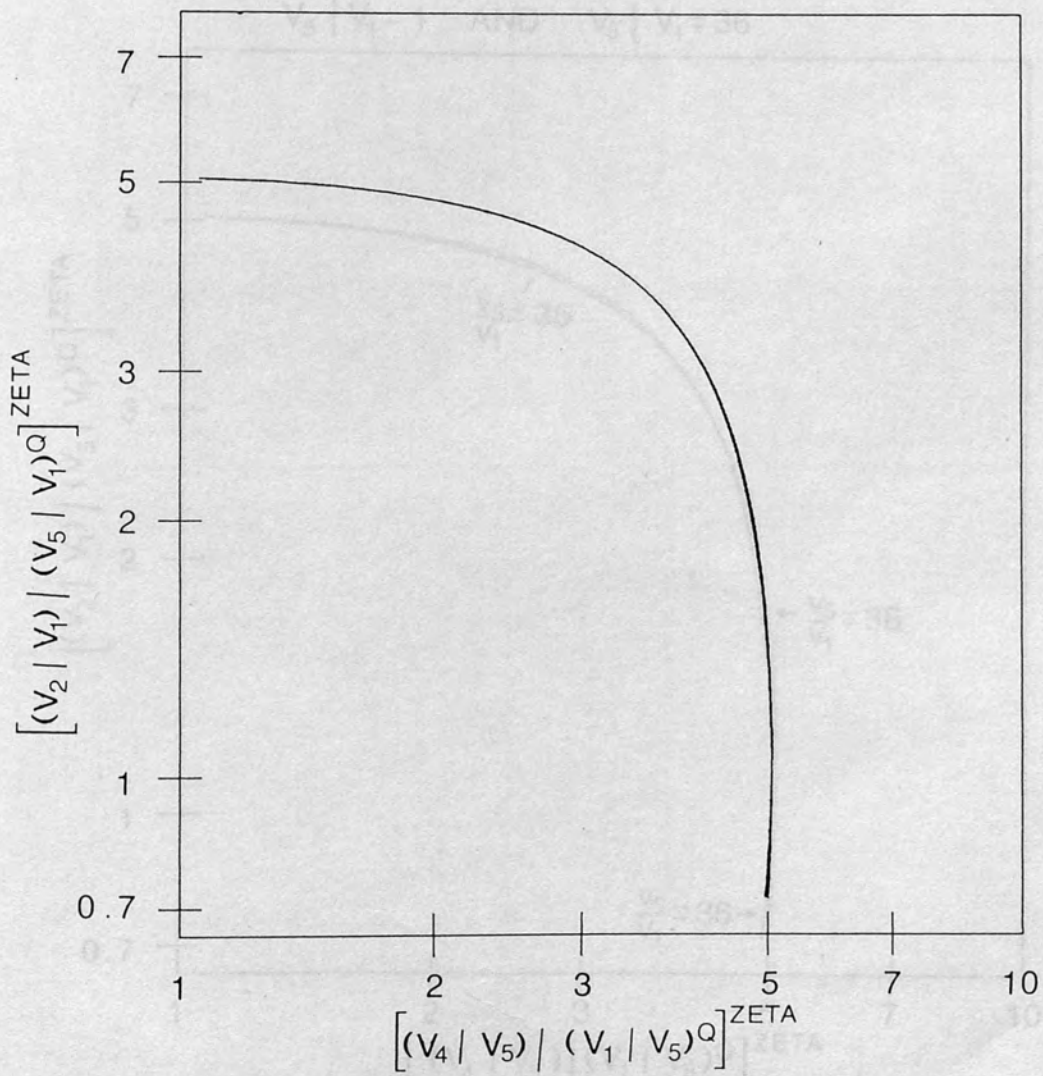


Figure 5.15

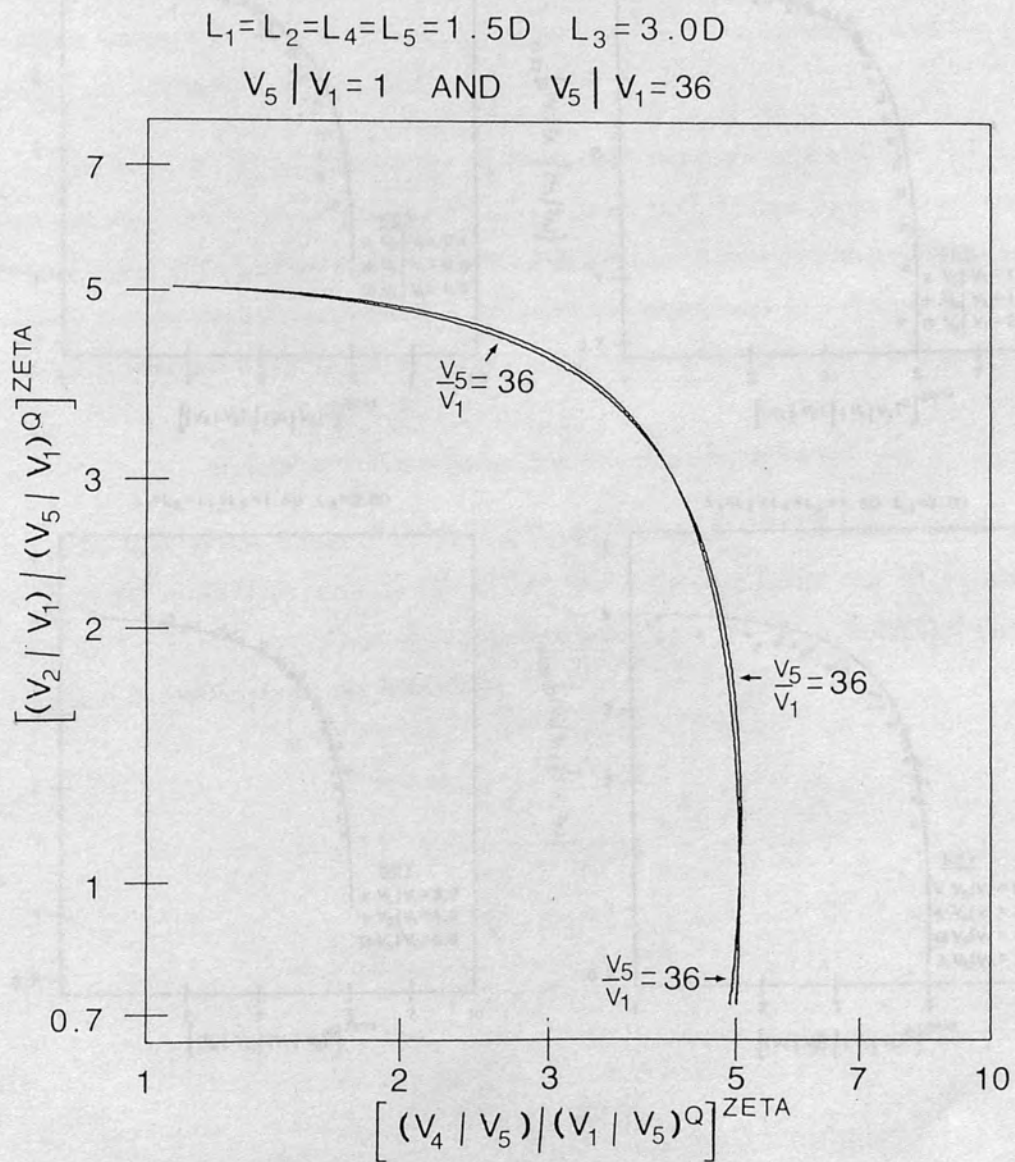


Figure 5.16

by experiment, are plotted in figure 5.17 for the HP lens. The solid line represents the calculated values of V_{AULT} and V_{EULT} .

The agreement between calculation and experiment is within 10% for the experimental points plotted in figure 5.17. The agreement is best for data where $V_2/V_1 \geq 1$ and close to 1. Where $V_2/V_1 < 1$ the agreement between calculation and experiment becomes progressively worse; the experimental values of V_{AULT} becoming progressively less than the calculated values where $V_{AULT,calc} > V_{AULT,exp}$. Where $V_2/V_1 > 1$, the agreement between calculation and experiment becomes progressively worse; the experimental values of V_{AULT} becoming progressively less than the calculated values where $V_{AULT,calc} > V_{AULT,exp}$.

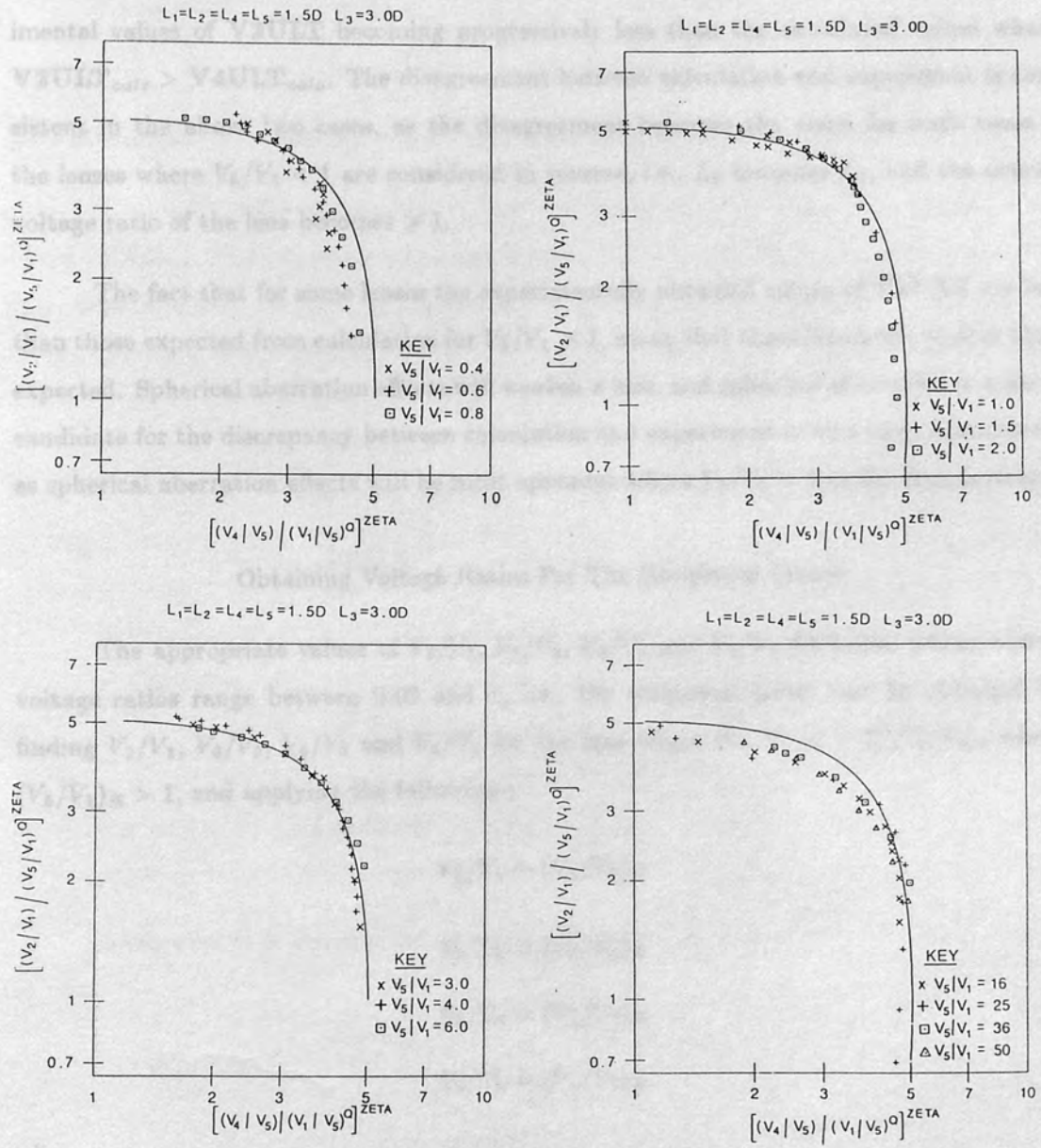


Figure 5.17

by experiment, are plotted in figure 5.17 for the **HP** lens. The solid line represents the calculated values of **V2ULT** and **V4ULT**.

The agreement between calculation and experiment is within 10% for the experimental points plotted in figure 5.17. The agreement is best for data where $V_5/V_1 \geq 1$ and close to 1. Where $V_5/V_1 < 1$ the agreement between calculation and experiment becomes progressively worse; the experimental values of **V4ULT** becoming progressively less than the calculated values where $V4ULT_{calc} > V2ULT_{calc}$. Where $V_5/V_1 > 16$, the agreement between calculation and experiment becomes progressively worse; the experimental values of **V2ULT** becoming progressively less than the calculated values where $V2ULT_{calc} > V4ULT_{calc}$. The disagreement between calculation and experiment is consistent in the above two cases, as the disagreement becomes the same for both cases if the lenses where $V_5/V_1 < 1$ are considered in reverse, i.e., L_5 becomes L_1 , and the overall voltage ratio of the lens becomes > 1 .

The fact that for some lenses the experimentally obtained values of **V2ULT** are less than those expected from calculation for $V_5/V_1 > 1$, mean that these lenses are weaker than expected. Spherical aberration effects will weaken a lens, and spherical aberration is a likely candidate for the discrepancy between calculation and experiment in this case, particularly as spherical aberration effects will be most apparent where $V_5/V_1 < 1$ or the lens is strong.

Obtaining Voltage Ratios For The Reciprocal Lenses

The appropriate values of V_2/V_1 , V_3/V_2 , V_4/V_3 and V_4/V_5 for lenses whose overall voltage ratios range between 0.02 and 1, i.e., the reciprocal lenses can be obtained by finding V_2/V_1 , V_3/V_2 , V_4/V_3 and V_4/V_5 for the lens where $(V_5/V_1)_R = 1/(V_5/V_1)$, where $(V_5/V_1)_R > 1$, and applying the following-;

$$V_2/V_1 = (V_4/V_5)_R$$

$$V_3/V_2 = (V_3/V_4)_R$$

$$V_4/V_3 = (V_2/V_3)_R$$

$$V_4/V_5 = (V_2/V_1)_R$$

also

$$MAG = (1/MAG)_R \quad (5.11)$$

5.6 THE 'UNIVERSAL CURVE' FOR THE MAGNIFICATION

Figure 5.12 i.e., UCV, the universal curve for the voltage ratios for the HP lens, enable all the possible useful values of V_2/V_1 and V_4/V_3 for conjugate points to be deduced. However, it is also necessary to be able to deduce the magnification for the lens for given values of V_5/V_1 , V_2/V_1 and V_4/V_3 . A second universal curve was therefore derived relating the magnification to V_2/V_4 for a given value of V_5/V_1 , and hence via UCV to V_2/V_1 and V_4/V_3 .

It was found that plotting

$$B \times (MAG^A) \text{ versus } (C \times (V_2/V_4))^D \quad (5.12)$$

gave a universal curve over the same range of values of V_2/V_1 and V_4/V_3 as UCV.

A value for A for values of $V_5/V_1 \neq 1 = W$ is obtained by causing the difference between $(MAG_{max})^A$, (i.e., maximum magnification, V_2/V_1 and $V_4/V_3 \geq 1$) and $(MAG_{min})^A$, (i.e., minimum magnification, V_2/V_1 and $V_4/V_3 \geq 1$) to be the same as the difference between MAG_{max} and MAG_{min} for $V_5/V_1 = 1$, (V_2/V_1 and $V_4/V_3 \geq 1$) on a \log_{10} scale; i.e.,

$$\begin{aligned} & \log_{10} ((MAG_{max})^A) - \log_{10} ((MAG_{min})^A) \\ &= \log_{10} \left(MAG_{max, \frac{V_5}{V_1}=1} \right) - \log_{10} \left(MAG_{min, \frac{V_5}{V_1}=1} \right) \\ \Rightarrow A &= \frac{2 \log_{10} \left(MAG_{max, \frac{V_5}{V_1}=1} \right)}{\log_{10} \left(MAG_{max, \frac{V_5}{V_1}=W \neq 1} \right) - \log_{10} \left(MAG_{min, \frac{V_5}{V_1}=W \neq 1} \right)} \quad (5.13) \\ & \left(\text{as } MAG_{max, \frac{V_5}{V_1}=1} = \frac{1}{MAG_{min, \frac{V_5}{V_1}=1}} \right) \end{aligned}$$

A value for B is obtained by offsetting the resultant curve of (MAG^A) versus V_2/V_4 so that

$$MAG_{max, \frac{V_5}{V_1}=W \neq 1} = MAG_{max, \frac{V_5}{V_1}=1} \quad \text{and} \quad (5.14)$$

$$MAG_{min, \frac{V_5}{V_1}=W \neq 1} = MAG_{min, \frac{V_5}{V_1}=1}$$

i.e., the curve of $(B \times (MAG^A))$ versus V_2/V_4 for $V_5/V_1 = W$ and the curve of MAG versus V_2/V_4 for $V_5/V_1 = 1$ are 'parallel' on a \log_{10} scale.

A value for C is obtained by offsetting the curve of $(B \times (MAG^A))$ versus V_2/V_4 so that the curve of $(B \times (MAG^A))$ versus $(C \times (V_2/V_4))$ passes through the origin (\log_{10} scale).

Finally D is used to scale $(B \times (MAG^A))$ versus $(C \times (V_2/V_4))$ so that the curves of $(B \times (MAG^A))$ versus $(C \times (V_2/V_4))^D$ where $V_5/V_1 = W$ and MAG versus V_2/V_4 where $V_5/V_1 = 1$ lie on top of one another (or nearly so), we thus have a universal curve. Figure 5.18 shows UCM. The curves obtained from plotting $(B \times (MAG^A))$ versus $(C \times (V_2/V_4))^D$ for different values of V_5/V_1 for values of V_5/V_1 are indistinguishable for values of V_5/V_1 between 1 and 10. Figure 5.19 shows $(B \times (MAG^A))$ versus $(C \times (V_2/V_4))^D$ for $V_5/V_1 = 1$ and $V_5/V_1 = 10$, for the **HP** lens. and Figure 5.20 shows $(B \times (MAG^A))$ versus $(C \times (V_2/V_4))^D$ for $V_5/V_1 = 1$ and $V_5/V_1 = 36$, for the **HP** lens. Again, as for figures 5.15 and 5.16 i.e., for the voltage ratio universal curves for different values of V_5/V_1 , the agreement is almost perfect for the smaller value of V_5/V_1 but is not quite as good for the larger value of V_5/V_1 . Figures 5.21 to 5.24 show A , B , C and D as functions of V_5/V_1 for the **HP** lens.

$(B \times (MAG^A))$ versus $(C \times (V_2/V_4))^D$ as derived from the values of MAG and V_2/V_4 obtained from experiment, are plotted in figure 5.25 for the **HP** lens. The solid line represents the calculated values of $(B \times (MAG^A))$ and $(C \times (V_2/V_4))^D$. The agreement between calculation and experiment is within 10% for most of the experimental points plotted, however where the value of V_5/V_1 is large i.e., ≥ 16 the discrepancy between calculation and experiment was found to be up to as much as 40% for large values of $(B \times (MAG^A))$ and $(C \times (V_2/V_4))^D$. As with the voltage data, i.e., figure 5.17, the agreement between calculation and experiment is best for data where $V_5/V_1 \geq 1$ and close to 1. The disagreement between calculation and experiment occurs when the magnification is at its largest, i.e., when the lens is strong. The magnification is found to have larger values than those predicted by calculation. The fact that it is difficult to judge when the lens is focussed using the method described in Chapter Three when the lens is strong, may possibly explain the discrepancy between calculation and experiment. When the lens is strong, lens action occurs close to the object plane, i.e., far away from the image plane. This means that the angle at which rays reach the image plane is shallow, causing the depth of field to be large, making it difficult to judge focus.

Deducing the values of V_2/V_1 and V_4/V_3 when the values
of V_5/V_1 and the Magnification are Specified

Using UCV followed by UCM allows a value for the magnification to be deduced

once the values of V_5/V_1 , V_2/V_1 and V_4/V_3 have been chosen. However, to obtain values for V_2/V_1 and V_4/V_3 for a lens where V_5/V_1 and the magnification are both known, it first is necessary to find the value of V_2/V_4 using UCM i.e., figure 5.18 and figures 5.21 to 5.24. V_2/V_1 and V_4/V_3 can then be deduced from UCV plotted on linear axes (figure 5.26) using the argument given below. The tangent of the angle θ_u of UCV, i.e., $V2ULT/V4ULT$ plotted on linear axes is equal to $(V_2/V_4) / (V_5/V_1)^{(2Q-1)ZETA}$, i.e.,

$$\tan\theta_u = (V_2/V_4) / (V_5/V_1)^{(2Q-1)ZETA} \quad (5.15)$$

therefore the values of

$((V_2/V_1)/(V_5/V_1)^Q)^{ZETA}$ (i.e., **V2ULT**) and $((V_4/V_5)/(V_1/V_5)^Q)^{ZETA}$ (i.e., **V4ULT**) can be read off UCV once the value of the angle θ_u is known and is found by calculating the arctangent of $(V_2/V_4 \times (V_5/V_1)^{(2Q-1)})$, obtaining the appropriate value of Q from figure 5.11. The values of V_2/V_1 and V_4/V_3 may then be deduced by using the values of Q , $(V_5/V_1)^Q$ and $ZETA$ obtained from figures 5.11, 5.13, and 5.14, and remembering that V_3/V_1 is constrained to equal $\sqrt{V_5/V_1}$.

5.7 THE 'UNIVERSAL CURVE' FOR THE ANGULAR MAGNIFICATION

It was found that plotting $(B' \times (MAG_\alpha^{A'}))$ versus $(C \times (V_2/V_4))^D$ gave a universal curve for the angular magnification over the same range of values of V_2/V_1 and V_4/V_3 as UCV and UCM, where

$$A' = -A$$

$$B' = \frac{B}{\left(\frac{V_5}{V_1}\right)^{\frac{1}{2}A}} \quad (5.16)$$

5.8 THE INVESTIGATION OF THE ABERRATION BEHAVIOUR OF A FIVE-ELEMENT LENS

The aberration behaviour of a five-element lens with $L_1 = L_5 = 1.5D$, $L_2 = L_4 = 1.0D$ and $L_3 = 3.0D$ was investigated. It was decided to study the aberration behaviour of this lens in preference to the **HP** lens as it is slightly shorter, a shorter lens perhaps being easier to use as it requires less vacuum space, a slightly shorter lens is also slightly stronger which may also be useful. The aberration behaviour of this particular lens is also slightly better than the **HP** lens because the lengths of its second and fourth elements L_2 and L_4 are shorter than the lengths of the second and fourth elements of the **HP** lens.

$$L_1 = L_2 = L_4 = L_5 = 1.5D \quad L_3 = 3.0D$$

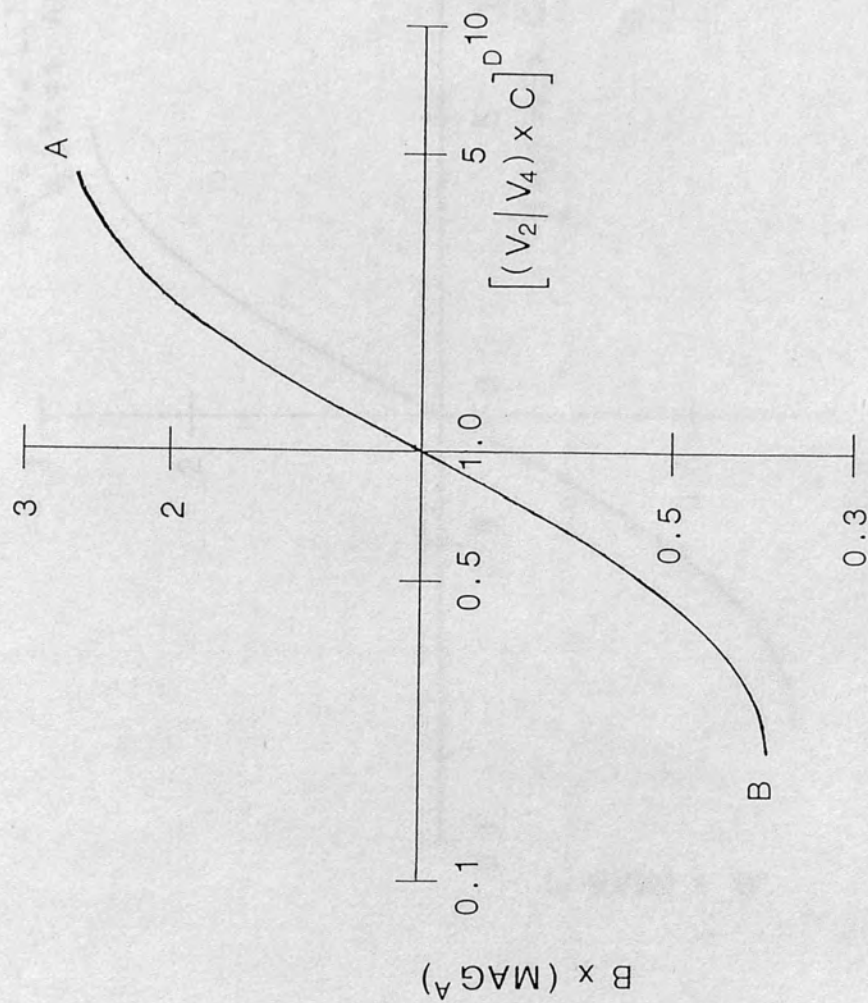


Figure 5.18

$L_1=L_2=L_4=L_5=1.5D$ $L_3=3.0D$
 $V_5/V_1=1$ AND $V_5/V_1=10$

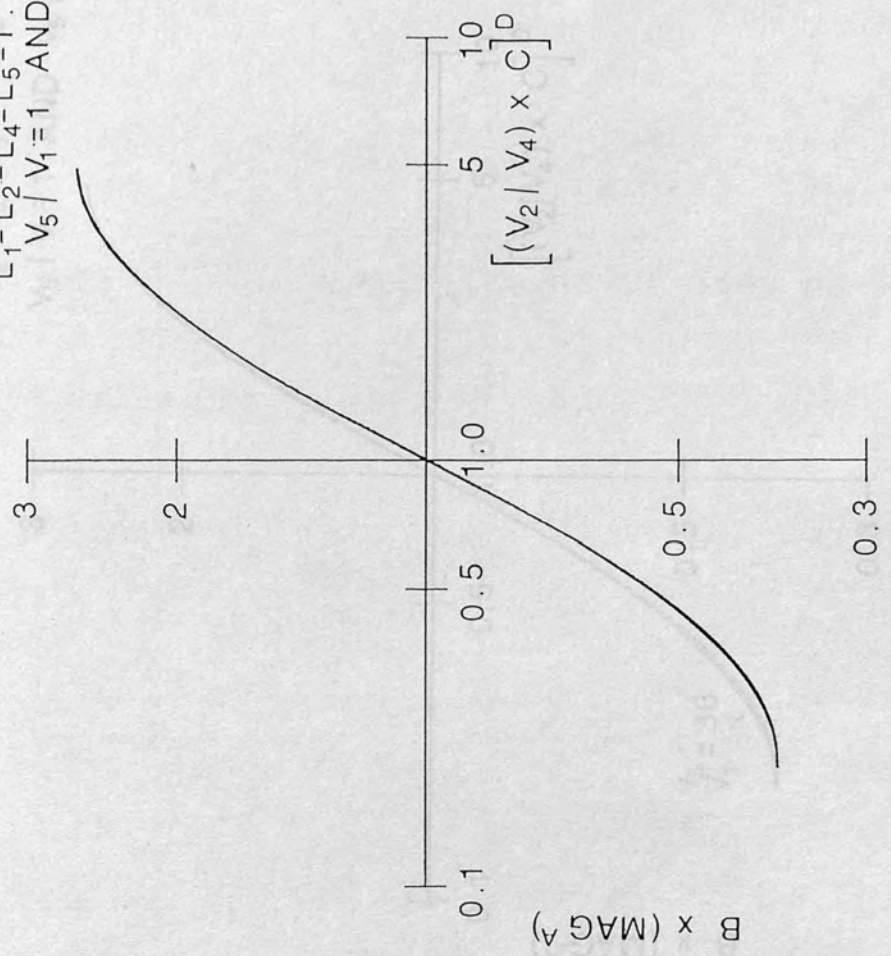


Figure 5.19

$L_1 = L_2 = L_4 = L_5 = 1.5D$ $L_3 = 3.0D$
 $V_5 / V_1 = 1$ AND $V_5 / V_1 = 36$

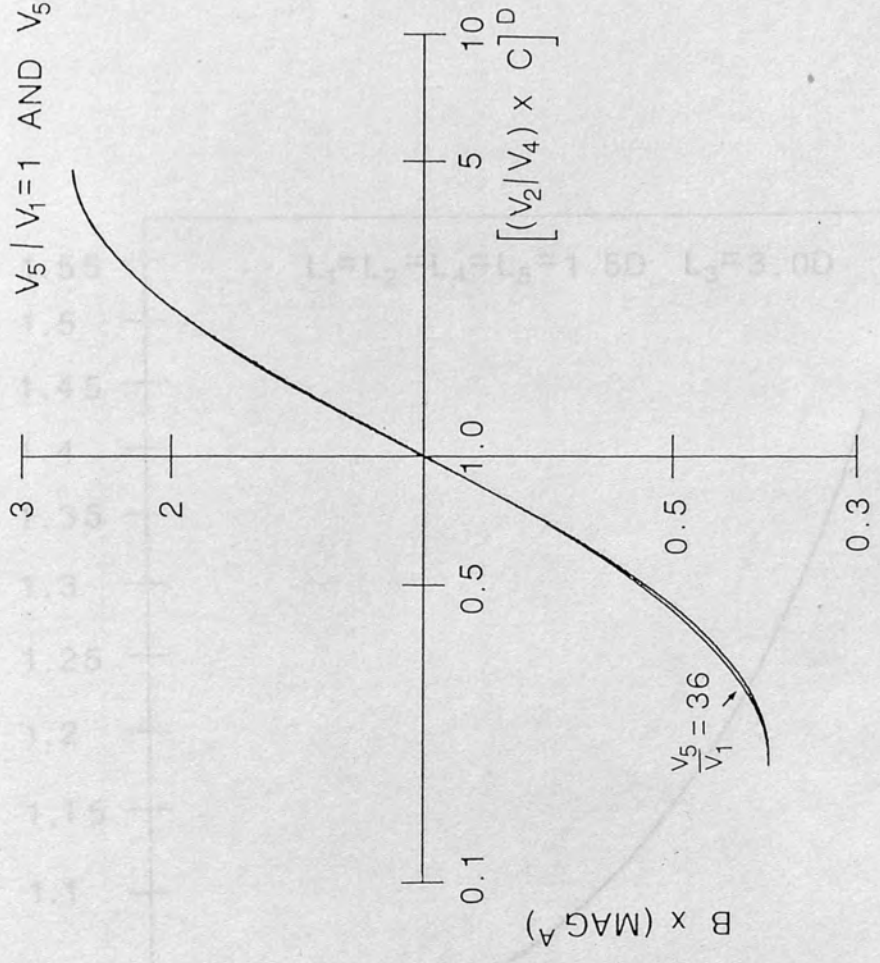


Figure 5.20

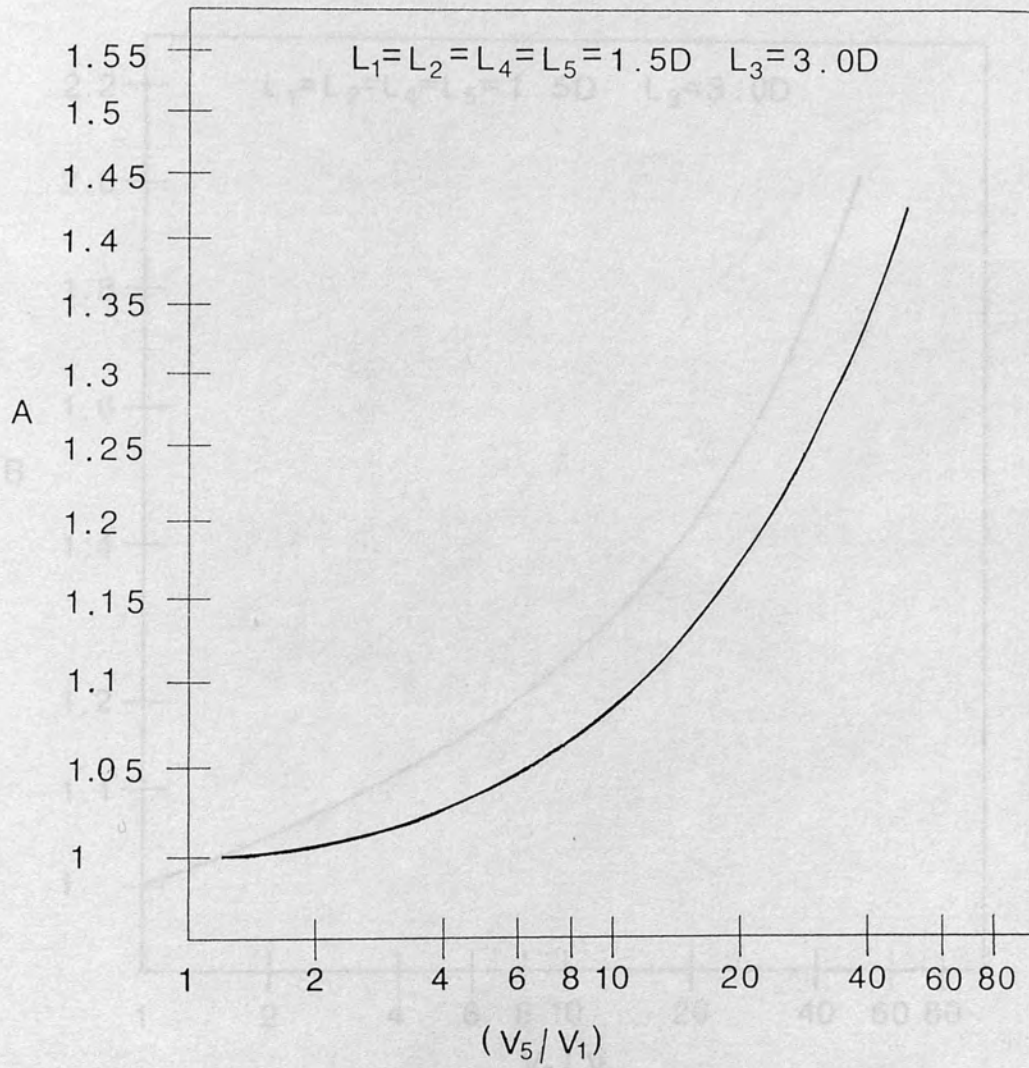


Figure 5.21

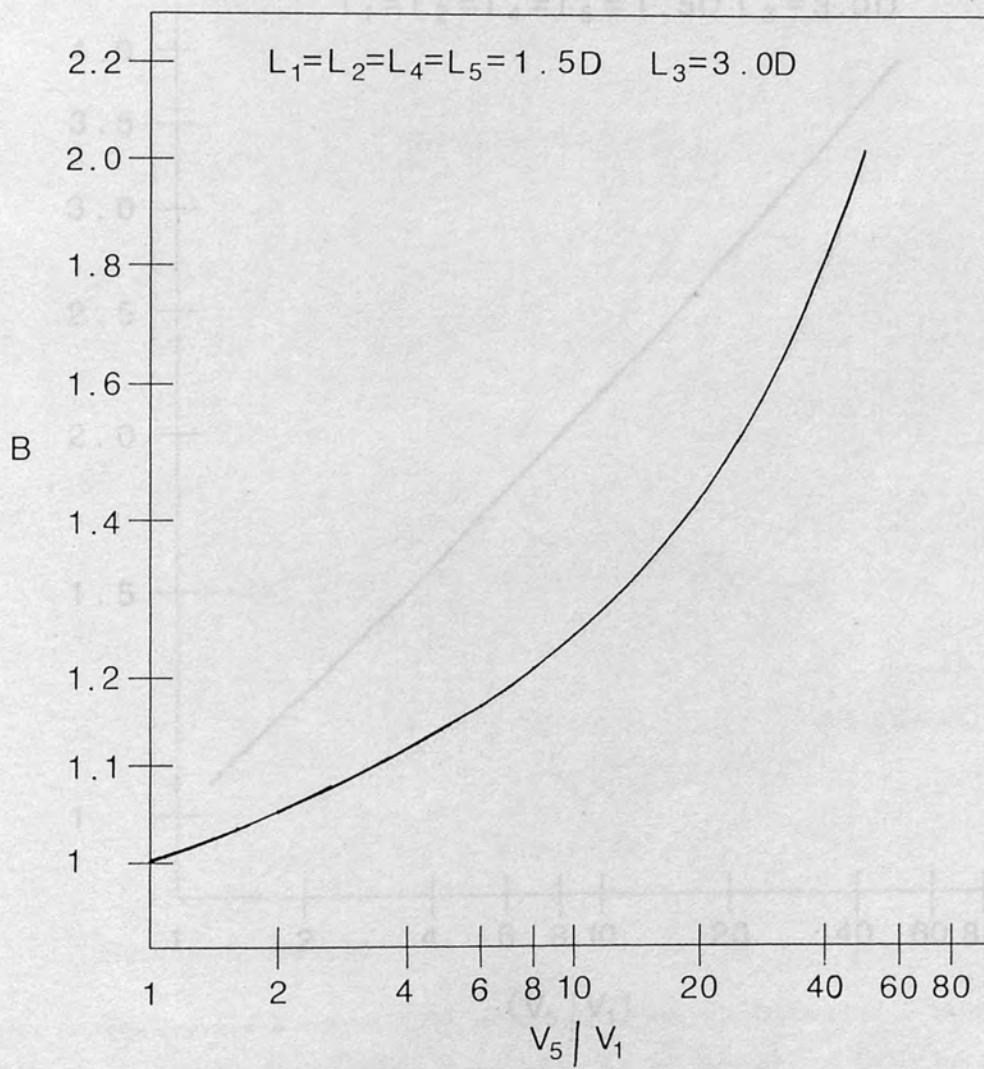
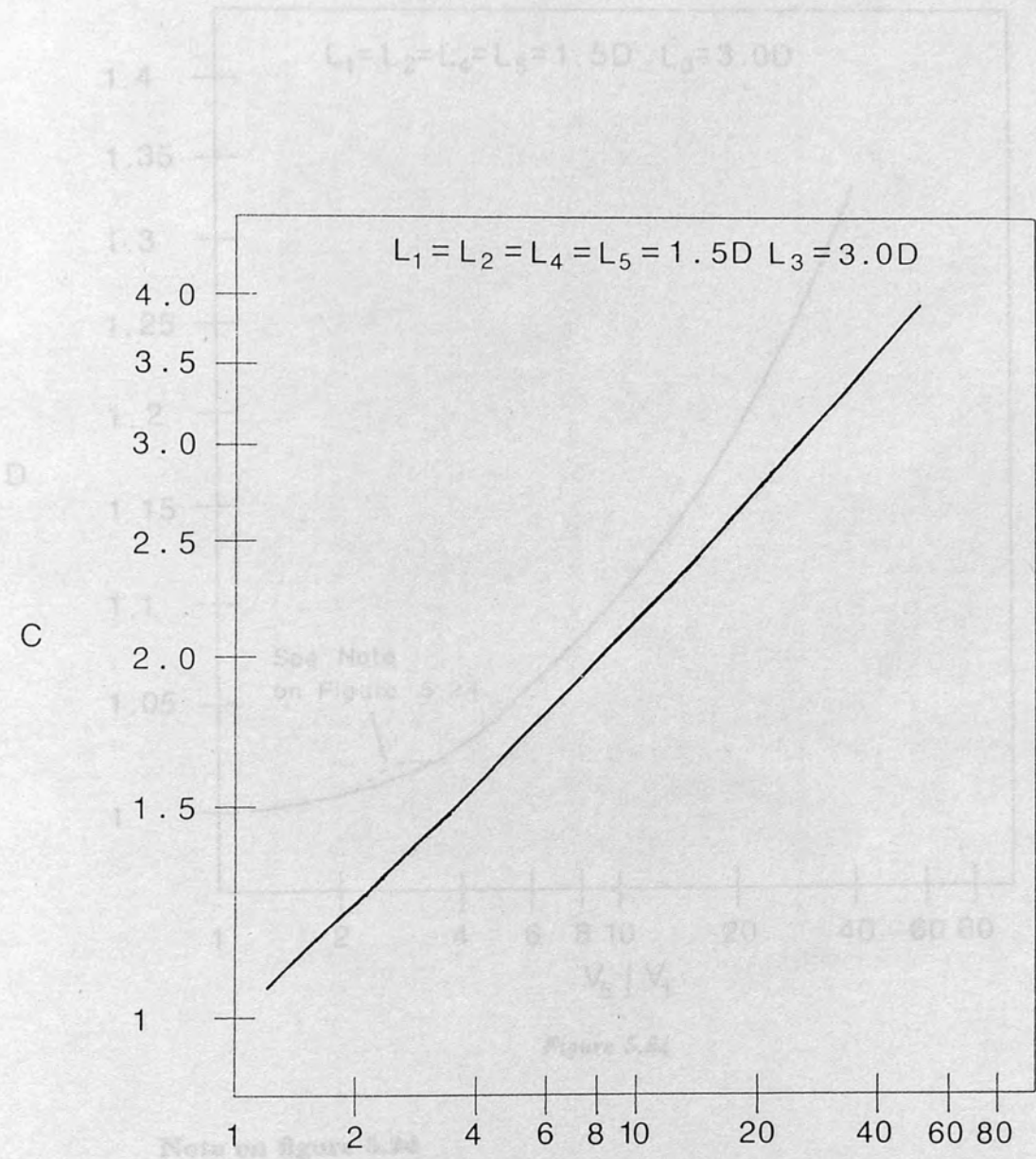


Figure 5.22



The curve of D versus V_5/V_1 as shown in the above figure has a 'bump' as shown by the dashed line in the above figure. The 'bump' may be due to an anomaly in the calculations, therefore a curve (full line) is shown which ignores the 'bump'.

Figure 5.23

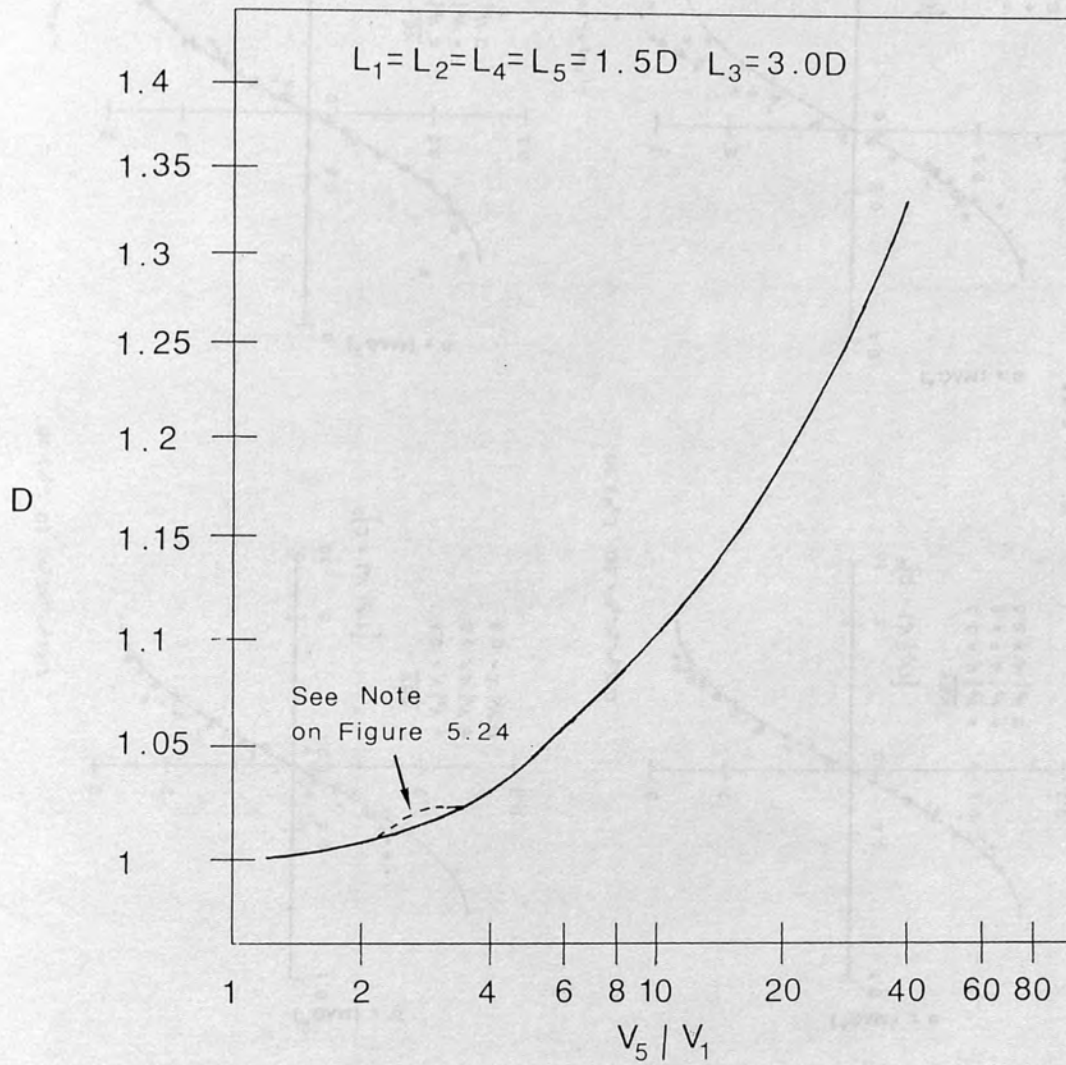
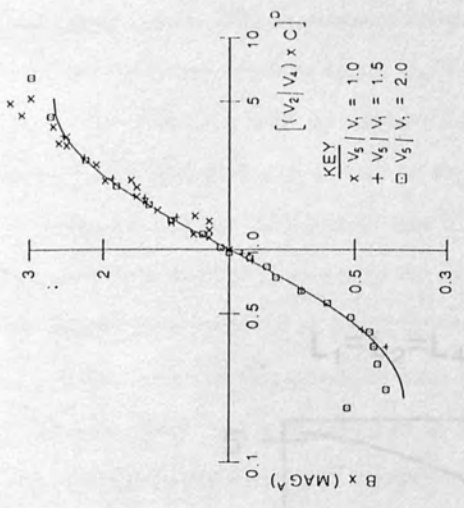


Figure 5.24

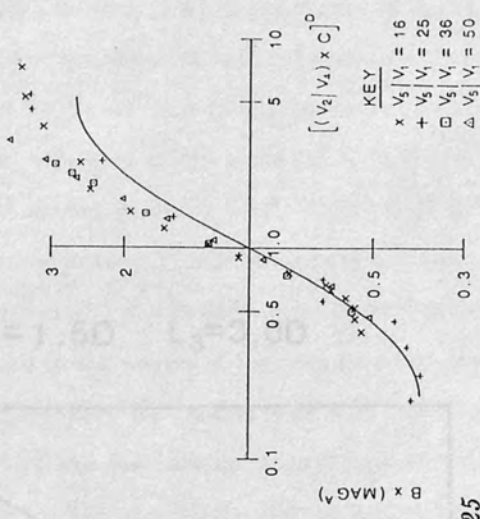
Note on figure 5.24

The curve of D versus V_5/V_1 as produced from calculations has a 'bump' as shown by the dashed line in the above figure. The 'bump' may be due to an anomaly in the calculations, therefore a curve (full line) has been drawn which ignores the 'bump'.

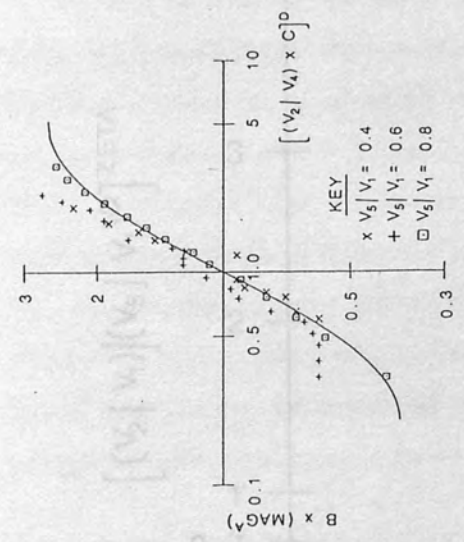
$L_1=L_2=L_4=L_5=1.5D$ $L_3=3.0D$



$L_1=L_2=L_4=L_5=1.5D$ $L_3=3.0D$



$L_1=L_2=L_4=L_5=1.5D$ $L_3=3.0D$



$L_1=L_2=L_4=L_5=1.5D$ $L_3=3.0D$

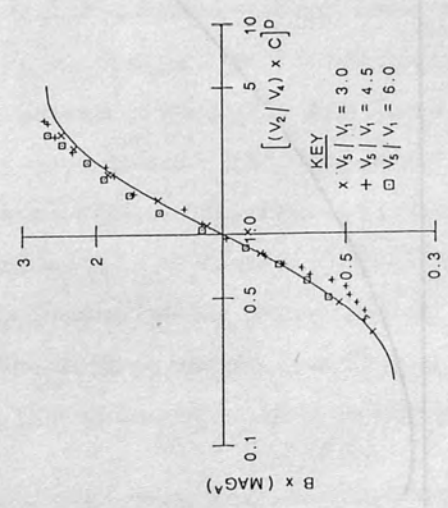


Figure 5.25

The aberration behaviour of this lens as a function of V_5/V_1 was investigated, where V_2/V_1 was constrained to equal 1 and V_3/V_1 and $V_4/V_5 > V_3/V_1$ were constrained to be equal, and equal to or greater than V_5/V_1 ; i.e., the magnification was 1. It was found that C_s varied inversely with V_5/V_1 , C_s changing most rapidly where V_5/V_1 is small and less than 1, the rate of change of C_s decreasing as V_5/V_1 is increased to values greater than 1 up to a maximum value. The maximum value of V_5/V_1 is reached when the values of $V_2/V_1 = V_4/V_5$ equal to four the lens equal V_2/V_1 , i.e., the five-element lens reduces to a three-element lens. For this lens the maximum value of $V_5/V_1 = 11.5$ (deduced from calculation, see below). C_s was deduced from the measured values of Δ and ν for $0.5 \leq V_5/V_1 \leq 1.2$, from pictures on the oscilloscope screen like that shown in Figure 5.27. Figure 5.27 differs from Figure 5.25 in that it shows only six dots instead of ten. This is because it was found that for an overall voltage ratio of 1 and a magnification of 1 it was only possible to illuminate three of the five holes of the aperture disc A placed in the centre of the lens (see Chapter Three). (The disc used was a circular disc with five holes and two of the holes were in horizontal direction and a separation of 3.5mm between its central hole and the off-axis holes in the vertical direction.) However, it was possible to deduce values for both Δr_1 and Δr_2 from pictures like that of figure 5.27, i.e., values of C_s could be obtained and compared from independently obtained values of Δr_1 where $i = \Delta$ or ν for each value of V_5/V_1 it was felt that the results obtained could be accepted with reasonable confidence. Values of C_s were also obtained for values of $V_5/V_1 > 1.2$, as it was not possible to measure Δr_1 or Δr_2 for $V_5/V_1 > 1.2$, as it was not possible to resolve the dots from which Δr_1 and Δr_2 were deduced. The results obtained are shown in figure 5.26. The curves show the agreement between the values of C_s obtained from the two methods. The agreement between the values of C_s obtained from the two methods for values of V_5/V_1 is within 7% for all values of V_5/V_1 . The agreement between the values of C_s calculated by Heide, (private communication) using the Heide expansion method and the Fox-Groenin method, (see Chapter Two) (the agreement in this experiment is shown to be within 32% which is within experimental error).

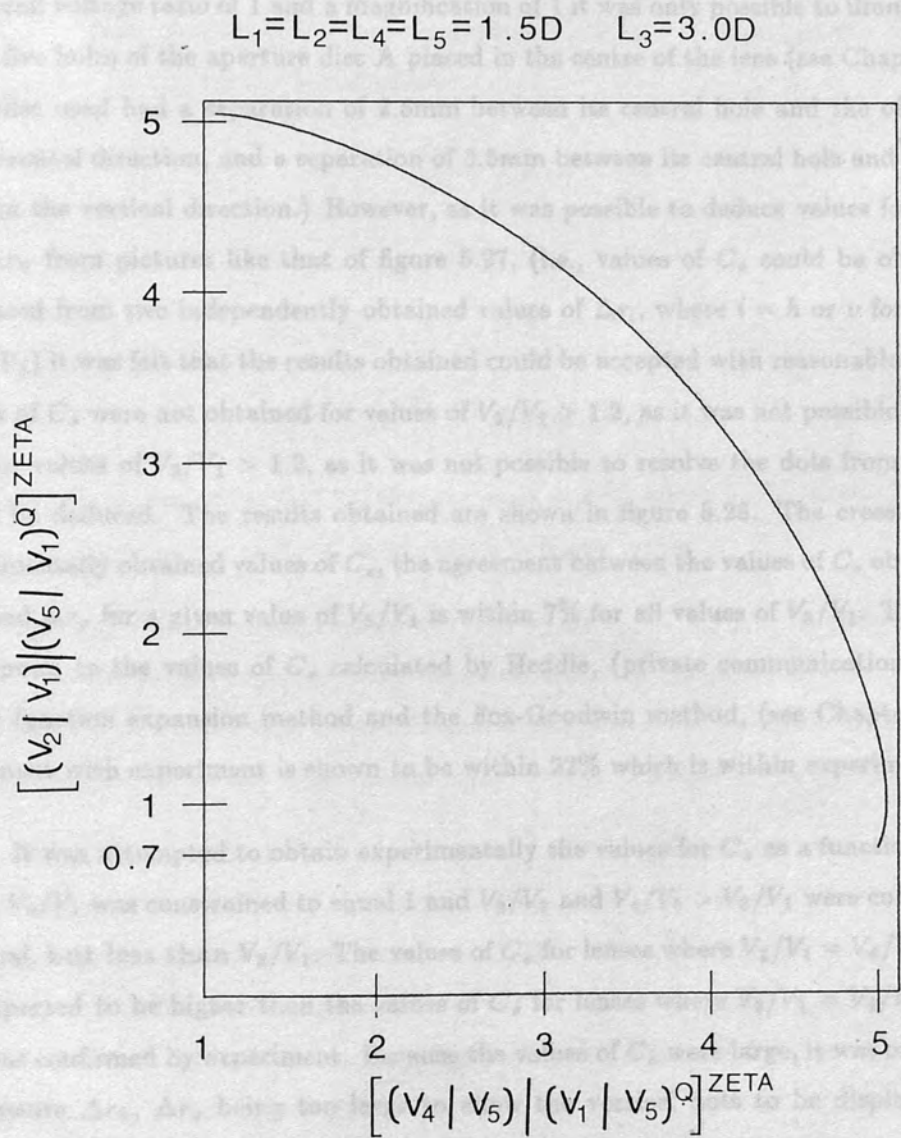


Figure 5.26

The aberration behaviour of this lens as a function of V_3/V_1 was investigated, where V_5/V_1 was constrained to equal 1 and V_2/V_1 and $V_4/V_5 > V_3/V_1$ were constrained to be equal, and equal to or greater than V_3/V_1 ; i.e., the magnification was 1. It was found that C_s varied inversely with V_3/V_1 , C_s changing most rapidly where V_3/V_1 is small and less than 1, the rate of change of C_s decreasing as V_3/V_1 is increased to values greater than 1 up to a maximum value. The maximum value of V_3/V_1 is reached when the values of $V_2/V_1 = V_4/V_5$ required to focus the lens equal V_3/V_1 , i.e., the five-element lens reduces to a three-element lens. For this lens the maximum value of $V_3/V_1 = 11.8$ (deduced from calculation, see below). C_s was deduced from the measured values of h and v for $0.5 \leq V_3/V_1 \leq 1.2$, from pictures on the oscilloscope screen like that shown in figure 5.27. Figure 5.27 differs from figure 3.15 in that it shows only six dots instead of ten. This is because it was found that for an overall voltage ratio of 1 and a magnification of 1 it was only possible to illuminate three of the five holes of the aperture disc **A** placed in the centre of the lens (see Chapter Three). (The disc used had a separation of 2.5mm between its central hole and the off-axis holes in horizontal direction, and a separation of 3.5mm between its central hole and the off-axis holes in the vertical direction.) However, as it was possible to deduce values for both Δr_h and Δr_v from pictures like that of figure 5.27, (i.e., values of C_s could be obtained and compared from two independently obtained values of Δr_i , where $i = h$ or v for each value of V_3/V_1) it was felt that the results obtained could be accepted with reasonable confidence. Values of C_s were not obtained for values of $V_3/V_1 > 1.2$, as it was not possible to measure Δr_h for values of $V_3/V_1 > 1.2$, as it was not possible to resolve the dots from which Δr_h would be deduced. The results obtained are shown in figure 5.28. The crosses show the experimentally obtained values of C_s , the agreement between the values of C_s obtained from Δr_h and Δr_v for a given value of V_3/V_1 is within 7% for all values of V_3/V_1 . The asterisks correspond to the values of C_s calculated by Heddle, (private communication) using the Bessel function expansion method and the Fox-Goodwin method, (see Chapter Two) the agreement with experiment is shown to be within 22% which is within experimental error.

It was attempted to obtain experimentally the values for C_s as a function of V_3/V_1 , where V_5/V_1 was constrained to equal 1 and V_2/V_1 and $V_4/V_5 > V_3/V_1$ were constrained to be equal, **but less than** V_3/V_1 . The values of C_s for lenses where $V_2/V_1 = V_4/V_5 < V_3/V_1$, are expected to be higher than the values of C_s for lenses where $V_2/V_1 = V_4/V_5 > V_3/V_1$, this was confirmed by experiment. Because the values of C_s were large, it was only possible to measure Δr_h , Δr_v being too large to allow the vertical dots to be displayed on the oscilloscope screen. The value of Δr_h for a given V_3/V_1 was found to be very sensitive to the value of $V_2/V_1 = V_4/V_5$, this fact coupled with the fact that only Δr_h could be measured

made it impossible to obtain values of C_s with any degree of confidence. However, they were within 50% of the values of C_s calculated by Heddle. The calculations by Heddle showed that as with the lens where $V_2/V_1 = V_4/V_5 > V_3/V_1$, C_s varies inversely with V_3/V_1 , changing most rapidly where V_3/V_1 is small and less than 1, the rate of change of C_s decreasing as V_3/V_1 is increased to values greater than 1 up to a maximum value, the maximum value of V_3/V_1 occurring when $V_2/V_1 = V_4/V_5 \approx (V_3/V_1)^{1/2}$.

The aberration behaviour of the afocal lens was also investigated. C_s was obtained experimentally for $V_5/V_1 = 0.5, 0.666, 1.5$ and 2.0 . Figure 5.29 shows the experimentally obtained values of C_s as a function of V_5/V_1 , and shows how they compare with those obtained from calculation, again the experimental results obtained are within experimental error of those calculated. Both experiment and calculation show that C_s varies inversely with V_5/V_1 . Note that $C_s = C_{sr}$ for lenses where $V_5/V_1 < 1 = (V_5/V_1)_r$, can be expressed in terms of $C_s = C_{sa}$ for the lenses where

$$\frac{V_5}{V_1} = \frac{1}{\left(\frac{V_5}{V_1}\right)_r}$$

i.e.,

$$\begin{aligned} C_{sr} &= C_{sa} M^4 \left(\frac{V_5}{V_1}\right)^{3/2} \\ &= C_{sa} \left(\frac{V_5}{V_1}\right)^{1/2} \text{ for the afocal lens} \end{aligned}$$

Heddle's calculations show that C_s changes most rapidly where V_5/V_1 is small, the rate of change of C_s decreasing as V_5/V_1 is increased to larger values.

Finally, C_s was investigated for the lens where $V_5/V_1 = V_3/V_1 = 1$, $V_2/V_1 \neq V_4/V_5$. Figure 5.30 shows the experimentally obtained values of C_s as a function of V_4/V_1 and shows how they compare with those obtained from calculation, and again the experimental results obtained are within experimental error of those calculated.

When considering the overall performance of a lens the important parameter is not C_s but the product of C_s and the magnification $MAG \times C_s$, as it is this product which determines by how much the aberrated image differs from the perfect image. In the case where C_s was investigated as a function of V_3/V_1 the magnification was equal to 1 in all cases. However, for the afocal lens the magnification is a function of the overall voltage ratio V_5/V_1 , in fact it is inversely proportional to V_5/V_1 . As C_s is also inversely proportional to V_5/V_1 , the product $MAG \times C_s$ is therefore also inversely proportional to V_5/V_1 . In the last case considered, i.e., $V_5/V_1 = V_3/V_1 = 1$, $V_2/V_1 \neq V_4/V_5$, the magnification is

proportional to V_2/V_1 . As C_s is inversely proportional to V_2/V_1 , the product $MAG \times C_s$ will reach a minimum i.e., **optimum** value (see figures 5.31 and 5.32). From calculation the optimum value of $MAG \times C_s$ is found to correspond to a value of $V_2/V_1 \approx 4.7$, and a value of $MAG \approx 1.4$.

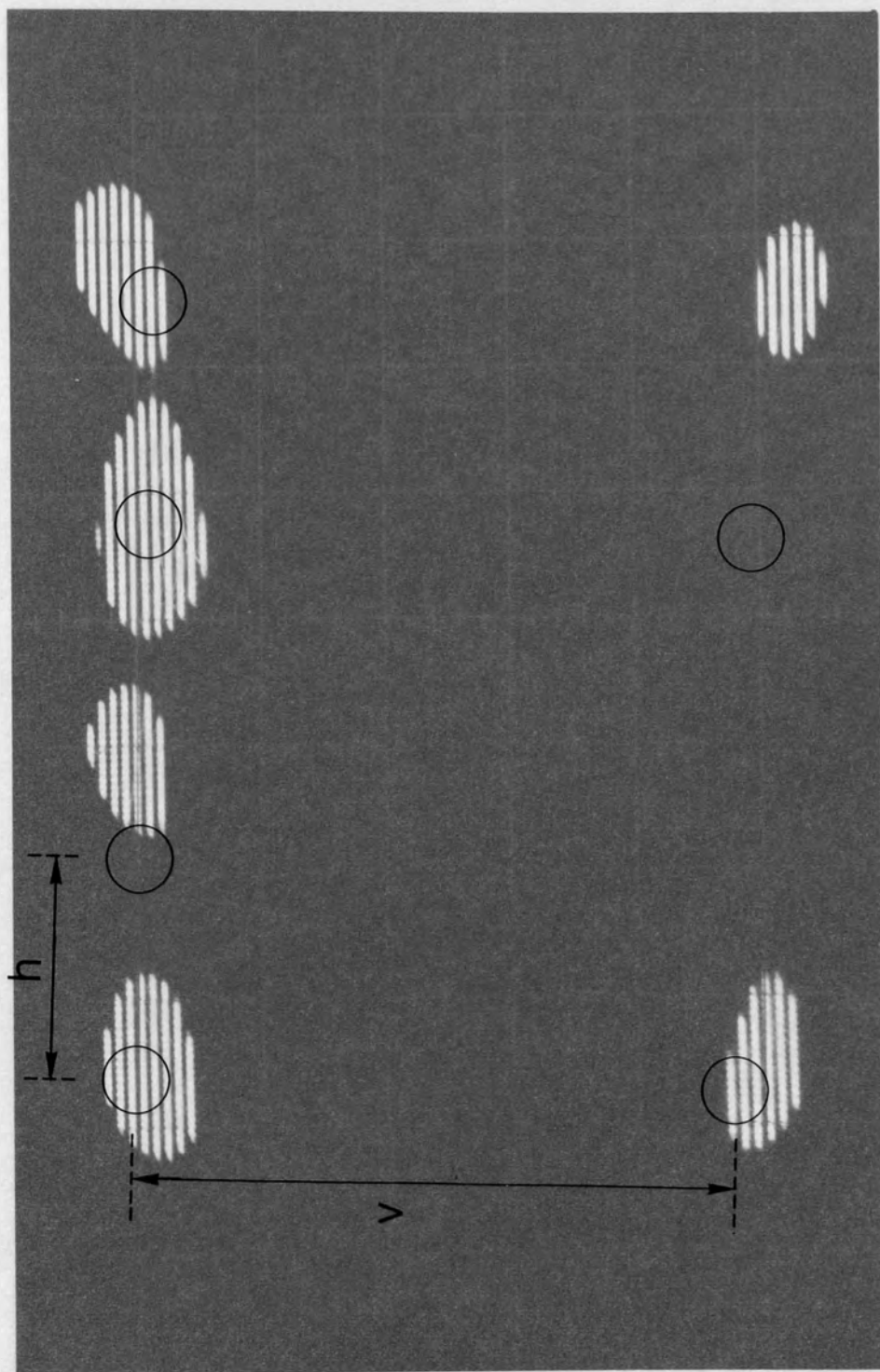
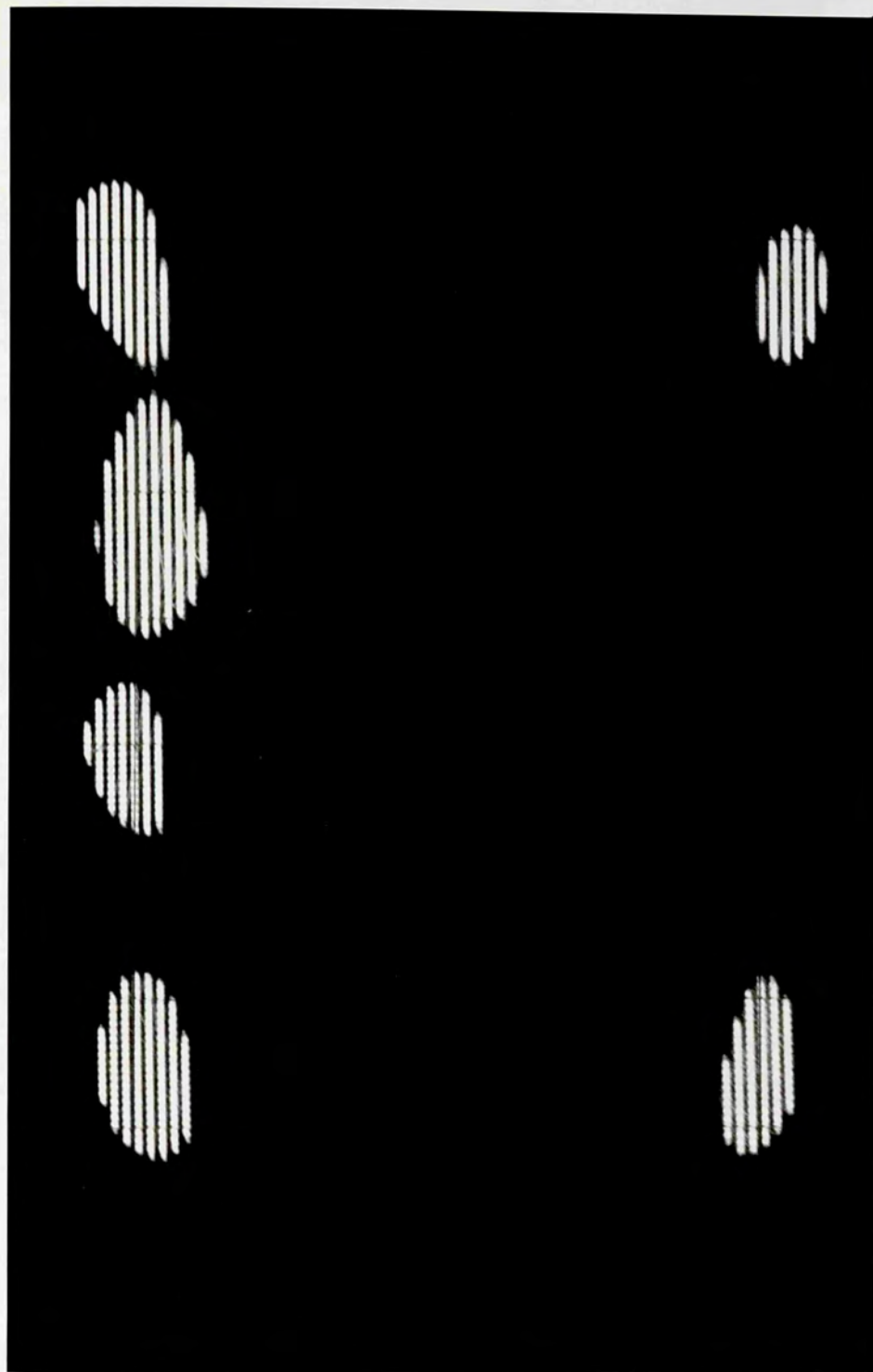


Figure 5.27



$L_1=L_5=1.5D$ $L_2=L_4=1.0D$ $L_3=3.0D$
 $V_5 \mid V_1=1.0$ $V_2 \mid V_1=V_4 \mid V_5 > V_3 \mid V_1$

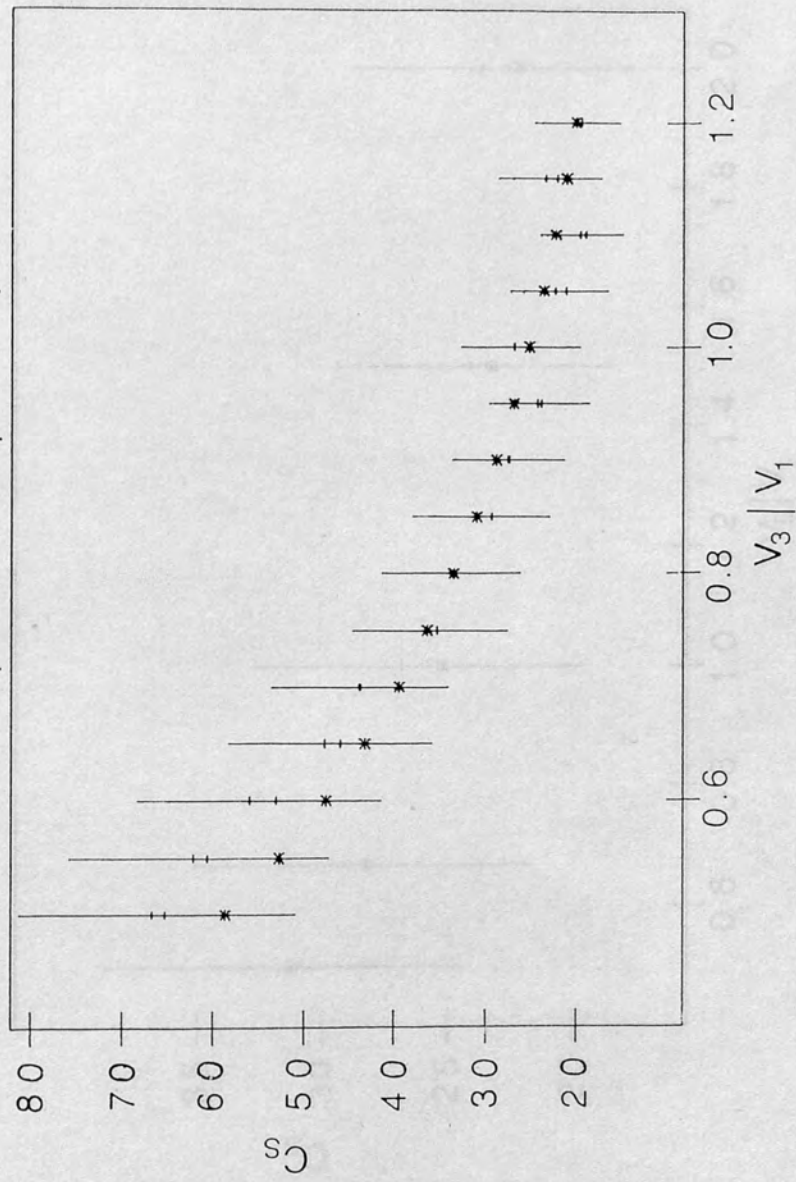


Figure 5.28

$L_1=L_5=1.5D$ $L_2=L_4=1.0D$ $L_3=3.0D$
 AFOCAL LENS

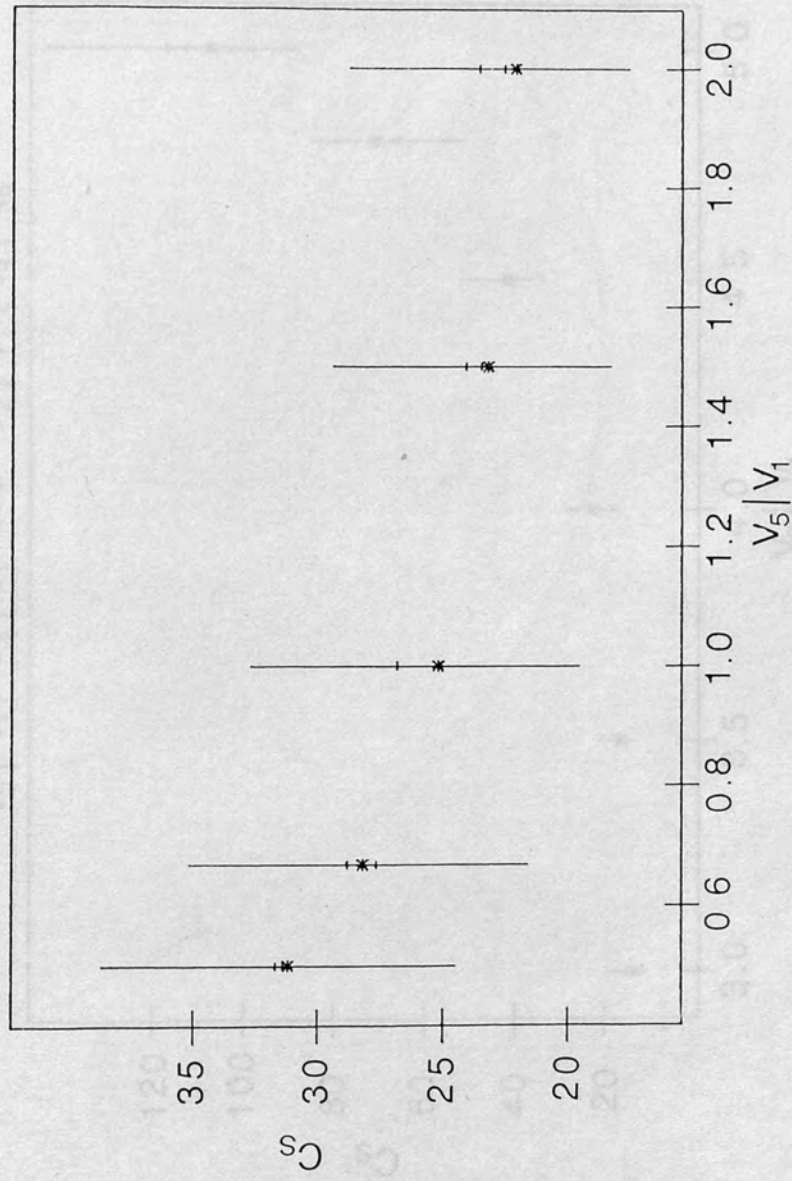


Figure 5.29

$$L_1=L_5=1.5D \quad L_2=L_4=1.0D \quad L_3=3.0D$$

$$V_5 \mid V_1=V_3 \mid V_1=1.0 \quad V_2 \mid V_1 \neq V_4 \mid V_5$$

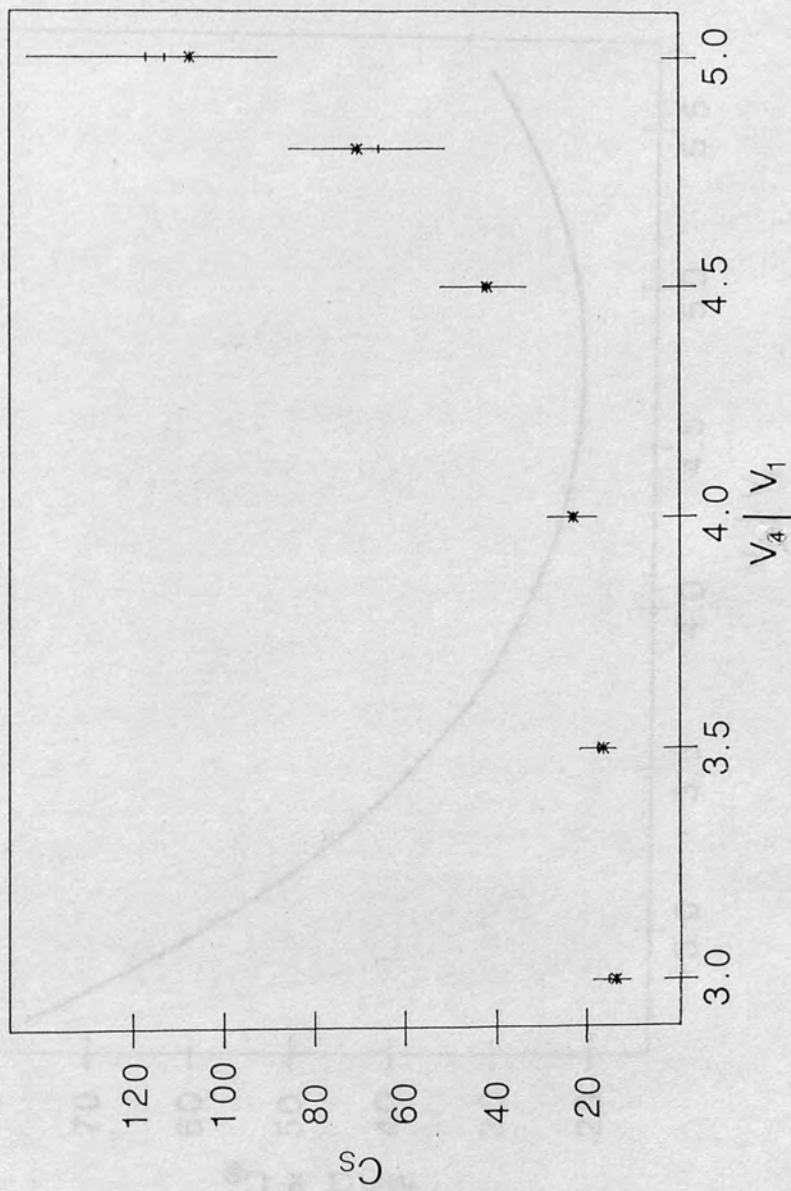


Figure 5.80

$L_1 = L_5 = 1.5D$ $L_2 = L_4 = 1.0D$ $L_3 = 3.0D$
 $V_5 \mid V_1 = V_3 \mid V_1 = 1.0$ $V_2 \mid V_1 \neq V_4 \mid V_5$

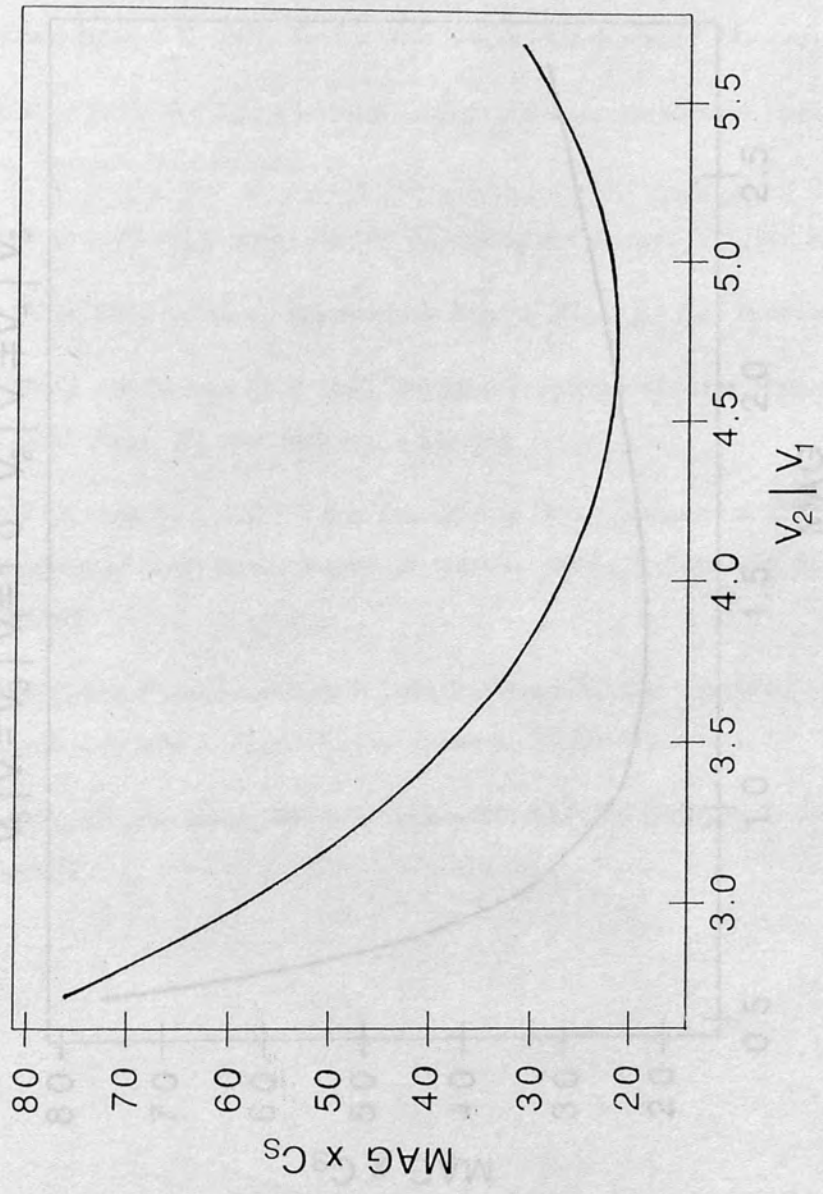


Figure 5.81

REFERENCES : CHAPTER FIVE

DjChio D, Natali J V and Kuyati C E 1974 Focal properties of the two tube electrostatic lens for and base-unity voltage ratio *Rev. Sci. Instrum.* 45 558-565

DjChio D, Natali J V, Kuyati C E and Galija A 1974 Use of matrices to represent electron lenses. Matrices for the two tube electrostatic lens *Rev. Sci. Instrum.* 45 586-590

Bartling E and Joad P H, 1970 *Electrostatic Lenses* (Amsterdam : Elsevier)

Hedilla D W O 1969 The design of three element electrostatic electron lenses *J. Phys. E. Sci. Instrum.* 2 1045-1050

Hedilla D W O 1970 *JILA report No.204* University of Colorado, Boulder, Colorado

Kuyati C E, 1971 An afocal Electrostatic Lens *J. Phys. E. Sci. Instrum.* 4 981-982

Kuyati C E and Kuyati M V 1970 The focal properties of the two element electrostatic lens *J. Phys. E. Sci. Instrum.* 3 552-554

Kuyati C E, Papadimitrakaki N and Yatseny A M 1982 Measurement of magnification behaviour of some three element electrostatic lenses *J. Phys. E. Sci. Instrum.* 15 1113-1114

Kuyati C E and Papadimitrakaki N 1984 The magnification behaviour of a five element electrostatic lens *J. Phys. E. Sci. Instrum.* 17 595-596

National Standards Bureau 1984 Subcommittee ED1BAF, 2025 *IEEE Library Manual* Mark II 2

$$L_1=L_5=1.5D \quad L_2=L_4=1.0D \quad L_3=3.0D$$

$$V_5 | V_1=V_3 | V_1=1.0 \quad V_2 | V_1 \neq V_4 | V_5$$

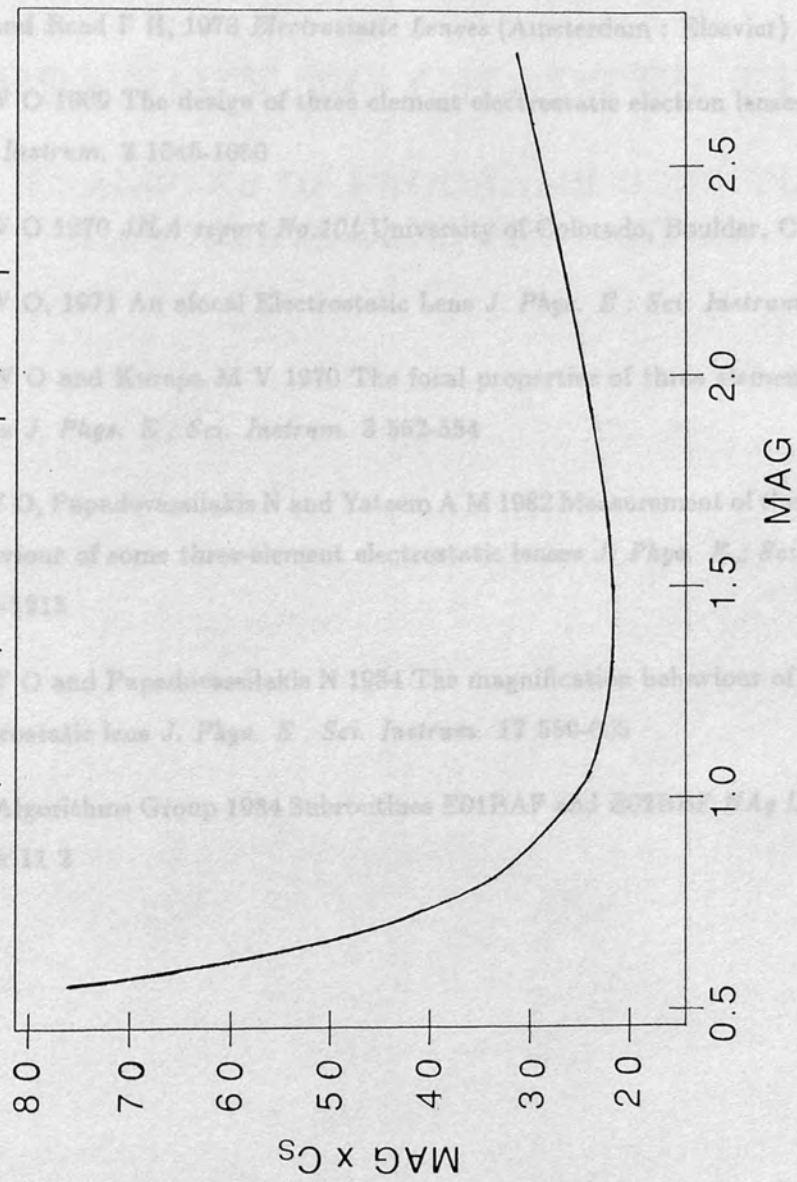


Figure 5.92

REFERENCES : CHAPTER FIVE

- DiChio D, Natali S V and Kuyatt C E 1974 Focal properties of the two tube electrostatic lens for and near-unity voltage ratios *Rev. Sci. Instrum.* **45** 559-565
- DiChio D, Natali S V, Kuyatt C E and Galejs A 1974 Use of matrices to represent electron lenses. Matrices for the two tube electrostatic lens *Rev. Sci. Instrum.* **45** 566-569
- Harting E and Read F H, 1976 *Electrostatic Lenses* (Amsterdam : Elsevier)
- Heddle D W O 1969 The design of three element electrostatic electron lenses *J. Phys. E : Sci. Instrum.* **2** 1046-1050
- Heddle D W O 1970 *JILA report No.104* University of Colorado, Boulder, Colorado
- Heddle D W O, 1971 An afocal Electrostatic Lens *J. Phys. E : Sci. Instrum.* **4** 981-983
- Heddle D W O and Kurepa M V 1970 The focal properties of three element electrostatic lenses *J. Phys. E : Sci. Instrum.* **3** 552-554
- Heddle D W O, Papadovassilakis N and Yateem A M 1982 Measurement of the magnification behaviour of some three-element electrostatic lenses *J. Phys. E : Sci. Instrum.* **15** 1210-1213
- Heddle D W O and Papadovassilakis N 1984 The magnification behaviour of a five-element electrostatic lens *J. Phys. E : Sci. Instrum.* **17** 559-605
- Numerical Algorithms Group 1984 Subroutines E01BAF and E02BBF *NAG Library Manual* Mark 11 **2**

CONTENTS

Section (5A.1) Description of Program CR5AFDCALLOCUS 185
Section (5A.2) Listing of CR5AFDCALLOCUS 191
Section (5A.3) Listing of PNDVMD 196

LIST OF FIGURES

APPENDIX TO CHAPTER FIVE

**EXAMPLES OF PROGRAMS USED TO
CALCULATE LENS PROPERTIES**

LIST OF TABLES

Table 5A.1 Table Defining the Points A through to H 189

CONTENTS

Section (5A.1) Description of Program CR5AFOCALLOCUS	185
--	-----

Section (5A.2) Listing of CR5AFOCALLOCUS	191
--	-----

Section (5A.3) Listing of FNDV51D	196
-----------------------------------	-----

LIST OF FIGURES

Figure 5A.1 Diagram showing Afocal Locus, Defining the Points A through to H	187
---	-----

LIST OF TABLES

Table 5A.1 Table Defining the Points A through to H	188
---	-----

DESCRIPTION OF PROGRAM CR5AFOCALLOCUS
WHICH PRODUCES A GRAPH OF $\log(V_5/V_1)$ VERSUS $\log(V_2/V_1)$
FOR AN AFOCAL FIVE-ELEMENT LENS WITH A SEPARATION
OF CONJUGATE POINTS INDEPENDENT OF OBJECT POSITION

This program finds the values for V_5/V_1 and V_2/V_1 so that the locus, i.e., the graph of $\log(V_5/V_1)$ versus $\log(V_2/V_1)$ can be drawn, for a five-element lens comprising two identical three-element lenses. The program is written in Fortran and incorporates two **NAg Library Subroutines E01BAF** and **E02BBF**. **E01BAF** is used to fit a cubic spline curve to the voltage ratio V'/V versus matrix element, (this routine therefore needs to be called eight times once for each matrix element a_{11} , a_{12} , a_{21} , and a_{22} , where V'/V is greater than one, and once for each matrix element d_{11} , d_{12} , d_{21} , and d_{22} , where V'/V is less than one), and **E02BBF** finds the value of a matrix element for a specific value of V'/V . A more complete description of these routines can be found in the **NAg FORTRAN Library Manual**, Mark 11, Volume 2. The program was run on the VAX/780 VMS4.2 mini-computer at RHBNC.

The program consists of two nested DO loops. In the inside DO loop the value of V_2/V_1 is incremented until the program converges on a value of V_2/V_1 which will focus the lens along with the current value of V_5/V_1 . The value of V_5/V_1 is set in the outside DO loop. It was found that to obtain values of V_5/V_1 which would cover the range of possible values of V_5/V_1 (10^{-3} to 10^3) in a smooth and even manner, it was better to increment $\log(V_5/V_1)$ rather than simply V_5/V_1 itself.

The locus may be divided into 8 sections, (see figure 5A.1) denoted as **A** to **B**, **B** to **C**, **C** to **D**, **D** to **E**, **E** to **F**, **F** to **G** and **G** to **H**. The values of $V_5/V_1 = (V_3/V_1)^2$ and $V_2/V_1 = V_4/V_3$ at the beginning and end of these sections, i.e., at the points **A**, **B**, **C**, **D**, **E**, **F**, **G** and **H**, can be deduced from the properties of appropriate two-element lenses, or may be deduced during the running of the program. At point **D** $V_2/V_1 = V_4/V_3 = 1$, and the two identical three-element lenses which the five-element lens comprises, with a constant value of $F_2 - F_1 = SUMF$, (where F_2 and F_1 are the first and second focal distances of the three-element lens, and their sum, $SUMF$ (the minus sign is due to the sign convention used) is equal to the separation of the reference planes of the two three-element lenses), reduce to two identical two-element lenses with constant $F_2 - F_1 = SUMF$. The voltage ratio of such a two-element lens, i.e., a two-element lens with $F_2 - F_1 = SUMF$ can easily be derived from the tabulated data of Harting and Read (1976), by interpolating between values of V'/V until the value of V'/V found which corresponds to the desired value of

$F_2 - F_1 = SUMF$. The value of V_3/V_1 for the five-element lens with $V_2/V_1 = V_4/V_3 = 1$ is equal to this value of V'/V , and V_5/V_1 equals $(V'/V)^2$. The same argument can be applied at point **H** where the value of V_2/V_1 is the same as that at point **D** i.e., $V_2/V_1 = V_4/V_3 = 1$, however, at point **D** V_5/V_1 has a value which is greater than 1, whereas at point **H** V_5/V_1 has a value which is less than 1, in fact, at point **H** the value of V_5/V_1 is the reciprocal of its value at point **D**. At points **B** and **F** the voltage ratio $V_3/V_2 = V_5/V_4 = 1$, and again the arguments used at point **D** can be applied. V_5/V_1 at point **B** therefore equals V_5/V_1 at point **D** and V_5/V_1 at point **F** is the reciprocal. V_2/V_1 at points **B** and **F** equals the reciprocal of the respective values of V_3/V_1 . Points **A** and **E** are the points where $V_5/V_1 = 1$, the corresponding values for V_2/V_1 can be found during the course of running the program. The values for both V_5/V_1 and V_2/V_1 at points **C** and **G** can be deduced during the running of the program. Point **C** corresponds to the maximum value of V_5/V_1 . If a value of V_5/V_1 is set in the outside loop which is greater than the maximum possible value of V_5/V_1 , then no corresponding value of V_2/V_1 can be found by the inside loop which will focus the lens, and convergence will not occur. Therefore, a test for non-convergence will allow the maximum value of V_5/V_1 to be deduced, and therefore the values of V_5/V_1 and V_2/V_1 at point **C**. Point **G** corresponds to the minimum value of V_5/V_1 , again the values of V_5/V_1 and V_2/V_1 at point **G** can be deduced from a test for non-convergence. The table listed on the next few pages summarises how the values of V_5/V_1 and V_2/V_1 can deduced.

TABLE 5A.1

TABLE DEFINING THE POINTS A THROUGH TO H

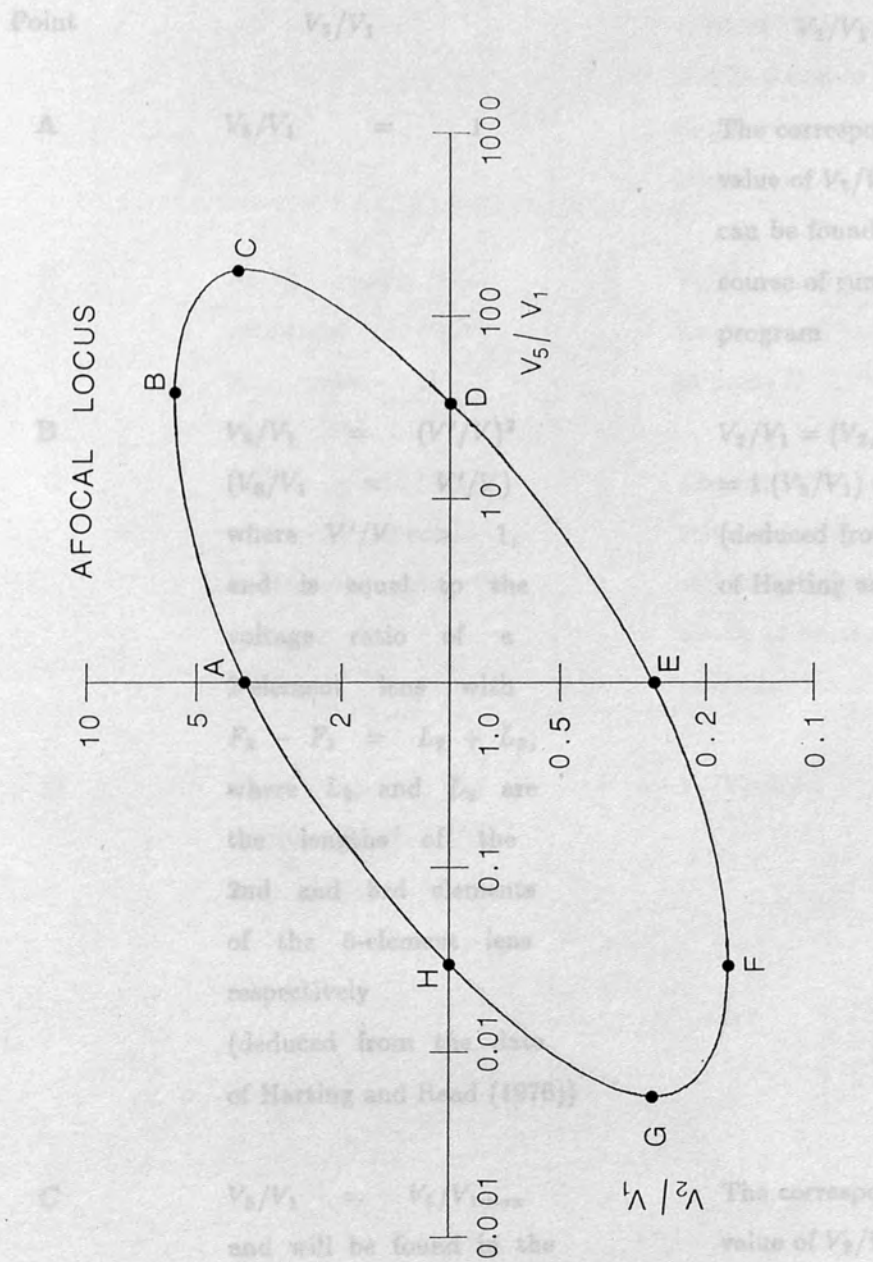


Figure 5A.1

TABLE 5A.1

TABLE DEFINING THE POINTS A THROUGH TO H

Point	V_5/V_1	The corresponding value of V_2/V_1 will be found in the
A	$V_5/V_1 = 1$	The corresponding value of $V_2/V_1 > 1$ can be found in the course of running the program
B	$V_5/V_1 = (V'/V)^2$ $(V_3/V_1 = V'/V)$ where $V'/V > 1$, and is equal to the voltage ratio of a 2-element lens with $F_2 - F_1 = L_2 + L_3$, where L_2 and L_3 are the lengths of the 2nd and 3rd elements of the 5-element lens respectively (deduced from the data of Harting and Read (1976))	$V_2/V_1 = (V_2/V_3)(V_3/V_1) = 1.(V_3/V_1) = (V_5/V_1)^{(1/2)} > 1$ (deduced from the data of Harting and Read (1976))
C	$V_5/V_1 = V_5/V_{1max}$ and will be found in the course of running the program	The corresponding value of $V_2/V_1 > 1$ will be found in the course of running the program
D	V_5/V_1 equals the V_5/V_1 at point B	$V_2/V_1 = 1$

Point V_5/V_1 V_2/V_1

E $V_5/V_1 = 1$ The corresponding value of $V_2/V_1 < 1$ will be found in the course of running the program

F V_5/V_1 equals the reciprocal of V_5/V_1 at point **B** V_2/V_1 equals the reciprocal of V_2/V_1 at point **B**

G $V_5/V_1 = V_5/V_{1min}$ and will be found in the course of running the program The corresponding value of $V_2/V_1 < 1$ will be found in the course of running the program

H V_5/V_1 equals the reciprocal of V_5/V_1 at point **B** $V_2/V_1 = 1$


```

C          PROGRAM CR5AFOCALLOCUS

C THIS PROGRAM PRODUCES THE LOCUS I.E., THE GRAPH OF LOG(V5/V1) VERSUS
C LOG(V2/V1) FOR A FIVE-ELEMENT LENS WHICH COMPRISES TWO IDENTICAL
C THREE-ELEMENT LENSES. IT USES NAG LIBRARY ROUTINES E01BAF AND E02BBF.
C E01BAF FITS A SPLINE TO V'/V VERSUS MATRIX ELEMENT, AND E02BBF FINDS
C THE SPECIFIC VALUE OF A MATRIX ELEMENT FOR A GIVEN VALUE OF V'/V.
C THE MATRIX ELEMENTS WERE DERIVED FROM THE DATA OF HARTING AND READ (1)
C AND ALSO FROM DATA CALCULATED BY DICHIO ET AL (2). THE MATRIX ELEMENTS
C ARE AS DEFINED BY DICHIO ET AL (2). THE PROGRAM CONSISTS OF TWO NESTED
C DO LOOPS, IN THE OUTSIDE DO LOOP A VALUE FOR LOG(10 TO THE BASE 10) OF V5/V1
C IS INCREMENTED AND IN THE INSIDE LOOP THE CORRESPONDING VALUE OF V2/V1
C IS SOUGHT. LOG(10)(V5/V1) IS INCREMENTED INSTEAD OF V5/V1 BECAUSE OF THE
C RANGE OF VALUES OF V5/V1, I.E.,  $1E-3 < V5/V1 < 1E+3$ .

C INTEGERS NEEDED BY NAG SUBROUTINES
      INTEGER NO,LCK,LWRK,IFAIL

C INTEGERS NEEDED BY REST OF PROGRAM
      INTEGER COUNT

C          COUNT KEEPS A COUNT OF THE VALUE OF J FOR
C          THE INSIDE DO LOOP, I.E., THE INSIDE DO
C          LOOP WHICH FINDS THE APPROPRIATE VALUE OF
C          V2/V1 FOR THE CURRENT VALUE OF V5/V1, AND
C          ALLOWS A CHECK TO BE MADE AS TO WHETHER
C          CONVERGENCE TO A SOLUTION IS ACTUALLY
C          OCCURRING, AND THEREFORE WHETHER A
C          SOLUTION EXISTS FOR THE CURRENT VALUE
C          OF V5/V1
      INTEGER CHECKSEC

C          CHECKSEC KEEPS A CHECK ON WHICH SECTION
C          OF THE LOCUS IS BEING CALCULATED

C REAL VALUES NEEDED BY MY SUBROUTINES
      REAL*8 LVA
C          ACCELERATING VOLTAGES
      REAL*8 A11A,A21A,A12A,A22A
C          MATRIX ELEMENTS FOR ACCELERATING VOLTAGES
      REAL*8 LVD
C          DECELERATING VOLTAGES
      REAL*8 D11D,D21D,D12D,D22D
C          MATRIX ELEMENTS FOR DECELERATING VOLTAGES

C END POINTS
      REAL V21H,V51H,V21D,V51D

C ARRAYS NEEDED BY NAG SUBROUTINES
      REAL*8 WRK(210)
      REAL*8 CNA11(210),CNA21(210),CNA12(210),CNA22(210)
      REAL*8 KA11(35),KA21(35),KA12(35),KA22(35)
      REAL*8 CND11(210),CND21(210),CND12(210),CND22(210)
      REAL*8 KD11(35),KD21(35),KD12(35),KD22(35)

C ARRAYS IN WHICH TABLES OF VOLTAGE RATIO,LOG OF VOLTAGE RATIO AND THE
C CORRESPONDING MATRIX ELEMENTS ARE STORED
      REAL*8 RV(35),LRV(35),A11(35),A21(35),A12(35),A22(35)
      REAL*8 RVD(35),LRVD(35),D11(35),D21(35),D12(35),D22(35)

C STARTING VALUES
      REAL*8 V32,LV32,V21,LV21,V51,LV51

C INCREMENTS FOR LOG(V5/V1) AND V2/V1 RESPECTIVELY
      REAL*8 ADD,INCR

C LENGTHS OF LENS ELEMENTS
      REAL L1,L2,L3,L4,L5

C DERIVED MATRIX ELEMENTS
      REAL*8 A1121,A2121,A1221,A2221,A1132,A2132,A1232,A2232
      REAL*8 A1131,A2131,A1231,A2231

C          DERIVED QUANTITIES
C THE FINAL OBJECT-IMAGE MATRIX HAS FINAL ELEMENTS ALPHA,BETA,GAMMA AND DELTA.
C BETA=0 FOR A FOCUSSED LENS, BETATEST IS SET TO ALLOW A CHECK OF THE
C PREVIOUSLY CALCULATED VALUE OF BETA.
C MAG : MAGNIFICATION

```

```

C RF : f2/f1 WHERE f1 AND f2 ARE THE FOCAL LENGTHS OF THE FIVE-ELEMENT LENS
C RVS : THE SQUARE ROOT OF (V5/V1), SHOULD EQUAL RF FOR FOCUSSED LENS,
C CF31 : F1 FOR THE THREE-ELEMENT LENS
C CF32 : F2 FOR THE THREE-ELEMENT LENS
C SUMCF : F2-F1
C NEWV21 IS AN INTERMEDIATE VALUE FOR V2/V1 OBTAINED WHEN USING THE METHOD
C OF FALSE POSITION TO SPEED UP CONVERGENCE.
      REAL*8 ALPHA,BETA,GAMMA,DELTA,BETATEST
      REAL*8 MAG,RF,RVS,CF31,CF32,SUMCF,NEWV21

C INTERMEDIATE VALUES WHEN CALCULATING FINAL MATRIX ELEMENTS
      REAL*8 A,B,C,D,W,X,Y,Z,R,S,T,V

C OUTPUT FILE
      CHARACTER*20 TITLE
      COMMON /A/ CNA11,CNA21,CNA12,CNA22,KA11,KA21,KA12,KA22
      COMMON /B/ CND11,CND21,CND12,CND22,KD11,KD21,KD12,KD22

C OPENING DATA FILES IN WHICH TABLES OF VOLTAGE RATIOS AND MATRIX ELEMENTS
C ARE STORED.
C ACCELERATING VOLTAGES
      OPEN(UNIT=1,FILE='ACCMATP1',STATUS='OLD',READONLY)
      DO I=1,31
      READ(1,*) RV(I),A11(I),A21(I),A12(I),A22(I)
      LRV(I)=DLOG10(RV(I))
      END DO

C DECELERATING VOLTAGES
      OPEN(UNIT=2,FILE='WDECMATP1',STATUS='OLD',READONLY)
      DO I=1,31
      READ(2,*) RVD(I),D11(I),D21(I),D12(I),D22(I)
      LRVD(I)=DLOG10(RVD(I))
      END DO

      PRINT*,'WHAT DO YOU WISH TO CALL THE OUTPUT DATA FILE?'
      READ(5,'(A)') TITLE
      OPEN(UNIT=3,FILE=TITLE,STATUS='NEW')

C PROMPTING FOR THE LENGTHS OF THE LENS ELEMENTS
      PRINT*,'PLEASE INPUT THE VALUES FOR L1,L2,L3,L4,L5'
      READ(5,*)L1,L2,L3,L4,L5
      WRITE(3,*)L1,L2,L3,L4,L5

C READING IN THE VALUES FOR V5/V1 AT POINT D AS DERIVED FROM THE
C TWO-ELEMENT DATA OF HARTING AND READ, (CALCULATED IN PROGRAM
C FNDV51D). V5/V1D=V5/V1B=1/(V5/V1H)=1/(V5/V1F)
      OPEN(UNIT=4,FILE='INFOV51D',STATUS='OLD',READONLY)
      READ(4,*)V51D
      V51H=1.0/V51D
      V21D=1.0
      V21H=1.0

C SETTING VALUES FOR CONSTANTS FOR NAG ROUTINES
      NO=31
      IFAIL=0
      LCK=36
      LWRK=210

C SETTING UP THE SPLINE CURVES
      CALL EO1BAF(NO,LRV,A11,KA11,CNA11,LCK,WRK,LWRK,IFAIL)
      CALL EO1BAF(NO,LRV,A21,KA21,CNA21,LCK,WRK,LWRK,IFAIL)
      CALL EO1BAF(NO,LRV,A12,KA12,CNA12,LCK,WRK,LWRK,IFAIL)
      CALL EO1BAF(NO,LRV,A22,KA22,CNA22,LCK,WRK,LWRK,IFAIL)
      CALL EO1BAF(NO,LRVD,D11,KD11,CND11,LCK,WRK,LWRK,IFAIL)
      CALL EO1BAF(NO,LRVD,D21,KD21,CND21,LCK,WRK,LWRK,IFAIL)
      CALL EO1BAF(NO,LRVD,D12,KD12,CND12,LCK,WRK,LWRK,IFAIL)
      CALL EO1BAF(NO,LRVD,D22,KD22,CND22,LCK,WRK,LWRK,IFAIL)

C SETTING STARTING VALUES
      CHECKSEC=0
10      CHECKSEC=CHECKSEC+1
      IF(CHECKSEC.EQ.1)THEN
      V21=V21H
      V51=V51H

```



```

DO J=1,500
COUNT=COUNT+1

V21=V21+ADD
LV21=DLOG10(V21)

V32=DSQRT(V61)/V21
LV32=DLOG10(V32)

C FINDING THE MATRIX VALUES FOR A GIVEN VOLTAGE RATIO
IF (V21 .GE. 1.0) THEN
CALL CALAMAT(LV21, A1121, A2121, A1221, A2221)
ELSE
CALL CALDMAT(LV21, A1121, A2121, A1221, A2221)
END IF

IF (V32 .GT. 1.0) THEN
CALL CALAMAT(LV32, A1132, A2132, A1232, A2232)
ELSE
CALL CALDMAT(LV32, A1132, A2132, A1232, A2232)
END IF

C FINDING THE MATRIX ELEMENTS
A=A1121*(L2*A2121)
B=(L1*A1121)+A1221+(L1*L2*A2121)+(L2*A2221)
C=A2121
D=(L1*A2121)+A2221
W=(A*(A1132+(L3*A2132)))+(C*(A1232+(L3*A2232)))
X=(B*(A1132+(L3*A2132)))+(D*(A1232+(L3*A2232)))
Y=(A*A2132)+(C*A2232)
Z=(B*A2132)+(D*A2232)
R=(W*(A1121+(L4*A2121)))+(Y*(A1221+(L4*A2221)))
S=(X*(A1121+(L4*A2121)))+(Z*(A1221+(L4*A2221)))
T=(W*A2121)+(Y*A2221)
V=(X*A2121)+(Z*A2221)
ALPHA=(R*(A1132+(L5*A2132)))+(T*(A1232+(L5*A2232)))
BETA=(S*(A1132+(L5*A2132)))+(V*(A1232+(L5*A2232)))
GAMMA=(R*A2132)+(T*A2232)
DELTA=(S*A2132)+(V*A2232)

C THE MATRIX ELEMENTS OF THE THREE-ELEMENT LENSES CAN BE DERIVED, ALLOWING
C THE FOCAL DISTANCES F1 AND F2 TO BE CALCULATED, AND F2-F1 = CONSTANT
C CAN BE CHECKED
A2131=A2132*(A1121+L2*A2121)+A2232*A2121
A1131=A1132*(A1121+L2*A2121)+A1232*A2121-((L2/2.0)*A2131)
A2231=A2132*(A1221+L2*A2221)+A2232*A2221-((L2/2.0)*A2131)
A1231=A1132*(A1221+L2*A2221)+A1232*A2221-((L2/2.0)*A1131)
-(((L2/2.0)**2)*A2131)-((L2/2.0)*A2231)

C CHECK SIGN OF BETA SO THAT ADD HAS CORRECT SIGN OF CONVERGENCE
IF (BETA .LT. (0.0) .AND. COUNT .EQ. 1) ADD=-ADD

C TEST FOR CONVERGENCE USING METHOD OF FALSE POSITION
IF (COUNT .EQ. 1) THEN
BETATEST=BETA

ELSE IF ((BETA*BETATEST) .LE. (0.0)) THEN
NEWV21=((V21-ADD)*BETA-V21*BETATEST)/(BETA-BETATEST)
V21=NEWV21+ADD/2.0
ADD=-ADD/2.0
BETATEST=BETA

ELSE IF (ABS(BETATEST) .LT. ABS(BETA)) THEN
V21=V21-ADD
ADD=-ADD/2.0
BETATEST=BETA

ELSE
BETATEST=BETA

END IF

PRINT*, 'BETA = ', BETA, ' V2/V1 = ', V21

IF (ABS(BETA) .LE. 1E-04) GOTO 20
ONCE BETA IS EQUAL TO A VALUE

```

C

```

C                                     LESS THAN 1E-04 THE PROGRAM
C                                     JUMPS OUT OF THE INSIDE LOOP
C                                     INTO THE OUTSIDE LOOP
C                                     IF (CHECK.GT.50)THEN
C                                     IF (CHECKSEC.EQ.4)STOP
C                                     GOTO 10
C                                     END IF
C                                     IF A VALUE OF V2/V1 CANNOT BE
C                                     FOUND WHICH WILL FOCUS THE LENS
C                                     ALONG WITH THE CURRENT VALUE OF
C                                     VALUE OF V5/V1 IT IS ASSUMED
C                                     THAT NO SOLUTION EXISTS FOR THIS
C                                     VALUE OF V5/V1. THE CURRENT VALUE
C                                     MUST THEREFORE BE GREATER THAN THE
C                                     MAXIMUM VALUE OF V5/V1 OR LESS
C                                     THE MINIMUM VALUE, THE PROGRAM
C                                     THEREFORE JUMPS OUT OF THE INSIDE
C                                     LOOP INTO THE OUTSIDE LOOP AND
C                                     INTO THE NEXT SECTION. IF THE LAST
C                                     SECTION HAS BEEN REACHED THE
C                                     PROGRAM IS STOPPED
C                                     END DO
C                                     END OF INSIDE DO LOOP
C                                     END OF OUTSIDE DO LOOP
20      MAG=-ALPHA
      RF=-1/(ALPHA+DELTA)
      RVS=DSQRT(V51)
      CF31=A2232/A2131
      CF32=-A1131/A2131
      SUMCF=CF32-CF31
      WRITE(6,60)V51,V21,MAG,V51**-0.25,RF,RVS,CF31,CF32,SUMCF
60      FORMAT(' V5/V1 = ',F7.3,' V2/V1 = ',F7.3,' MAG = ',F7.3,
      + ' V5/V1^(-1/4)',F7.3,' f2/f1 = ',F7.3,' SQRT(V5/V1) = ',F7.3,
      + ' F1(3-e1) = ',F7.3,' F2(3-e1) = ',F7.3,' F2(3-e1) - F1(3-e1) = ',F7.3)
C f2/f1, V5/V1^(1/2), AND F1, F2, F2-F1 FOR THE 3-ELEMENT LENS AND BETA
      WRITE(3,*)V51,V21,MAG,RF,RVS,F1,F2,SUMCF,BETA
      END DO
C                                     END OF OUTSIDE DO LOOP
      END
C SUBROUTINES USED TO FIND APPROPRIATE MATRIX ELEMENTS
      SUBROUTINE CALAMAT(LVA,A11A,A21A,A12A,A22A)
      REAL*8 CNA11(210),CNA21(210),CNA12(210),CNA22(210)
      REAL*8 KA11(35),KA21(35),KA12(35),KA22(35)
      COMMON /A/ CNA11,CNA21,CNA12,CNA22,KA11,KA21,KA12,KA22
      CALL EO2BBF(35,KA11,CNA11,LVA,A11A,IFAIL)
      CALL EO2BBF(35,KA21,CNA21,LVA,A21A,IFAIL)
      CALL EO2BBF(35,KA12,CNA12,LVA,A12A,IFAIL)
      CALL EO2BBF(35,KA22,CNA22,LVA,A22A,IFAIL)
      END
      SUBROUTINE CALDMAT(LVD,D11D,D21D,D12D,D22D)
      REAL*8 CND11(210),CND21(210),CND12(210),CND22(210)
      REAL*8 KD11(35),KD21(35),KD12(35),KD22(35)
      COMMON /B/ CND11,CND21,CND12,CND22,KD11,KD21,KD12,KD22
      CALL EO2BBF(35,KD11,CND11,LVD,D11D,IFAIL)
      CALL EO2BBF(35,KD21,CND21,LVD,D21D,IFAIL)
      CALL EO2BBF(35,KD12,CND12,LVD,D12D,IFAIL)
      CALL EO2BBF(35,KD22,CND22,LVD,D22D,IFAIL)
      END

```

```

C PROGRAM FNDV51D

C THIS PROGRAM FINDS THE VALUE OF V5/V1 AT THE POINT D, I.E., AT THE
C POINT WHERE V2/V1 = 1.0 AND V5/V1 > 1.0. FOR THE LOCUS I.E.,
C THE GRAPH OF LOG(V5/V1) VERSUS LOG(V2/V1) FOR A FIVE-ELEMENT
C LENS WHICH COMPRISES TWO IDENTICAL THREE-ELEMENT LENSES. THE DATA
C OF HARTING AND READ (1976) FOR TWO-ELEMENT LENSES IS USED TO GIVE A
C FIRST APPROXIMATION TO V5/V1. THIS VALUE OF V5/V1 IS THEN CHECKED
C BY OBTAINING THE OBJECT-IMAGE MATRIX FOR THIS LENS. THE MATRIX ELEMENT
C BETA SHOULD EQUAL ZERO FOR A FOCUSSED LENS. IF THE VALUE OF V5/V1 AS
C DERIVED FROM THE DATA OF HARTING AND READ GIVES A VALUE FOR BETA
C SUFFICIENTLY CLOSE TO ZERO, I.E., < 1E-04, THEN THE PROGRAM STORES
C THIS VALUE AND STOPS. IF THE VALUE FOR BETA IS NOT SUFFICIENTLY CLOSE
C TO ZERO THE VALUE OF V5/V1 IS ITERATED BY A DO LOOP UNTIL A VALUE FOR
C V5/V1 FOUND WHICH GIVES A VALUE OF BETA < 1E-04.
C THE PROGRAM USES NAG LIBRARY ROUTINES EO1BAF AND EO2BBF. EO1BAF FITS
C A SPLINE TO V'/V VERSUS MATRIX ELEMENT, AND EO2BBF FINDS THE SPECIFIC
C VALUE OF A MATRIX ELEMENT FOR A GIVEN VALUE OF V'/V. THE MATRIX
C ELEMENTS WERE DERIVED FROM THE DATA OF HARTING AND READ (1976) AND
C ALSO FROM DATA CALCULATED BY DICHIO ET AL (1974). THE MATRIX ELEMENTS
C ARE AS DEFINED BY DICHIO ET AL (1974).

C INTEGERS NEEDED BY NAG SUBROUTINES
      INTEGER NO,LCK,LWRK,NF,LCKF,LWRKF,IFAIL

C INTEGERS NEEDED BY REST OF PROGRAM
      INTEGER COUNT

C
C COUNT KEEPS A COUNT OF THE VALUE OF I
C FOR THE DO LOOP

C REAL VALUES NEEDED BY MY SUBROUTINES
      REAL*8 LVA
C
C ACCELERATING VOLTAGES
      REAL*8 A11A,A21A,A12A,A22A
C
C MATRIX ELEMENTS FOR ACCELERATING VOLTAGES

C ARRAYS NEEDED BY NAG SUBROUTINES
      REAL*8 WRK(210)
      REAL*8 CNA11(210),CNA21(210),CNA12(210),CNA22(210)
      REAL*8 KA11(35),KA21(35),KA12(35),KA22(35)
      REAL*8 KLVV(30),CHLVV(30),WRKF(200)

C ARRAYS IN WHICH TABLES OF VOLTAGE RATIO, LOG OF VOLTAGE RATIO AND THE
C CORRESPONDING MATRIX ELEMENTS ARE STORED
      REAL*8 RV(35),LRV(35),A11(35),A21(35),A12(35),A22(35)

C ARRAYS IN WHICH TABLES OF VOLTAGE RATIO, LOG VOLTAGE RATIO, f1, F1,
C f2, F2, F2-F1 AND LOG(F2-F1) ARE STORED, (MINUS SIGN IS SIGN CONVENTION)
      REAL*8 VV(25),LVV(25),SF21(25),SF22(25),CF21(25),CF22(25)
      REAL*8 SUMCF2(25),LSUMCF2(25)

C STARTING VALUES
      REAL*8 V32,LV32,V21,LV21,V51,LV51

C INCREMENT FOR LOG(V5/V1)
      REAL*8 ADD

C LENGTHS OF LENS ELEMENETS
      REAL L1,L2,L3,L4,L5

C DERIVED MATRIX ELEMENTS
      REAL*8 A1132,A2132,A1232,A2232

C
C DERIVED QUANTITIES
C THE FINAL OBJECT-IMAGE MATRIX HAS FINAL ELEMENTS ALPHA,BETA,GAMMA AND DELTA
C BETA=0 FOR A FOCUSSED LENS, BETATEST IS SET TO ALLOW A CHECK OF THE PREVIOUSLY
C CALCULATED VALUE OF BETA
C NEWV51 IS AN INTERMEDIATE VALUE FOR V5/V1 OBTAINED WHEN USING THE METHOD
C OF FALSE POSITION TO SPEED UP CONVERGENCE.
C CF31 : 1ST FOCAL LENGTH OF THE THREE-ELEMENT LENS
C CF32 : 2ND FOCAL LENGTH OF THE THREE-ELEMENT LENT
C SUMCF3 : CF32-CF31, LSUMCF3 : LOG(SUMCF3)
C V51D : V5/V1 AT POINT D, LV51D : LOG(V5/V1D).
C V31DFSTAP : 1ST APPROX TO V3/V1D DERIVED FROM THE TWO-ELEMENT DATA
C V51DFSTAP : 1ST APPROX TO V5/V1D DERIVED FROM THE TWO-ELEMENT DATA
C OF HARTING AND READ.

```

```

C V21D : V2/V1 AT POINT D = 1
      REAL*8 ALPHA,BETA,GAMMA,DELTA,BETATEST,NEWV51
      REAL*8 CF31,CF32,SUMCF3,LSUMCF3
      REAL*8 V51D,LV51D,V31DFSTAP,V51DFSTAP,V21D

C INTERMEDIATE VALUES WHEN CALCULATING FINAL MATRIX ELEMENTS
      REAL*8 A,B,C,D

C FILE IN WHICH V5/V1D IS STORED
      CHARACTER*20 TITLE

      COMMON /A/ CNA11,CNA21,CNA12,CNA22,KA11,KA21,KA12,KA22

C OPENING DATA FILES IN WHICH TABLES OF VOLTAGE RATIOS AND MATRIX ELEMENTS
C ARE STORED.

C ACCELERATING VOLTAGES
      OPEN(UNIT=1,FILE='ACCMATP1',STATUS='OLD',READONLY)
      DO I=1,31
      READ(1,*) RV(I),A11(I),A21(I),A12(I),A22(I)
      LRV(I)=DLOG10(RV(I))
      END DO

C DATA FOR TWO-ELEMENT CYLINDER LENS(HARTING AND READ)
      OPEN(UNIT=2,FILE='ACCFOCAL',STATUS='OLD',READONLY)
      DO I=1,25
      READ(2,*)VV(26-I),SF21(26-I),CF21(26-I),SF22(26-I),CF22(26-I)
      SUMCF2(26-I)=CF21(26-I)+CF22(26-I)
      LVV(26-I)=LOG10(VV(26-I))
      LSUMCF2(26-I)=LOG10(SUMCF2(26-I))
      END DO

      PRINT*,'WHAT DO YOU WISH TO CALL THE OUTPUT DATA FILE?'
      READ(5, '(A)') TITLE
      OPEN(UNIT=3,FILE=TITLE,STATUS='NEW')

C PROMPTING FOR THE DIMENSIONS OF THE LENS
      PRINT*,'PLEASE INPUT THE LENGTHS OF THE LENS ELEMENTS'
      READ(5,*)L1,L2,L3,L4,L5
      SUMCF3=L2+L3
      LSUMCF3=LOG10(SUMCF3)

C SETTING VALUES FOR CONSTANTS FOR NAG ROUTINES
      NO=31
      NF=25
      IFAIL=0
      LCK=36
      LCKF=30
      LWRK=210
      LWRKF=200

C SETTING UP THE SPLINE CURVES
      CALL EO1BAF(NO,LRV,A11,KA11,CNA11,LCK,WRK,LWRK,IFAIL)
      CALL EO1BAF(NO,LRV,A21,KA21,CNA21,LCK,WRK,LWRK,IFAIL)
      CALL EO1BAF(NO,LRV,A12,KA12,CNA12,LCK,WRK,LWRK,IFAIL)
      CALL EO1BAF(NO,LRV,A22,KA22,CNA22,LCK,WRK,LWRK,IFAIL)

C FINDING A FIRST APPROXIMATION FOR V5/V1D FROM HARTING AND READ DATA
      CALL EO1BAF(NF,LSUMCF2,LVV,KLVV,CNLVV,LCKF,WRKF,LWRKF,IFAIL)
      CALL EO2BBF(NF,KLVV,CNLVV,LSUMCF3,LV51D,IFAIL)
      V31DFSTAP=(10**LV51D)
      V51DFSTAP=(10**LV51D)**2.0
      PRINT*,'THE FIRST APPROXIMATION OF V3/V1D =',V31DFSTAP
      PRINT*,'THE FIRST APPROXIMATION OF V5/V1D =',V51DFSTAP

C SETTING STARTING VALUES
      COUNT=0
      BETA=-100
      BETATEST=BETA
      ADD=0.1
      V21D=1.0
      V51=V51DFSTAP-ADD

      DO I=1,500
      COUNT=COUNT+1
      V51=V51+ADD

```

```
V32=DSQRT(V51)
LV32=DLOG10(V32)
```

```
C FINDING THE MATRIX VALUES FOR A GIVEN VOLTAGE RATIO
CALL CALAMAT(LV32,A1132,A2132,A1232,A2232)
```

```
C FINDING THE MATRIX ELEMENTS
A=A1132+((L3+L4)*A2132)
B=((L1+L2)*A1132)+A1232+((L1+L2)*(L3+L4)*A2132)+((L3+L4)*A2232)
C=A2132
D=((L1+L2)*A2132)+A2232
ALPHA=(A*(A1132+(L5*A2132)))+(C*(A1232+(L5*A2232)))
BETA=(B*(A1132+(L5*A2132)))+(D*(A1232+(L5*A2232)))
DELTA=(A*A2132)+(C*A2232)
GAMMA=(B*A2132)+(D*A2232)
```

```
C CHECK SIGN OF BETA SO THAT ADD HAS CORRECT SIGN OF CONVERGENCE
IF(BETA.LT.(0.0).AND.COUNT.EQ.1)ADD=-ADD
```

```
C TEST FOR CONVERGENCE USING METHOD OF FALSE POSITION
IF(COUNT.EQ.1)THEN
BETATEST=BETA
```

```
ELSE IF((BETA+BETATEST).LE.(0.0))THEN
NEWV51=((V51-ADD)*BETA-V51*BETATEST)/(BETA-BETATEST)
V51=NEWV51+ADD/2.0
ADD=-ADD/2.0
BETATEST=BETA
```

```
ELSE IF(ABS(BETATEST).LT.ABS(BETA)) THEN
V51=V51-ADD
ADD=-ADD/2.0
BETATEST=BETA
```

```
ELSE
BETATEST=BETA
```

```
END IF
```

```
PRINT*,'BETA = ',BETA,' V5/V1 = ',V51
```

```
IF(ABS(BETA).LE.1E-04)THEN
```

```
WRITE(3,*)V51
```

```
STOP
```

```
END IF
```

```
END DO
```

```
END
```

```
C SUBROUTINE USED TO FIND APPROPRIATE MATRIX ELEMENTS
```

```
SUBROUTINE CALAMAT(LVA,A11A,A21A,A12A,A22A)
REAL*8 CNA11(210),CNA21(210),CNA12(210),CNA22(210)
REAL*8 KA11(35),KA21(35),KA12(35),KA22(35)
COMMON /A/ CNA11,CNA21,CNA12,CNA22,KA11,KA21,KA12,KA22
```

```
CALL EO2BBF(35,KA11,CNA11,LVA,A11A,IFAIL)
```

```
CALL EO2BBF(35,KA21,CNA21,LVA,A21A,IFAIL)
```

```
CALL EO2BBF(35,KA12,CNA12,LVA,A12A,IFAIL)
```

```
CALL EO2BBF(35,KA22,CNA22,LVA,A22A,IFAIL)
```

```
END
```

CONTENTS : CHAPTER SIX

	Page No.
Section (6.1) Introduction	204
Section (6.2) Construction and Operation of the Multi-Disc Lens	206
Section (6.3) Acquiring data for the Multi-disc Lens	
(a) Experimental Data	214
(b) Calculated Data	218
Section (6.4) Presentation of the Data for the Multi-Disc Lens	218
CHAPTER SIX	
MULTI-DISC LENS	
Section (6.5) Concluding Remarks	222
References	244

CONTENTS : CHAPTER SIX

	Page No
Section (6.1) Introduction	204
Section (6.2) Construction and Operation of the Multi-Disc Lens	206
Section (6.3) Acquiring data for the Multi-disc Lens	
(a) Experimental Data	214
(b) Calculated Data	218
Section (6.4) Presentation and Discussion of the Data for the Multi-Disc Lens	218
Section (6.5) Concluding Remarks	222
References	244
Figure 6.5 Schematic Diagram of a disc	210
Figure 6.6 Diagram showing how discs were stacked to form the Disc Lens	213
Figure 6.7 End View of Disc Lens Sandwich	215
Figure 6.8 Schematic Diagram of Switching Unit	216
Figure 6.9 Photograph of Front Panel of Switching Unit	216
Figure 6.10 Diagram showing that if the change in voltage in the regions of 'stepping' voltage are approximated by a linear voltage variation, then the effective length of L_2 is (no. of discs connected together to form $L_2 - 1$) \times 0.10	217
Figure 6.11 Typical Example of the 'image' displayed on the Display Scope from the Disc Lens	219
Figure 6.12 Example of a 'bad' image from the Disc lens	220
Figure 6.13 Lines of constant V_2/V_1 and lines of Constant magnification M plotted on axes of V_2/V_1 versus V_3/V_1 for various values of V_4/V_1 for the Disc Lens with a Centre Element length of 0.50 as obtained from the calculated data of Heddle	224
Figure 6.14 Lines of constant V_2/V_1 and lines of Constant magnification M plotted on axes of V_2/V_1 versus V_3/V_1 for the Disc Lens with a Centre Element length of 1.00 as obtained from the calculated data of Heddle	225

LIST OF FIGURES : CHAPTER SIX

	Page No
Figure 6.1 Read's Movable Electrostatic Lens	205
Figure 6.2 Photograph of Discs sandwiched between two Cylindrical Lens Elements	207
Figure 6.3 Diagram showing how the Voltages are stepped between L_1 and L_2 and L_2 and L_3 respectively	208
Figure 6.4 Photograph of a disc	209
Figure 6.5 Schematic Diagram of a disc	210
Figure 6.6 Diagram showing how discs were stacked to form the Disc Lens	212
Figure 6.7 End View of Disc Lens Sandwich	213
Figure 6.8 Schematic Diagram of Switching Unit	215
Figure 6.9 Photograph of Front Panel of Switching Unit	216
Figure 6.10 Diagram showing that if the change in voltage in the regions of 'stepping' voltage are approximated by a linear voltage variation, then the effective length of L_2 is (no. of discs connected together to form L_2 -1) \times 0.1D	217
Figure 6.11 Typical Example of the 'image' displayed on the Display Scope from the Disc Lens	219
Figure 6.12 Example of a 'bad' image from the Disc lens	220
Figure 6.13 Lines of constant V_3/V_1 and lines of Constant magnification M plotted on axes of n_c Versus V_2/V_1 for various values of V_3/V_1 for the Disc Lens with a Centre Element length of 0.6D as obtained from the calculated data of Heddle	224
Figure 6.14 Lines of constant V_3/V_1 and lines of Constant magnification M plotted on axes of n_c Versus V_2/V_1 for various values of V_3/V_1 for the Disc Lens with a Centre Element length of 1.0D as obtained from the calculated data of Heddle	225

LIST OF FIGURES : CHAPTER SIX (cont)

	Page No
Figure 6.15 Lines of constant V_3/V_1 and lines of Constant magnification M plotted on axes of n_c Versus V_2/V_1 for various values of V_3/V_1 for the Disc Lens with a Centre Element length of 2.0D as obtained from the calculated data of Heddle	226
Figure 6.16 V_2/V_1 Versus n_c for various values of V_3/V_1 for the Disc Lens with a Centre Element length of 0.6D as obtained from experiment	228
Figure 6.17 V_2/V_1 Versus n_c for various values of V_3/V_1 for the Disc Lens with a Centre Element length of 1.0D as obtained from experiment	229
Figure 6.18 V_2/V_1 Versus n_c for various values of V_3/V_1 for the Disc Lens with a Centre Element length of 2.0D as obtained from experiment	230
Figure 6.19 Experimentally obtained and calculated values of V_2/V_1 Versus n_c for $V_3/V_1 = 0.6, 1.0$ and 3.0 for the Disc Lens with a Centre Element length of 0.6D	232
Figure 6.20 Experimentally obtained and calculated values of V_2/V_1 Versus n_c for $V_3/V_1 = 0.6, 1.0$ and 3.0 for the Disc Lens with a Centre Element length of 01.0D	233
Figure 6.21 Experimentally obtained and calculated values of V_2/V_1 Versus n_c for $V_3/V_1 = 0.6, 1.0$ and 3.0 for the Disc Lens with a Centre Element length of 2.0D	234
Figure 6.22 Experimentally obtained and calculated values of Magnification M Versus n_c for $V_3/V_1 = 0.6$ for the Disc Lens with a Centre Element Length of 0.6D	236
Figure 6.23 Experimentally obtained and calculated values of Magnification M Versus n_c for $V_3/V_1 = 1.0$ for the Disc Lens with a Centre Element Length of 0.6D	237
Figure 6.24 Experimentally obtained and calculated values of Magnification M Versus n_c for $V_3/V_1 = 3.0$ for the Disc Lens with a Centre Element Length of 0.6D	238

LIST OF FIGURES : CHAPTER SIX (cont)

	Page No
Figure 6.25 Experimentally obtained and calculated values of Magnification M Versus n_c for $V_3/V_1 = 0.6$ for the Disc Lens with a Centre Element Length of 1.0D	239
Figure 6.26 Experimentally obtained and calculated values of Magnification M Versus n_c for $V_3/V_1 = 1.0$ for the Disc Lens with a Centre Element Length of 1.0D	240
Figure 6.27 Experimentally obtained and calculated values of Magnification M Versus n_c for $V_3/V_1 = 3.0$ for the Disc Lens with a Centre Element Length of 1.0D	241
Figure 6.28 Experimentally obtained and calculated values of Magnification M Versus n_c for $V_3/V_1 = 0.6$ and 1.0 for the Disc Lens with a Centre Element Length of 2.0D	242
Figure 6.29 Experimentally obtained and calculated values of Magnification M Versus n_c for $V_3/V_1 = 0.6$ and 3.0 for the Disc Lens with a Centre Element Length of 2.0D	243

MULTI-DISC LENS

6.1 INTRODUCTION

In this chapter the properties, construction and operation of a lens built from 31 discs electrically insulated from each other and sandwiched between two ordinary cylindrical lens elements will be discussed.

The focal properties of a given cylindrical electrostatic electron lens are dependent on a number of its physical properties. These are

- (1) The number of lens elements.
- (2) The ratio of the length to diameter of each element.
- (3) The length of the gap between a pair of lens elements.

Once (1), (2) and (3) have been chosen, the lens is constructed and placed in vacuum. It is usually not possible to change (1), (2) and (3) without opening the vacuum system, removing the lens, and constructing a new lens. However, the method used to construct the lens studied in the present work, in principle allows (1), (2) and (3) to be changed without any physical change being made to the lens itself, and so the lens does not need to be removed from the vacuum system. Any alterations which are required can be made externally, via the electrical connections to the discs which make up the lens.

In 1983 Read proposed a lens constructed from several short closely spaced cylinders sandwiched between two longer ones. He suggested that it should be possible to connect a number of neighbouring discs to the same voltage V_2 while connecting the remaining discs on the left (including the left-hand long cylinder) to a voltage V_1 and those to the right to a voltage V_3 , thus making a three-element lens whose element lengths are variable within a range dictated by the number of discs and by the number and position of discs chosen to be connected together to form the middle element. Read investigated the properties of a three-element lens constructed using the discs, in the manner described below, using the three-cylinder lens data of Harting and Read (1976) calculated using the charge density method. The data used was that calculated for a three cylinder lens having $A/D = 1$ and $g/D = 0.1$, where A is the distance between the lens gaps, D is the diameter of the lens elements and g is the length of the gaps between the cylinders. Where the data of Harting and Read was insufficient, i.e., when $V_3/V_1 > 30$, additional data was calculated

using the charge density method. The lens was envisaged as being constructed from 22 short lengths of thickwalled cylinders insulated from each other and sandwiched between two longer lengths of cylinders of the same internal diameter D , where 10 of these short cylinders were chosen to be connected together to form the centre element (see figure 6.1).

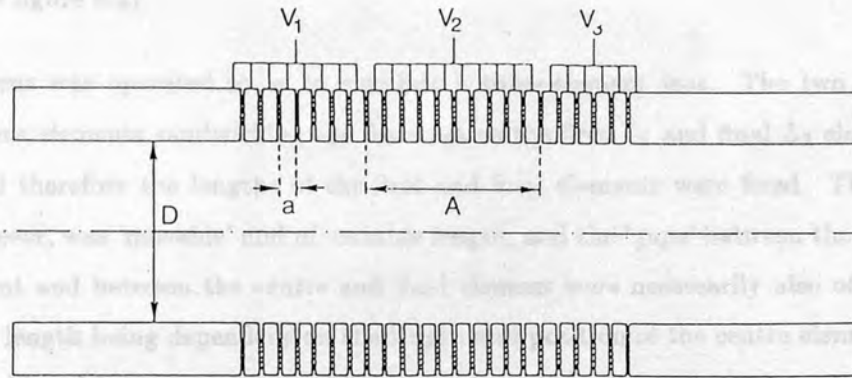


Figure 6.1 (from Read 1983, figure 1)

The spacing a of the mid-points of the gaps between the short cylinders was equal to $0.1D$ and the length of each gap was $0.02D$. The system therefore acts as a three-element lens with $A/D = 1$. Read proposed that a trapezoidal voltage distribution with sloping sides of width s could be applied to the short elements, and that $V(z)$ would be given by

$$V(z) = V_1 \quad \text{for } z < z_0 - \frac{1}{2}A - \frac{1}{2}s$$

$$V(z) = V_1 + \frac{V_2 - V_1}{s} \left[z - \left(z_0 - \frac{1}{2}A - \frac{1}{2}s \right) \right]$$

$$\text{for } z_0 - \frac{1}{2}A - \frac{1}{2}s \leq z \leq z_0 - \frac{1}{2}A + \frac{1}{2}s$$

$$V(z) = V_2 \quad \text{for } z_0 - \frac{1}{2}A + \frac{1}{2}s \leq z \leq z_0 + \frac{1}{2}A - \frac{1}{2}s$$

$$V(z) = V_2 + \frac{V_3 - V_2}{s} \left[z - \left(z_0 - \frac{1}{2}A - \frac{1}{2}s \right) \right]$$

$$\text{for } z_0 + \frac{1}{2}A - \frac{1}{2}s \leq z \leq z_0 + \frac{1}{2}A + \frac{1}{2}s$$

$$V(z) = V_3 \quad \text{for } z > z_0 + \frac{1}{2}A + \frac{1}{2}s$$

Read chose to take $s = a$ so that the properties of the disc lens could be deduced from the focal properties of a three cylinder lens as described above, as the focal properties of the

disc lens with $s = a$ do not differ significantly from the three cylinder lens with $A/D = 1$ and $g/D = 0.1$.

The lens investigated in the present work was similar to the lens proposed by Read in that as described at the beginning of this chapter, it was constructed from 31 discs electrically insulated from each other and sandwiched between two ordinary cylindrical elements (see figure 6.2).

The lens was operated so as to simulate a three-element lens. The two ordinary cylindrical lens elements sandwiching the discs act as the first L_1 and final L_3 elements of the lens, and therefore the lengths of the first and final elements were fixed. The centre element however, was 'movable' and of variable length, and the 'gaps' between the first and centre element and between the centre and final element were necessarily also of variable length, their length being dependent on the length and position of the centre element. The above was achieved by connecting together a number of the discs at a voltage V_2 to form the centre element L_2 . The voltages on the discs on either side of L_2 were stepped between V_1 the voltage applied to the first element L_1 and V_2 , and between V_2 and V_3 the voltage applied to the third and final element L_3 of the lens respectively. Figure 6.3 illustrates this, the regions on either side of L_2 where the voltages are stepped, act as the 'gaps' between L_1 and L_2 and L_2 and L_3 .

As the voltage is stepped in the 'gaps', the 'gap' voltage is therefore known and controllable irrespective of the size of the 'gap', i.e., the voltage in the 'gap' is not affected by the presence of stray fields as can be the case with ordinary lenses with large 'air gaps' between elements. A fuller description of the methods used to construct the lens are discussed in the next section. From the above description of the lens it can be seen that this lens differs from the lens proposed by Read in that instead of the lengths of the first and final elements of the three-element lens being variable and the 'gap' size fixed, the lengths of the first and final lens elements were fixed and the 'gaps' between the first and middle element and between the middle and final element were variable.

6.2 CONSTRUCTION AND OPERATION OF THE MULTI-DISC LENS

The discs used to construct the lens are 0.86mm thick and have an external diameter of 30mm and an internal diameter of 13.5mm. Figure 6.4 is a photograph of a disc, and a schematic diagram of a disc is given in figure 6.5.

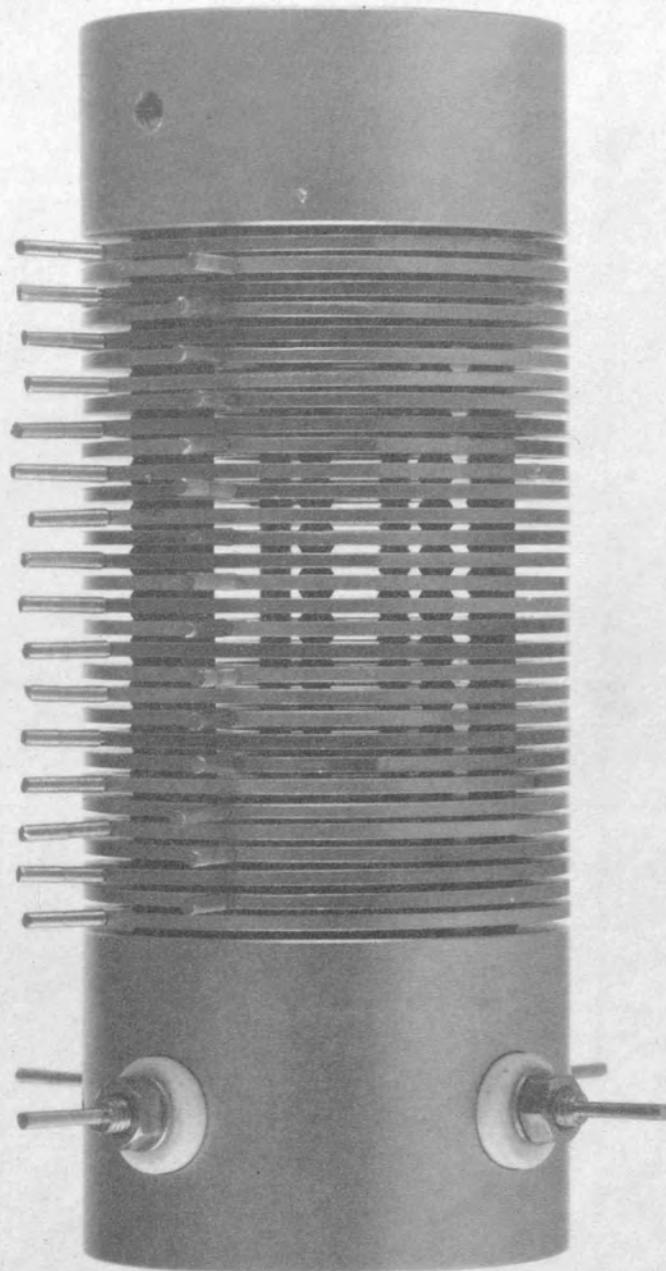
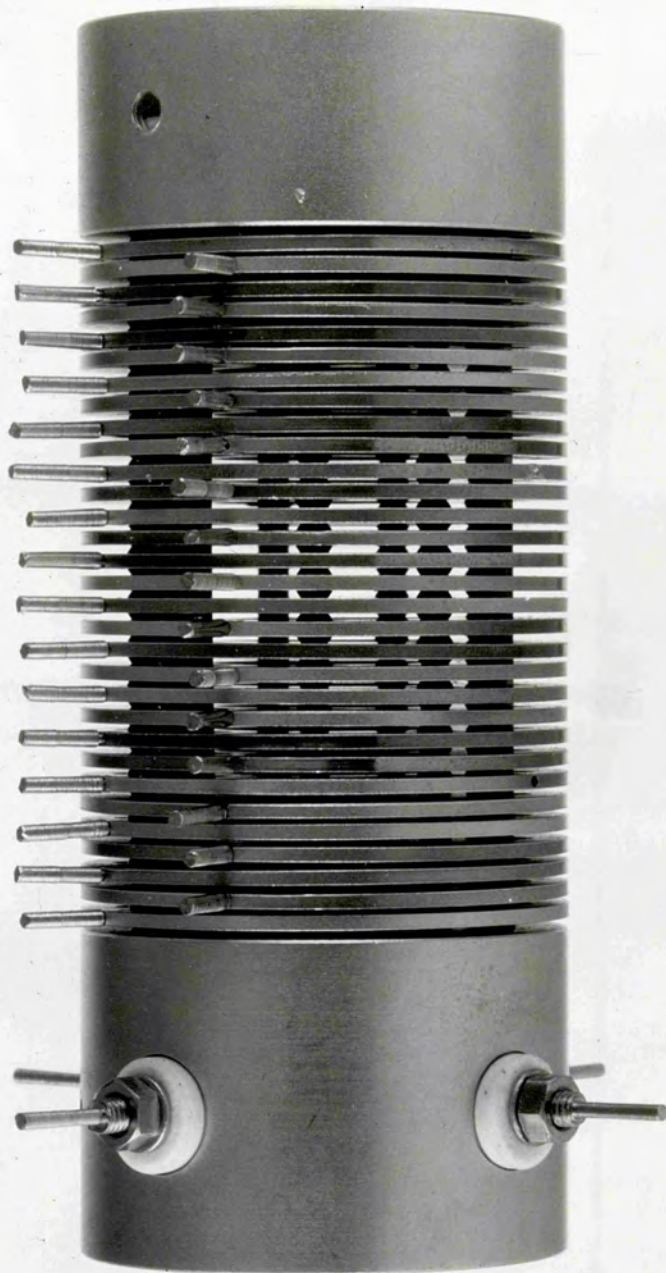


Figure 6.2



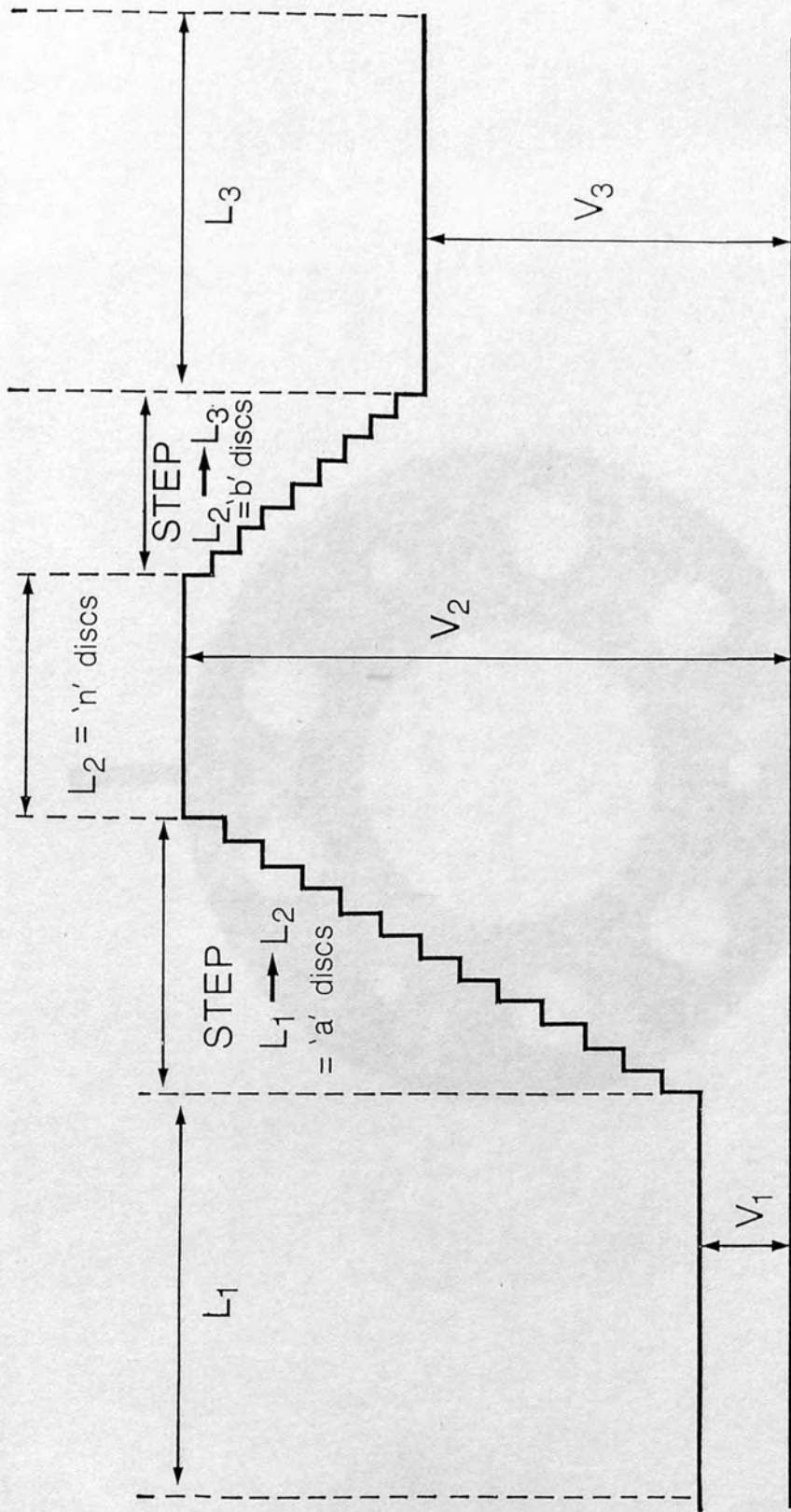


Figure 6.3

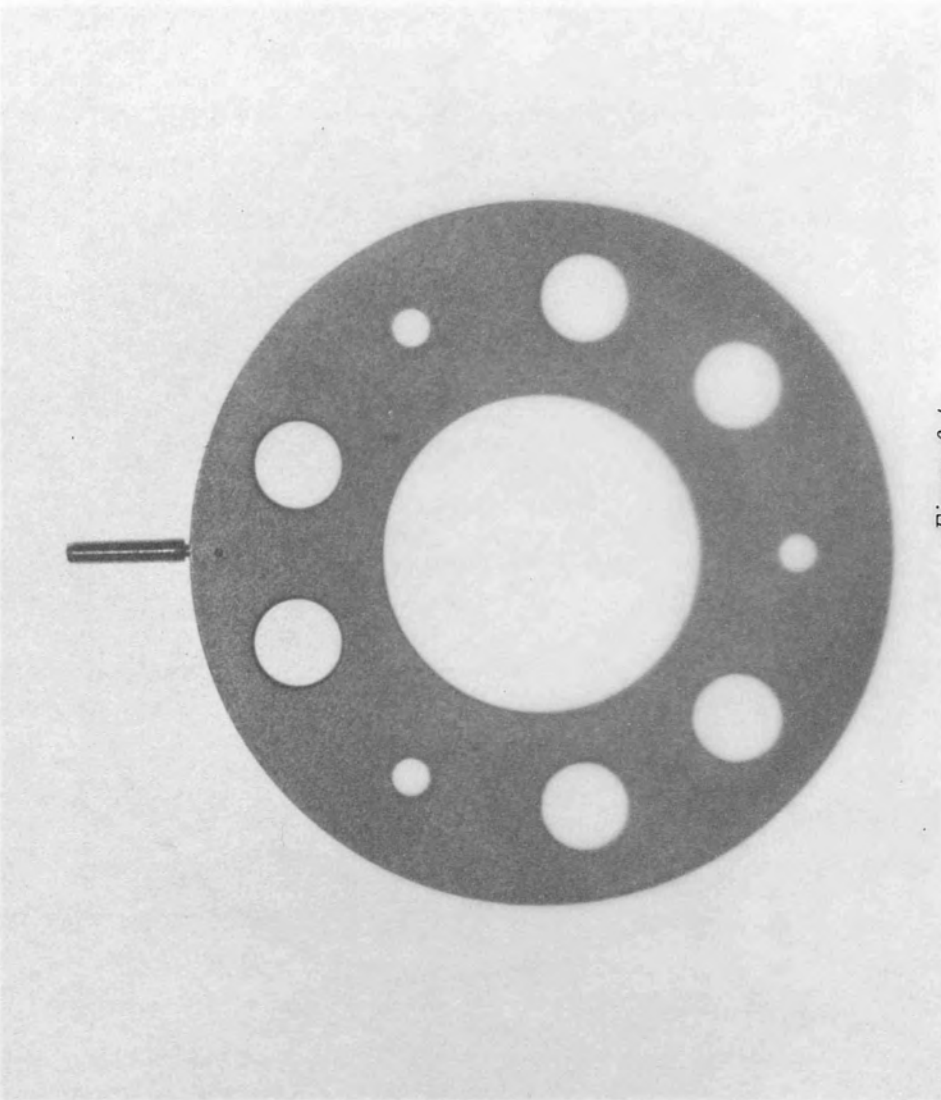
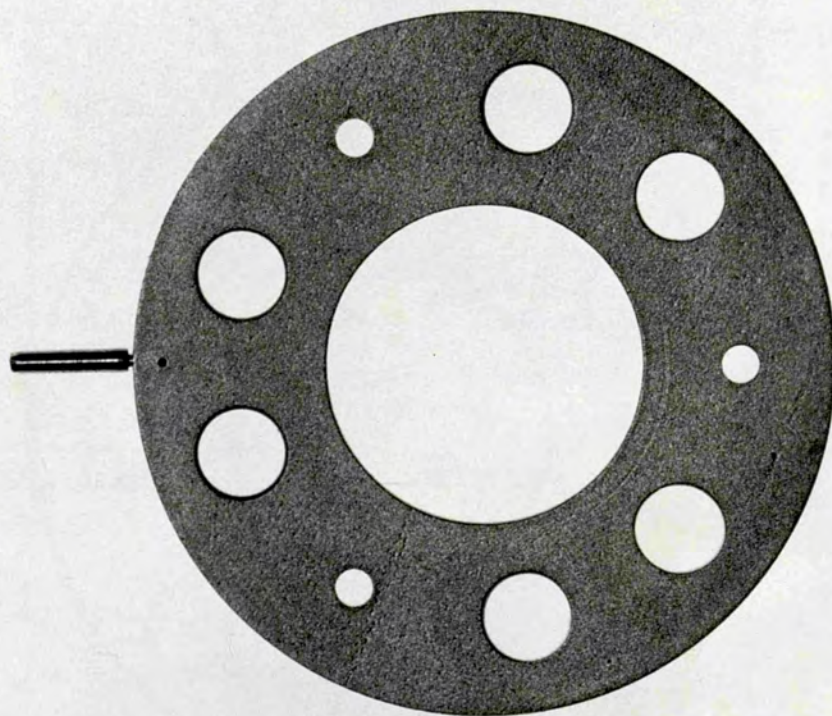
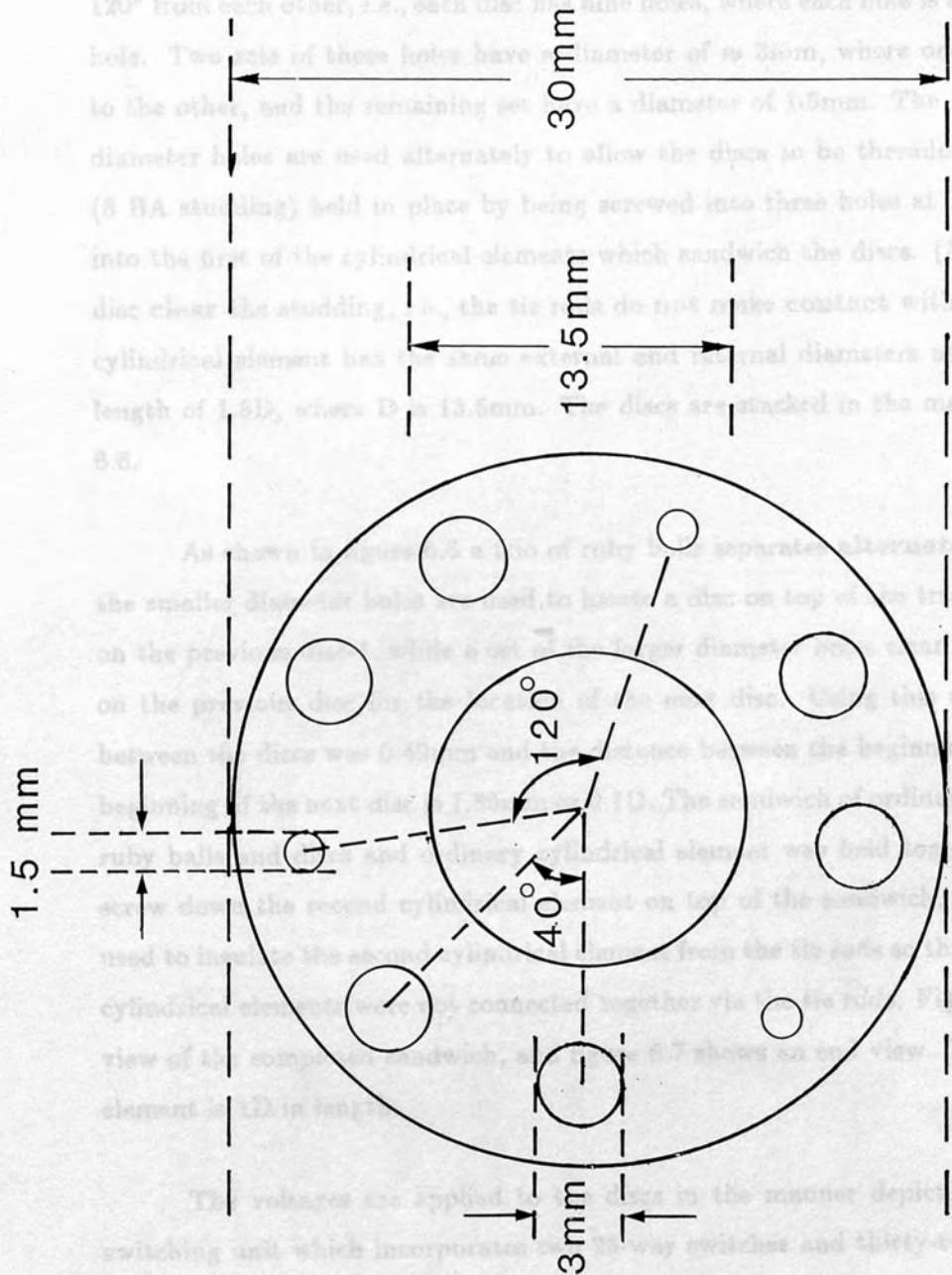


Figure 6.4



The discs are insulated from each other and from the ordinary cylindrical elements sandwiching the discs, using ruby ball bearings 3.38mm in diameter in the manner described below. Each disc has three sets of three holes, where one three holes in a set are offset by 120° from each other, i.e., each disc has nine holes, where each hole is at 40° to the previous hole. Two sets of these holes have a diameter of ≈ 30 mm, where one set is offset by 40° to the other, and the remaining set has a diameter of 13.5mm. The two sets of the larger diameter holes are used alternately to allow the discs to be threaded onto three tie rods (8 BA studding) held in place by being screwed into three holes spaced 120° intervals tapped into the first of the cylindrical elements which sandwich the discs. (Note the holes in the disc clear the studding, i.e., the tie rods do not make contact with the discs.) The first cylindrical element has a diameter of 13.5mm and a length of 1.5D, where D = 13.5mm. The discs are stacked in the manner shown in figure 6.5.



SCHEMATIC DIAGRAM OF A DISC

Figure 6.5

As shown in figure 6.5 a series of ruby ball bearings separate alternate pairs of discs where the smaller diameter holes are used to pass a disc on top while the larger diameter holes are resting on the previous disc. The larger diameter holes are used to pass a disc on top while the smaller diameter holes are resting on the previous disc. The larger diameter holes are used to pass a disc on top while the smaller diameter holes are resting on the previous disc. The larger diameter holes are used to pass a disc on top while the smaller diameter holes are resting on the previous disc.

The voltages are applied to the discs in the manner depicted by figure 6.5, by a switching unit which incorporates 32 two-way switches and thirty-two 100K resistors in a chain. As shown in the schematic diagram of the switching unit, (figure 6.8) the first switch allows the voltages to the discs to be stepped between V_1 and V_2 across n_1 of R_1 to R_{32} , i.e., 23 resistors, the second switch allows the voltages to the discs to be stepped between V_2 and V_3 across n_2 of R_3 to R_{34} , i.e., 23 resistors. LEDs are used to indicate the switch positions. A line of red LEDs numbered 1 to 32 are coupled to the first switch, and a line of green LEDs numbered 33 to 64 are coupled to the second switch. If for example, the voltages V_1 and V_2 are stepped across R_1 and R_2 , the fourth LED in the line of red LEDs will light

The discs are insulated from each other and from the ordinary cylindrical elements sandwiching the discs, using ruby ball bearings 2.38mm in diameter in the manner described below. Each disc has three sets of three holes, where the three holes in a set are offset by 120° from each other, i.e., each disc has nine holes, where each hole is at 40° to the previous hole. Two sets of these holes have a diameter of $\approx 3\text{mm}$, where one set is offset by 40° to the other, and the remaining set have a diameter of 1.5mm. The two sets of the larger diameter holes are used alternately to allow the discs to be threaded onto three tie rods (8 BA studding) held in place by being screwed into three holes at 120° intervals tapped into the first of the cylindrical elements which sandwich the discs. (Note, the holes in the disc clear the studding, i.e., the tie rods do **not** make **contact** with the discs.) The first cylindrical element has the same external and internal diameters as the discs and has a length of $1.5D$, where D is 13.5mm. The discs are stacked in the manner shown in figure 6.6.

As shown in figure 6.6 a trio of ruby balls separates **alternate** pairs of discs where the smaller diameter holes are used to locate a disc on top of the trio of ruby balls resting on the previous disc-1, while a set of the larger diameter holes clear the ruby balls resting on the previous disc for the location of the next disc. Using this arrangement, the gap between the discs was 0.49mm and the distance between the beginning of one disc and the beginning of the next disc is 1.35mm or $0.1D$. The sandwich of ordinary cylindrical element, ruby balls and discs and ordinary cylindrical element was held together by using nuts to screw down the second cylindrical element on top of the sandwich, ceramic washers were used to insulate the second cylindrical element from the tie rods so that the first and second cylindrical elements were not connected together via the tie rods. Figure 6.2 shows the side view of the completed sandwich, and figure 6.7 shows an end view. The second cylindrical element is $1D$ in length.

The voltages are applied to the discs in the manner depicted by figure 6.3, by a switching unit which incorporates two 23-way switches and thirty-two 100K resistors in a chain. As shown in the schematic diagram of the switching unit, (figure 6.8) the first switch allows the voltages to the discs to be stepped between V_2 and V_3 across n_1 of R_1 to R_{23} , i.e., 23 resistors, the second switch allows the voltages to the discs to be stepped between V_2 and V_3 across n_2 of R_9 to R_{32} , i.e., 23 resistors. LEDs are used to indicate the switch positions. A line of red LEDs numbered 1 to 23 are coupled to the first switch, and a line of green LEDs numbered 9 to 31 are coupled to the second switch. If for example, the voltages V_1 and V_2 are stepped across R_1 and R_4 , the fourth LED in the line of red LEDs will light

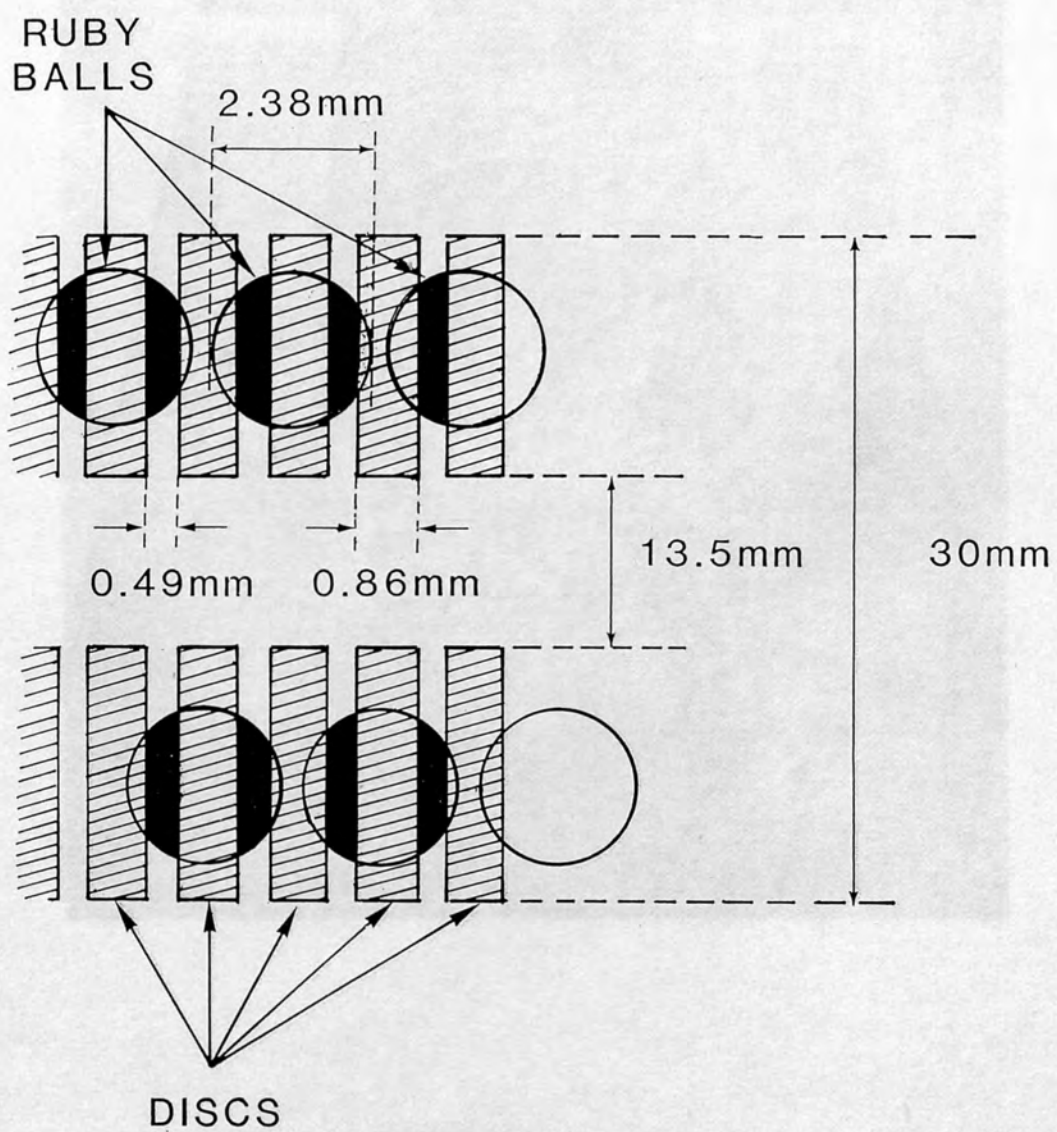


Figure 6.6

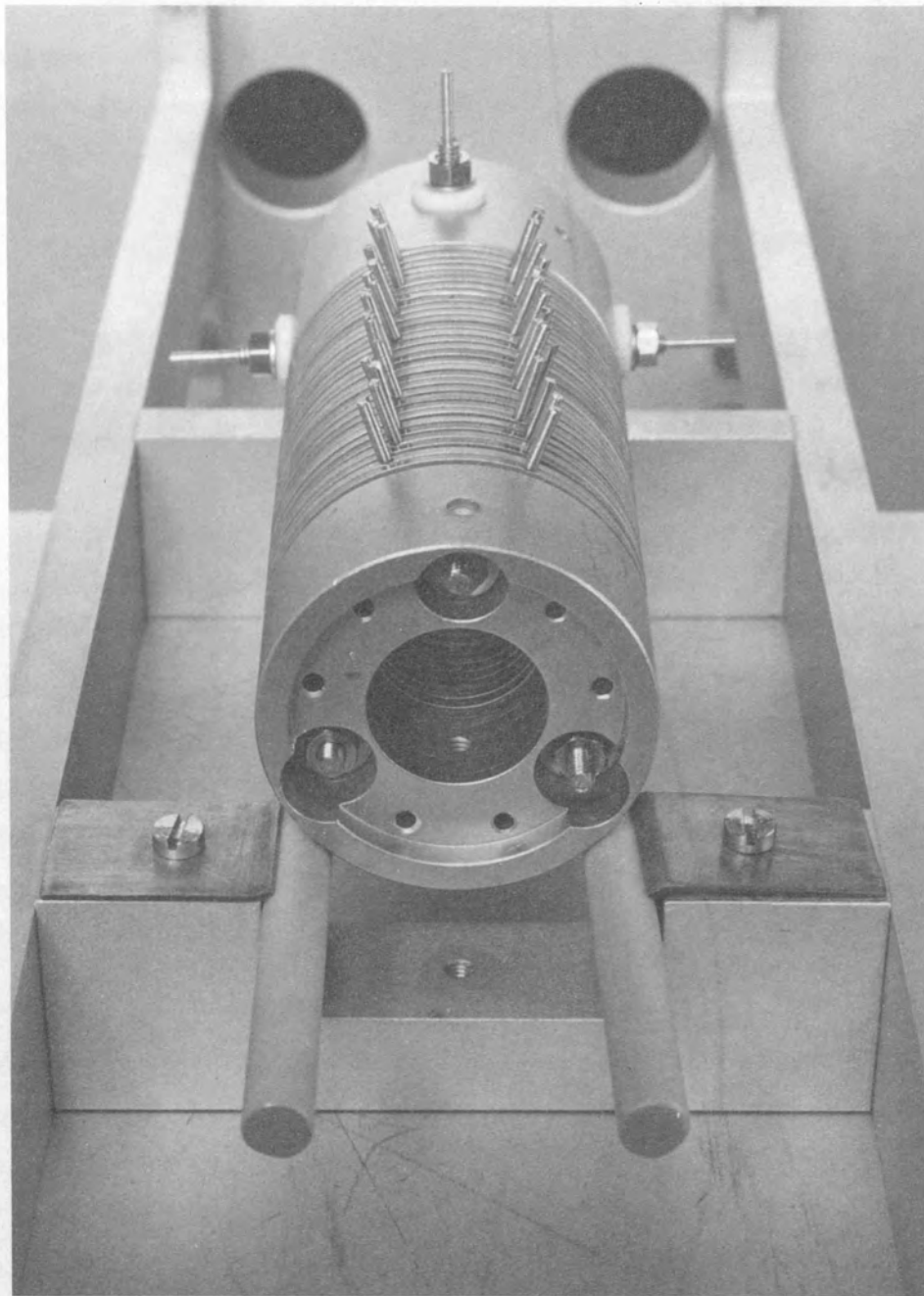
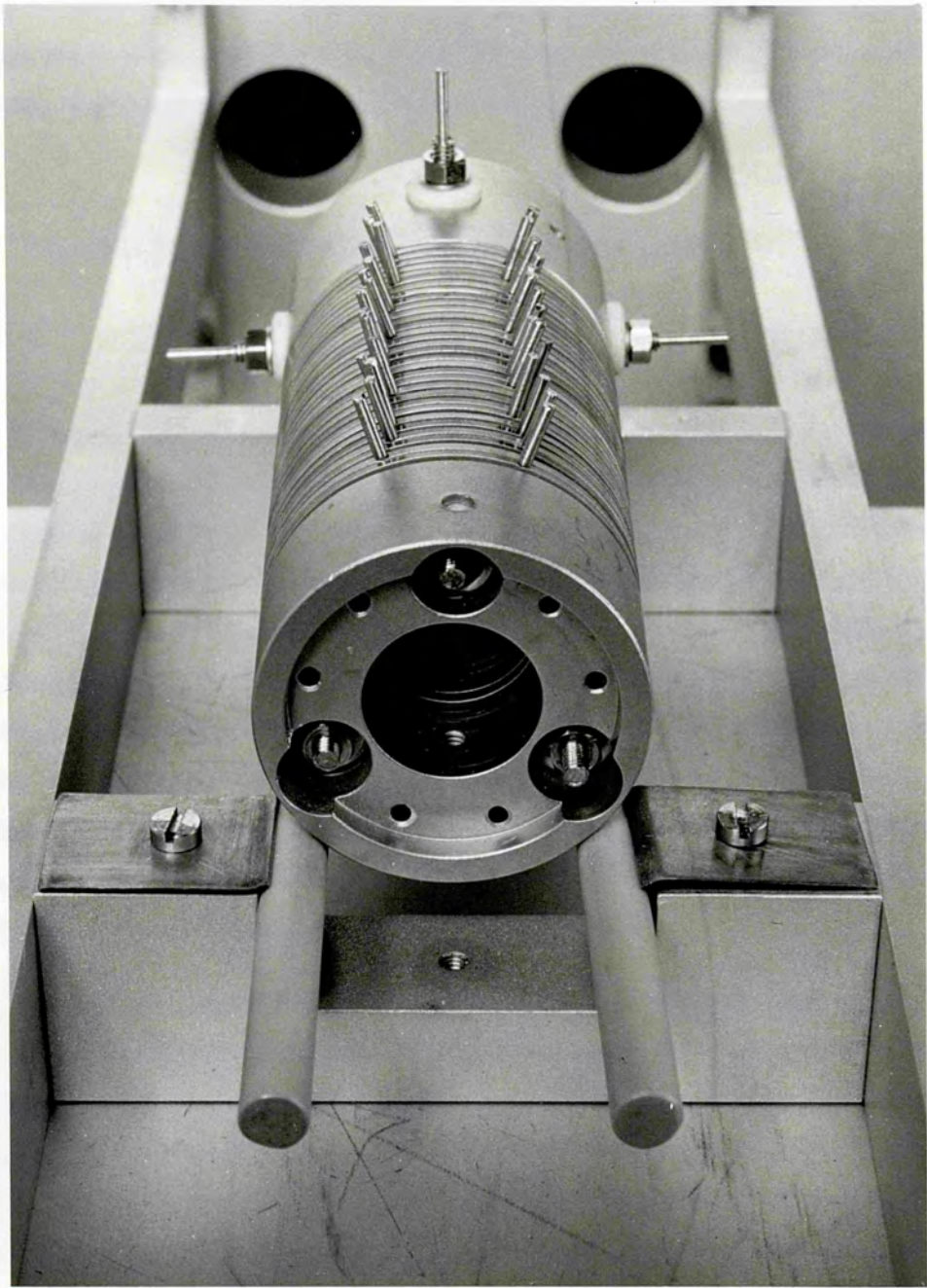


Figure 6.7



up to indicate that the centre element L_2 begins at disc 4; and if the voltages V_2 and V_3 are stepped across R_{15} and R_{32} the 7th LED in the line of green LEDs (numbered 15) will light up to indicate the centre element L_2 ends at disc 15. Figure 6.9 is a photograph of the front panel of the switching unit, the LEDs show that a lens with a centre element 11 discs long, starting at disc 10 and ending at disc 20 is being investigated.

6.3 ACQUIRING DATA FOR THE MULTI-DISC LENS

Experimental Data

It was decided to investigate three lenses out of the many possible three-element lenses incorporating the 31 discs. All three lenses had a first element length L_1 of 2.72D and a final element length L_3 of 1.80D. As the ordinary elements which sandwich the discs are shorter than 2.72D and 1.80D respectively, an additional cylindrical element was placed in front of and electrically connected to the first ordinary cylinder of the 'sandwich', and a second additional cylinder was placed behind and connected to the second ordinary cylindrical element of the 'sandwich'. An aperture disc with a single central hole of 1.5mm, was placed between the two cylindrical elements which make up L_1 to act as an angle stop. The three lenses differed in the number of elements which were chosen to be connected together to form the centre element L_2 . The first lens studied had an L_2 of 0.6D, the second had an L_2 of 1.0D and the third had an L_2 of 2.0D.

For each lens, experimental data was obtained by finding for fixed values of L_2 and V_3/V_1 , the value of V_2/V_1 which focussed the lens, and the resultant magnification M , for a given position of the central disc n_c of the centre element L_2 , using the method described in chapter three. Once V_2/V_1 and M had been noted, new values of V_2/V_1 and M were found for the next value of n_c . This process was repeated until the values of V_2/V_1 (where $V_2/V_1 > V_3/V_1$) and M had been found for all possible values of n_c for a given V_3/V_1 . The process was then repeated for the next value of V_3/V_1 . Data was taken for V_3/V_1 equal to 0.5, 0.6, 0.7, 0.8, 0.9, 1.0, 2.0, 3.0, 4.0 and 5, for each of the three values of L_2 . n_c had values of between 6 and 26 for the lens with a centre element of length L_2 of 0.6D, (i.e., 7 discs, see figure 6.10) and values of between 8 and 24 for the lens with an L_2 of 1.0D, (i.e., 11 discs) and values of between 13 and 19 for the lens with an L_2 of 2.0D, (21 discs).

Figure 6.11 shows a typical example of the type of 'image' appearing on the display scope screen when the disc lens was focussed, and from which the focussing voltage V_2/V_1

SCHEMATIC DIAGRAM OF SWITCHING
UNIT

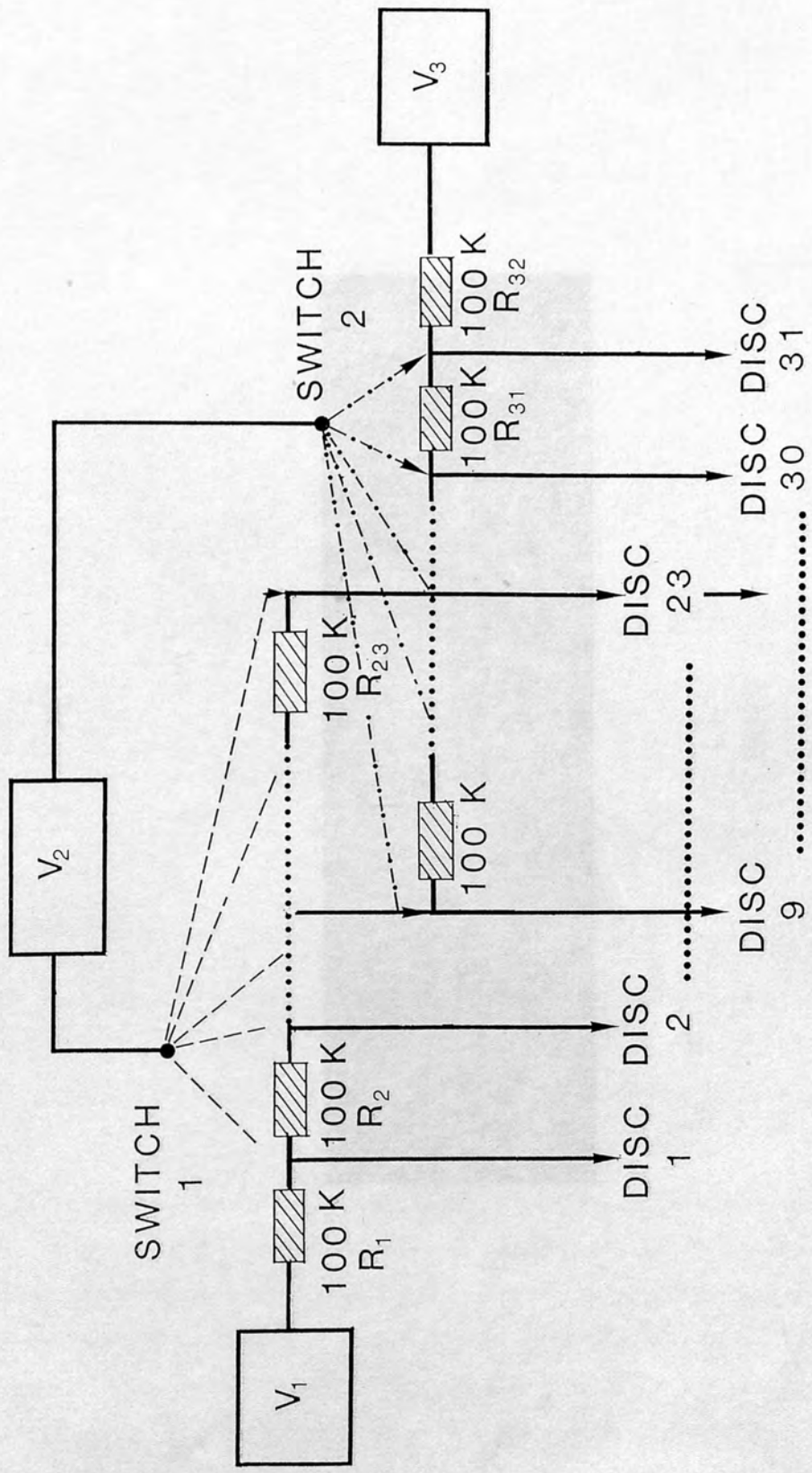


Figure 6.8

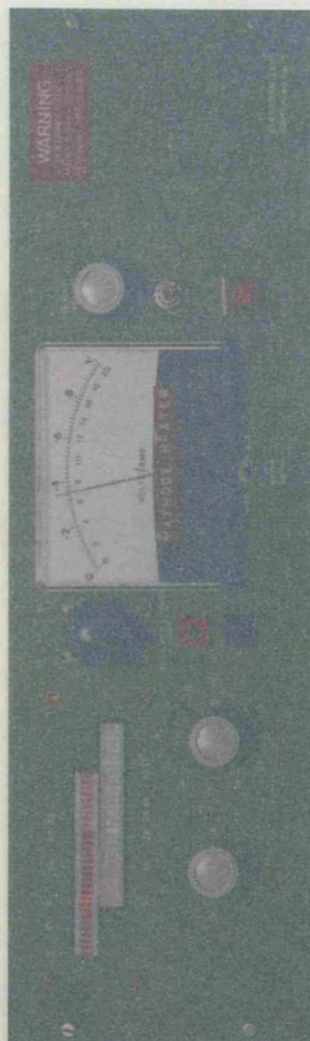


Figure 6.9

If the voltage drops are measured across the bridge arms above, then the middle segment will effectively represent the average of the first and second arms to which V_1 is applied, and will be at the centre of the gap between the first and second feet to which V_2 is applied. Therefore, as the distance between the centres of two gaps is $2L$, the effective length of the centre segment L_0 will be

$$L_0 = L_1 + L_2 = 2L$$

i.e. the distance between the centres of the two gaps is $2L$.



Figure 6.9

and M were determined. Figure 6.12 shows another example of an 'image' from the disc lens, but in this case, the 'image' is not good, making the determination of the magnification difficult. 'Bad images' occur when:

- (1) The signal to noise ratio is small, due to the current collected at the Faraday cup being small. If the voltage V_1 is small, as it must be when the voltage ratio V_2/V_1 is large, the current entering the lens will be small, causing the current exiting the lens to be small.
- (2) Aberrations will also cause 'distortion' of the image, particularly when the lens acts as a focusing lens, i.e., $V_2/V_1 < 1$ or the lens is strong, i.e., V_2/V_1 is large.

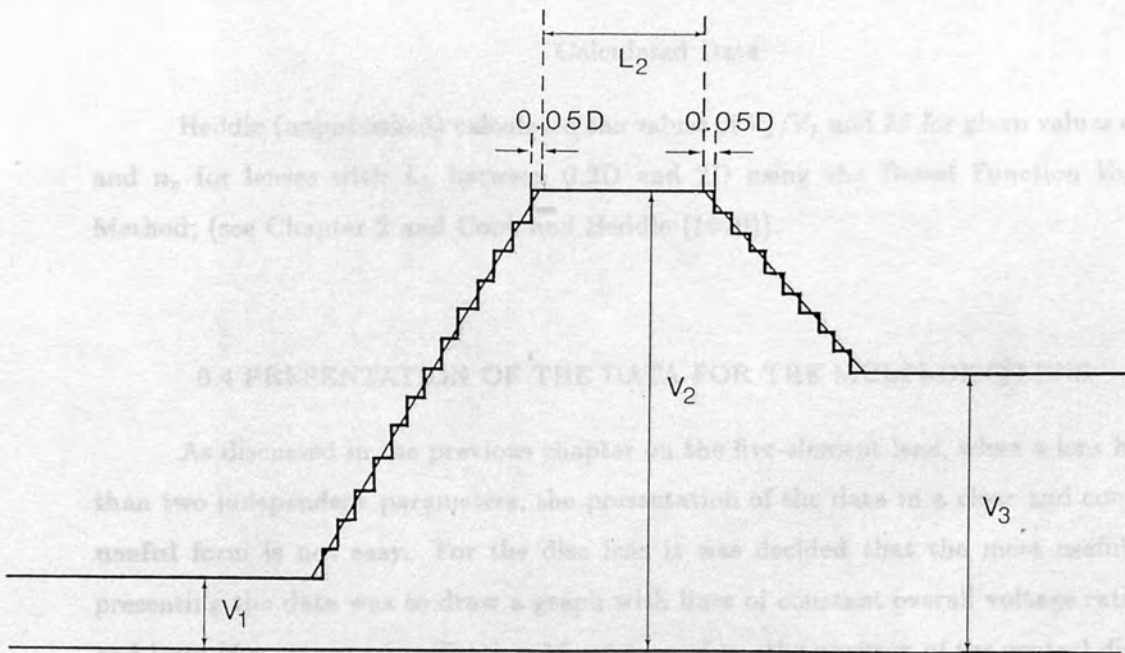


Figure 6.10

If the voltage 'steps' are approximated by a linear change in voltage as shown above, then the middle element will effectively begin at the centre of the gap between the first and second disc, to which V_2 is applied, and will end at the centre of the gap between the last and second last disc to which V_2 is applied. Therefore, as the distance between the centres of two gaps is $0.1D$, the effective length of the centre element L_2 will be

$$L_2 = (\text{no. of discs connected together to form } L_2 - 1) \times 0.1D$$

i.e., 11 Discs connected together form an element with an effective length of $1.0D$.

and M were determined. Figure 6.12 shows another example of an 'image' from the disc lens, but in this case, the 'image' is not good, making the determination of the magnification difficult. 'Bad images' occur when

- (1) The signal to noise ratio is small, due to the current collected at the Faraday cup being small. If the voltage V_1 is small, as it must be when the voltage ratio V_3/V_1 is large, the current entering the lens will be small, causing the current leaving the lens to be small.
- (2) Aberrations will also cause 'distortion' of the image, particularly when the lens acts as a retarding lens, i.e., $V_3/V_1 < 1$ or the lens is strong, i.e., V_3/V_1 is large.

Calculated Data

Heddle (unpublished) calculated the values of V_2/V_1 and M for given values of V_3/V_1 and n_c for lenses with L_2 between 0.2D and 2D using the Bessel Function Expansion Method, (see Chapter 2 and Cook and Heddle (1976)).

6.4 PRESENTATION OF THE DATA FOR THE MULTI-DISC LENS

As discussed in the previous chapter on the five-element lens, when a lens has more than two independent parameters, the presentation of the data in a clear and concise and **useful** form is not easy. For the disc lens it was decided that the most useful way of presenting the data was to draw a graph with lines of constant overall voltage ratio V_3/V_1 and lines of constant magnification M , on axes of n_c , the position of the central disc of the centre element L_2 , versus V_2/V_1 . An electron lens is normally required to be operated at a **given** overall voltage ratio, (V_3/V_1 in the case of the disc lens) and a **given** magnification M . The information that remains to be found in the case of the disc lens once V_3/V_1 and M have been specified, are the values of V_2/V_1 and n_c necessary to focus the lens. From the graph described above it is possible to find the values of V_2/V_1 and n_c for given values of V_3/V_1 and M . Figures 6.13 to 6.15 show lines of constant V_3/V_1 and M drawn on axes of n_c versus V_2/V_1 as obtained from the calculated data of Heddle for the three lenses which were investigated experimentally.

Lines of constant V_3/V_1 drawn on axes of n_c versus V_2/V_1 , can also easily be produced from the experimentally obtained data, as the method used to obtain the data, as described

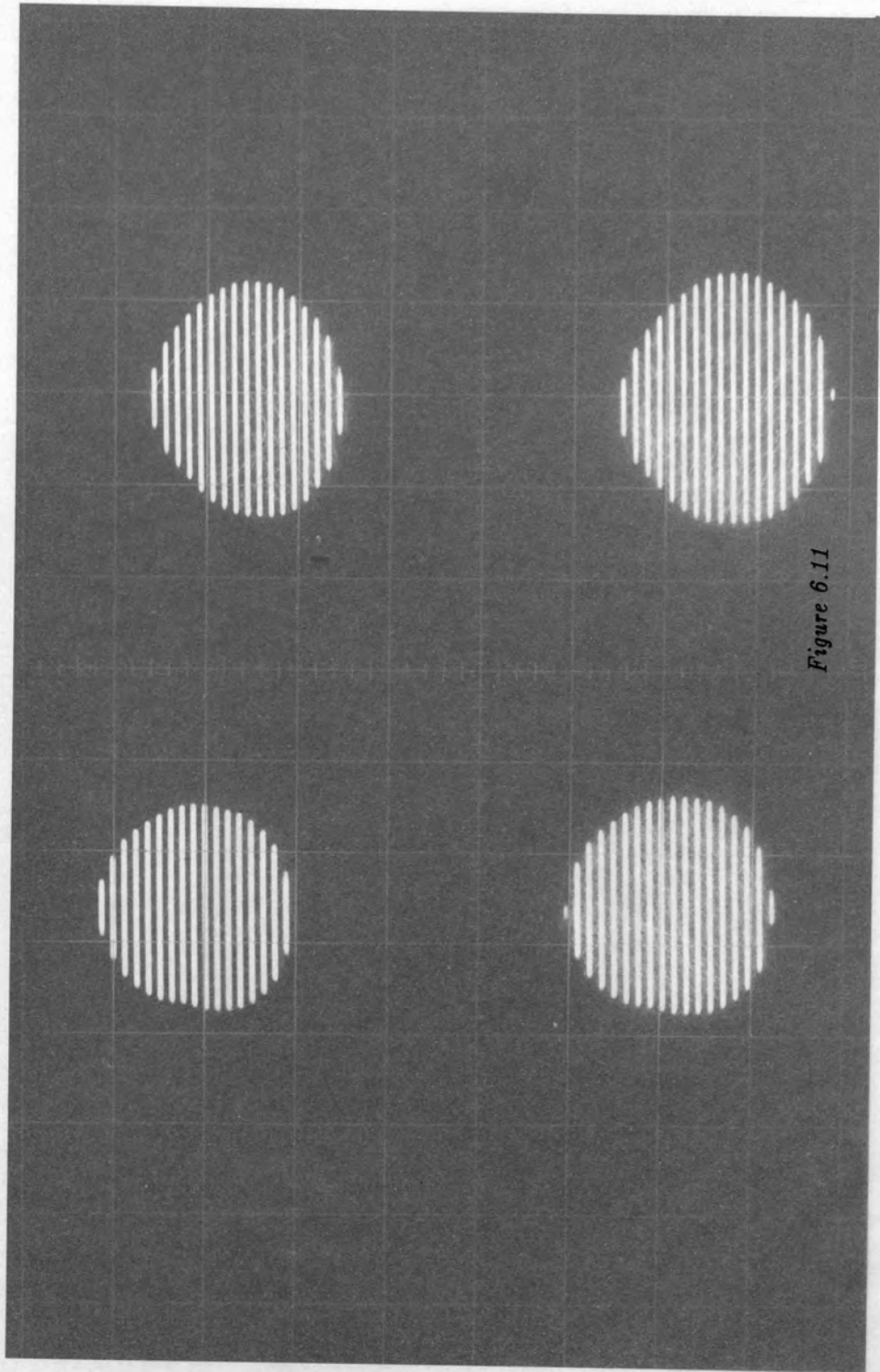
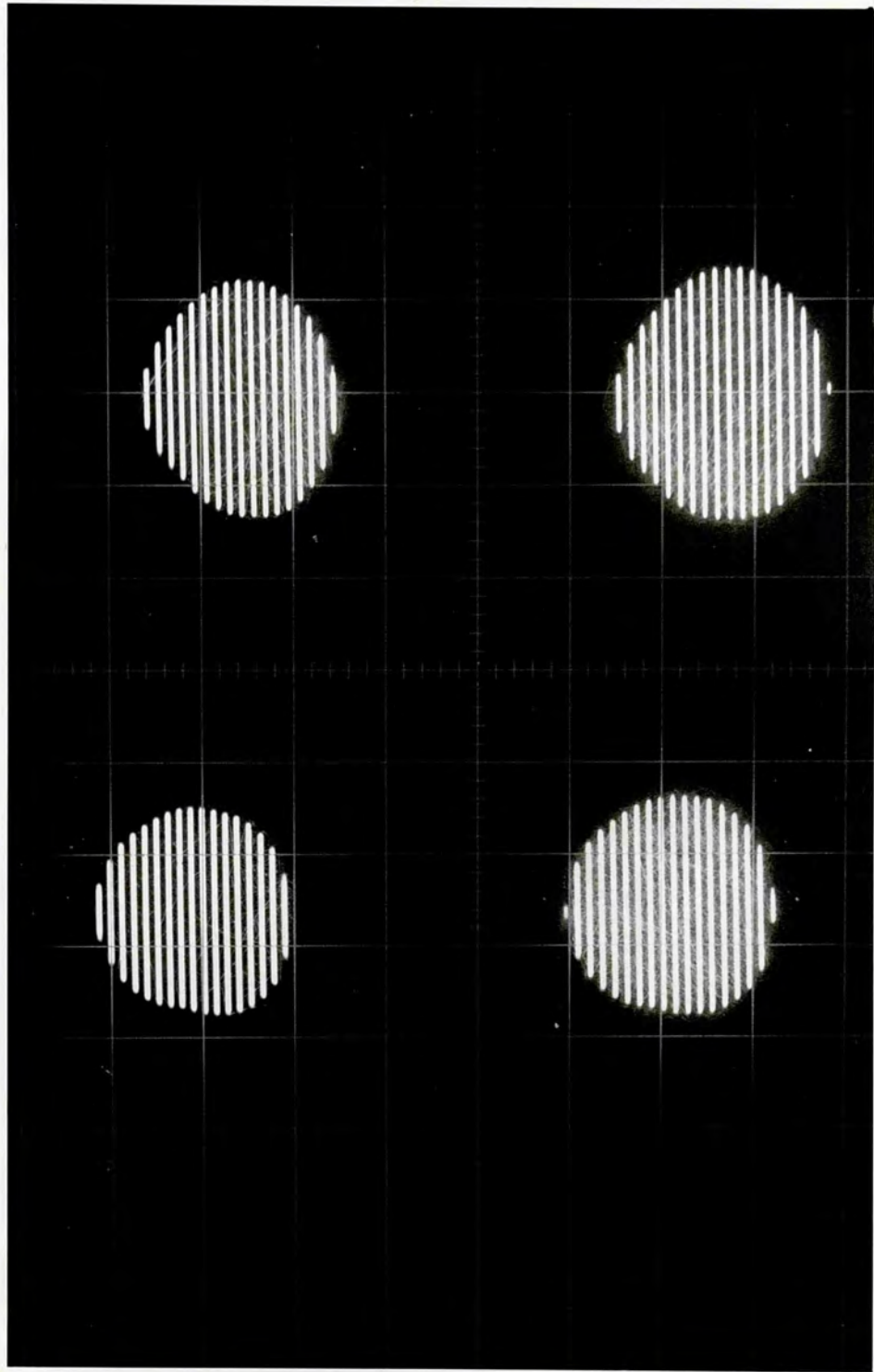


Figure 6.11



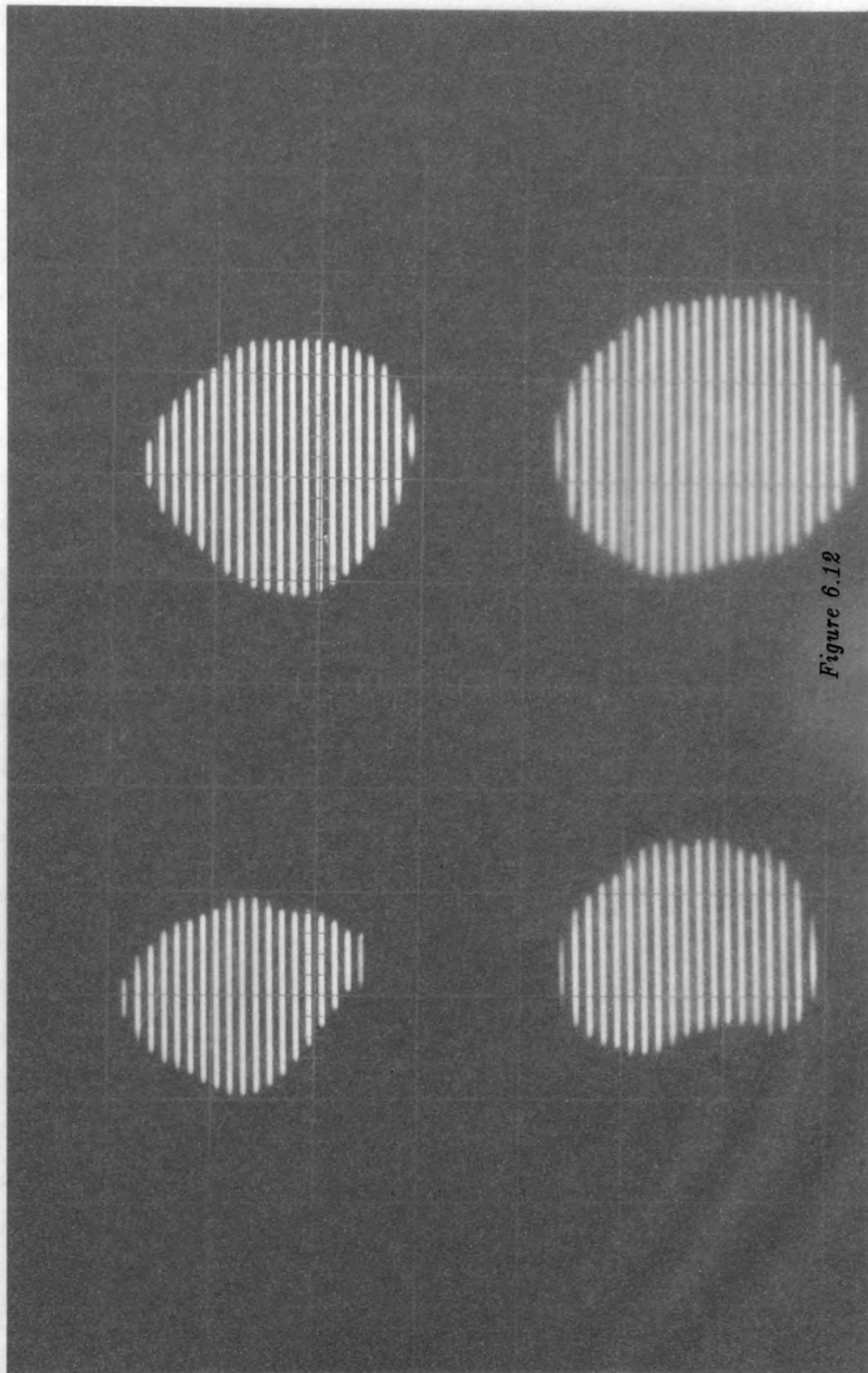
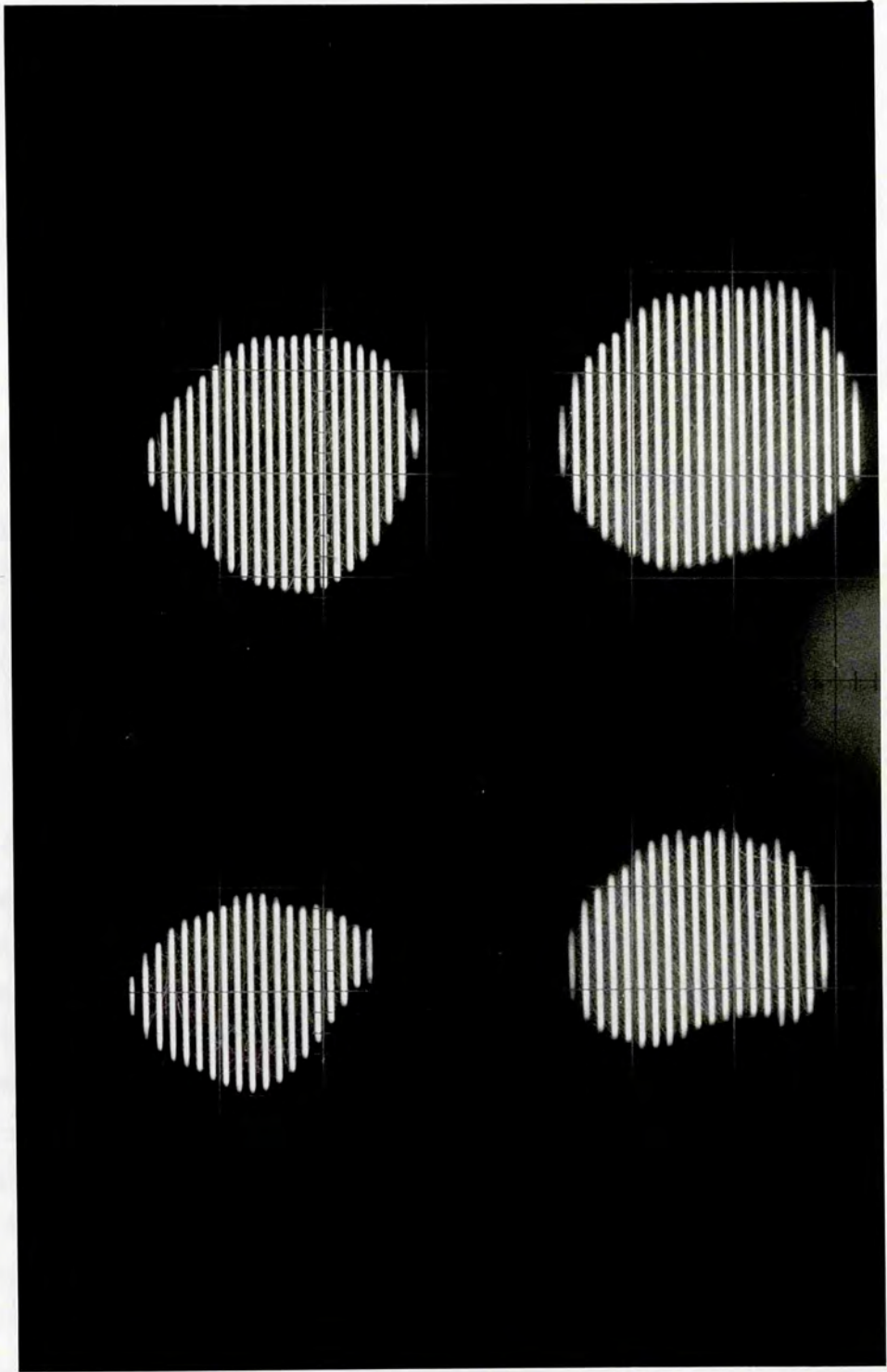


Figure 6.12



in the last section, produces tables of n_c , V_2/V_1 and M for constant values of V_3/V_1 for a given lens, i.e., for a given value of L_2 . In figures 6.16 to 6.18 the experimentally obtained values of n_c and V_2/V_1 are plotted for the same constant values of V_3/V_1 , as figures 6.13 to 6.15 i.e., the same values of V_3/V_1 as used for the calculated data. Figures 6.19 to 6.21 show both the calculated and experimentally obtained values for n_c and V_2/V_1 for V_3/V_1 equal to 0.6, 1.0 and 3.0 for the three values of L_2 , and from these figures it can be seen that the agreement obtained between the calculation and experiment is very satisfactory. The worst agreement occurs when the lens acts as a retarding lens and V_3/V_1 has its smallest values, or when the lens is at its strongest, i.e., when V_3/V_1 has its largest values. The agreement is particularly bad where the first 'gap', i.e., the region between L_2 and L_1 is large. This is because for accelerating lenses, i.e., those lenses where $V_3/V_1 > 1$, the lens is particularly strong when the first 'gap' is large, and the second 'gap' small, i.e., when the action of the lens is due predominately to the second gap.

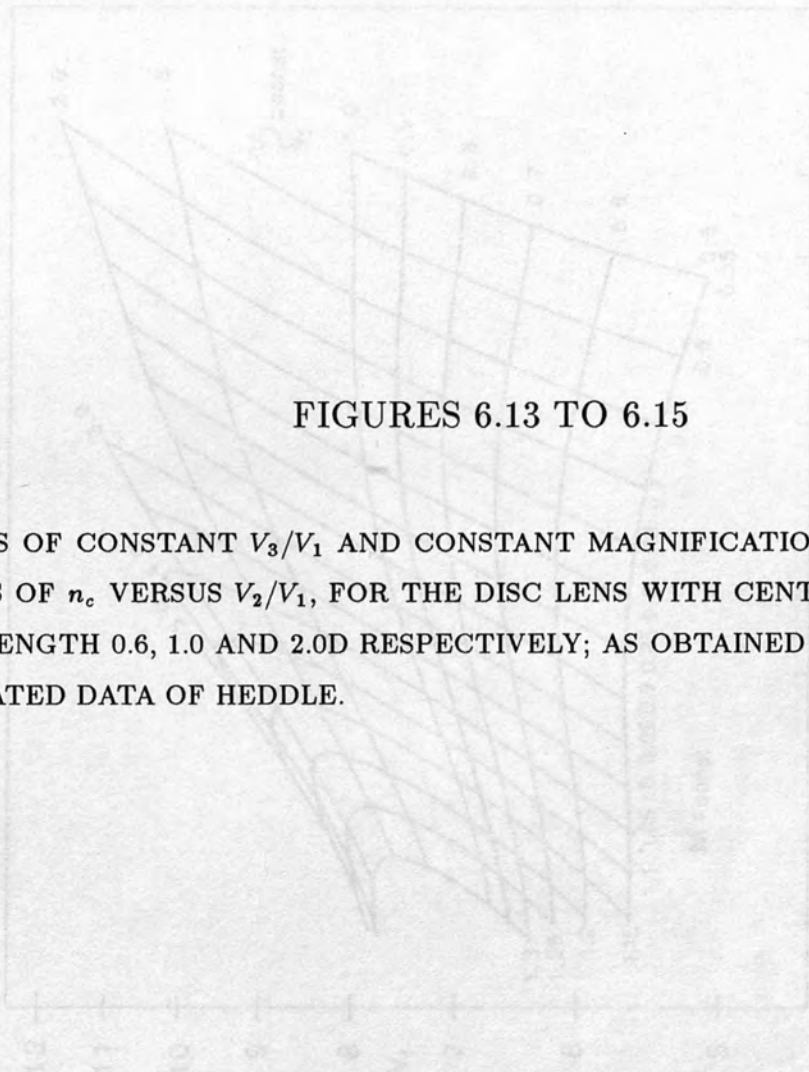
That the worst agreement between calculation and experiment occurs for those lenses described above, is not surprising, as it is for these lenses that lens aberrations would be expected to have their greatest effect. The experimentally obtained values of V_2/V_1 tend to be lower than the calculated values of V_2/V_1 , this is consistent with the argument that the differences between calculation and experiment are the effect of spherical aberration, as spherical aberration will cause a lens to appear to be focussed at a value of V_2/V_1 lower than would be expected for the ideal lens, and the calculated data refers to the ideal lens.

Experimentally, there is no straightforward method to obtain values of n_c and V_2/V_1 for constant M , therefore to present the experimentally obtained magnification data n_c was plotted versus M for constant values of V_3/V_1 . Figures 6.22 to 6.29 show both the calculated and experimentally obtained values for n_c and M for V_3/V_1 equal to 0.6, 1.0 and 3.0 for the three values of L_2 . From these figures it can be seen that the agreement obtained is satisfactory, the worst agreement occurring again for the retarding and strongest lenses. They also illustrate the 'zoom' action of this lens, i.e., for a given V_3/V_1 it is possible to vary the magnification from between 0.5 to 1.3. The agreement between calculation and experiment is not as good for the magnification data as for the voltage data, and this is a reflection of the relative ease with which it is possible to judge focus and measure the magnification using the technique described in chapter three, i.e., it is easier to decide from the 'image' of four dots when the lens is focussed than it is to determine the magnification, particularly when the 'image' is poor, it is impossible to determine with confidence the separation of dots such as those shown in figure 6.12, the error incurred in measuring the

the magnification from such an image is therefore larger, ($\approx 15\%$ of the measured value) than the error incurred ($\approx 6\%$) when a good 'image' is obtained. From figures 6.22 to 6.29 it can be seen that the experimentally obtained values of M tend to go from being smaller than the calculated values of M where the 'gap' between L_2 and L_1 is small, i.e., n_c is small, to being larger than the calculated values where the 'gap' between L_2 and L_1 is small, i.e., n_c is large. There is no obvious reason why this should be so, however, the experimental values of M being lower than the calculated values of M at small values of n_c , is consistent with them being higher at large values of n_c . There is also no easy way to explain why for large values of V_3/V_1 , the experimentally obtained values of M lie consistently below the calculated values. Although, as aberrations tend to cause a lens to appear to be focussed at voltages lower than those expected if only paraxial rays are considered, (i.e., the ideal lens) as is the case for the calculated data, then it could be argued that aberrations cause the lens to behave as an apparently weaker lens than the ideal lens, and will therefore have a smaller magnification than the ideal lens.

6.5 CONCLUDING REMARKS

A three-element lens with a 'movable' centre element of variable length has been studied. Experimental data has been compared with data calculated using the Bessel function expansion method and the agreement was found to be satisfactory.



FIGURES 6.13 TO 6.15

LINES OF CONSTANT V_3/V_1 AND CONSTANT MAGNIFICATION M DRAWN ON AXES OF n_c VERSUS V_2/V_1 , FOR THE DISC LENS WITH CENTRE ELEMENT L_2 OF LENGTH 0.6, 1.0 AND 2.0D RESPECTIVELY; AS OBTAINED FROM THE CALCULATED DATA OF HEDDLE.

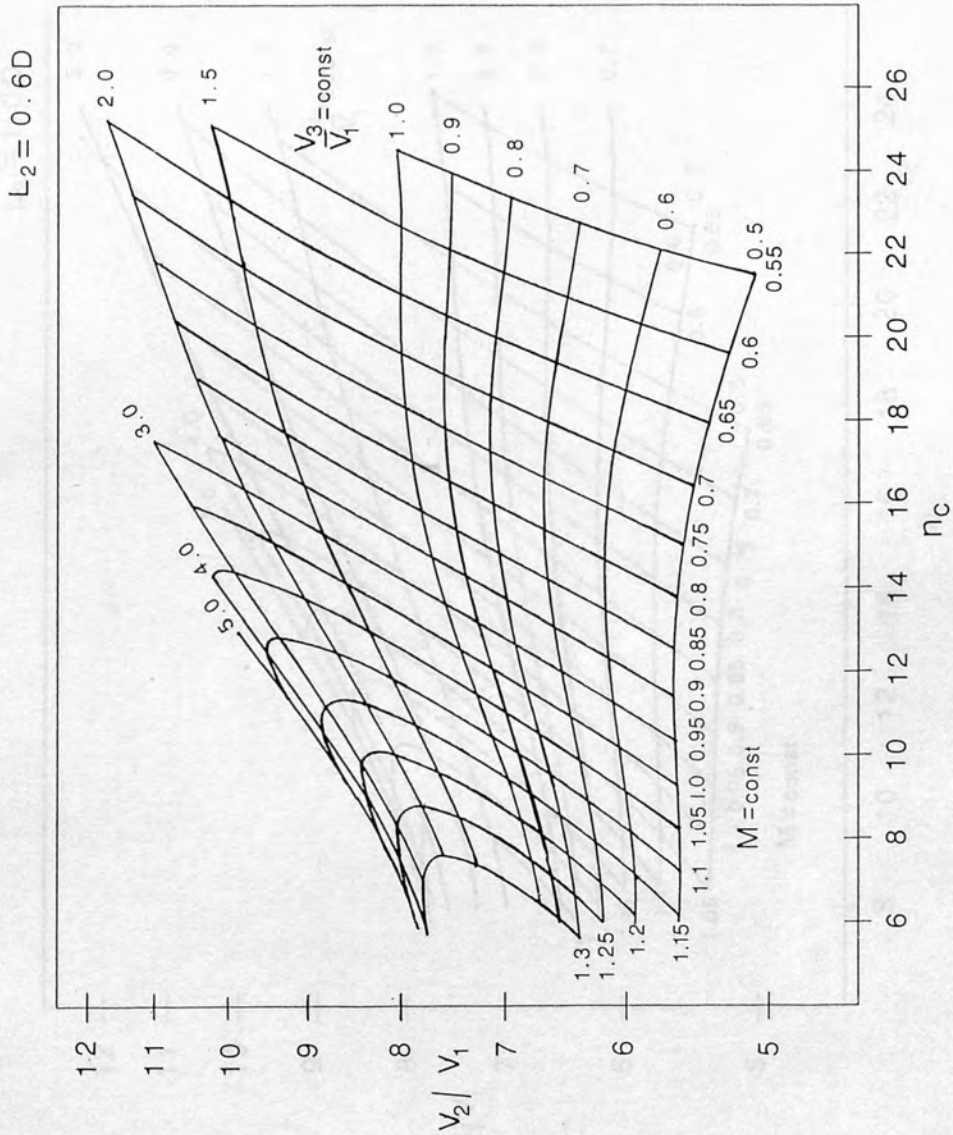


Figure 6.13

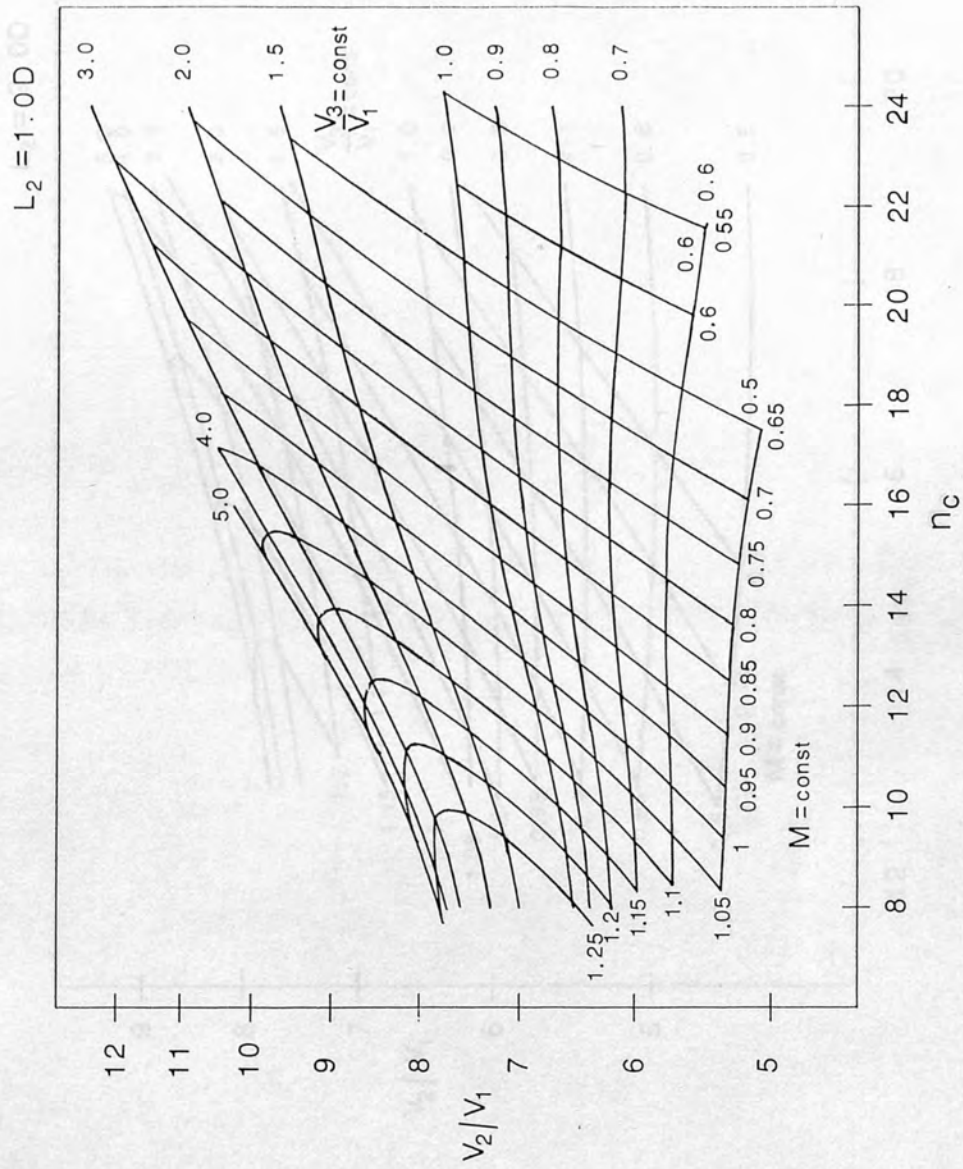


Figure 6.14

$L_2 = 2.0D$

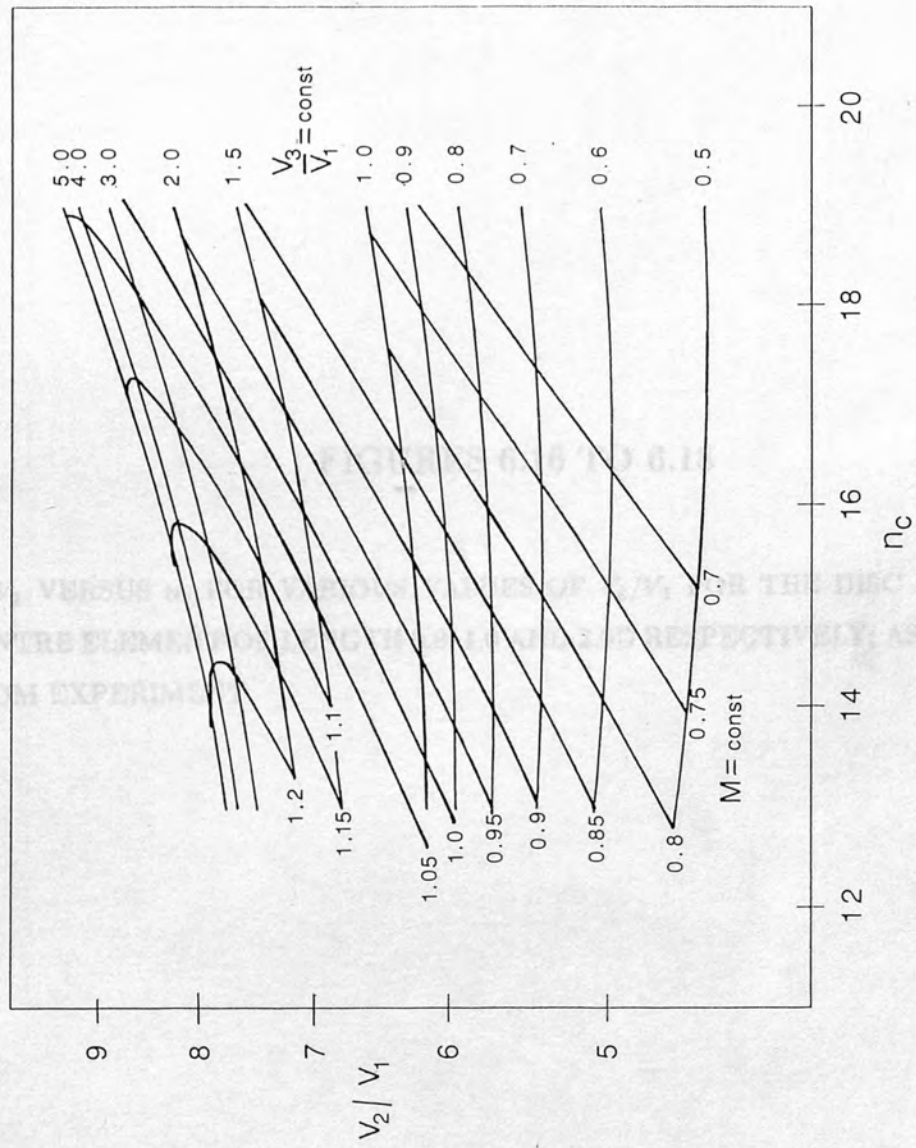


Figure 6.15

FIGURES 6.16 TO 6.18

V_2/V_1 VERSUS n_c FOR VARIOUS VALUES OF V_3/V_1 FOR THE DISC LENS WITH CENTRE ELEMENT OF LENGTH 0.6, 1.0 AND 2.0D RESPECTIVELY; AS OBTAINED FROM EXPERIMENT.

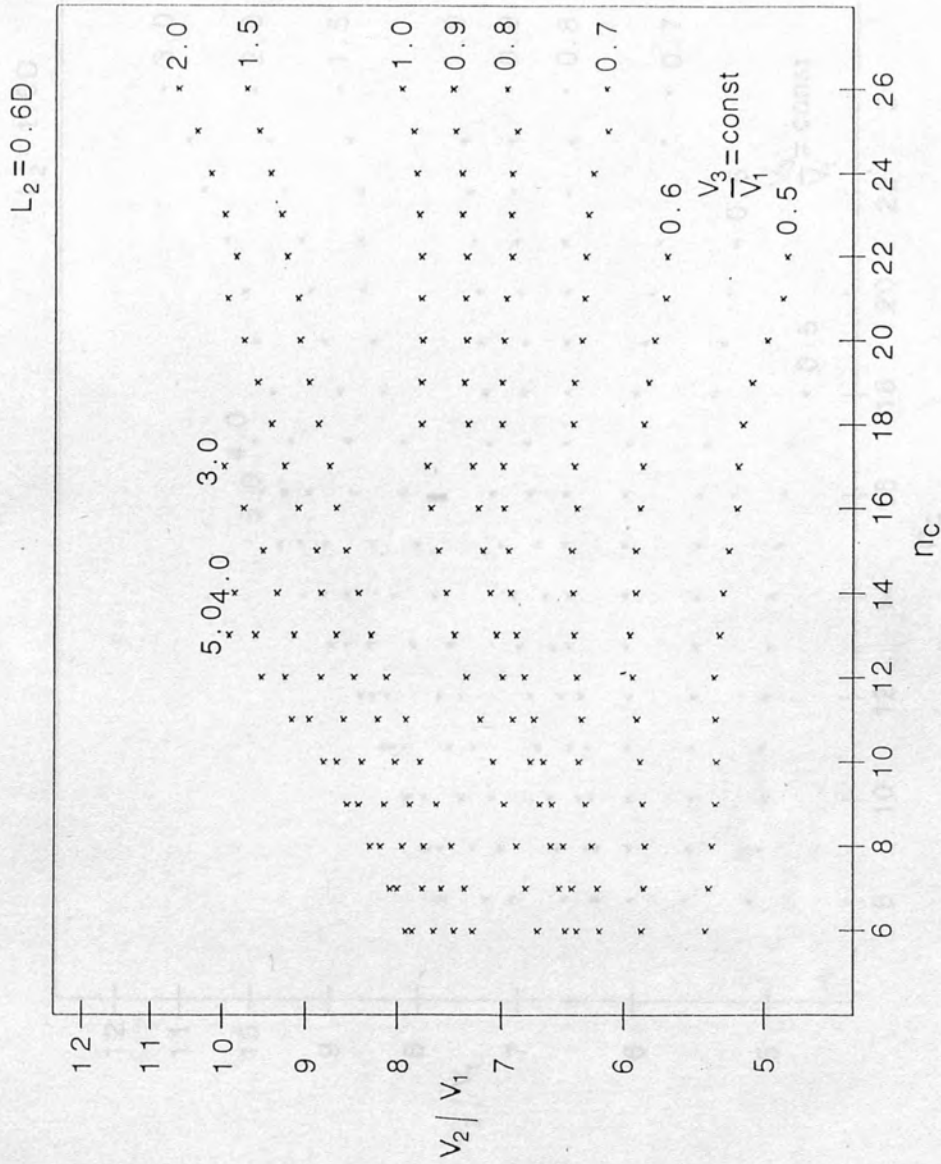


Figure 6.16

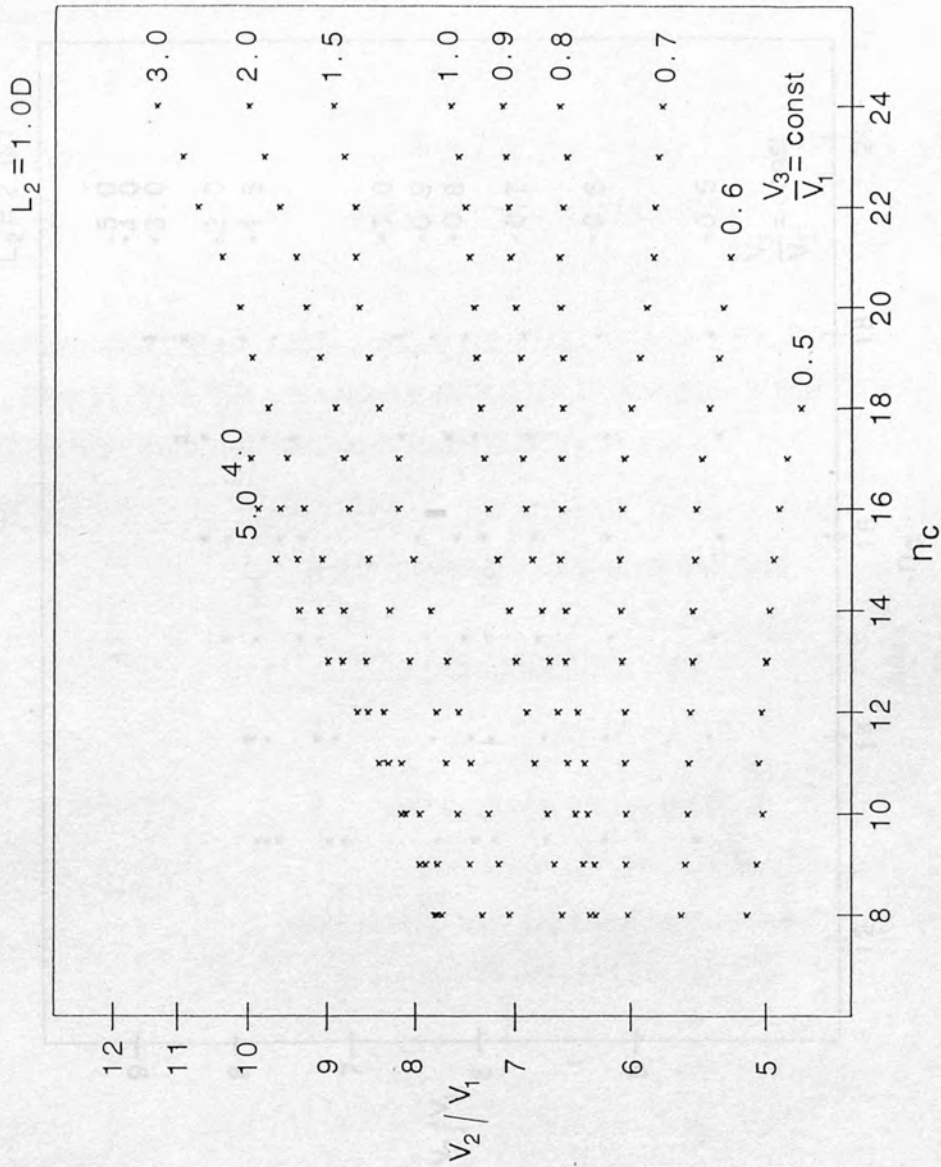


Figure 6.17

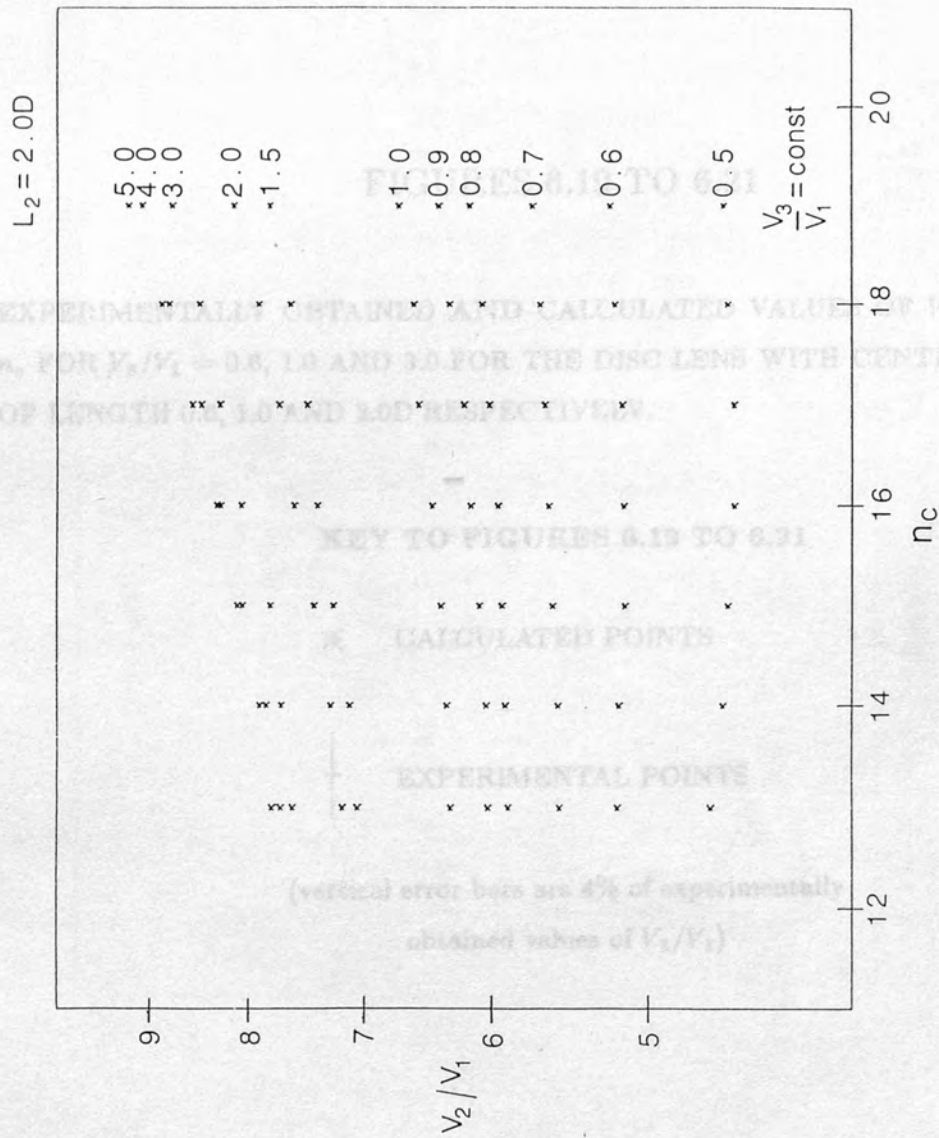


Figure 6.18

FIGURES 6.19 TO 6.21

EXPERIMENTALLY OBTAINED AND CALCULATED VALUES OF V_2/V_1 VERSUS n_c FOR $V_3/V_1 = 0.6, 1.0$ AND 3.0 FOR THE DISC LENS WITH CENTRE ELEMENT OF LENGTH $0.6, 1.0$ AND $2.0D$ RESPECTIVELY.

KEY TO FIGURES 6.19 TO 6.21

* CALCULATED POINTS

† EXPERIMENTAL POINTS

(vertical error bars are 4% of experimentally obtained values of V_2/V_1)

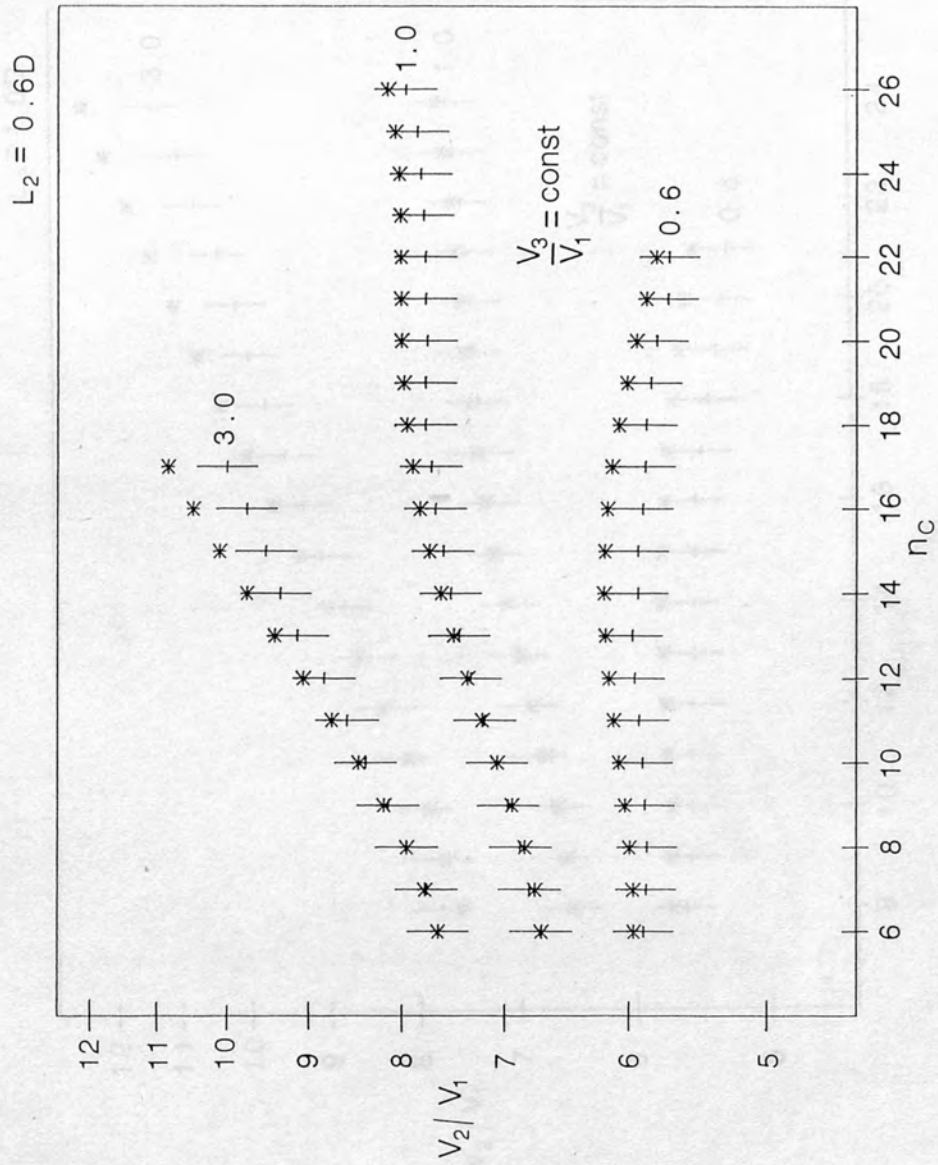


Figure 6.19

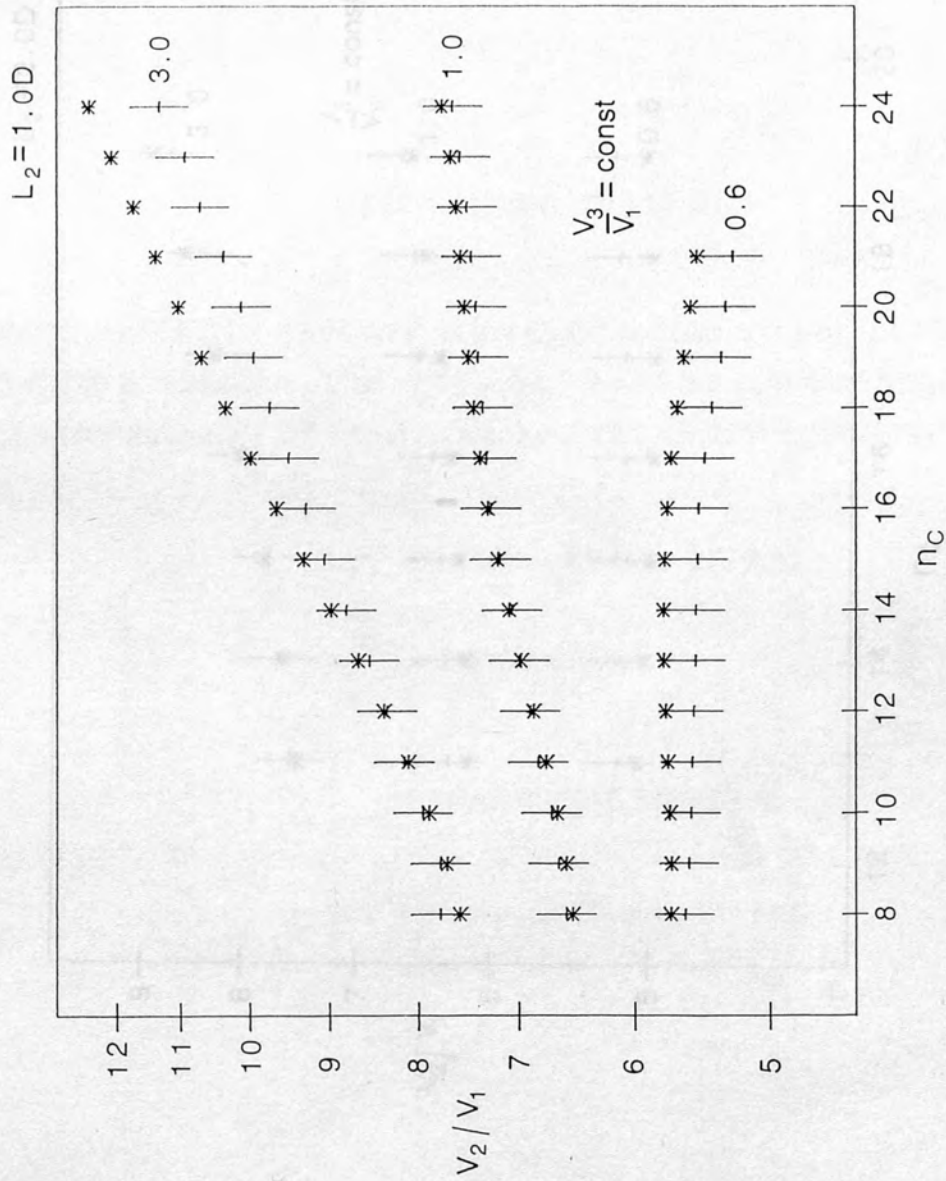


Figure 6.20

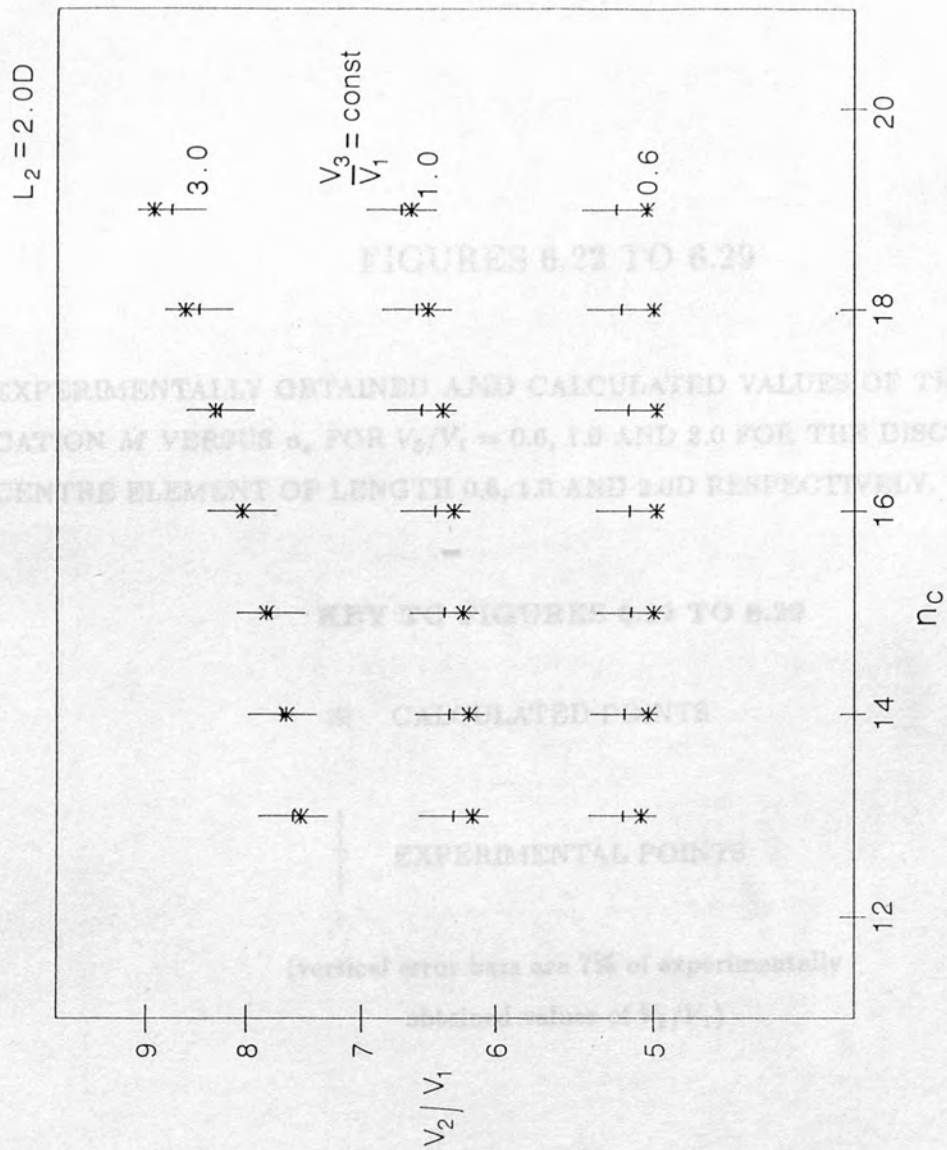


Figure 6.21

FIGURES 6.22 TO 6.29

EXPERIMENTALLY OBTAINED AND CALCULATED VALUES OF THE MAGNIFICATION M VERSUS n_c FOR $V_3/V_1 = 0.6, 1.0$ AND 3.0 FOR THE DISC LENS WITH CENTRE ELEMENT OF LENGTH $0.6, 1.0$ AND $2.0D$ RESPECTIVELY.

KEY TO FIGURES 6.22 TO 6.29

* CALCULATED POINTS

† EXPERIMENTAL POINTS

(vertical error bars are 7% of experimentally
obtained values of V_2/V_1)

$L_2 = 0.6D$

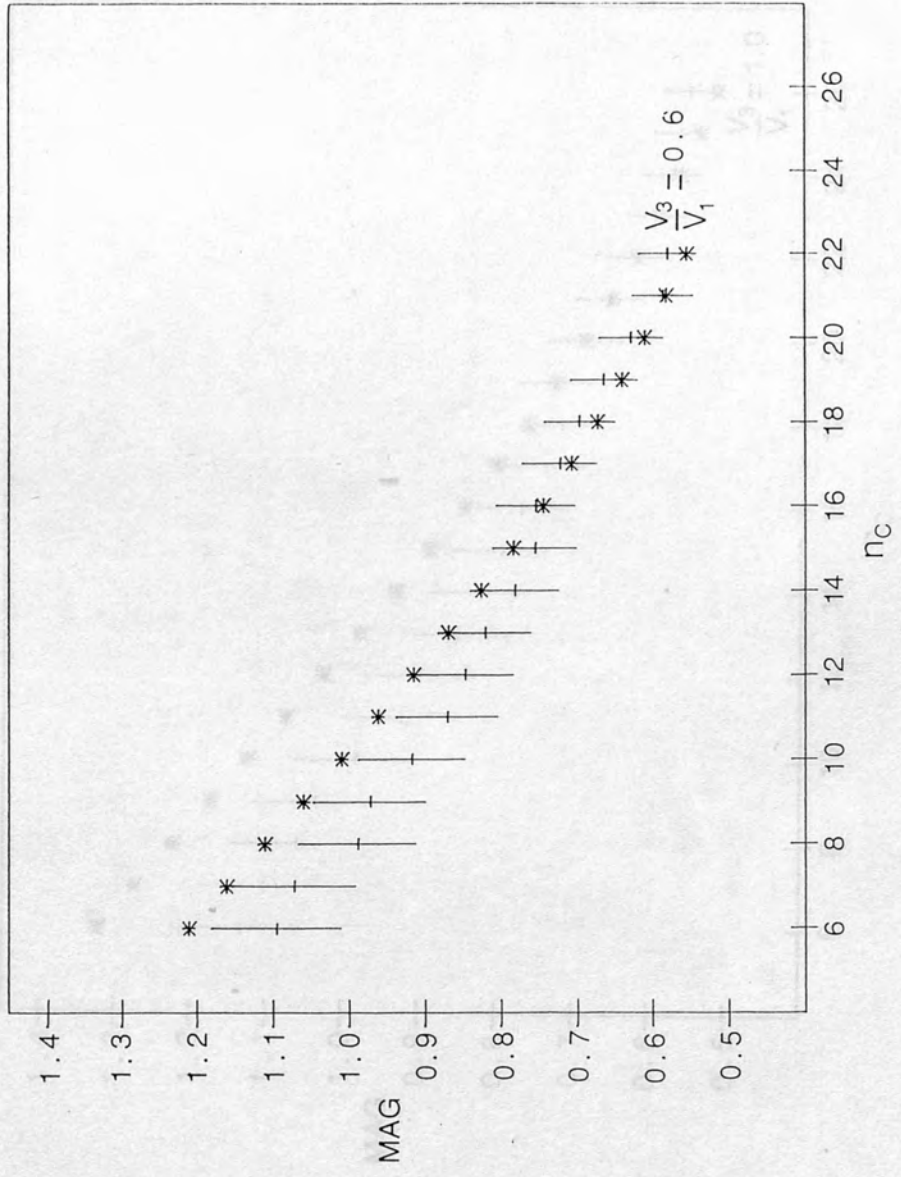


Figure 6.22

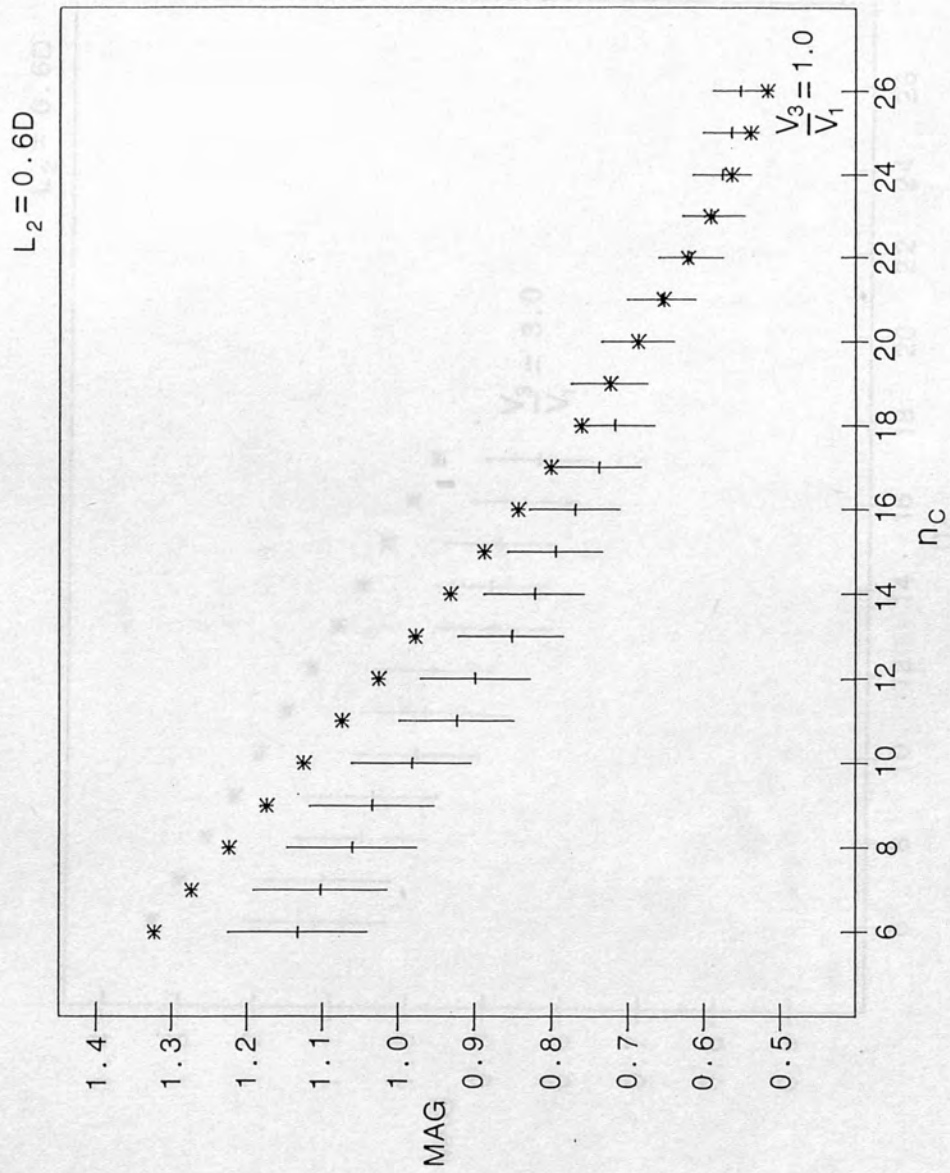


Figure 6.23

$L_2 = 0.6D$

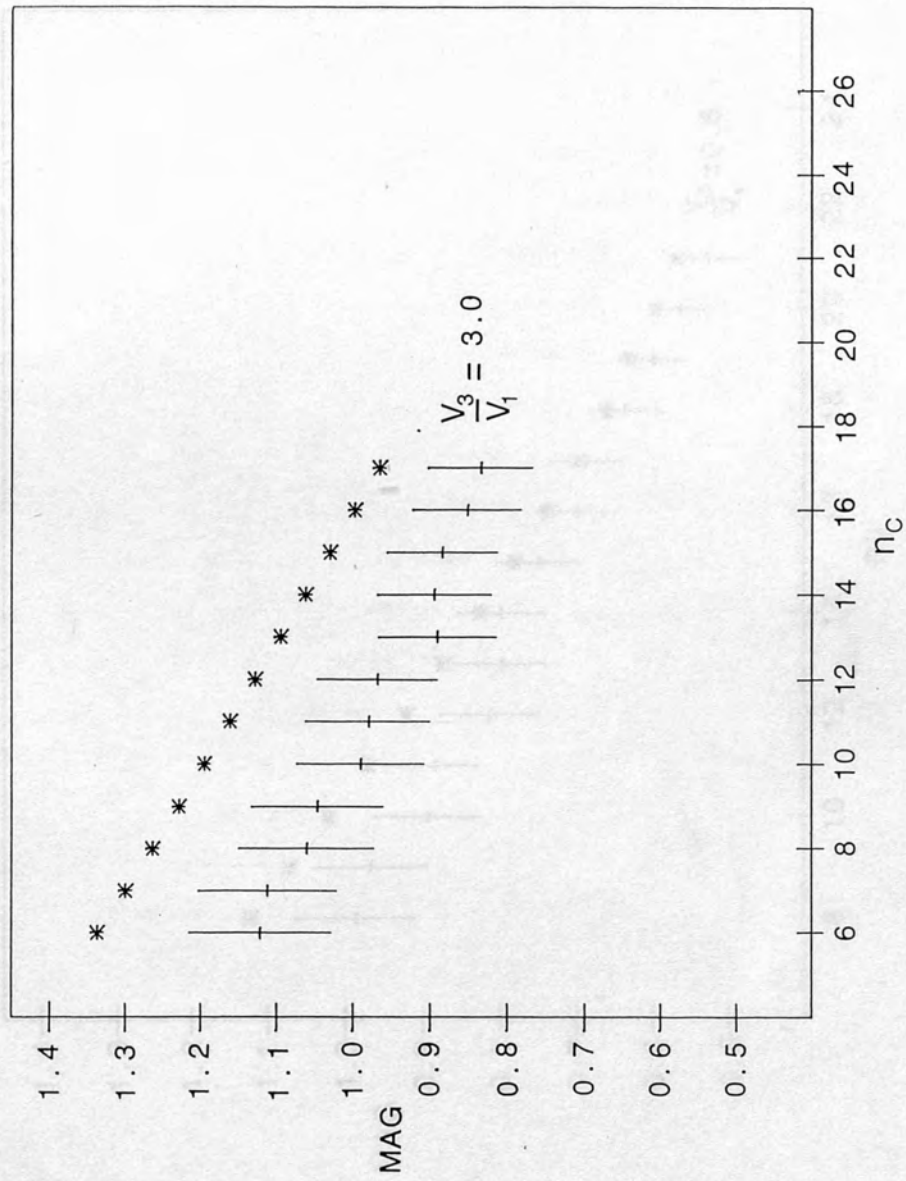


Figure 6.24

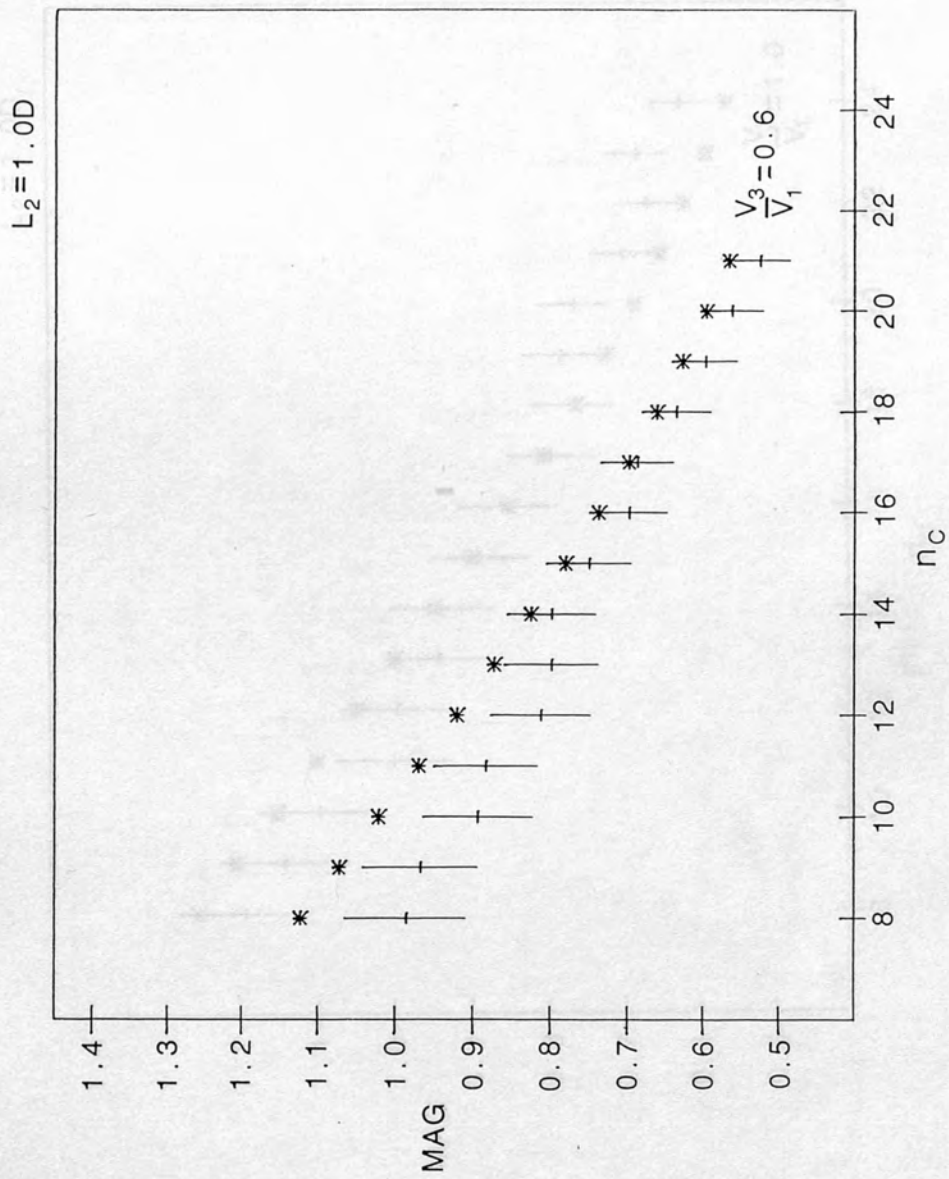


Figure 6.25

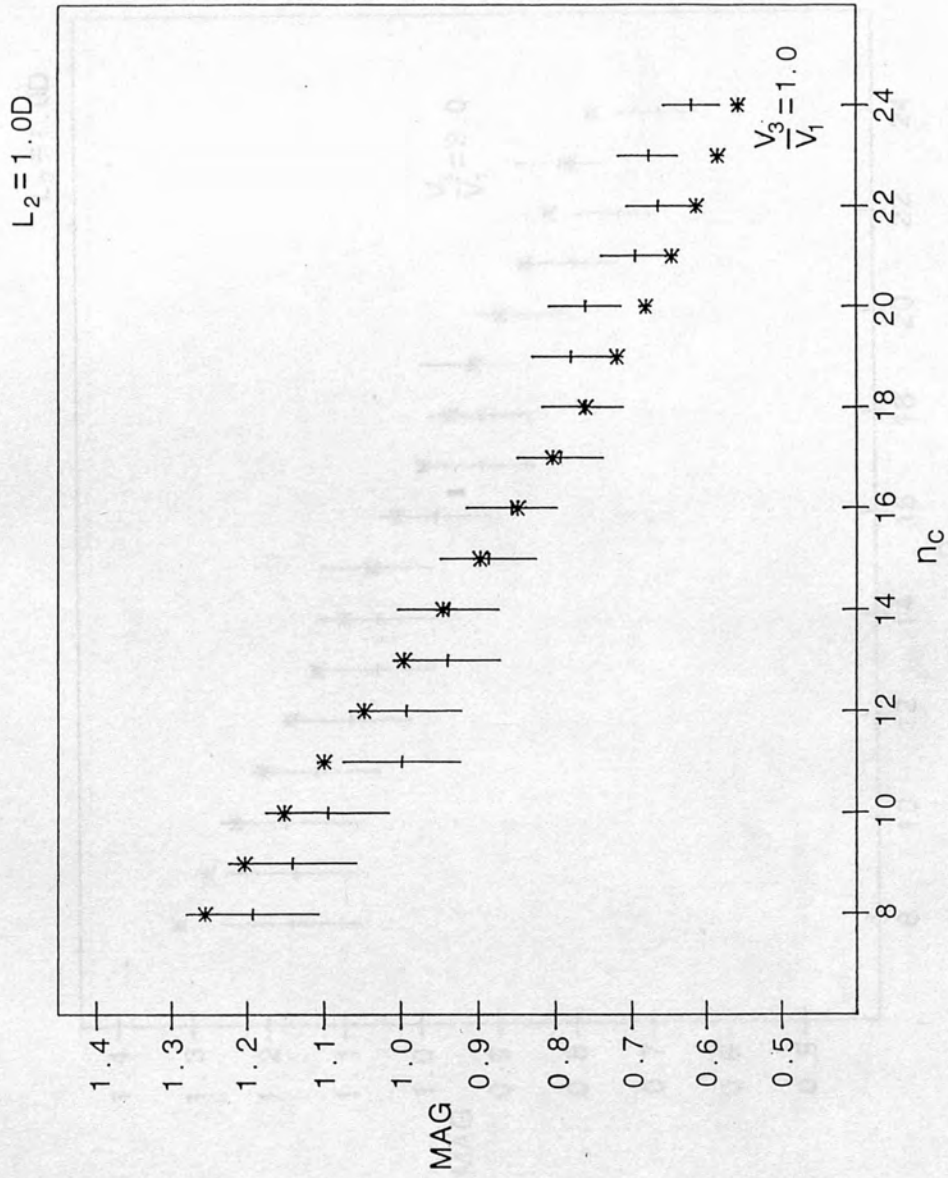


Figure 6.26

$L_2 = 1.0D$

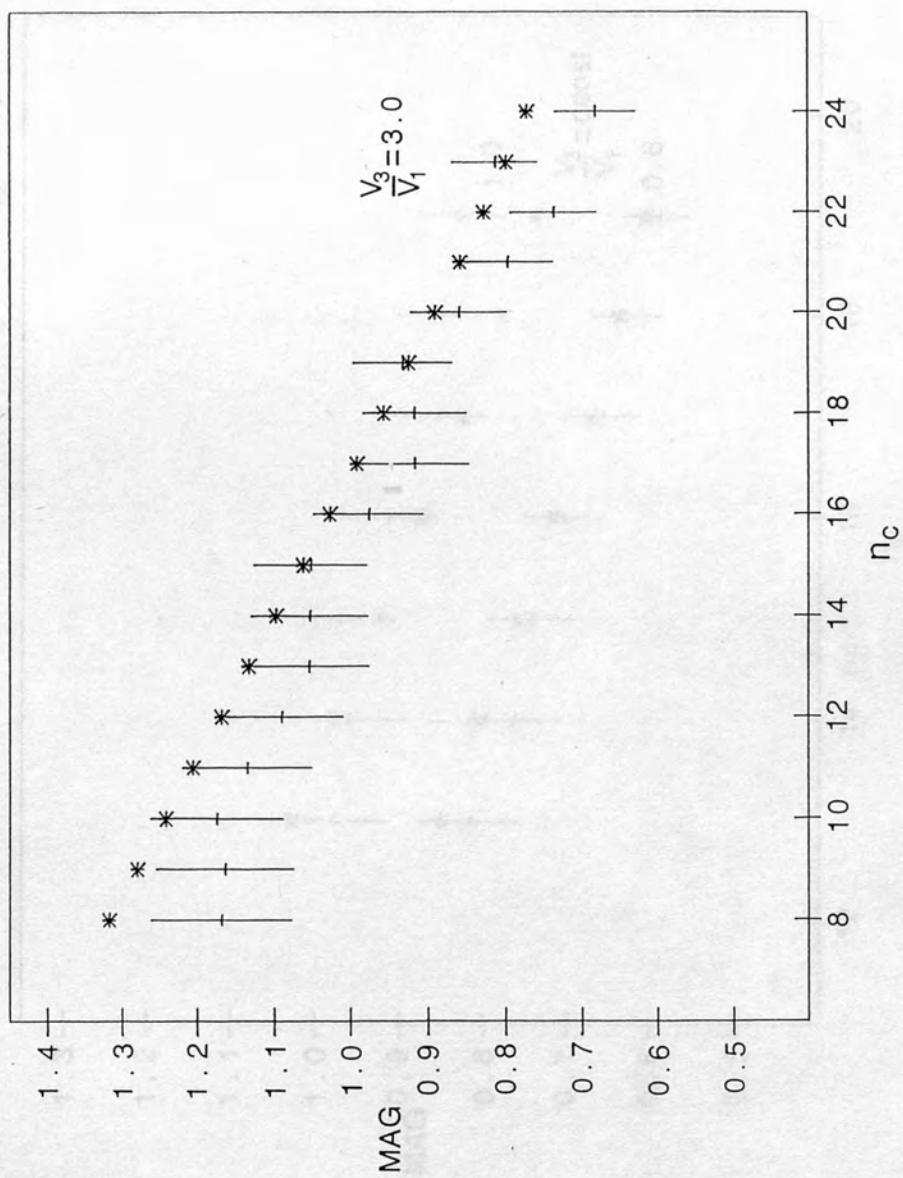


Figure 6.27

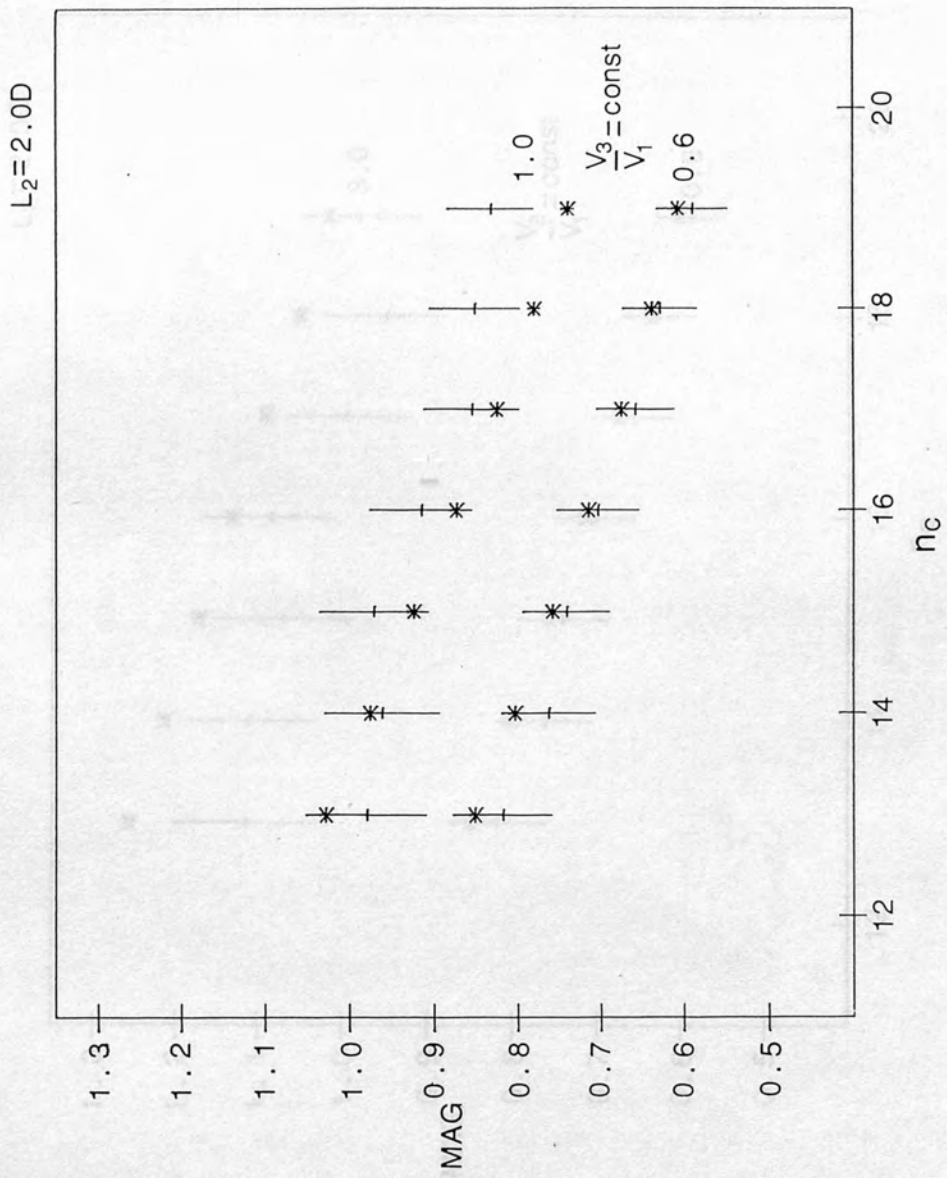


Figure 6.28

REFERENCES : CHAPTER SIX

- Cook R D and Hoddle D W O 1976 The simple accurate calculation of cylinder lens potentials and local properties *J. Phys. E : Sci. Instrum.* 9 279-82
- Read F H 1983 A 'reversible' electrostatic lens *J. Phys. E : Sci. Instrum.* 16 630-642
- Harting E and Read F H 1976 *Electrostatic Lenses (Academic Press)*

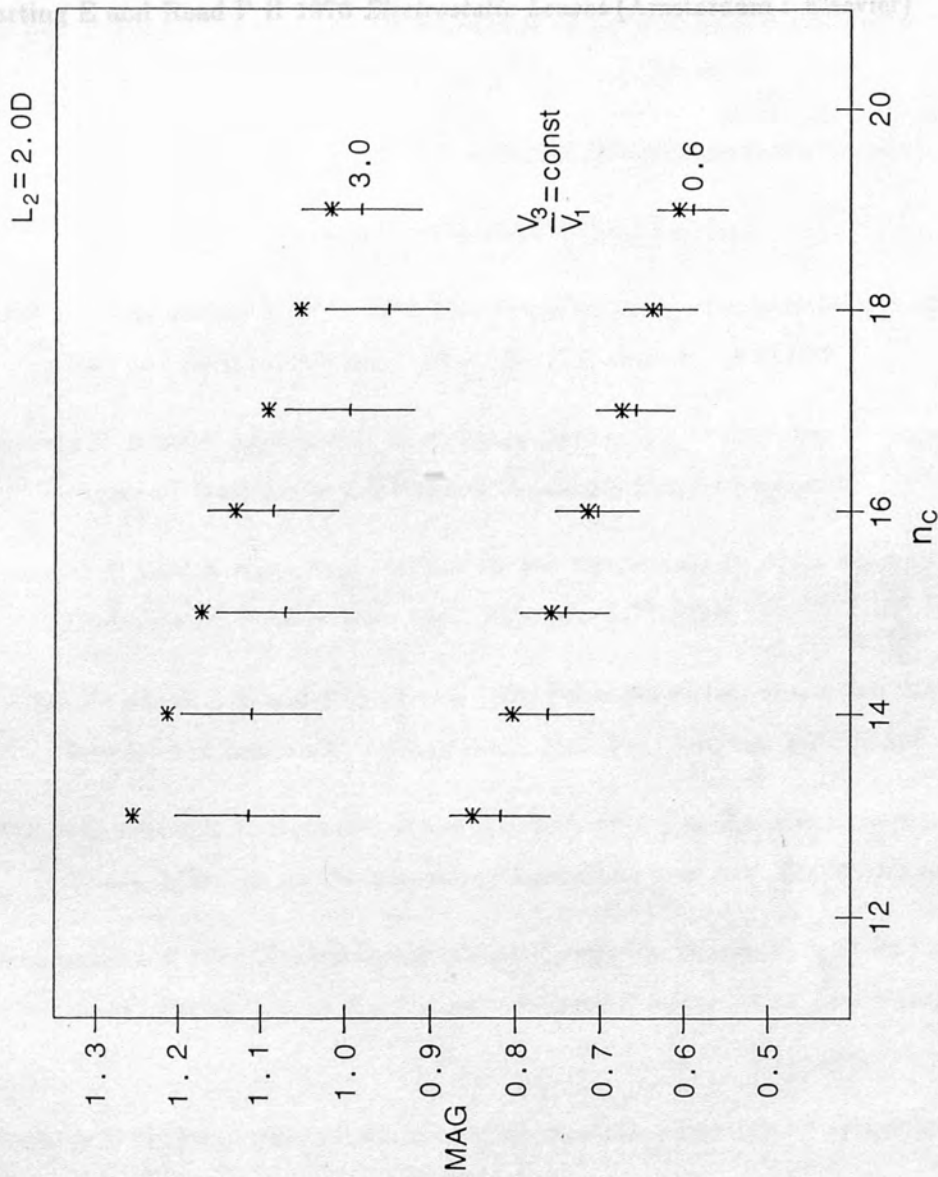


Figure 6.29

REFERENCES : CHAPTER SIX

- Cook R D and Heddle D W O 1976 The simple accurate calculation of cylinder lens potentials and focal properties *J. Phys. E : Sci. Instrum.* **9** 279-82
- Read F H 1983 A 'movable' electrostatic lens *J. Phys. E : Sci. Instrum.* **16** 636-642
- Harting E and Read F H 1976 *Electrostatic Lenses* (Amsterdam : Elsevier)
- British Association of Mathematical Tables 6 1958 (Cambridge Royal Society)
- Buckingham R A 1962 *Numerical Methods* (Pitman : London)
- Cook R D and Heddle D W O 1976 The simple accurate calculation of cylinder lens potentials and focal properties *J. Phys. E : Sci. Instrum.* **9** 279-82
- Comolli V E 1980 *Introduction to Electron Optics, the Production, Propagation, and Focusing of Electron Beams* (Oxford University Press : England)
- Cramer D R 1963 A Numerical Method for the Determination of an Electric Field about a Complicated Boundary *J. Appl. Phys.* **34** 2477-2479
- DiChio D, Natali S V and Kuyatt C E 1974 Focal properties of the two tube electrostatic lens for and near-unity voltage ratios *Rev. Sci. Instrum.* **45** 559-565
- DiChio D, Natali S V, Kuyatt C E and Galejs A 1974 Use of matrices to represent electron lenses. Matrices for the two tube electrostatic lens *Rev. Sci. Instrum.* **45** 566-569
- Drummond I W 1964 The Ion Optics of Low Energy Ion Beams *Vacuum 36 (Vacuum Special Issue, Proceedings of the 3rd International Conference on Low Energy Ion Beams)* 1-8
- Edwards D 1963 Accurate calculations of electrostatic potentials for cylindrically symmetric lenses *Rev. Sci. Instrum.* **34** 1729-1735
- El-Karek A B and El-Karek J C 1976 *Electron Beams, Lenses, and Optics* Vols. I and II (Academic Press : New York)
- Epstein D W 1936 Electron Optical System of Two Cylinders as applied to Cathode-Ray Tubes *Proc. Inst. Radio Eng.* **24** 1095-1129

REFERENCES : ALL

- Bertram S 1940 Determination of the Axial Potential Distribution in Axially Symmetric Electrostatic Fields *Proc. IRE* **28** 418-20
- Bertram S 1942 Calculation of Axially Symmetric Fields *J. Appl. Phys.* **13** 496-502
- Bonjour P 1979 A simple accurate expression of the potential in electrostatic lenses. Part I : Two cylinder lenses *Revue Phys. Appl.* **14** 533-40
- British Association Mathematical Tables **6** 1958 (Cambridge Royal Society)
- Buckingham R A 1966 *Numerical Methods* (Pitman : London)
- Cook R D and Heddle D W O 1976 The simple accurate calculation of cylinder lens potentials and focal properties *J. Phys. E : Sci. Instrum.* **9** 279-82
- Cosslett V E 1950 *Introduction to Electron Optics, the Production, Propagation, and Focusing of Electron Beams* (Oxford University Press : England)
- Cruise D R 1963 A Numerical Method for the Determination of an Electric Field about a Complicated Boundary *J. Appl. Phys.* **34** 3477-3479
- DiChio D, Natali S V and Kuyatt C E 1974 Focal properties of the two tube electrostatic lens for and near-unity voltage ratios *Rev. Sci. Instrum.* **45** 559-565
- DiChio D, Natali S V, Kuyatt C E and Galejs A 1974 Use of matrices to represent electron lenses. Matrices for the two tube electrostatic lens *Rev. Sci. Instrum.* **45** 566-569
- Drummond I W 1984 The Ion Optics of Low Energy Ion Beams *Vacuum* **34** (*Vacuum Special Issue, Proceedings of the 3rd International Conference on Low Energy Ion Beams*) 1-61
- Edwards D 1983 Accurate calculations of electrostatic potentials for cylindrically symmetric lenses *Rev. Sci. Instrum.* **54** 1729-1735
- El-Kareh A B and El-Kareh J C 1970 *Electron Beams, Lenses, and Optics* Vols. I and II (Academic Press : New York)
- Epstein D W 1936 Electron Optical System of Two Cylinders as applied to Cathode-Ray Tubes *Proc. Inst. Radio Engrs* **24** 1095-1139

- Fink J and Kisker E 1980 A method for rapid calculations of electron trajectories in multi-element electrostatic cylinder lenses *Rev. Sci. Instrum.* **51** 918-920
- Gabor D 1945 *The Electron Microscope* (Hutton : London)
- Grivet P 1972 *Electron Optics* 2nd Edition (1st Ed. 1965) (Pergamon : Oxford)
- Hall C E 1966 *Introduction to Electron Microscopy* 2nd Edition (1st Ed. 1953) (McGraw-Hill : New York)
- Hamming R W 1973 *Numerical Methods for Scientists and Engineers* (MacGraw Hill : London)
- Harting E and Read F H 1976 *Electrostatic Lenses* (Amsterdam : Elsevier)
- Hawkes P W and Armstrong R J 1970 Note on the Calculation of Potential and Field Functions in Electron Optics *Optik* **30** 546-548
- Hawkes P W 1972 *Electron Optics and Electron Microscopy* (Taylor and Frances Ltd : London)
- Hawkes P W (editor) 1973 *Image Processing and Computer Aided Design in Electron Optics* (Academic Press : London)
- Heddle D W O 1969 The design of three element electrostatic electron lenses *J. Phys. E : Sci. Instrum.* **2** 1046-1050
- Heddle D W O and Kurepa M V 1970 The focal properties of three-element electrostatic electron lenses *J. Phys. E : Sci. Instrum.* **3** 552-4
- Heddle D W O 1970 *JILA report No.104* University of Colorado, Boulder, Colorado
- Heddle D W O, 1971 An afocal Electrostatic Lens *J. Phys. E : Sci. Instrum.* **4** 981-983
- Heddle D W O, Papadovassilakis N and Yateem A M 1982 Measurement of the magnification behaviour of some three-element electrostatic lenses *J. Phys. E : Sci Instrum.* **15** 1210-1213
- Heddle D W O and Papadovassilakis N 1984 The magnification behaviour of a five-element electrostatic lens *J. Phys. E : Sci. Instrum.* **17** 559-605 Jacob L 1950 *An Introduction to Electron Optics* (Methuen : London)

- Kisker E 1982 Simple method for accurate ray tracing in electrostatic lenses *Rev. Sci. Instrum.* **53** 114-116
- Klemperer O and Wright W D 1939 The Investigation of Electron Lenses *Proc. Phys. Soc.* **51** 296-317,376-377
- Klemperer O 1953 *Electron Optics* 2nd Edition (Cambridge University Press : England)
- Klemperer O and Barnett M E 1971 *Electron Optics* 3rd Edition (Cambridge University Press : England)
- Lawson J D 1977 *The Physics of Charged Particle Beams* (Oxford University Press : England)
- Mautz J R and Harrington R F 1970 Computation of Rotationally Symmetric Laplacian Potentials *Proc. IEE* **117** 850-852
- Meyers L M 1939 *Electron Optics* (Chapman and Hall : London)
- Mulvey T and Wallington M J 1973 Electron Lenses *Rep. Prog. Phys.* **36** 347-421
- Munro E 1973 Computer-Aided Design of Electron Lenses by the Finite Element Method in *Image Processing and Computer Aided Design in Electron Optics*, ed. Hawkes P W (Academic Press : London) 284-323
- Natali S, DiChio D and Kuyatt C E 1972 Accurate Calculations of Properties of the Two-Tube Electrostatic Lens. 1. Improved Digital Methods for the Precise Calculation of Electric Fields and Trajectories *J. Research NBS* **76A** 27-35
- Numerical Algorithms Group 1984 Subroutines E01BAF and E02BBF *NAG Library Manual* Mark 11 **2**
- Paszkowski B 1968 *Electron Optics* (Iliffe : London)
- Pierce J R 1954 *Theory and Design of Electron Beams* (D. Van Nostrand Company, Inc. : U.S.A)
- Ralston A 1965 *A first Course in Numerical Analysis* (McGraw-Hill:New York)
- Read F H 1969a Accurate Calculations of double-aperture electrostatic immersion lenses *J. Phys. E: Sci. Instrum.* **2** 165-169

- Read F H 1969b Calculated properties of electrostatic einzel lenses of three apertures *J. Phys. E: Sci. Instrum.* **2** 679-684
- Read F H 1970 Asymmetric electrostatic lenses of three apertures *J. Phys. E: Sci. Instrum.* **3** 127-31
- Read F H, Adams A and J R Soto-Montiel 1971 Electrostatic cylinder lenses 1: Two element lenses *J. Phys. E: Sci. Instrum.* **4** 625-632
- Read F H 1983 A 'movable' electrostatic lens *J. Phys. E: Sci. Instrum.* **16** 636-642
- Renau A, Read F H and Brunt J N H 1982 The charge-density method of solving electrostatic problems with and without the inclusion of space-charge *J. Phys. E: Sci. Instrum.* **15** 347-354
- Renau A and Heddle D W O 1986 Geometric aberrations in electrostatic lenses I. A simple and accurate computer model *J. Phys. E: Sci. Instrum.* **19** 284-288
- Septier A (editor) 1967 *Focusing of charged particles* (Academic Press : London)
- Singer B and Braun M 1970 Integral Equation Method for Computer Evaluation of Electron Optics *IEEE Trans. Electron. Devices* **17** 926-934
- Spangenberg K R and Field L M 1942 Some Simplified Methods of Determining the Optical Characteristics of Electron Lenses *Proc. Inst Radio Engrs.* **30** 138-144 & *Elect. Commun.* **20** 305-313
- Spangenberg K R 1948 *Vacuum Tubes* (McGraw-Hill : New York)
- Sturrock P A 1955 *Electron Optics* (Cambridge University Press : England)
- Weber C 1950 *Electromagnetic Fields* Vol. 1 (Wiley : New York)
- Weber C 1967 Numerical Solution of Laplace's and Poissons's equations and the Calculation of Electron Trajectories and Electron Beams in *Focusing of Charged Particles* Vol 1, ed Septier A (Academic Press : London) 45-99
- Ximen Jiye 1986 *Aberration Theory in Electron and Ion Optics*; Suppl. *Advances in Electronic and Electron Physics* **17**
- Zworykin V K, Morton G A, Ramberg E G, Hillier J and Vance A W 1945 *Electron Optics and the Electron Microscope* (Wiley : New York)

Zworykin V K and Morton 1956 *Television. The Electronics of Image Transmission in Colour and Monochrome* 2nd Edition (1st Ed. 1940 *Television*) (Wiley : New York)

Carrott V B 1950 *Introduction to Electron Optics, the Production, Propagation, and Focusing of Electron Beams* (Oxford University Press : England)

Diamond I W 1984 The Ion Optics of Low Energy Ion Beams *Vacuum 34 (Vacuum Special Issue, Proceedings of the 3rd International Conference on Low Energy Ion Beams)* 1-61

El-Kazeh A B and El-Razek I C 1970 *Electron Beams, Lenses, and Optics* Vols. 1 and 2 (Academic Press : New York)

Gabor D 1945 *The Electron Microscope* (Hottel : London)

Grivet P 1973 *Electron Optics* 2nd Edition (1st Ed. 1955) (Penguin : Oxford)

Hall C E 1968 *Introduction to Electron Microscopy* 2nd Edition (1st Ed. 1953) (McGraw-Hill : New York)

Harting E and Read P H 1970 *Electrostatic Lenses* (Amsterdam : Elsevier)

Hawkes P W 1972 *Electron Optics and Electron Microscopy* (Taylor and Francis Ltd : London)

Hawkes P W (editor) 1973 *Image Processing and Computer Aided Design in Electron Optics* (Academic Press : London)

Jacob L 1950 *An Introduction to Electron Optics* (Methuen : London)

Klemperer O 1955 *Electron Optics* 2nd Edition (Cambridge University Press : England)

Klemperer O and Barnatt M B 1971 *Electron Optics* 3rd Edition (Cambridge University Press : England)

Lawson J D 1977 *The Physics of Charged Particle Beams* (Oxford University Press : England)

Meyers U M 1958 *Electron Optics* (Chapman and Hall : London)

Mulvey T and Wallington M J 1973 *Electron Lenses* *Rep. Prog. Phys.* 36 347-424

Paschowski B 1938 *Electron Optics* (Hill : London)

BIBLIOGRAPHY

- Cosslett V E 1950 *Introduction to Electron Optics, the Production, Propagation, and Focusing of Electron Beams* (Oxford University Press : England)
- Drummond I W 1984 The Ion Optics of Low Energy Ion Beams *Vacuum* **34** (*Vacuum Special Issue, Proceedings of the 3rd International Conference on Low Energy Ion Beams*) 1-61
- El-Kareh A B and El-Kareh J C 1970 *Electron Beams, Lenses, and Optics* Vols. I and II (Academic Press : New York)
- Gabor D 1945 *The Electron Microscope* (Hutton : London)
- Grivet P 1972 *Electron Optics* 2nd Edition (1st Ed. 1965) (Pergamon : Oxford)
- Hall C E 1966 *Introduction to Electron Microscopy* 2nd Edition (1st Ed. 1953) (McGraw-Hill : New York)
- Harting E and Read F H 1976 *Electrostatic Lenses* (Amsterdam : Elsevier)
- Hawkes P W 1972 *Electron Optics and Electron Microscopy* (Taylor and Frances Ltd : London)
- Hawkes P W (editor) 1973 *Image Processing and Computer Aided Design in Electron Optics* (Academic Press : London)
- Jacob L 1950 *An Introduction to Electron Optics* (Methuen : London)
- Klemperer O 1953 *Electron Optics* 2nd Edition (Cambridge University Press : England)
- Klemperer O and Barnett M E 1971 *Electron Optics* 3rd Edition (Cambridge University Press : England)
- Lawson J D 1977 *The Physics of Charged Particle Beams* (Oxford University Press : England)
- Meyers L M 1939 *Electron Optics* (Chapman and Hall : London)
- Mulvey T and Wallington M J 1973 Electron Lenses *Rep. Prog. Phys.* **36** 347-421
- Paszkowski B 1968 *Electron Optics* (Iliffe : London)

- Pierce J R 1954 *Theory and Design of Electron Beams* (D. Van Nostrand Company, Inc. : U.S.A)
- Septier A (editor) 1967 *Focusing of charged particles* (Academic Press : London)
- Spangenberg K 1948 *Vacuum Tubes* (McGraw-Hill : New York)
- Sturrock P A 1955 *Electron Optics* (Cambridge University Press : England)
- Ximen Jiye 1986 *Aberration Theory in Electron and Ion Optics*; Suppl. *Advances in Electronic and Electron Physics* 17
- Zworykin V K, Morton G A, Ramberg E G, Hillier J and Vance A W 1945 *Electron Optics and the Electron Microscope* (Wiley : New York)
- Zworykin V K and Morton 1956 *Television. The Electronics of Image Transmission in Colour and Monochrome* 2nd Edition (1st Ed. 1940 *Television*) (Wiley : New York)